

ANALYSIS OF OPTIMAL FACADE SYSTEM DESIGN IN HIGH PERFORMANCE
BUILDINGS

A Dissertation

by

QINBO LI

Submitted to the Office of Graduate and Professional Studies of
Texas A&M University
in partial fulfillment of the requirements for the degree of

DOCTOR OF PHILOSOPHY

Chair of Committee,	Jeff S. Haberl
Committee Members,	Juan-Carlos Baltazar
	Wei Yan
	Michael B. Pate
Head of Department,	Gregory A. Luhan

December 2020

Major Subject: Architecture

Copyright 2020 Qinbo Li

ABSTRACT

This dissertation presents a new, optimal window design procedure for an office that uses a combined daylighting and thermal simulation in a hot and dry climate. The purpose of this work is to better inform the design of building windows used for daylighting in the preliminary design stage for improving building performance.

This study used a simple office model to develop and test a prototype for the combined daylighting+thermal simulation by comparing the combined simulation methods of DOE-2+Split-Flux, EnergyPlus+Split-Flux, EnergyPlus+Radiosity, and EnergyPlus+Radiance. The results showed that different window size and location designs could have very different annual energy consumption results when using the combined EnergyPlus+Radiance simulation tool for North, South, East, and West orientations. However, the other three combined simulation methods could not simulate the differences between the different window size and placement designs (with same window areas). Therefore, this study proposes guidelines for how to conduct a combined daylighting and thermal simulation to obtain more accurate results.

This study demonstrated the use of an improved procedure for using the Radiance simulation for speeding up the daylighting optimization. This new method produces accurate annual daylighting results while minimizing run time. This study also proposes a new customized, Radiance rendering parameters (called custom preset) into the DIVA software to simulate the annual daylighting. This custom preset only took 30 seconds to obtain annual daylighting results, while the most accurate preset (high-quality

preset) in DIVA takes over one hour to complete the same simulation. The statistical software JMP Pro 14 was used to calculate the correlation between high-quality preset and custom preset. The results show that the high accuracy annual daylighting results can be predicted using the simulation results from the custom preset together with the multi-linear regression method that was developed.

This study developed a window design plugin in grasshopper using Python. This new window design plugin was used generate thousands of different window sizes and placement designs. The window design plugin used a Multi-Objective Optimization (MOO) tool for analyzing different window size and placement designs. Finally, four optimization studies were conducted for the case-study office. The results showed that top positioned windows had the best daylighting and thermal performance, whereas lower positioned windows had the worst results. Therefore, national standards, such as ASHRAE Standard 90.1 and the IECC should not give the same credits for all the window location placements on an external wall. The Standard should provide the guidelines for the combined thermal and daylighting simulation. In addition, standardized testing of combined simulation programs that model the daylighting and thermal characteristics of a building, similar to the existing ASHRAE Standard 140 procedures, need to be developed and used by whole-building energy simulation programs.

DEDICATION

To my friends and family

ACKNOWLEDGEMENTS

I would like to thank the following people, without whom I would not have been able to complete this research. Without their help I would not have made it through my Ph.D. degree. First of all, I would like to gratefully thank my committee chair, Dr. Haberl, for his enthusiasm for my study, for his support, encouragement and patience. The meetings and conversations were vital in inspiring me to think outside the box and to overcome many difficulties. I also would like to express my sincere gratitude to my committee member Dr. Baltazar for his guidance during this research. He helped me with the coding issues of my window design program.

I would like to thank my committee member, Dr. Yan, for his guidance in learning parametric modeling and Python. Also, I would like to thank my committee member Dr. Pate, for his guidance and support throughout the course of this research.

I would like to express my gratitude and appreciation to Yanze Li. He helped me in coding and efficiently designing my program. I am also grateful for the help from Huanjun Zhang and Jiangyuan Li, who helped me to select the statistic model in the analysis of data.

Thanks also go to my friends and colleagues and the department faculty and staff for making my time at Texas A&M University a great experience.

Finally, thanks to my family for their encouragement.

CONTRIBUTORS AND FUNDING SOURCES

Contributors

This work was supervised by a dissertation committee consisting of Professor Dr. Jeff S. Haberl and Dr. Juan-Carlos Baltazar and Dr. Wei Yan of the Department of Architecture and Professor Dr Michael B. Pate of the Department of Mechanical Engineering.

Funding Sources

This study was supported by a fellowship from ASHRAE Graduate Student Research Grant-In-Aid for the 2019-2020 and a scholarship from China Scholarships Council.

NOMENCLATURE

BES	Building Energy Simulation
BES/DL	Building Energy Simulation and DayLighting
BEM	Building Energy Modeling
IRC	Internal Reflected Component
HVAC	Heating Ventilation and Air Conditioning
CFSs	Complex Fenestration Systems
LBNL	Lawrence Berkeley National Laboratory
CIE	International Commission on Illumination
ASHRAE	American Society of Heating, Refrigerating and Air-Conditioning Engineers
IECC	International Energy Conservation Code
ACEEE	American Council for an Energy-Efficient Economy
IES	Illuminating Engineering Society
IBPSA	International Boarding & Pet Services Association
LEED	Leadership in Energy and Environmental Design
IEQ	Indoor Environment Quality
DF	Daylight Factor
DA	Daylight Autonomy
UDI	Useful Daylight Illuminance
sDA	Spatial Daylight Autonomy

ASE	Annual Sunlight Exposure
DGI	The Daylight Glare Index
VCP	Visual Comfort Probability
CGI	CIE glare index
UGR	Unified Glare Rating System
DGP	Daylight Glare Probability
DGPs	Simplified Daylight Glare Probability
HDR	High Dynamic Range
HDRI	High-Dynamic-Range Imaging
PMV	Predicted Mean Vote
PPD	Predicted Percent Dissatisfied
SET	Standard Effective Temperature
DC	Daylight Coefficient
SC	Shading Coefficient
ERC	Externally Reflected Component
IRC	Internally Reflected Component
GPS	Generalized Pattern Search algorithms
FC	Foot-candles
BSDF	Bi-directional Scattering Distribution Function
BTDF	Bi-directional Transmission Distribution Function
BRDF	Bi-directional Reflection Distribution Function
SHGC	Solar Heat Gain Coefficient

RGB	Red, Green, and Blue
GPS	Generalized Pattern Search algorithms
CDS	Conceptual Dynamic Shading
DDS	Detailed Dynamic Shading
SOO	Single-Objective Optimization
MOO	Multi-Objective Optimization
GAs	Genetic Algorithms
NSGA-II	Non-dominated Sorting Genetic Algorithm
PSO	Particle Swarm Optimization
TAR	Transmittance Absorbance Reflectance
MLW	Multi-Layer Window

TABLE OF CONTENTS

	Page
ABSTRACT	ii
DEDICATION	iv
ACKNOWLEDGEMENTS	v
CONTRIBUTORS AND FUNDING SOURCES.....	vi
NOMENCLATURE.....	vii
TABLE OF CONTENTS	x
LIST OF FIGURES.....	xiii
LIST OF TABLES	xx
1. INTRODUCTION.....	1
1.1. Background	1
1.2. Purpose and Objectives	5
1.3. Significance and Limitations.....	5
1.4. Organization of the Dissertation	7
2. LITERATURE REVIEW	9
2.1. Overview	9
2.2. Sky Models.....	9
2.3. Building Performance	11
2.3.1. Visual Comfort	11
2.3.2. Thermal Comfort.....	16
2.3.3. Summary	20
2.4. Daylighting Calculation Methods	21
2.4.1. Daylight Factor Methods (DF).....	21
2.4.2. Daylight Coefficient Methods.....	24
2.4.3. Summary	27
2.5. Simulation tools	28
2.5.1. Daylighting simulation tools	28

2.5.2. Self-Contained energy and daylighting simulation program.....	30
2.5.3. Summary	39
2.6. Parametric Modeling Tools – Rhino & Grasshopper.....	41
2.7. Coupled Simulation Methods: Integrated the thermal and daylighting simulation.....	41
2.8. Optimization Techniques for Building Simulation	47
2.8.1. Single-Objective Optimization and Multi-Objective Optimization Methods	47
2.8.2. Continuous and Discrete Optimization Methods	48
2.8.3. Optimization Design Application.....	55
2.8.4. Summary	60
2.9. Design Strategies.....	61
2.9.1. Daylighting systems	62
2.9.2. Building Shape and Orientation	65
2.9.3. Window size and placement.....	68
2.9.4. Complex Façades Systems	80
2.9.5. Shading Devices.....	86
2.10. Overall Summary of the Literature Review	97
2.11. Issues Identified.....	102
 3. METHODOLOGY	 107
3.1. Overview	107
3.2. Reproduce the Caldas Office Model Using Empirical Testing	109
3.3. Propose Prototype for the Simulation Process and Tools.....	110
3.4. Propose an Improved Radiance Annual Daylighting Simulation Method.....	111
3.5. Parametric Modeling and Optimization	114
 4. RESULTS OF THE COMBINING DAYLIGHTING AND THERMAL SIMULATION	 117
4.1. Build the Simulation Model	117
4.1.1. Caldas Office Model	117
4.1.2. Empirical Testing of Input Parameters.....	119
4.1.3. Limitations of the Caldas Simulation Model	125
4.1.4. The Improved Office Model.....	127
4.2. Propose a Prototype for the Daylighting and Thermal Simulation Process.....	130
4.2.1. Small Size Office Model	131
4.2.2. Match Models in DOE-2 and EnergyPlus.....	132

4.2.3. Model Parameters of Window Layout and Placement Designs	138
4.2.4. Daylighting Settings in DIVA.....	140
4.2.5. Combined Daylighting and Thermal Simulation	144
4.2.6. Combined Daylighting and Energy Simulation Results	146
4.2.7. Dynamic Daylighting Metric Analysis.....	177
4.3. Overall Summary	182
5. RESULTS OF THE PARAMETRIC ANALYSIS	189
5.1. An Improved Radiance Simulation Method in Optimization.....	189
5.1.1. Grid Spacing Setting	193
5.1.2. Radiance Rendering settings	195
5.2. Window Size and Placement Design Plugin in Grasshopper.....	217
5.3. Window Design Optimization Process and Results in Office Models.....	221
5.3.1. The Results for South-Facing Windows	225
5.3.2. The Results for East-Facing Windows.....	236
5.3.3. The Results for West-Facing Windows.....	240
5.3.4. The Results for North-Facing Windows	242
5.4. Summary	246
6. SUMMARY, RESULTS, CONCLUSIONS, AND FUTURE WORK	252
6.1. Summary	252
6.2. Results	253
6.2.1. Results from the Combined Daylighting and Thermal Simulation.....	253
6.2.2. Results from Improved Radiance Simulation Method in Optimization	256
6.2.3. Results from Window Design Optimization in Office Models.....	257
6.3. Conclusion.....	259
6.4. Future Work	261
REFERENCES.....	263
APPENDIX A	
DAYLIGHTING AND THERMAL SIMULATION RESULTS.....	290

LIST OF FIGURES

	Page
Figure 2.1 Different Components of Daylight Calculation (Source: Adapted from (Gharpedia, 2017))	22
Figure 2.2 Daylight Coefficient Concept of Discretization of Sky Dome into Patches (Source: Adapted from (Mardaljevic, 2000)).....	25
Figure 2.3 Daylighting Coefficient Basics (Source: Adapted from (Mardaljevic, 1999))	25
Figure 2.4 Forward Ray-Tracing Method (Source: Adapted from (Kim, 2011))	26
Figure 2.5 Backward Ray-Tracing Method (Source: Adapted from (Kim, 2011))	27
Figure 2.6 Types of Light Shelf and Their Operation (Source: Adapted from (Littlefair, 1990)).....	63
Figure 2.7 Prismatic Glazing (Source: Adapted from (Aiziewood, 1993)).....	64
Figure 2.8 Mirrored Louvres (Source: Adapted from (Aiziewood, 1993)).....	65
Figure 2.9 Building Shape (Source: Adapted from (Tuhus-Dubrow and Krarti, 2010))	66
Figure 2.10 The Main Types of Skylights (Source: Adapted from (Yoon et al., 2008)).....	75
Figure 2.11 Monitor Skylight Reflectors Types: Rectangular, Slanted, Sawtooth or Curved (Source: Adapted from (Acosta,Navarro, et al., 2015))	76
Figure 2.12 Initial Calculation Model of Lightscoops (Source: Adapted from (Acosta et al., 2012))	77
Figure 2.13 Nine Different Lightscoops with Same Reflector Surface (Source: Adapted from (Acosta et al., 2012))	78

Figure 2.14 Selection of CFS-Models Currently Supported by the FHG-IBP CFS-Sample Generator with Key Configuration Parameters (Source: Adapted from (Andersen and de Boer, 2006)).....	81
Figure 2.15 Bi-directional Scattering Distribution Function (BSDF) Showing the two Components Bi-directional Reflected Distribution Function (BRDF) and Bi-directional Transmittance Distribution Function (BTDF) (Source: Adapted from (BSDF, n.d.))	83
Figure 2.16 Main Shading Type (Source: Adapted from (Bellia et al., 2014)).....	88
Figure 2.17 Shaded Area Calculation Process Using the Polygon Method (Source: Adapted from (Choi et al., 2015))	94
Figure 3.1 Overview of Research Methodology	108
Figure 3.2: Reproduced Office Model	109
Figure 3.3: Proposed prototype for simulation process and tools (Source: (Li and Haberl, 2020)).....	111
Figure 3.4: Improved Annual Daylighting Simulation Method in DIVA (Radiance).....	112
Figure 3.5 Parametric Modeling and Optimization Simulation	116
Figure 4.1: The Office Model in DOE2.1e (Source: Adapted from (Caldas and Norford, 2002)).....	118
Figure 4.2: Daylighting Reference Points in the Four Perimeter Zones.....	120
Figure 4.3: Annual Energy Consumption of Five Cases to the Phoenix climate (Source: Adapted from (Caldas and Norford, 2002)).....	124
Figure 4.4: Comparison of Total Annual Energy Consumption	125
Figure 4.5: Reference Point Location Difference Causes Lighting Control Differences	126
Figure 4.6: The Energy Difference of the Five Reproduced Models	129

Figure 4.7: The Energy Difference of the Five Improved Models.....	129
Figure 4.8: Six Different Window Models with the Same Window Area (Source: (Li and Haberl, 2020)).....	132
Figure 4.9: Reference Points in Small Office Room.....	133
Figure 4.10: The DIVA Daylighting Grid and Lighting Control Setting.....	141
Figure 4.11: Illuminance Map of Six South-Facing Windows at a Solar Time 12:00 noon, July 24 in the Location of Phoenix, AZ. (Floor Visual Reflectance=0.2).....	142
Figure 4.12: Illuminance Map of Six South-Facing Windows at a Solar Time 12:00 noon, July 24 in the Location of Phoenix, AZ. (Floor visual reflectance=0.5).....	143
Figure 4.13: Illuminance Map of Six South-Facing Windows at a Solar Time 12:00 noon, July 24 in the Location of Phoenix, AZ. (Floor visual reflectance=0.9).....	144
Figure 4.14: The creation of the lighting schedule in DIVA (Solemma, n.d.-a).....	145
Figure 4.15: A sample of lighting schedule image in DIVA (Solemma, n.d.-a).....	145
Figure 4.16: Honeybee system and outputs editing in Grasshopper (Solemma, n.d.-a).....	146
Figure 4.17: Annual Lighting Electricity Use with Floor Visual Reflectance 0.2 (South Facing Window, Phoenix, AZ) (Source: (Li and Haberl, 2020)).....	150
Figure 4.18: Annual Cooling Load Use with the Floor Visual Reflectance 0.2 (South Facing Window, Phoenix, AZ) (Source: (Li and Haberl, 2020)).....	151
Figure 4.19: Annual Heating Load Use with Floor Visual Reflectance 0.2 (South Facing Window, Phoenix, AZ) (Source: (Li and Haberl, 2020)).....	152
Figure 4.20: Annual Lighting Electricity Use with Floor Visual Reflectance 0.5 (South Facing Window, Phoenix, AZ).....	153

Figure 4.21: Annual Cooling Load Use with Floor Visual Reflectance 0.5 (South Facing Window, Phoenix, AZ)	153
Figure 4.22: Annual Heating Load Use with Floor Visual Reflectance 0.5 (South Facing Window, Phoenix, AZ)	154
Figure 4.23: Annual Lighting Electricity Use with Floor Visual Reflectance 0.9 (South Facing Window, Phoenix, AZ) (Source: (Li and Haberl, 2020)).....	155
Figure 4.24: Annual Cooling Load Use with Floor Visual Reflectance 0.9 (South Facing Window, Phoenix, AZ) (Source: (Li and Haberl, 2020)).....	156
Figure 4.25: Annual Heating Load Use with Floor Visual Reflectance 0.9 (South Facing Window, Phoenix, AZ) (Source: (Li and Haberl, 2020)).....	156
Figure 4.26: Annual Lighting Energy Use with Floor Visual Reflectance 0.2 (East Facing Window, Phoenix, AZ).....	158
Figure 4.27: Annual Cooling Load Use with Floor Visual Reflectance 0.2 (East Facing Window, Phoenix, AZ).....	158
Figure 4.28: Annual Heating Load Use with Floor Visual Reflectance 0.2 (East Facing Window, Phoenix, AZ).....	159
Figure 4.29: Annual Lighting Energy Use with Floor Visual Reflectance 0.5 (East Facing Window, Phoenix, AZ).....	159
Figure 4.30: Annual Cooling Load Use with Floor Visual Reflectance 0.5 (East Facing Window, Phoenix, AZ).....	160
Figure 4.31 Annual Heating Load Use with Floor Visual Reflectance 0.5 (East Facing Window, Phoenix, AZ).....	160
Figure 4.32: Annual Lighting Energy Use with Floor Visual Reflectance 0.9 (East Facing Window, Phoenix, AZ).....	161
Figure 4.33: Annual Cooling Load Use with Floor Visual Reflectance 0.9 (East Facing Window, Phoenix, AZ).....	161
Figure 4.34 Annual Heating Load Use with Floor Visual Reflectance 0.9 (East Facing Window, Phoenix, AZ).....	162

Figure 4.35: Annual Lighting Energy Use with Floor Visual Reflectance 0.2 (North Facing Window, Phoenix, AZ)	164
Figure 4.36: Annual Cooling Load Use with Floor Visual Reflectance 0.2 (North Facing Window, Phoenix, AZ)	165
Figure 4.37: Annual Heating Load Use with Floor Visual Reflectance 0.2 (North Facing Window, Phoenix, AZ)	165
Figure 4.38: Annual Lighting Energy Use with Floor Visual Reflectance 0.5 (North Facing Window, Phoenix, AZ)	166
Figure 4.39: Annual Cooling Load Use with Floor Visual Reflectance 0.5 (North Facing Window, Phoenix, AZ)	166
Figure 4.40: Annual Heating Load Use with Floor Visual Reflectance 0.5 (North Facing Window, Phoenix, AZ)	167
Figure 4.41: Annual Lighting Energy Use with Floor Visual Reflectance 0.9 (North Facing Window, Phoenix, AZ)	167
Figure 4.42: Annual Cooling Load Use with Floor Visual Reflectance 0.9 (North Facing Window, Phoenix, AZ)	168
Figure 4.43: Annual Heating Load Use with Floor Visual Reflectance 0.9 (North Facing Window, Phoenix, AZ)	168
Figure 4.44: Annual Lighting Energy Use with Floor Visual Reflectance 0.2 (West Facing Window, Phoenix, AZ)	170
Figure 4.45: Annual Cooling Load Use with Floor Visual Reflectance 0.2 (West Facing Window, Phoenix, AZ)	170
Figure 4.46: Annual Heating Load Use with Floor Visual Reflectance 0.2 (West Facing Window, Phoenix, AZ)	171
Figure 4.47: Annual Lighting Energy Use with Floor Visual Reflectance 0.5 (West Facing Window, Phoenix, AZ)	171
Figure 4.48: Annual Cooling Load Use with Floor Visual Reflectance 0.5 (West Facing Window, Phoenix, AZ)	172
Figure 4.49: Annual Heating Load Use with Floor Visual Reflectance 0.5 (West Facing Window, Phoenix, AZ)	172

Figure 4.50: Annual Lighting Energy Use with Floor Visual Reflectance 0.9 (West Facing Window, Phoenix, AZ)	173
Figure 4.51: Annual Cooling Load Use with Floor Visual Reflectance 0.9 (West Facing Window, Phoenix, AZ)	173
Figure 4.52: Annual Heating Load Use with Floor Visual Reflectance 0.9 (West Facing Window, Phoenix, AZ)	174
Figure 5.1: Radiance Reference Rendering Settings (Source from (LBL, 2019)).....	190
Figure 5.2: The Illuminance Map of the Four Presets in DIVA.	190
Figure 5.3: Radiance Rendering Setting in DIVA for Grasshopper.	196
Figure 5.4: The Lighting Energy Changes with Different Rendering Settings.....	201
Figure 5.5: The sDA Changes with The Different Rendering Settings	202
Figure 5.6: Window Positions.....	204
Figure 5.7: Window Shade Examples	205
Figure 5.8: Lighting Energy Use in the Small Size Office	207
Figure 5.9: Lighting Energy Use in the Medium Size Office	207
Figure 5.10: The sDA Correlation Between the sDA_custom and the sDA_high in Categories: Small size office and Medium size office	208
Figure 5.11: The sDA Correlation between the sDA_custom and the sDA_high in Categories: No Shades, Dark Shades, and White Shades	209
Figure 5.12: The Final True Runs (Purple) Used to Find the sDA Correlation between the sDA_custom and the sDA_high.....	210
Figure 5.13: Actual Data by Predicted Data Plot	216
Figure 5.14: Window Design Generator in Grasshopper (Rutten, 2014).....	218

Figure 5.15: Window Parameters on Surface.....	218
Figure 5.16: Overlapped Windows Change to a Boolean Union Window.....	220
Figure 5.17: The Genes Used for Selecting	223
Figure 5.18: The Objectives of Optimization.....	224
Figure 5.19: Shading Device for South-Oriented Window.....	225
Figure 5.20: Generation 1.....	226
Figure 5.21: Generation 5 (Brown Points are Generation 5; The Green Points are the Previous Generations).....	227
Figure 5.22: Generation 10 (Brown Points are Generation 10; The Green Points are the Previous Generations).....	227
Figure 5.23: Generation 15 (Brown Points are Generation 15; The Green Points are the Previous Generations).....	228
Figure 5.24: Generation 20 (Brown Points are Generation 20; The Green Points are the Previous Generations).....	228
Figure 5.25: Generation 25 (Brown Points are Generation 25; The Green Points are the Previous Generations).....	229
Figure 5.26: Generation 30 (Brown Points are the Generation 30; The Green Points are the Previous Generations).....	229
Figure 5.27: Generation 35 (Brown Points are Generation 35; The Green Points are the Previous Generations).....	230
Figure 5.28: Generation 40 (Brown Points are Generation 40; The Green Points are the Previous Generations).....	230
Figure 5.29: Shading Device for East-Oriented Windows.....	236
Figure 5.30: 40 Generation Results of East-Facing Window Designs.....	237
Figure 5.31: 40 Generation Results of West-Facing Window Designs.	240
Figure 5.32: 40 Generation Results of North-Facing Window Designs	243

LIST OF TABLES

	Page
Table 2-1 CIE 15 Sky Model (Darula and Kittler, 2002).....	10
Table 2-2 Glare Prediction Value (color) Assignments Used in All Visualizations (Jakubiec and Reinhart, 2012)	13
Table 2-3 The ASHRAE Comfort Scale (ASHRAE, 2004)	17
Table 2-4 The Comparison of Different Simulation Tools/Platform (Kota, 2020).....	40
Table 2-5 Coupled Simulation Methods	46
Table 4-1: Empirically Determined Office Building Parameters in the Caldas Model	119
Table 4-2: Parameter Change List.....	121
Table 4-3: Simulation Procedure for the Office Model	122
Table 4-4: The Parameter changes in order to test the window design strategies.....	128
Table 4-5: The small size office model dimension	131
Table 4-6: The Construction Material Values in DOE-2 and EnergyPlus.....	134
Table 4-7: Selected Target Windows from DOE-2 library (Winkelmann et al., 1993b)	135
Table 4-8: Simulation window output parameters	136
Table 4-9: The input parameters and output in DOE-2 and EnergyPlus.....	137
Table 4-10: Simulation results in Cooling Load Energy and Heating Load Energy.....	138
Table 4-11: The input parameters and output of the office building (Source: (Li and Haberl, 2020)).....	139

Table 4-12: The Simulation Runtimes of Different Simulation Methods	147
Table 4-13: sDA and ASE with Floor Visual Reflectance 0.2 (South-Facing Window, Phoenix, AZ).....	178
Table 4-14: sDA and ASE with Floor Visual Reflectance 0.5 (South-Facing Window, Phoenix, AZ).....	179
Table 4-15: sDA and ASE with Floor Visual Reflectance 0.9 (South-Facing Window, Phoenix, AZ).....	179
Table 4-16: sDA and ASE with Floor Visual Reflectance 0.2 (East-Facing Window, Phoenix, AZ)	179
Table 4-17: sDA and ASE with Floor Visual Reflectance 0.5 (East-Facing Window, Phoenix, AZ)	179
Table 4-18: sDA and ASE with Floor Visual Reflectance 0.9 (East-Facing Window, Phoenix, AZ)	179
Table 4-19: sDA and ASE with Floor Visual Reflectance 0.2 (North-Facing Window, Phoenix, AZ).....	180
Table 4-20: sDA and ASE with Floor Visual Reflectance 0.5 (North-Facing Window, Phoenix, AZ).....	180
Table 4-21: sDA and ASE with Floor Visual Reflectance 0.9 (North-Facing Window, Phoenix, AZ).....	180
Table 4-22: sDA and ASE with Floor Visual Reflectance 0.2 (West Facing Window, Phoenix, AZ)	181
Table 4-23: sDA and ASE with Floor Visual Reflectance 0.5 (West Facing Window, Phoenix, AZ)	181
Table 4-24: sDA and ASE with Floor Visual Reflectance 0.9 (West Facing Window, Phoenix, AZ)	181
Table 4-25: The Lighting Energy Difference between EnergyPlus+Radiance and EnergyPlus+Split-Flux/Radiosity.....	186
Table 5-1: The Daylighting Simulation Runtimes and Results with Different Simulation Programs.....	192

Table 5-2: Model Parameters in Daylighting Simulation	194
Table 5-3: Daylighting Simulation Results with Different Grid Spacing in the Room Condition of No Shades with a Dark Floor.....	195
Table 5-4: Daylighting Simulation Results with Different Grid Spacings with the Room Condition of Shades with a Bright Floor	195
Table 5-5: Daylighting Simulation Results with Different Grid Spacings with the Room Condition of Shades with a Dark Floor.....	195
Table 5-6: DIVA presets of the Radiance Rendering Parameters (Solemma, n.d.).....	197
Table 5-7: Daylighting Results of Different Preset of Radiance Rendering.....	200
Table 5-8: The daylighting simulation parameters and variables	205
Table 5-9: Independent Variables	212
Table 5-10: Parameter Estimates of Single Variable	213
Table 5-11: Minimum AICc Stepwise Regression Results.....	213
Table 5-12: Associations Between Y Response and Variables from the Multiple Regression Model.....	215
Table 5-13: Summary of fit.....	215
Table 5-14: The Input Parameters and Output Setting for Simualtion.....	222
Table 5-15: Optimal Designs of South-Facing Windows	232
Table 5-16: The Optimal Designs of East-Facing Windows	238
Table 5-17: The Optimal Designs of West-Facing Windows.....	241
Table 5-18: The Optimal Designs of West-Facing Windows.....	244
Table A-1: The Simulation Results of Different Model Conditions.....	290
Table A-2: Statistical Analysis and Predicted Results	296

1. INTRODUCTION

1.1. Background

Currently, about 40% of the world's source energy is consumed in buildings (UNEP, 2016). Since this represents a significant amount of the world's energy use, energy efficiency, the use of renewable energy, and even net-zero buildings have become important trends in architectural design. During the design process, many factors are involved in and affect the quality of the architectural design, which will ultimately affect the energy consumption of the building once it is built. Unfortunately, the dynamic interaction between the architectural design features, climate, daylighting, thermal performance, and lighting systems in a building is a complex process. To fully understand the performance of integrated daylighting and thermal analysis, the simulation tools used in daylighting and thermal analysis should be combined during the analysis process.

In the past, there have been attempts to integrate thermal and daylighting simulation tools to achieve a combined simulation. Unfortunately, such combined methods may not provide the same result as the single-purpose tools, which are run independently. Therefore, the success of an architecture design that uses a combined daylighting and thermal simulation depends heavily on the analysis of the daylighting and efficient envelope strategies a designer chooses to use. Previously, it was hypothesized that better informed design decisions would create optimal design that consists of more comfortable living and working environments, which would reduce the

energy usage for lighting, cooling and heating (An and Mason, 2010). Therefore, the use of a combined Building Energy Simulation and DayLighting (BES/DL) analysis tools must first consider whether or not the tool is accurately modeling the daylighting and thermal envelope design strategies before results are fed to design optimization routines.

There are several combined simulation tools in the U.S. that can both simulate the daylighting and thermal performance to analyze the impact of both on the annual energy performance of a building, such as: DOE2.1e (Winkelmann, 1983); eQuest (Hirsch, 2006, 2017), and EnergyPlus (Crawley et al., 2000). However, the daylighting calculation methods they employ may not represent the most accurate methods. For example, DOE2.1e and eQUEST (DOE-2.2) use limited sky models (i.e., only two sky models: the CIE overcast and clear sky models) and employ the split-flux method calculation to calculate the Internal Reflected Component (IRC) that predicts the illumination levels at two points in one zone for limited room configurations.

In contrast, EnergyPlus offers four different sky models (i.e., clear, clear turbid, intermediate and overcast), and the Split-flux and Radiosity methods for calculating the IRC. Therefore, the use of EnergyPlus for daylighting simulation was only a modest improvement over the accuracy available with DOE2.1e/eQuest. This is because the radiosity method underpredicts the daylight harvesting potential as distance increases away from the window, and it also cannot model specular reflection effectively (Tsangrassoulis and Bourdakis, 2003). More accurate tools that perform only daylighting simulation, such as RADIANCE (Reinhart and Herkel, 2000) and DAYSIM (Reinhart, 2010; Reinhart, 2017) use the backward ray-tracing method to calculate the internal

reflection, which can calculate more accurate daylighting simulation results for more configurations and can simulate more complicated shading devices. However, they cannot directly simulate the impact of daylight on a building's thermal energy consumption nor can they directly calculate the thermal comfort of a space.

There have been previous attempts to link the thermal and daylighting simulation tools to achieve better results. Such a combined method would be an improvement for evaluating changes in designs versus methods that use several special purpose tools that require passing results back-and-forth between tools. For example, the study by Koti and Addison (2007) demonstrated improved results by linking the DOE2.1e thermal energy simulation and the DAYSIM daylighting simulation versus what could be obtained by only using DOE2.1e. The method they developed showed lower energy savings when the DAYSIM daylighting results were used instead of using the DOE2.1e daylighting results for selected daylighting strategies. In another study, An and Mason (2010) integrated eQUEST and DAYSIM. Their study showed that the combined simulation had higher energy savings than those simulated by DOE-2.2 using only the split-flux method. Since these combined simulation methods showed an differences in the simulated performance, there is a significant motivation to use combined simulation methods to analyze the thermal performance of buildings incorporating daylighting strategies.

In another of the previous studies, Caldas and Norford (2002) used Genetic Algorithms (GAs) (Goldberg, 1989) combined with the DOE2.1e simulation program for the combined thermal and daylighting analysis within DOE2.1e to inform the

architectural design practice. In this analysis, feedback loops between the architecture design decisions and the environmental impact (i.e., energy consumption) were used to provide information about the performance changes of the specific designs. However, there were limitations in the simulation process used in this study that were not fully explained. First was the fact that all the windows in the simulations were centered in the middle of each façade, which does not reflect all types of daylighting strategies related to window locations. Second, no supporting documentation was provided to help the reader with details about the simulations (e.g., the placement of the daylight sensors within the zone, simulation inputs etc.). Therefore, there is a need to reinvestigate the daylighting strategies in this research using a more sophisticated daylighting analysis that can analyze off-center placement of fenestration, and advanced daylighting strategies such as light-shelves.

In summary, although the previous literatures have used combined daylighting and thermal simulation methods to analyze the daylighting impact on the building energy usage, the data exchange between the different simulation programs was not fully automatic, nor was it well-documented in all cases. In addition, combined simulation methods were seldom used by the previous studies to develop the optimal design decisions that included daylighting strategies. Therefore, there is a need to further analyze and classify the capabilities of different design simulation tools to obtain improved building energy simulation methods that adequately address daylighting. To accomplish this, improved, combined simulation programs will be used to analyze building façade design strategies to provide improved guidance to architects to help

them select the best combinations of architectural features (i.e., building shape, size, orientation, window placement, daylighting, utilization, heating/cooling loads, etc.).

1.2. Purpose and Objectives

The purpose of this study is to better inform the building façade design process in the preliminary design stage for improving building performance.

The following objectives are proposed to accomplish this purpose:

- 1) Find and test the most accurate simulation methods to evaluate the coupled daylighting and thermal performance of window size and placement.
- 2) Reproduce the Caldas office model to better understand how to build an improved simulation model.
- 3) Develop an improved Radiance annual daylighting simulation method that produces acceptable results while minimizing run time.
- 4) Using the Multi-Objective Optimization to determine the best window size and placement design for North, South, East, and West orientations.
- 5) Develop a new prototype to guide architects/engineers about the proper window size and placement on a façade based on indoor visual comfort and annual energy consumption.

1.3. Significance and Limitations

Significance of the Study:

- 1) This work is significant because it resolved the issues of Radiance, and

proposed an improved annual daylighting simulation method in optimization.

- 2) This work is significant because it used sophisticated daylighting and thermal simulations to better analyze optimal building façade design strategies to provide improved guidance to architects to help them better select the best combination of architectural features.
- 3) This work is significant because it created a command to automatically select the window size and placement in Grasshopper using Python scripts.
- 4) This work is significant because it analyzed the proper placement of a window within the wall, and it also analyze the daylighting and thermal performance compared to the acceptable visual and thermal comfort levels.

The following are the limitations of the study:

- 1) There are many types of commercial, classrooms, and residential buildings. However, for the present study, only office buildings will be studied with their operation times that coincide with the available of daylighting.
- 2) There are many types of daylighting strategies available for office buildings. For this study, only few predominantly used strategies will be selected, and will be studied, such as window size, window placement, and shading.
- 3) The study will primarily analyze different daylighting systems. Interaction with HVAC system will not be considered.
- 4) The study of the Complex Fenestration Systems (CFSs) and dynamic shading will not be considered for the present study, since the development of custom scripting and use of BSDF which is beyond the scope of the present study.

1.4. Organization of the Dissertation

This dissertation is organized as follows:

In Chapter 1, the study background is provided as well as the study purpose and objectives, followed by the study significance and the limitations.

In Chapter 2, a comprehensive literature review was performed, covering the history of thermal and daylighting simulation methods, thermal and visual comfort, simulation tools, optimization techniques for building simulation, and design strategies.

In Chapter 3, the research methodology is presented. The methodology is composed of five tasks: 1) reproduce the office models used by Caldas and Norford (2002) to build an improved office model used in their study; 2) Develop and test a prototype for the combined daylighting + thermal simulation; 3) develop an improved Radiance annual daylighting simulation method that produces acceptable results while minimizing run time; 4) develop a window design plugin in grasshopper using Python script; 5) apply window design plugin in parametric modeling with Multi-Objective Optimization for window size and placement to determine the best design for North, South, East, and West orientations.

In Chapter 4, the results of the combining daylighting and thermal simulation are shown. Part I of this chapter illustrate how to build the simulation model. Part II proposed a prototype for the daylighting and thermal simulation process. Part III shows the summary of the findings.

In Chapter 5, this chapter shows the results of parametric analysis. Part I develop an improved Radiance daylighting simulation method for optimization. Part II create a

window size and placement design plugin in Grasshopper. Part III illustrate the window design optimization process and results for an office model. Part IV shows the summary of the findings.

Chapter 6, results, summary, and conclusions are provided from the study and the potential future work is discussed.

2. LITERATURE REVIEW

2.1. Overview

The categories of the previous literature that are the most relevant to this dissertation are:

1) daylighting sky models, 2) performance indicators, 3) daylighting simulation methods, 4) building simulation tools, 5) coupled simulation tools (i.e., integrated BES and Daylighting Simulation: BES/DL), 6) optimization tools, 7) building design strategies, 8) applications of optimization tools, 9) predictions of indoor thermal comfort, and 10) predictions of visual comfort.

The sources of literature reviewed include journals (e.g., ASHRAE Transactions, ASHRAE Science and Technology for the Built Environment Journal, Journal of Building Performance Simulation, Building and Environment, Energy and Buildings, Solar Energy, Building Simulation, LEUKOS and the Lighting Research & Technology Journal); conference proceedings (ASHRAE, ACEEE, IES, IBPSA, ASHRAE Simbuild and SIGGRAPH); ASHRAE Handbooks (ASHRAE, 2017a); building energy codes ASHRAE Standard 90.1 (ASHRAE, 2016), and the IES Lighting Handbook 10th Edition (DiLaura et al., 2011).

2.2. Sky Models

Sky models are used to generate numerical sky brightness patterns from measured solar radiation quantities. Over the years a number of models have been developed that vary in complexity and accuracy, including Clear Sky, Overcast Sky, Uniform Sky, and Intermediate sky models. Moon and Spencer (1942) was one of the earliest studies that proposed a luminance distribution model for an overcast sky. This

model was later recommended as the CIE Standard Overcast Sky model (CIE, 1995). Later, Kittler (1967) proposed a luminance distribution model for clear sky condition. Kittler's clear sky model was then recommended as the CIE Standard Clear Sky model (CIE, 1973). In addition, Kittler et al. (1997) classified sky conditions into 15 categories (Table 2.1), and proposed numerical equations for the 15 sky luminance distributions, which were also later recommended as the CIE Standard General Sky (CIE, 2003)

Table 2-1 CIE 15 Sky Model (Darula and Kittler, 2002)

Typ e	Grad ation	Indik atrix	a	b	c	d	e	Description of luminance distribution
1	I	1	4	-0.7	0	-1	0	CIE Standard Overcast Sky, alternative form Steep luminance gradation towards zenith, azimuthal
2	I	2	4	-0.7	2	-1.5	0.15	Overcast, with steep luminance gradation and slight brightening
3	II	1	1.1	-0.8	0	-1	0	Overcast, moderately graded with azimuthal uniformity
4	II	2	1.1	-0.8	2	-1.5	0.15	Overcast, moderately graded and slight brightening towards the sun
5	III	1	0	-1	0	-1	0	Sky of uniform luminance
6	III	2	0	-1	2	-1.5	0.15	Partly cloudy sky, no gradation towards zenith, slight brightening
7	III	3	0	-1	5	-2.5	0.3	Partly cloudy sky, no gradation towards zenith, brighter circumsolar
8	III	4	0	-1	10	-3	0.45	Partly cloudy sky, no gradation towards zenith, distinct solar corona
9	IV	2	-1	-0.55	2	-1.5	0.15	Partly cloudy, with the obscured sun
10	IV	3	-1	-0.55	5	-2.5	0.3	Partly cloudy, with brighter circumsolar region
11	IV	4	-1	-0.55	10	-3	0.45	White-blue sky with distinct solar
12	V	4	-1	-0.32	10	-3	0.45	CIE Standard Clear Sky, low illuminance turbidity
13	V	5	-1	-0.32	16	-3	0.3	CIE Standard Clear Sky, polluted atmosphere
14	VI	5	-1	-0.15	16	-3	0.3	Cloudless turbid sky with broad solar corona
15	VI	6	-1	-0.15	24	-2.8	0.15	White-blue turbid sky with broad solar corona

Later, in 1990s, the Perez All-Weather Sky Model (Perez et al., 1993) became the most popular model in daylighting simulation because it yielded the most accurate results. Perez All-Weather Sky Model is a mathematical model that is used to describe the relative luminance distribution of the sky dome using measured data gathered from weather stations all over the world. This sky model is an all-weather sky model, which includes overcast, clear, and partly cloudy. It is also the model LEED requires to be used for daylighting predictions (USGBC, 2014). The Perez sky models are also used in the RADIANCE program (Ward, 1996), the DAYSIM program (Reinhart, 2010; Reinhart, 2017), and the DIVA program (Reinhart et al., 2011)

2.3. Building Performance

To ensure a healthy indoor environment for building occupants, the building indoor environment must be carefully monitored to provide the desired thermal and visual conditions. Therefore, in order to improve a building's performance, the visual and thermal comfort of the space must be carefully considered. To accomplish this, Daylight Performance Indicators and Thermal Comfort Indicators provide information on how a building is performing in terms of visual and thermal comfort. Over the years, many indicators have been developed to quantify the daylighting and thermal performance of buildings.

2.3.1. Visual Comfort

The use of daylighting to enhance the Indoor Environment Quality (IEQ) and

reduce the energy consumption is one of the most effective strategies available to design high performance buildings. Daylighting technologies are usually aimed at balancing daylight transmission for energy and visual comfort. The visual comfort evaluates indicators include Daylighting Performance Indicators and Glare Indices.

2.3.1.1. Daylighting Performance Indicators

Daylight performance indicators evaluate the effectiveness of daylighting design on a building. There are five indicators that are commonly used to quantify the daylighting performance of a building, which are: the Daylight Factor (DF) (Trotter, 1911), the Daylight Autonomy (DA) (Reinhart et al., 2006), the Useful Daylight Illuminance (UDI) (Nabil and Mardaljevic, 2005), the Spatial Daylight Autonomy (sDA) (IESNA, 2012), and the Annual Sun Exposure (ASE) (IESNA, 2012).

The DF is the ratio of internal illuminance to external horizontal illuminance under an overcast sky defined by the CIE luminance distribution (CIE, 2003). The DA is the percentage of working hours when a minimum work plane illuminance is maintained by daylight alone (Reinhart et al., 2006). The UDI is a dynamic daylight performance measure that determines when daylight levels are useful for the occupant(s) (i.e., neither too dark (<100 lux) nor too bright (>2,000 lux)) (Nabil and Mardaljevic, 2005).

Recently, dynamic daylighting metrics (sDA+ASE) (IESNA, 2012) were introduced that are location-based because they use measured weather data and annualize the performance over the entire year. The dynamic daylighting metrics includes the Spatial Daylight Autonomy (sDA) index and the Annual Sun Exposure (ASE) index. The sDA index describes how much of a space receives sufficient daylight.

Specifically, it describes the percentage of floor area that receives at least 300 lux for at least 50% of the annual occupied hours. The ASE index describes how much of a space receives too much direct sunlight, which can cause visual discomfort (glare) or an increase in cooling loads. Specifically, the ASE measures the percentage of floor area that receives at least 1,000 lux for at least 250 occupied hours per year. The USGBC has codified these two metrics (i.e., sDA and ASE) in LEED v4 (USGBC, 2014). In order to obtain the LEED points for daylighting, interior spaces should achieve a Spatial Daylight Autonomy index (sDA 300 lux / 50% of the annual occupied hours) of 55% (2pts) or 75% (3pts) with an Annual Sunlight Exposure index (ASE_{1000lx, 250h}) below 10% in all regularly occupied floor areas.

2.3.1.2. Glare Indices

For the glare indices, there are five matrices that have been developed to evaluate lighting glare including: The Daylight Glare Index (DGI), the Visual Comfort Probability (VCP), the CIE Glare Index (CGI), the CIE Unified Glare Rating system (UGR), and the Discomfort Glare Probability (DGP). Glare Assessment scale according to glare index value range shown in Table 2.2. The glare classified four levels, which is imperceptible glare, perceptible glare, disturbing glare, and intolerable glare.

Table 2-2 Glare Prediction Value (color) Assignments Used in All Visualizations (Jakubiec and Reinhart, 2012)

Discomfort Classification	Color	Glare Value Range				
		DGI	VCP	CGI	UGR	DGP
Imperceptible Glare	GREEN	<18	80-100	<13	<13	<0.35
Perceptible Glare	YELLOW	18-24	60-80	13-22	13-22	0.35-0.40
Disturbing Glare	ORANGE	24-31	40-60	22-28	22-28	0.4-0.45
Intolerable Glare	RED	>31	<40	>28	>28	>0.45

2.3.1.2.1. The Daylight Glare Index (DGI)

DGI was developed by Hopkinson (Hopkinson, 1972). The DGI predicts glare from a large glare source: the sky viewed through a window. The New Daylight Glare Index (DGIN), developed by Nazzal (Nazzal, 2001), is a modification of Hopkinson's original equation (Hopkinson, 1972).

2.3.1.2.2. The Visual Comfort Probability (VCP)

VCP (IESNA, 1993) is an estimate of the percentage of people who do not find a lighting system uncomfortable from a glare perspective, and therefore is expressed as a number between 0 and 100 (Mistrick and An-Seop, 1999). The VCP is only valid for typically-sized luminaire sources, it cannot be used for the evaluation of daylight conditions, metal halide fixtures, incandescent, or small compact fluorescent downlights (Jakubiec and Reinhart, 2012).

2.3.1.2.3. The CIE Glare Index (CGI)

CGI was an attempt by Einhorn to develop a formula that takes into account all the peer-reviewed glare research in order to be used as a standard glare index adopted by the CIE (Einhorn, 1979). The CGI calculations require both direct and diffuse illuminance.

2.3.1.2.4. The CIE Unified Glare Rating system (UGR)

UGR (Akashi et al., 1996) was developed by the International Commission on Illumination, CIE, for applications of interior lighting. UGR is based on a measurement of the luminance of a fixture for a specified line of sight.

2.3.1.2.5. The Discomfort Glare Probability (DGP)

DGP (Wienold and Christoffersen, 2006) can evaluate direct sunlight falling on a work-plane as a glare source (Jakubiec and Reinhart, 2012). The DGP is the evaluation of glare, which considers the largest number of factors that contribute to discomfort.

The previous studies introduced many tools to evaluate the glare indices (i.e., DGI, VCP, CGI, UGR, and DGP) to prevent the problem of indoor glare. One of the most popular tools is Evalglare (Wienold, 2004), which was created to assess the glare potential in an interior space.

Evalglare (Wienold, 2004) is a glare assessment tool developed to evaluate glare problems due to daylight in an space. Evalglare detects glare sources in a ± 180 degree fish-eye scene, and evaluates the anticipated magnitude of the glare source. The algorithm in evalglare is based on an empirical study of over 100 test subjects in a controlled office setting who rated whether or not they experienced glare under different conditions, and rated the magnitude of the glare experience (An and Mason, 2010). Evalglare software can calculate DGP (Daylight Glare Probability), DGI (Daylight Glare Index), UGR (Unified Glare Rating), VCP (Visual Comfort Probability), and CGI (CIE Glare Index).

An and Mason (2010) used Evalglare to estimate the glare potential in an office building. In this study, they evaluated a daylight design for overall glare risk in a space over the course of one year. However, it is extremely difficult to conduct an hourly glare assessment over an entire year due to the time and cost required to conduct such a study. Therefore, in this study, two weeks in each month were used, where every other day was

selected for the assessment. Their results showed that in a West office, from September to April, there was disturbing or intolerable glare that occurred in the mid-afternoon. During the remainder of the time, the glare conditions were imperceptible.

Yun et al. (Yun et al., 2014) analyzed visual comfort and energy savings in an office building. They evaluated visual environmental comfort using a quantitative criterion (illuminance) and a qualitative criterion (glare index) in daylighting. In their study, they used HDR¹ images that captured the actual scene and the simulation tool DIVA-for-Rhino (Solemma, n.d.-a) in the Evalglare tool for glare evaluation. In their study, the simulation tool was validated by comparing measured data from a mock-up room and a scale model. In the study, the EnergyPlus program was used to calculate the annual energy consumption. The study suggested lighting and shading control strategies for visual comfort and building energy savings.

2.3.2. Thermal Comfort

Thermal comfort conditions in a room usually require measuring indoor air temperature, inner surface temperatures, indoor humidity, and airflow within the room. Achieving thermal comfort means providing an indoor climate that building occupants will find thermally comfortable. The ASHRAE Standard 55 determined the desired indoor thermal conditions of a room with respect to the room's function, the properties

¹ High Dynamic Range (HDR) is a dynamic range higher than what is considered to be standard dynamic range. High-Dynamic-Range Imaging (HDRI) is the compositing and tone-mapping of images to extend the dynamic range beyond the native capability of the capturing device ("HDR", 2017).

of the user, and the activity level for which the room will be used (ASHRAE, 1981, 2010, 2013, 2017b).

2.3.2.1. Conventional Thermal Comfort Indicators

Common applications of thermal comfort indicators include: the Predicted Mean Vote (PMV) index (Fanger, 1970), the Predicted Percent Dissatisfied (PPD) index (Fanger, 1970), and the Standard Effective Temperature (SET) (Gagge et al., 1986). Fanger's (1970) PMV index was defined in terms of the heat load that would be required to restore a state of "Comfort" as evaluated by his Comfort Equation.

ISO 7730 (ISO, 1994) uses the Fanger (1970) PMV formula to predict a numerical value for the mean subjective response to the thermal environment on the ASHRAE standard 55 scale (ASHRAE, 2004) (Table 2.3) using six thermal variables. Fanger (Fanger, 1986) related the PPD to the PMV: A PPD of 10% corresponds to the PMV range of ± 0.5 . It should be noted that even with $PMV = 0$, about 5% of the people are dissatisfied when average air speeds do not exceed 0.2 m/s. In general, the PMV-PPD model is widely used and accepted for design and field assessment of comfort conditions. For example, ASHRAE Standard 55 (ASHRAE, 2013, 2017b) and ISO standard 7730 (ISO, 2005). ISO Standard 7730 includes a short computer program that facilitates the calculation of the PMV and PPD for a wide range of parameters.

Table 2-3 The ASHRAE Comfort Scale (ASHRAE, 2004)

	Hot	Warm	Slightly warm	Neutral	Slightly cool	Cool	Cold
Numerical value	3	2	1	0	-1	-2	-3

The SET* is defined as the equivalent air temperature of an isothermal environment at 50% RH in which a subject, wearing clothing that is standardized for the

activity concerned. The SET has the same heat stress (i.e., skin temperature, t_{sk}) and thermoregulatory strain (i.e., skin wettedness, w) as was observed in the actual environment (ASHRAE, 2013, 2017b).

Finally, Building Energy Simulation (BES) often uses conventional thermal comfort theories to make decisions based on simulated indoor temperatures. Unfortunately, the conventional calculation of thermal comfort was set-up based on steady-state laboratory experiments, which may not represent real situations in buildings. For example, the PMV model works well in air-conditioned space. However, it does not provide useful results in naturally ventilated buildings because it was developed using principles of heat balance and experimental data collected in a controlled climate chamber under steady-state conditions (Fanger, 1970). In addition, the PMV tends to over-predict the subjective warmth in the built environment, especially in warmer climates (Yang et al., 2014).

2.3.2.2. Adaptive Thermal Comfort Models

Adaptive thermal comfort models (Moossavi, 2014; Oseland, 1998) mentioned a connection to the outdoors, which means people can control their immediate environment, allows them to adapt to a wider range of thermal conditions than are generally considered comfortable. The adaptive thermal comfort model was developed based on hundreds of field studies with occupants that thermal comfort dynamically interacts with their environment. Therefore, adaptive thermal comfort has a broader human comfort zone than the conventional thermal comfort. In addition, adaptive adjustments are typically conscious actions by the occupant such as altering clothing,

posture, activity schedules or levels, rate of working, diet, ventilation, air movement, and local temperature (Moossavi, 2014).

Using field studies that were performed on naturally ventilated and air-conditioned buildings, two adaptive thermal comfort standards have been developed: the American ASHRAE Standard 55-2017 (ASHRAE, 2017b) and the European EN15251 Standard (CEN, 2007).

2.3.2.2.1. ASHRAE Standard 55-2013,2017

ASHRAE conducted 21,000 measurements around the world, primarily in office buildings, and proposed an optional method for determining acceptable thermal conditions in naturally-conditioned spaces (ASHRAE, 2013, 2017b). In the latest published version, ASHRAE Standard 55-2017 adopted a prevailing mean outdoor air temperature ($T_{pma(out)}$), with an extended upper 80% acceptability limit based on higher air speed values (above 0.30 until 1.2 m/s). This method introduced the following equation:

$$\text{Upper 80\% acceptability limit } T_{CO} = 0.31 * T_{pma(out)} + 21.3 \text{ }^{\circ}\text{C} \quad \text{Equation 2-1}$$

$$\text{Lower 80\% acceptability limit } T_{CO} = 0.31 * T_{pma(out)} + 14.3 \text{ }^{\circ}\text{C} \quad \text{Equation 2-2}$$

Where

T_{CO} is the comfort temperatures.

$T_{pma(out)}$ is the prevailing mean outdoor air temperature (for a time period between last 7 and 30 days before the day in question (ASHRAE, 2013, 2017b).

2.3.2.2.2. EN15251

The EN15251 Standard (CEN, 2007) was based on the Smart Control And

Thermal comfort project (SCATs), commissioned by the European Commission. In this project, 26 European buildings in France, Greece, Portugal, Sweden and the UK were surveyed for three years covering free-running, conditioned and mixed-mode buildings (McCartney and Fergus Nicol, 2002). In 2007, the European Committee for Standardisation (CEN) released Standard EN15251:2007 (CEN, 2007) with the following equation for naturally ventilated buildings:

$$T_{CO} = 0.33 * T_{rm7} + 18.8 \text{ }^{\circ}\text{C} \quad \text{Equation 2-3}$$

Where

T_{CO} is the comfort temperatures.

T_{rm7} is the exponentially weighted running mean of the daily outdoor temperature of the previous seven days.

From Equation 2-3, the Adaptive Thermal Comfort (ATC) model (CEN, 2007) uses a comfortable operative temperature that is a function of the running mean outdoor air temperature. In this model, the upper limit for thermal comfort is not a fixed temperature, but a variable temperature that depends on recent outdoor temperatures.

2.3.3. Summary

In this section, the Daylighting Performance Indicator, Glare Indices, and Thermal Performance Indicators have been reviewed. The Daylighting Performance Indicators include: DF, DA, UDI, and aDA + ASE. A review of the literature showed the sDA+ASE indexes were seldom used to evaluate the daylighting environment in design strategies. For Glare Indices, the DGI, VCP, CGI, UGR, and DGP have been compared.

In addition, there are previous studies that showed how to use software to evaluate the glare value range to classify the visual discomfort level. Therefore, for a thermal performance analysis, this study will use the conventional thermal comfort indices (i.e., PMV and PPD), as well as adaptive thermal comfort model (i.e., ASHRAE Standard 55-2017 and European Standard EN15251).

However, in the previous studies that evaluated the daylighting strategies, such as Caldas' study (Caldas and Norford, 2002), the thermal and visual comfort were not been take an into account for the optimal design. The literature showed the use of sDA+ASE indicators and glare matrices provide an accurate criterion to evaluate the daylighting performance. In addition, the use of the adaptive thermal comfort model suggests a more sophisticate method to evaluate the indoor thermal environment. Therefore, there is a need to design high performance buildings that utilize daylighting strategies with a consideration of visual and thermal comfort.

2.4. Daylighting Calculation Methods

Daylighting calculation methods can be broadly classified into two types, Daylight Factor (DF) methods (Hopkinson et al., 1966) and Daylight Coefficient (DC) methods (Tregenza and Waters, 1983). Almost all the methods and tools used today use either the DF concept or the DC concept.

2.4.1. Daylight Factor Methods (DF)

The Daylight Factor (DF) is the ratio of internal illuminance to external

horizontal illuminance under an overcast sky defined by the CIE luminance distribution (Hopkinson et al., 1966). The daylight factor methods used in daylighting simulation are the amount of daylight reaching a point on a surface that is split into three components: The Sky Component, the External Reflected Component (ERC), and the Internal Reflected Component (IRC) (Figure 2.1). Depending on the method used to calculate the Internal Reflected Component (IRC), these methods can be represented in two categories: The Split-Flux Method and the Radiosity Method.

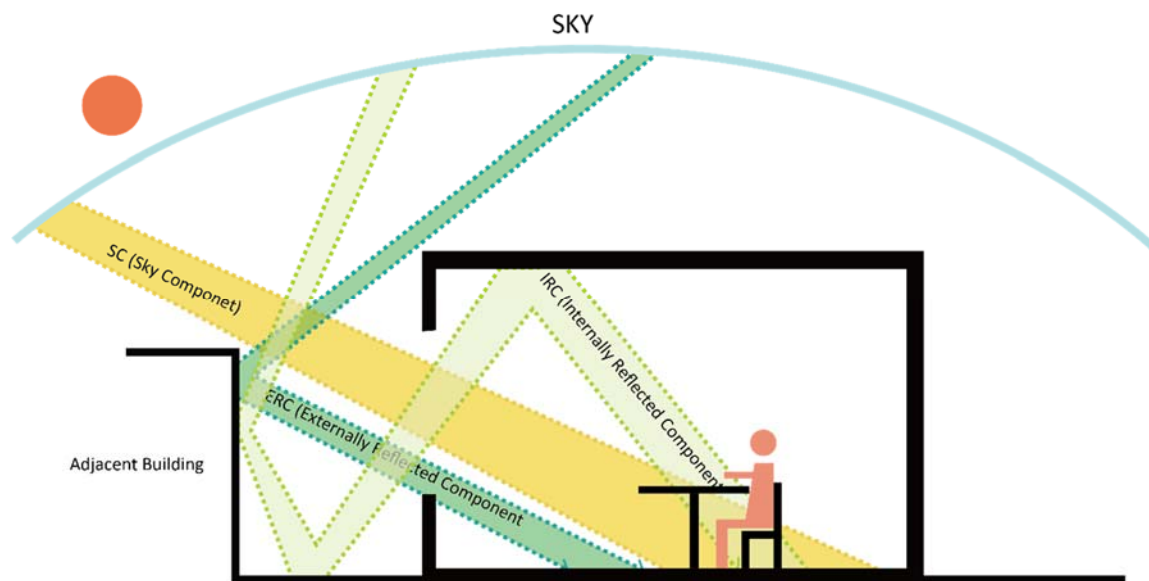


Figure 2.1 Different Components of Daylight Calculation (Source: Adapted from (Gharpedia, 2017))

2.4.1.1. Split-flux method

The split-flux method (Hopkinson et al., 1954) is an empirical formula for calculating the Internal Reflected Component (IRC). The split-flux method assumes that the luminous flux entering the room through a window is calculated in two parts. The first part is the flux coming down from the sky and any external obstructions above an

imaginary plane that is at the center of the window. The second portion is the luminous flux coming up from the ground and any external obstructions falling below the imaginary plane.

The limitation of split-flux method are: 1) The method only works well for square or rectangle-type shaped rooms; 2) The method cannot simulate complex daylighting strategies, such as: light shelves or reflective overhangs (Baker and Salem, 1990); 3) Since the split-flux method assumes perfectly diffuse interior surfaces with no internal obstructions, it over-predicts the internally reflected illuminance near the back of the rooms (Winkelmann and Selkowitz, 1985). Tools like DOE-2 (Winkelmann, 1983; Winkelmann and Selkowitz, 1985), eQuest (Hirsch, 2006, 2017), EnergyPlus (Crawley et al., 2000) and ECOTECT (Marsh, 2003; Marsh, 1997) currently use the Split-Flex Method.

2.4.1.2. Radiosity Method

The Radiosity method divides an interior space into a mesh of patches. Each patch is considered as a Lambertian reflector², which gives the surface a constant luminance that reflects the luminous flux according to Lambert's cosine law³ (Tsangrassoulis and Santamouris, 1997). Thus, each patch receives, absorbs, and reflects

² Lambertian Reflectance is the property that defines an ideal "matte" or diffusely reflecting surface. The apparent brightness of a Lambertian surface to an observer is the same regardless of the observer's angle of view ("Lambertian Reflectance", n.d.).

³ Lambert's Cosine Law says that the radiant intensity or luminous intensity observed from an ideal diffusely reflecting surface or ideal diffuse radiator is directly proportional to the cosine of the angle θ between the direction of the incident light and the surface normal ("Lambert's Cosine Law", n.d.).

flux back into a space. This process is iterative until all reflected flux has been absorbed (Tsangrassoulis and Santamouris, 1997). However, one of the most difficult tasks in this method is to calculate the view factors between different patches. Since view factors have to be stored, the amount of data storage required increases as a function of the number of patches. This method is easiest for materials that are uniform diffusors (Tsangrassoulis and Santamouris, 1997). However, due to the assumption that all the surfaces are perfectly diffuse, it is difficult to simulate specular materials (Geebelen et al., 2005). Therefore, it is difficult to accurately calculate the energy consumption under the influence of shading devices such as specular venetian blinds, specular light shelves, and mirrors. EnergyPlus (Crawley et al., 2000) and SUPERLITE (Hitchcock and Osterhaus, 1993; Selkowitz et al., 1982) both use the Radiosity method to calculate the IRC.

2.4.2. Daylight Coefficient Methods

The Daylight Coefficient (DC) method divides the sky into a large number of very small elements (Figure 2.2) (Tregenza and Waters, 1983). In this method the internal illuminance at a point in the space results from each corresponding element of the sky (Figure 2.3).

The advantage of the DC method is that it can calculate illumination levels at a reference point in a room for a wide variety of sky conditions (Tregenza and Waters, 1983). There are two main Daylight Coefficient methods for calculating the IRC: The Forward Ray-Tracing Method and Back Ray-Tracing Method.

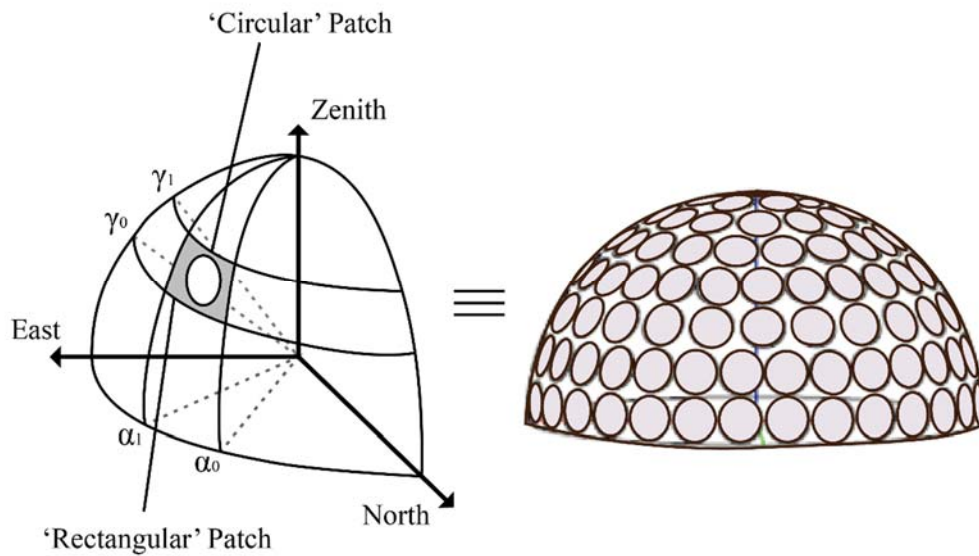


Figure 2.2 Daylight Coefficient Concept of Discretization of Sky Dome into Patches (Source: Adapted from (Mardaljevic, 2000))

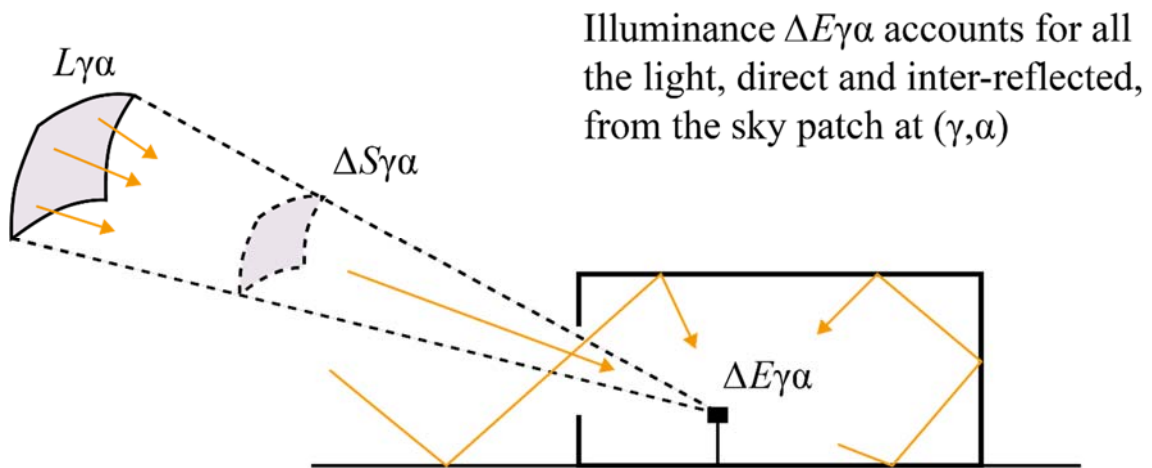


Figure 2.3 Daylighting Coefficient Basics (Source: Adapted from (Mardaljevic, 1999))

2.4.2.1. Forward Ray-Tracing Method

In the Forward ray-tracing method, light rays are emitted from the light source striking surfaces in all directions in a space, contributing to the luminances of these

surfaces, which finally reaches the eye (Tsangrassoulis and Santamouris, 1997) (Figure 2.4). Unfortunately, only a few of all the possible rays ever reach the viewer's eye contributing to an image. As a result, forward ray-tracing is computationally very time consuming to track all the rays that do not contribute to the image or reach the eye (Tsangrassoulis and Bourdakis, 2003; Tsangrassoulis and Santamouris, 1997).

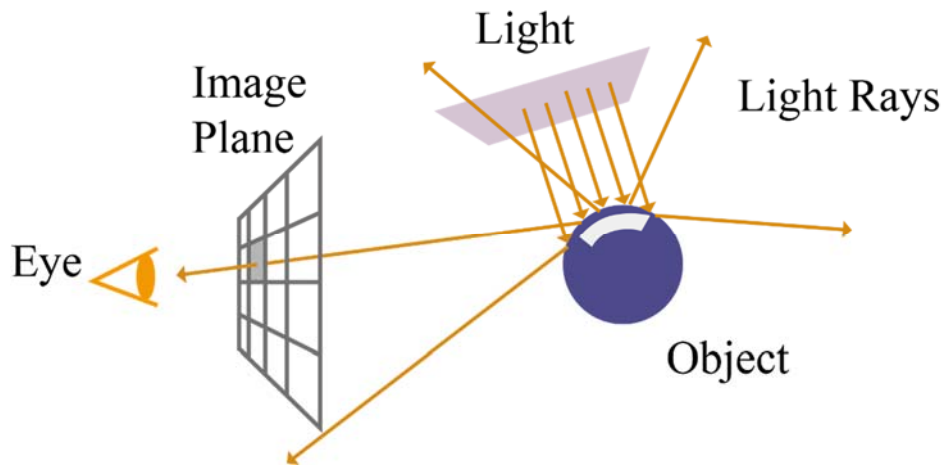


Figure 2.4 Forward Ray-Tracing Method (Source: Adapted from (Kim, 2011))

2.4.2.2. Backward Ray-Tracing Method

In the backward ray-tracing method, the rays are generated from a point (i.e., the viewer's eye) and are then traced backward towards the light source (Tsangrassoulis and Santamouris, 1997). In this method, only those rays are considered that strike the image plane and pass into the viewer's eye. Thus, backward ray-tracing is computationally much faster than the forward ray-tracing (Glassner, 1989) (Figure 2.5). Ray-tracing is also the most advanced technique to find the light levels on surfaces or the inside of a space. Ray-tracing techniques can model both Lambertian and specular surfaces with high accuracy. A well-known tool based on ray-tracing technique is Radiance (Ward,

1996). The simulation tools that used Radiance engine are ESP-r (Clarke, 1996; Clarke et al., 1998), DAYSIM (Reinhart, 2010; Reinhart, 2017), OpenStudio (Temkin, 2009), DesignBuilder (Documentation, 2006; Tindale, 2005), and DIVA (Reinhart et al., 2011).

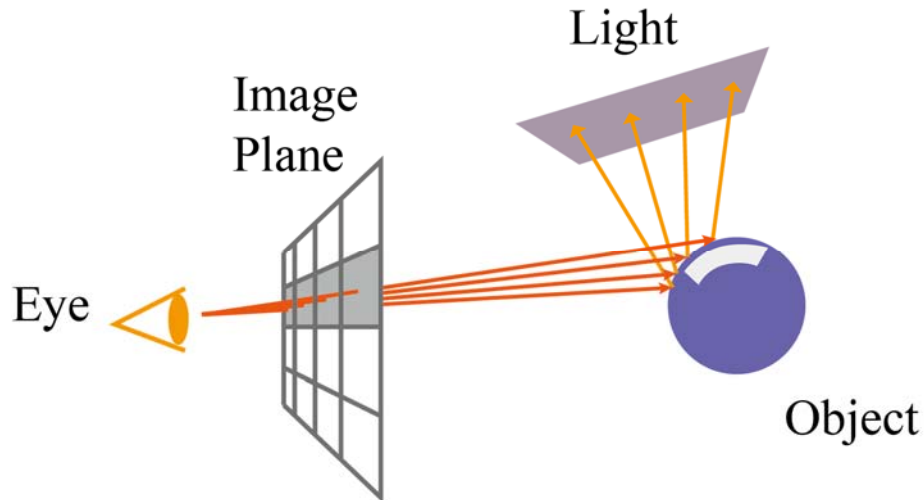


Figure 2.5 Backward Ray-Tracing Method (Source: Adapted from (Kim, 2011))

2.4.3. Summary

In summary, based on the previous discussion, the Daylight Factor methods do not predict the illumination levels at a point on a plane for all time varying sky luminance distributions as well as other methods. In addition, the Daylight Factor method does not accurately predict illumination levels directly from the sun (Tsangrassoulis and Bourdakis, 2003). In contrast, Daylight Coefficient (DC) methods can be used to calculate time varying illuminances and luminances in buildings accurately (Tsangrassoulis and Bourdakis, 2003). Furthermore, a climate-based DC method can be used to calculate annual dynamic daylight performance metrics such as daylight autonomies (DA) and Useful Daylight Illuminances (UDI) (Nabil and

Mardaljevic, 2005).

2.5. Simulation tools

Over the years, many daylighting and energy simulation tools have been developed. These tools can also divide into two categories, which include daylighting only simulation tools and self-contained building energy simulation tools that have daylighting calculations.

Tools such as Radiance (Ward, 1996) and DAYSIM (Reinhart, 2010; Reinhart, 2017) can only simulate daylighting. The most widely used self-contained tools, include: DOE2.1e (Winkelmann et al., 1993b), eQUEST, EnergyPlus (Energy, 2018), DIVA (Reinhart et al., 2011), DesignBuilder (Documentation, 2006; Tindale, 2005), TRNSYS (Klein et al., 2004; TRNSYS, 2017), the IES Virtual Environment (IES<VE>) (IES, 2011, 2017), and OpenStudio (OpenStudio, 2017) are described below.

2.5.1. Daylighting simulation tools

The most widely-used daylighting simulation tools that use ray-tracing in the U.S. are like Radiance (Ward, 1996) and DAYSIM (Reinhart, 2010; Reinhart, 2017) can only simulate daylighting. RADIANCE is a state-of-the-art illuminance prediction and synthetic imaging system based on the backward ray-tracing method (Ward, 1996; Ward and Rubinstein, 1988). DAYSIM (Reinhart, 2010; Reinhart, 2017) is a RADIANCE-based daylight simulation tool that uses the Daylight Coefficient (DC) method (Tregenza and Waters, 1983) and the Perez all-weather sky luminance model (Perez et al., 1993)

for predicting illumination levels in space.

2.5.1.1. RADIANCE

RADIANCE is a suite of different programs working together to generate an image. It comes with two programs to produce a sky luminance distribution for the daylighting calculations. The first program in RADIANCE is the GENSKY program that develops sky patterns such as the CIE standard overcast sky or a clear sky with and without sun. The second program, GENDAYLIT, is a sky model generator that produces a RADIANCE description based on the Perez all-weather sky model (Mardaljevic, 2000). RADIANCE uses the CIE Glare Index (CGI) to analyze the visual comfort of a space (Ward, 1996). In 2010, tools to simulate the Complex Fenestration Façade were added to Radiance to better track lighting contributions from complex windows (Saxena et al., 2010; Ward et al., 2011). This new method in Radiance is called the three-phase method, which separates the light transport between the sky patches and the illuminance sensor points into three phases: exterior transport, fenestration transmission and interior transport (McNeil et al., 2013; Saxena et al., 2010; Ward et al., 2011).

Radiance mainly has three main limitations when used for daylighting simulation listed below:

The first one is that it is very time-consuming climate-based daylighting simulation program. In order to obtain high accuracy annual daylighting results, the Radiance runtime would be more than one hour, which makes an optimization process extremely time consuming.

Second, Radiance simulations involve a stochastic process (i.e., randomly determined). Therefore, re-running the exact same case can produce a $\pm 5\%$ difference each time using the low-quality rendering simulation. However, in the high-quality rendering simulation can reduce these differences.

Third, Radiance annual daylighting simulation results can have a huge difference in rendering runtime. Unfortunately, this can be a problem since the low-quality preset rendering has the lowest sDA and highest lighting energy. This issue makes it is impossible to use the low quality preset in daylighting optimization to save the runtime.

2.5.1.2. DAYSIM

DAYSIM predicts illumination levels at a point in the space for all 8,760 hours of the year. It is a climate-based daylighting analysis tool that is able to calculate the short-time-step dynamics of an indoor illumination distribution with a time-varying sky luminance distribution (Reinhart and Walkenhorst, 2001). DAYSIM also provides a daylighting analysis matrices such as the Daylight Autonomy (DA) and Useful Daylight Illuminances (UDI), which can be used to graphically visualize the results using different tools such as ECOTECH (Marsh, 2003), SketchUp (Chopra, 2012), and Rhinoceros (McNeil, 1998).

2.5.2. Self-Contained energy and daylighting simulation program

During the past several decades, a wide variety of building energy simulation tools have been developed. Those tools can predict the hourly energy consumption, electric demand, temperature, humidity, and energy costs of a building for a given set of

input parameters. At the same time, these tools can also simulate the daylighting performance of the same building that is being analyzed for its energy performance. These combined calculations are typically performed based on inputs that describe the building envelope, daylighting, solar, infiltration, zone loads, mechanical systems and equipment for the corresponding weather condition. The most widely used self-contained tools, which include: DOE2.1e (Winkelmann et al., 1993b), eQUEST, EnergyPlus (Crawley et al., 2000), DIVA (Reinhart et al., 2011), DesignBuilder (Documentation, 2006), TRNSYS (Klein et al., 2004; TRNSYS, 2017), The IES Virtual Environment (IES<VE>) (IES, 2017), and OpenStudio (OpenStudio, 2017) are described below.

2.5.2.1. DOE2.1e

DOE2.1e (Winkelmann et al., 1993b) predicts the hourly energy use and energy cost of a building given hourly weather information, building geometry, HVAC description, and utility rate structure. DOE2.1e has one subprogram for the translation of user input (i.e., the BDL Processor), and four simulation subprograms (LOADS, SYSTEMS, PLANT and ECONOMICS). LOADS, SYSTEMS and PLANT are executed in sequence, with the output of LOADS becoming the input of SYSTEMS, etc. Each of the simulation sub-programs also produces printed reports of the results of its calculations. The shading calculations in DOE-2 use the Split-flux method. If any shadings elements are provided for windows, DOE-2 calculates the shading profile for the first day of the month and uses the same profile for the rest of the month instead of computing the shading for the everyday of the year (York and Cappiello, 1981). This

simplification does not always yield the best results when significant shading of window is used in DOE-2.

DOE-2 uses the split-flux method to calculate the Internal Reflected Component (IRC) (Winkelmann and Selkowitz, 1985). DOE-2.1b⁴ was the first version to calculate the impacts of daylighting strategies on the energy consumption of a building as well as the thermal impact of the fenestration. Unfortunately, DOE2.1e has limitations when it comes to daylighting calculations. DOE-2 uses only two sky models: the CIE overcast and clear sky models, which do not represent the entire range of naturally occurring skies. In addition, the split-flux method used to compute the IRC only works well for certain types of geometry that closely resemble a sphere (such as a square or rectangular-type shape) (Hopkinson et al., 1966). In addition, DOE-2 cannot simulate daylighting strategies such as light shelves because only the shading impact of shelf is considered (i.e., no internal or external reflectance is considered) (Winkelmann et al., 1993a; Winkelmann et al., 1993b). In addition, DOE-2 cannot simulate Complex Fenestration Systems (CFS), and it cannot account for light coming from adjacent spaces or atrium spaces. In addition, because DOE-2 treats surfaces as perfect diffusers it cannot take into consideration material properties such as specularly or glossiness. As a result, the daylighting algorithms in DOE-2 are limited to calculating simple geometries, without complex daylighting strategies such as light shelves or atrium spaces.

⁴ The different versions of DOE-2 include: DOE-2.1 January 1980 release; DOE-2.1a February 1982 release; DOE-2.1b January 1983 release; DOE-2.1c May 1984 release; DOE2.1e released in the Spring of 1992.

2.5.2.2. eQUEST

The Quick Energy Simulation Tool (eQUEST) (Hirsch, 2006) is an easy-to-use building energy simulation program that is based on the DOE-2.2 calculation engine (Hirsch, 2017). In contrast to DOE2.1e, this program provides the user with two options: a Graphical User Interface (GUI) that includes a building creation wizard; and Energy Efficiency Measure (EEM) wizard. The building input wizard option enables users to quickly specify building details without the need for a detailed knowledge of building energy simulation, or detailed input information. Using the EEM wizard, users are able to quickly walk through the process of evaluating the building energy savings and specific design decisions.

DOE-2.2 is the simulation program behind eQUEST (Hirsch, 2017). Both DOE-2.2 and eQUEST 3.64 use the same daylight calculation methods as the DOE2.1e program performs. Therefore, both DOE-2.2 and eQUEST have the same daylighting simulation limitations as the DOE2.1e program has.

2.5.2.3. EnergyPlus

EnergyPlus is an advanced whole-building, energy simulation tool that incorporates the best features of DOE-2 and BLAST⁵ into a new platform (Crawley et al., 2000). In a similar fashion as DOE2.1e and DOE-2.2, EnergyPlus also uses the response factor method for the transient heat transfer through multi-layered walls. The simulation modules in EnergyPlus are integrated with a heat balance-based zone

⁵ BLAST was sponsored by the US Department of Defense (DOD), has its origins in the NBSLD program developed at the US National Bureau of Standards (now NIST) in the early 1970s.

simulation. In addition, input and output data structures are tailored to facilitate third party interface development. EnergyPlus allows user specified time steps of less than one hour, and performs load calculations and simulations of the response of the systems and plant at each time step. In this way, EnergyPlus provides more accurate space temperature predictions, which is crucial for system and plant sizing, occupant comfort and occupant health calculations (Crawley et al., 2008). It also allows users to evaluate realistic system controls, moisture adsorption and desorption in building elements, radiant heating and cooling systems, and inter-zone air flow, photovoltaic systems and fuel cells.

The daylighting calculations in EnergyPlus are performed using a built-in, split-flux daylighting module as well as a special program called DELIGHT. Both methods can simulate daylighting as well as supplemental electric lighting. The built-in module in EnergyPlus is referred to as detailed calculation method. The detailed method and the DELIGHT method allow for the choice of four different sky models: clear, clear turbid, intermediate and overcast for generating sky luminance distribution for daylight calculations (Ellis et al., 2004). The detailed method and the earlier versions of DELIGHT used the split-flux method for calculating Inter Reflected Component (IRC). Later versions of DELIGHT uses the Radiosity-based algorithms that were developed for SUPERLITE⁶ (Hitchcock and Carroll, 2003; Selkowitz et al., 1982). The detailed

⁶ SUPERLITE is a large computer program that predicts the spatial distribution of the illuminance in a room based on exterior sun and sky conditions, site obstruction, varying fenestrations, and includes shading device details and interior room properties. This program was extensively validated against physical models under an artificial sky (Moore, 1985).

method allows for only two sensor points for a space for electric lighting control, whereas DELIGHT allows 100 sensor points that can be placed arbitrarily in the space. DELIGHT 2.0 (Hitchcock and Carroll, 2003) has the capability of simulating Complex Fenestration Systems (CFS) by reading the Bi-directional Scattering Distribution Function (BSDF) dataset files for simulating CFS that are either generated experimentally or generated using tools such as WINDOWS 6 (Mitchell et al., 2008). In a similar fashion as DOE2.1e and eQUEST, EnergyPlus can also assess the overall impact of different daylighting strategies on the hourly supplemental lighting electricity use and the impact of the internal heat gain (heating and cooling loads) of the building.

2.5.2.4. DIVA

DIVA (Reinhart et al., 2011) is an environmental analysis plugin for the Rhino (McNeel, 2002, 2010; McNeil, 1998) and Grasshopper (Rutten, 2010, 2014). DIVA has two versions, which are DIVA for Rhino (Solemma, n.d.-a) and DIVA for Grasshopper (Solemma, n.d.-b). DIVA performs a daylight analysis on an existing Rhinoceros architectural model using Radiance and DAYSIM (Reinhart, 2010; Reinhart, 2017). DIVA constructs a simplified perimeter-zone geometry for energy analysis based on the existing detailed daylighting model. Schedules generated by the daylighting analysis, such as shading schedule and lighting schedule, can be automatically shared with the energy simulation. This method allows the rapid visualization of daylight and thermal energy consequences from a design model where users can easily test multiple design variants for daylighting and energy performance without manually exporting the output file to multiple software. The schedules are automatically saved into Comma Separated

Value (CSV) files which can be used as inputs into more complex energy models, such as EnergyPlus.

DIVA can also simulate dynamic shading devices, which includes have two types of dynamic shading simulating systems: Conceptual Dynamic Shading (CDS) and Detailed Dynamic Shading (DDS). Conceptual Dynamic Shading considers the operation of an idealized blind that covers all windows in the scene without the need for modeling the device geometrically. This procedure considers the effect of this blind to reflect all direct sunlight and allow only 25% of diffuse sunlight into the space (Solemma, 2017).

The Detailed Dynamic Shading interface has two shading-type modes: Mechanical and Switchable. The mechanical mode is used to control dynamic geometric shading such as blinds or rotating louvers that are modeled on separate layers in Rhino. The switchable mode is used to control glazing that changes state from mostly transparent to mostly opaque by switching-out material definitions for a specific glazing material (Solemma, 2017).

2.5.2.5. DESIGN BUILDER

DesignBuilder is a user-friendly modelling environment that works with virtual building models. It provides a range of environmental performance data such as: annual energy consumption, maximum summertime temperatures and HVAC component sizes (Tindale, 2005).

DesignBuilder uses the EnergyPlus simulation engine to generate performance data. The Daylighting module calculates the daylight illuminance, average daylight

factor and uniformity outputs for each zone using the advanced Radiance simulation engine (Tindale, 2005). However, in DesignBuilder daylighting and thermal simulation, the daylighting simulation results in Radiance model cannot connect to the EnergyPlus for thermal simulation directly.

Internal and external shading obstructions and daylighting features such as light shelves and window frames can be included in the DesignBuilder model using component blocks or assemblies at the building or block level (Tindale, 2005).

2.5.2.6. TRNSYS

TRNSYS (Klein et al., 2004; TRNSYS, 2017) an extremely flexible graphically based software environment used to simulate the behavior of transient systems.

TRNSYS is based on a modular approach to simulate the dynamic hourly performance of building energy models. Functional blocks in the software are called Types, which can be compiled into DLLs (Dynamically Linked Libraries) for easy sharing and high computational speed (Michele et al., 2015). The TRNSYS Types can be linked together to model the interactions between the building components and systems. The “Type56” is dedicated to the thermal building simulations and is used Radiance for daylighting simulation. In the latest version, they added innovative glazing layer used for use of daylighting, reduction of unwanted solar gains, and the avoidance of glare effects. They also applied the ability to read the Bi-directional Scattering Distribution Function (BSDF) data to simulate Complex Fenestration Systems (CFSs) (TRNSYS, 2017). As in the existing window model in TRNSYS, the calculation of optical properties of the CFS occurs in the external program Window 7 (LBNL, 2017). Window 7 not only includes a

large product database, but also algorithms to calculate different shading systems like horizontal or vertical slat systems, perforated screens or woven layers, etc. and offers the option to import own data (TRNSYS, 2017).

2.5.2.7. IES Virtual Environment (IES<VE>)

The IES Virtual Environment (IES<VE>) program is an integrated collection of applications linked by a common user interface and a single integrated data model (IES, 2011, 2017), which allows the data input for one application to be used by others. The program provides an environment for the detailed evaluation of building and system designs, allowing them to be optimized with regard to comfort criteria and energy use. It consists of different modules, each of them performing specific calculations, such as “Apachesim” for thermal simulation, “Radiance” for lighting simulation, “Mechanical” for mechanical simulation, and “SunCast” for solar shading analysis (Muhaisen and Gadi, 2006).

2.5.2.8. OpenStudio

OpenStudio (OpenStudio, 2017) is an open source analysis platform that supports whole building energy modeling using EnergyPlus and advanced daylight analysis using Radiance. OpenStudio can simulate the CFSs by accessing the BSDF data. The three-phase method (Saxena et al., 2010; Ward et al., 2011) algorithm provides climate-based daylighting simulation using the BSDF file. One limit is in the usage of BSDF data that are only contained in the OpenStudio’s database (Michele et al., 2015). Another limitation is that dynamic shading control is not supported, and lighting schedules for each window and shading state combination are pre-calculated and then passed to

EnergyPlus for the thermal simulations (Michele et al., 2015).

2.5.2.9. Ladybug & Honeybee

Ladybug & Honeybee (Roudsari, 2016) are two open source plugins for Grasshopper. Ladybug imports and analyzes the standard EnergyPlus Weather files (.EPW) in Grasshopper, and provides a variety of 3D interactive graphics in drawing diagrams like Sun-path, wind-rose, and radiation-rose; and running radiation analysis and shadow studies. Honeybee connects Grasshopper3D to EnergyPlus, Radiance, Daysim and OpenStudio for building energy, comfort, and daylighting simulation. The honeybee plugin makes these simulation tools available in a parametric way.

2.5.3. Summary

Many studies have compared and validated the accuracy of the daylighting simulation tools. In 2015, Gibson and Krarti compared the real measured daylighting performance data with the simulated data by EnergyPlus Detailed, EnergyPlus DELight, SPOT V4.0, and DAYSIM, and they concluded that the DAYSIM was the most accurate mode (Gibson and Krarti, 2015).

All RADIANCE-based daylighting simulation tools are by far the most accurate daylighting simulation tools that are presently available such tools can be climate-based and have adopted the ray-tracing and daylighting coefficient methods for predicting indoor illumination levels. Table 2.4 shows a comparative analysis (i.e., their strengths and limitations) of different daylight simulations tools.

Table 2-4 The Comparison of Different Simulation Tools/Platform (Kota, 2020)

Characteristics/Tools	EnergyPlus	DOE-2.1e	eQUEST	ECOTECH	Design Builder	RADIANCE	DAYSIM	DIVA	ESP-r	IES<VE>	OpenStudio	TRNSYS
Thermal Simulation	Yes	Yes	Yes	Yes	Yes	No	No	No	Yes	Yes	Yes	Yes
Daylighting Simulation	Yes	Yes	Yes	Yes	Yes	Yes	Yes	Yes	Yes	Yes	Yes	Yes
Sky model	Clear, Clear Turbid, Intermediate and Overcast with Sun	Clear, Overcast with Sun	Clear, Overcast with Sun	Clear, Intermediate and Overcast with and without Sun	Perez All-Weather Sky Model	Perez All-Weather Sky Model	Perez All-Weather Sky Model	Perez All-Weather Sky Model	Perez All-Weather Sky Model	Perez All-Weather Sky Model	Perez All-Weather Sky Model	Perez All-Weather Sky Model
Daylighting Method Adopted	Daylight Factor	Daylight Factor	Daylight Factor	Daylight Factor	Daylight Coefficient	Daylight Coefficient	Daylight Coefficient	Daylight Coefficient	Daylight Coefficient	Daylight Coefficient	Daylight Coefficient	Daylight Coefficient
Method used for computing internal reflected component	Radiosity Method	Split-Flux Method	Split-Flux Method	Split-Flux Method	Backward Ray-Tracing	Backward Ray-Tracing & Forward Ray-Tracing	Backward Ray-Tracing	Backward Ray-Tracing	Backward Ray-Tracing	Backward Ray-Tracing	Backward Ray-Tracing	Backward Ray-Tracing
External Overhangs	Yes	Yes	Yes	Yes	Yes	Yes	Yes	Yes	Yes	Yes	Yes	Yes
Light Shelves Simulation	Yes	No	No	No	Yes	Yes	Yes	Yes	Yes	Yes	Yes	Yes
Specularly Reflecting Louvers	Yes	No	No	No	No	Yes	No	No	No	No	Yes	Yes
Complex Fenestration Systems	Yes	No	No	No	No	Yes	No	No	No	No	Yes	Yes
Capability of Reading BSDF Datasets	Yes	No	No	No	No	Yes	No	No	No	No	Yes	Yes
Dynamic Shading	No	No	No	No	No	No	No	Yes	No	No	No	No
Side light simulation	Yes	Yes	Yes	Yes	Yes	Yes	Yes	Yes	Yes	Yes	Yes	Yes
Sky light simulation	Yes	Yes	Yes	Yes	Yes	Yes	Yes	Yes	Yes	Yes	Yes	Yes
Light from adjacent spaces	No	No	No	No	Yes	Yes	Yes	Yes	Yes	Yes	Yes	Yes
Shading of room	Daily	Daily	Daily	Daily	Daily	Daily	Daily	Daily	Daily	Daily	Daily	Daily

2.6. Parametric Modeling Tools – Rhino & Grasshopper

Parametric models are essential tools to obtain optimal building design. The term “parametric” refers to the digital modeling practice of using a series of design variables whose relationships to each other are pre-defined through one or more mathematical relationships (i.e., parameters). These variants form a parametric space that may comprise dozens or thousands of related but distinct forms. Such parametric models are essential to finding optimal design methods.

A number of parametric modeling tools have been developed, include BIM (Eastman et al., 2011; Ghaffarianhoseini et al., 2017), AutoCAD (Hamad, 2018), and Grasshopper (Rutten, 2014). Grasshopper is one of the friendliest software for architecture to use with parametric design. Grasshopper has a graphical editor that is integrated with the Rhinoceros 3D modelling tool (Rutten, 2010, 2014). Grasshopper can model geometries with parametrically controlled variables. Several scripts have been developed for grasshopper to integrate different simulation tools to evaluate building thermal and daylight performance. One example of an integrated tool is DIVA, which was previously discussed. DIVA the plugin for Grasshopper allows for an environmental analysis using Rhinoceros and its Grasshopper components.

2.7. Coupled Simulation Methods: Integrated the thermal and daylighting simulation

Recently, many attempts have been made by different researchers to integrate thermal and daylighting simulation tools at run-time to achieve improved results and

also take advantages of the best of both the thermal and daylighting tools. These previous efforts have integrated ESP-r with Radiance, DOE2.1e with DAYSIM, eQuest with DAYSIM, and so forth. In addition, there are many studies that have presented coupled simulation methods, including: Janak (1997), Bodart and De Herde (2002), Koti and Addison (2007), An and Mason (2010), Versage et al. (2010), Motamedi and Liedl (2017), and Solemma (2017).

Janak (1997) coupled ESP-r and RADIANCE to evaluate the performance of a building incorporating daylighting technologies. Since the daylight factor method in ESP-r failed to simulate the dynamic performance of the daylighting, they decided to use RADIANCE to obtain the dynamic behavior of lighting control system. They found that such a coupled building thermal and lighting simulation is a promising approach to study the impact of daylighting strategies on the thermal performance of the buildings.

Bodart and De Herde (2002) studied an integrative simulation approach combining daylighting and thermal performance, and evaluated the impact of lighting energy savings on the cooling/heating load consumption in office buildings. They coupled a daylighting simulation tool ADELIN (Szerman, 1993) and the thermal simulation software TRNSYS. They concluded that daylighting can reduce artificial lighting consumption from 50 to 80%, and reduced lighting internal loads around 40%.

Koti and Addison (2007) demonstrated a successful linking of DOE2.1e and DAYSIM. DOE-2 is a widely used building energy simulation software, but it also has limitations in daylighting simulation. The split-flux method employed by DOE2.1e cannot simulate the daylighting strategies such as light shelves. Thus, they implemented

DAYSIM to determine the impact of selected strategies (i.e., Light shelves) on the overall building energy consumption. To accomplish this, the DAYSIM hourly results for the entire year were read into the simulation using FUNCTION commands in DOE2.1e. Compared to the energy results of DOE2.1e with the split-flux daylighting calculation, the coupled DAYSIM/DOE2.1e simulation was able to simulate daylighting systems that not supported by DOE2.1e and it gave more accurate results for certain daylighting systems supported by both.

An and Mason (2010) described linking DOE-2.2 (eQUEST) and DAYSIM to calculate the energy performance in an office building. They used eQUEST as the whole-building energy analysis tool, and substituted the daylight controls schedule created by eQUEST with schedules that generated by DAYSIM. Results from the integrated process were compared against the conventional daylighting control calculation method in DOE-2.2. The daily lighting fraction generated by DAYSIM reduced the lighting related energy use by 25% during the school year. In addition, for the annual lighting consumption, the results from the integrated method saved around 30% in winter months to 40% in spring and fall months. In difference to Koti and Addison's results, their study showed that the use of DAYSIM daylighting method had higher energy savings than using the split-flux method in DOE-2.2 in lighting energy.

Versage et al. (2010) linked EnergyPlus with DAYSIM in order to study the impact of different daylighting simulations on the total energy consumption in buildings. In this study, the results obtained by EnergyPlus using the built-in daylighting module were compared to the results obtained when DAYSIM was linked with EnergyPlus. The

comparison revealed that the split-flux method over predicts the illumination levels compared to that of DAYSIM. As a result, the EnergyPlus/DAYSIM simulation method has resulted in lower energy savings when compared with savings in split-flux or DELIGHT method used in EnergyPlus.

Motamedi and Liedl (2017) also implemented EnergyPlus as the thermal simulation and Radiance as daylighting simulation through its host, Ladybug and Honeybee (Roudsari, 2016) which are environmental plugins for Grasshopper to visualize geometries and to display the results of EnergyPlus models. Although this tool can separately simulate the thermal and daylighting performance of a building, it could not consider the combined impact of daylighting in lighting, cooling, and heating load. Thus, they coupled the thermal and daylighting simulation using Python scripting (Langtangen, 2006) in Grasshopper. The Python script was written to transfer the daylighting results generated by Radiance simulation to the EnergyPlus simulation. They used this new combined simulation to find the optimal skylight to floor area ratio in office buildings. In their case studies in an office in San Francisco, the optimal skylight to floor ratio is 5.5–6% while decreasing the energy demand by 19%. In addition, energy efficiency only occurs for skylight ratios of 3–14%.

DIVA 4.0 and Archsim for Grasshopper (Solemma, n.d.-a) are several more examples of coupled tools with thermal and daylighting simulation. One important advantage of this combination is that this model can be changed very easy using the parametric model in Grasshopper. The newly released software DIVA 4.0 plugin for Grasshopper (Solemma, n.d.-a) uses the RADIANCE engine for calculating the

daylighting performance including the illuminance, shading schedules, and lighting schedules. The daylighting results in DIVA 4.0 can be connected to the grasshopper plugin Archsim (Solemma, n.d.-b), which allows the EnergyPlus engine to do the thermal simulation. This coupling of the lighting and energy simulations by connecting the shading and lighting schedules to Archism obtains more a more accurate energy and lighting consumption.

In summary, the previous studies have shown that a combined simulation that uses an advanced daylighting program (i.e., DIVA, DAYSIM, RADIANCE) can be combined with a building energy simulation program (i.e., DOE2.1e, DOE-2.2, eQuest, EnergyPlus) use the lighting schedules in DOE-2 or EnergyPlus were replaced with the lighting schedule from DAYSIM or RADIANCE to produce more accurate daylighting results. Table 2-5 shows the comparison of the different approaches to integrate the daylighting and thermal simulation. All of the previous studies showed that integrating the more advanced daylighting analysis into DOE-2 or EnergyPlus enabled the projects to be more accurate in their assessment of the energy benefits of a daylighting design. Of all the coupled daylighting and thermal simulation tools, DIVA 4.0 and Archsim/EnergyPlus for Grasshopper not only can simulate the more accurate daylighting performance, but can also automatically transfer the daylighting results into the thermal simulation. More importantly, the DIVA model in grasshopper can be used as a parametrical model, which can easily provide multiple optimal daylighting design strategies for an analysis.

Table 2-5 Coupled Simulation Methods

Author	Coupled Tools	Topic	Results
Janak (1997)	ESP-r and RADIANCE	Coupling building energy and lighting simulation	They found that such a coupled building thermal and lighting simulation is a promising approach to study the impact of daylighting strategies on the thermal performance of the buildings.
Bodart and De Herde (2002)	ADELIN and TRNSYS	Evaluated the impact of lighting energy savings on the cooling/heating load consumption	They concluded that daylighting can reduce artificial lighting consumption from 50 to 80%, and reduced lighting internal loads around 40%.
Koti and Addison (2007)	DOE2.1e and DAYSIM	Predict whole building energy performance with an accurately modeled daylighting	The coupled DAYSIM/DOE2.1e simulation was able to simulate daylighting systems that not supported by DOE2.1e and it gave more accurate results
An and Mason (2010)	DOE-2.2 (eQUEST) and DAYSIM	Integrate Daylight Analysis into Building Energy Analysis	The daily lighting fraction generated by DAYSIM reduced the lighting related energy use by 25% during the school year.
Versage et al. (2010)	EnergyPlus with DAYSIM	daylighting simulation results on the prediction of total energy consumption	The EnergyPlus/DAYSIM simulation method has resulted in lower energy savings when compared with savings in split-flux or DELIGHT method used in EnergyPlus.
Motamedi and Liedl (2017)	EnergyPlus with Radiance	Optimize skylights considering fully impacts of daylight on energy	The study showed optimal skylight to floor ratio is 5.5–6% while decreasing the energy demand by 19%. In addition, energy efficiency only occurs for skylight ratios of 3–14%.
Solemma (2016)	DIVA 4.0 and Archsim	Coupled tools with thermal and daylighting simulation with a parametric model	The coupling of the lighting and energy simulations by connecting the shading and lighting schedules in DIVA to Archism obtains more a more accurate energy and lighting consumption.

2.8. Optimization Techniques for Building Simulation

Optimization is the procedure of finding the minimum or maximum cost function given two or more opposing constraints (i.e., façade design, system, and construction cost). In mathematics, optimization is the process to find the best solution to a problem from a set of available options (Nguyen et al., 2014). Many design factors involved in building energy simulation ultimately affect the building performance. The generally accepted concept among the simulation-based, optimization community is that this term indicates an automated process, which is based on numerical simulation and mathematical optimization procedures. Mathematical optimization is the process of finding the best solution to a problem from a set of available alternatives (Nguyen et al., 2014). Optimization methods can be applied to a number of different building design problems, such as the building massing, orientation, façade design, shading devices, thermal comfort, and daylighting. Several types of optimization were reviewed for the proposed analysis, which including Single-Objective Optimization (SOO), Multi-Objective Optimization (MOO), and continuous and discrete optimization methods.

2.8.1. Single-Objective Optimization and Multi-Objective Optimization Methods

Optimization algorithms can be divided into single-objective optimization and multi-objective optimizations based on how many criteria have been used. Single-Objective Optimization (SOO) optimizes a problem by using a single-objective function. When there is more than one objective function for optimization then a multi-objective optimization problem arises. Multi-Objective Optimization (MOO) utilizes two or more

objective functions to solve a problem. There are two approaches for multi-objective problems. The first one uses a weighted sum function where each of the objectives is normalized and summed up with their associated weight factors to obtain one cost function (Aerts et al., 2003). However, this weighted sum function cannot evaluate the information on how the different sub-objectives interfere with each other (Machairas et al., 2014). The other popular method to solve multi-criteria optimization is called the Pareto front method (Balling et al., 1999), which results in a set of non-dominated solutions. When the optimization problem consists of two or three objective functions, the Pareto front can be reported as a curve (Machairas et al., 2014).

In summary, both MOO models (i.e., weighted sum function and Pareto front) have advantages and disadvantages. For example, although the Pareto front solutions focus on exploiting the diversity of solutions, they often present issues of inadequate efficiency and effectiveness. On the other hand, weighted sum methods are more efficient and easier to implement, but require prior knowledge of the two or more objective functions, and do not always provide information about how to resolve a compromise between the multiple objectives (Cao et al., 2012).

2.8.2. Continuous and Discrete Optimization Methods

Optimization techniques also can be classified as continuous or discrete. Most of the algorithms that deal with continuous design variables use mathematical programming techniques or optimal criteria approaches. Unfortunately, design variables are often discrete in most practical design problems. Therefore, continuous optimization

methods would require a procedure to analyze discrete data points into a continuous function prior to their use.

2.8.2.1. Continuous Optimization

Continuous optimization methods mean that the variables in the optimization model are allowed to take on any value within a range of values, usually real numbers. Continuous optimization methods include the Nelder-Mead simplex method (Glaudell et al., 1965), the Hooke-Jeeves method (Hooke and Jeeves, 1961), and various gradient-based approaches (Nash and Sofer, 1996).

The Hooke–Jeeves algorithm is a member of the family of Generalized Pattern Search algorithms (GPS) (Audet and Dennis Jr, 2002). It searches along each coordinate direction for a decrease in the objective function (Hooke and Jeeves, 1961). The initial mesh size for the search is given by a step size for each variable, and when no improvement in the objective function is achieved, the step size is divided by a mesh-size divider. When the local search around the current point finds a better point, the algorithm tries to make a global search move continuing in the same direction. As long as the global search finds a better point, it continues moving in the same direction until it fails, in which case the local search is restarted around the last best point. The local search and the algorithm ends once the maximal number of step reductions is attained (Hooke and Jeeves, 1961; Kämpf et al., 2010).

Several building energy simulation input parameters, such as aspect ratio, orientation, and window area can be considered continuous parameters. However, almost all other parameters, such as wall type, window type, and location, building shape, etc.,

have discrete options. Therefore, the continuous techniques are not well suited for use in these discrete optimizations.

2.8.2.2. Discrete Optimization

The variables in a discrete optimization model are required to belong to a discrete set. Variables may be binary (restricted to the values 0 and 1), or more abstract objects drawn from sets with many elements. Discrete optimization methods include global techniques such as sequential search used in BEopt (BEopt, 2017; Christensen et al., 2005), Genetic Algorithms (Goldberg, 1989), non-dominated sorting genetic algorithm (NSGA-II) (Deb, 2001), Tabu search (Glover, 1989, 1990), and Particle Swarm Optimization (Shi, 2001). Currently, all these methods that are widely used for optimization in the building design process. Each method uses discrete values of the cost function to determine the parameter values of the next iteration.

2.8.2.2.1. Sequential Search in BEopt

The sequential search technique used in BEopt⁷ is a direct search method that identifies the building option that will best decrease a cost function at each successive point (Christensen et al., 2005). The sequential search technique used in BEopt begins by simulating a user-defined reference building. It then runs a simulation for each potential option one at a time. The most cost-effective option is chosen and used in the building description for the next point along the path. There are a number of discrete

⁷ BEopt is a computer program designed to find optimal building designs along the path to accelerate the process of developing high-performance building designs. The BEopt software calls the DOE-2 and TRNSYS simulation engines (BEopt, 2017; Christensen et al., 2005).

options in different categories such as the building azimuth, the building aspect ratio, exterior wall type, ceiling insulation, etc. The process is repeated, ultimately defining a path from the reference building to least life cycle cost, which includes first costs and annual operating costs (Tuhus-Dubrow and Krarti, 2009).

2.8.2.2.2. Genetic Algorithms (GAs) & Non-dominated Sorting Genetic Algorithm (NSGA-II)

A popular evolutionary algorithm is the genetic algorithm (Holland, 1992) that uses the principle of natural selection to evolve a set of solutions towards an optimum solution. A genetic algorithm is a search technique for searching noisy solution spaces with local and global minima. GAs (Goldberg, 1989) operate on a finite set of points, called a population. The different populations are called generations. They are derived on the principles of natural selection and incorporate operators for (1) fitness assignment, (2) selection of points for recombination, (3) recombination of points, and (4) mutation of a point. Because it searches from a population of points, not a single point, the probability of the search getting trapped in a local minimum is limited. GAs start searching by randomly sampling within the solution space (Goldberg, 1989).

A genetic algorithm starts by generating a number of possible solutions to a problem, evaluates them, and applies the basic genetic operators to that initial population according to the fitness of each individual. This process generates a new population with higher average fitness than the previous one, which will in turn be evaluated. The cycle is repeated for the number of generations set by the user, which is dependent on problem complexity. Despite their apparent simplicity, GAs have proved to have a high efficacy

in solving complex problems than other, more conventional optimization methods, may have difficulties with, namely by being trapped in local minima (Goldberg, 1989). By maintaining a population of solutions, genetic algorithms can search for many non-inferior solutions in parallel. This characteristic makes GAs very attractive for solving MO problems (Fonseca and Fleming, 1993).

NSGA-II, a Non-dominated Sorting Genetic Algorithm (NSGA), was developed by Professor Kalyanmoy Deb's team at Kanpur Genetic Algorithms Laboratory, India (Deb, 2001; Deb et al., 2002). NSGA-II is one of the most efficient genetic algorithms for multi-objective optimization. Generally, NSGA-II initializes a population based on the problem range and constraints; and sorts the process into fronts based on non-domination criteria of the population. Once the non-domination sorting is completed, the crowding distance value is assigned, which is a measure of how close an individual is to its neighbors; a large average crowding distance indicates a high degree of diversity. The individuals in the population are selected using a binary tournament with a crowded-comparison operator. After undergoing the crossover and the mutation, the parents and their children are combined to form the next generation (Delgarm et al., 2016; KUMAR, 2011).

There are several tools used GAs to perform the optimization, such as Galapagos (Rutten, 2013), GenOpt (Wetter, 2009), and modeFRONTIER (Poles et al., 2008).

2.8.2.2.1. Galapagos

Galapagos (Rutten, 2007, 2017) is an evolutionary GA solver for the Grasshopper that was developed by David Rutten with McNeel and Associates.

Galapagos can automatically control the Grasshopper parameters by changing the input parameters, recalculating the solution, and then searching for the best results that meet the requirements preset by the user (Rutten, 2017). This optimum result involves searching by Galapagos under certain criteria, called the fitness number.

2.8.2.2.2.2. *GenOpt*

GenOpt (Wetter, 2009) is a genetic optimization program, which was developed by the LBNL's simulation Research Group. GenOpt can be used to minimize an objective function evaluated by an external simulation program (such as EnergyPlus, DOE-2, TRNSYS, etc.) (Wetter, 2009). GenOpt will work with any simulation engine that uses text files for input and output. However, currently, GenOpt is not capable of handling multi-objective optimization.

2.8.2.2.2.3. *modeFRONTIER*

modeFRONTIER is a multi-objective optimization and design environment tool that can couple almost any Computer Aided Engineering (CAE) tool, such as CAD, finite element structural analysis and Computational Fluid Dynamics (CFD) software (Poles et al., 2008). There are also direct interfaces for Excel, Matlab and Simulink. modeFRONTIER includes a wide range of possible algorithms that can be selected for solving different problems, such as Multi-Objective Genetic Algorithm (MOGA) and Non-dominated Sorting Genetic Algorithm (NSGA-II) (Poles et al., 2008). modeFRONTIER with NSGA-II provides a good spread of solutions for the multi-objective search.

2.8.2.2.3. *Tabu Search*

Tabu Search (TS) was developed for solving combinatorial optimization problems by Glover (Glover, 1989, 1990). Tabu Search (TS) is an optimization method that finds the optimum solution using the neighborhood search method in the solution space, which is also suitable for discrete design variables (Degertekin et al., 2008). The probability of becoming entrapped into a local optima is prevented with TS, because TS uses an artificial memory facility that records information about recent search moves and employs a “Tabu list” to forbid certain moves (Degertekin et al., 2008). In this study, TS has an artificial memory that prevents the algorithm from turning back to the old designs. In addition, the TS algorithm considers each design variable in the current design independently as it generates a new neighborhood design (Degertekin et al., 2008).

2.8.2.2.4. *Particle swarm optimization*

Particle Swarm Optimization (PSO) (Shi, 2001) is one of the simplest techniques to deal with discrete options. Eberhart and Kennedy (1995) first introduced PSO algorithms that are population-based Stochastic Optimization⁸ algorithms. PSO shares many similarities with genetic algorithms. Like GAs, the PSO technique works with a set of solutions called a population. At each iteration step, they compare the cost function value of a finite set of points, called particles. Each potential solution is then called a particle. The change of each particle from one iteration to the next is modeled

⁸ Stochastic Optimization: Stochastic optimization methods are optimization methods that generate and use random variables (“Stochastic Optimization”, n.d.).

based on the statistical methods used to describe the social behavior of flocks of birds or schools of fish (Eberhart and Kennedy, 1995). Each particle in the population encodes the values of all variables and represents a potential solution to the problem. An update equation, which models the social and cognitive behaviours, determines the position of each particle in the next generation (Eberhart and Kennedy, 1995; Rapone and Saro, 2012; Wetter and Wright, 2004).

2.8.2.2.5. Hybrid particle swarm and Hooke–Jeeves (HJ) algorithm

The idea of the hybridization is to use the PSO as a global optimization algorithm, which gets close to the global minimum and then refines the position of the minimum using the HJ algorithm. Practically, the PSO algorithm is executed for a user-specified number of generations, and then the HJ algorithm uses it as its initial search point the best individual obtained by the PSO algorithm (Kämpf et al., 2010).

2.8.3. Optimization Design Application

Optimization can simply divide into two main categories: Single-Objective Optimization (SOO) and Multi-Objective Optimization (MOO).

2.8.3.1. Single-Objective Optimization (SOO)

Single-Objective Optimization (SOO) can be described as optimizing a problem by using a single objective function. There are a number of studies have successfully used SOO to solve the design problems, including Coley and Schukat (2002), Caldas and Norford (2002), and Trubiano et al. (2013).

Coley and Schukat (2002) used Genetic Algorithms to find a set of building

envelope designs that exhibit similar energy performance, rather than just one absolute minimum. They used a simplified dynamic thermal model called EXCALIBUR⁹ (Crabb et al., 1987) for the energy simulations because of reduced computer simulation times. In their analysis, the aesthetic judgment has been used to obtain their final building design, which allows the architect's taste to come into play in choosing from a set of near-optimal designs. They took a single zone community hall design as an example, and tried to obtain the optimal design for the wall, roof, and floor construction, window type and area, shading location, and orientation. They used Genetic Algorithms to generate a large numbers of possible low-energy designs. Later, they used a histogram to encourage the design team to consider a wide range of possible high-performance designs. However, they did not consider the daylighting simulation. And the simulation program they used is a simplified one.

About the same time, Caldas and Norford (2002) developed a design tool for optimizing window areas in an office building using genetic algorithms and DOE2.1E. They used DOE2.1E for both daylighting and thermal simulation. The aim was to identify a solution that minimized annual energy use, while exploring the tradeoffs between heating, cooling and lighting. The genetic algorithm was validated by performing an exhaustive search for a case with a limited solution set before moving on to cases where a full set of solution may not be feasible. However, the window location

⁹ EXCALIBUR: Exeter Calculation in Building Thermal Response (EXCALIBUR) is a simplified dynamic thermal network simulation model intended for use as a design and energy-targeting tool (Crabb et al., 1987).

variation was not considered in the study. In addition, the daylighting simulation method split-flux in DOE-2 tool is not as sophisticated as more accurate RADIANCE based tools.

Trubiano et al. (2013) created an evolutionary optimization method to obtain improved design of office building forms and their adjacent atriums. They integrated the lighting and thermal performance by Radiance and EnergyPlus, and then used an automated script to connect the Grasshopper, EnergyPlus, MATLAB and RADIANCE program. Their combined programs can automate delivery the building's overall volumetric dimensions using GAs and a single objective function (i.e., minimum annual heating load, minimum annual cooling load, or lighting level between 300-800 lux). They also demonstrated the possibility of generating the optimal shape of atriums. However, they only evaluated a single objective: heating load, cooling load, or daylighting. They did not consider multi-objective optimization problems.

2.8.3.2. Multi-Objective Optimization (MOO)

Multi-Objective Optimization (MOO) seeks to optimize the components of a vector-valued cost function (Fonseca and Fleming, 1993). Unlike single objective optimization, the solution to this problem is not a single point, but a family of points known as the Pareto-optimal set (Fonseca and Fleming, 1993). Each point in this surface is optimal in the sense that no improvement can be achieved any one component that does not lead to degradation in at least one of the remaining components (Fonseca and Fleming, 1993). There are many studies have used MOO in building design, including: Ouarghi and Krarti (2006), Asadi et al. (2012), Futrell et al. (2015), Carlucci et al.

(2015), and Hou et al. (2017).

Ouarghi and Krarti (2006) examined building shape optimization for office buildings, where the building shape was described by its relative compactness. Relative compactness was defined as the ratio of the building volume to surface area. This study used a Bayesian Neural Network (BNN) (Bayes, 1970) to simulate building energy performance, which was trained by results from simulations using the DOE-2 engine. Input parameters included: weather files, wall and roof construction, window-to-wall ratio, solar heat gain coefficient, and relative compactness. The optimization technique utilized genetic algorithms, and optimizations were performed for total energy costs alone, as well as for construction and energy costs combined using weighting factors. This study showed that optimal building shapes were very sensitive to building volume and height, as well as to the chosen weighting factors. They concluded that buildings with lower heights are more energy efficient than high-rise buildings with the same total volume since they are more compact.

Asadi et al. (2012) built a simulation-based Multi-Objective Optimization (MOO) scheme, which consisted of TRNSYS (TRNSYS, 2000), GenOpt (Wetter, 2009), and a Tchebycheff optimization technique developed in MATLAB (MATLAB, 2019). TRNSYS was used for the thermal simulation. GenOpt was used to minimize the cost function. Tchebycheff was used to tackle the multi-objective optimization problem. They used this MOO to analyze building retrofit strategies. The decision variables that were chosen were: the external wall insulation materials, the roof insulation materials, the window types, and the solar collector type. The overall objective functions were to

decrease the retrofit costs, increase energy savings, and optimize the thermal comfort of a residential building. They concluded that their proposed approach could provide decisions regarding retrofit actions used in houses in Portugal.

Futrell et al. (2015) optimized early building design to maximize daylighting and thermal performance. The optimization method used GenOpt and an implementation of a Hooke Jeeves and Particle Swarm Optimization algorithm. Lighting performance was evaluated by the RADIANCE program based on the frequency and magnitude of the daylight levels. EnergyPlus was used to evaluate the thermal performance (i.e., how heat transfer across enclosure elements impacts hourly heating and cooling loads). The hourly lighting schedules generated in RADIANCE were connected to the EnergyPlus simulations to account for the offset in electric lighting power made possible by the daylight illuminance. In the analysis, they studied a single-zone classroom in Charlotte, NC, and optimized the façade designs for the North, South, East, and West orientations. The Pareto front was approximated to help evaluate trade-offs between thermal and daylighting objectives. Results show that for the South, East, and West orientations, thermal and daylighting objectives are not in strong conflict, however, for the North orientation there is a more marked conflict between these objectives. Conflict between thermal and lighting objectives is largely because the windows that provide daylight to a space are also the weakest thermal barrier between the inside and outside environments and have a significant impact on heating and cooling loads.

Carlucci et al. (2015) used Multi-Objective Optimization methods (MOO) to optimize nearly zero-energy buildings by evaluating the thermal and visual comfort. In

the analysis, they used EnergyPlus to perform the thermal and daylighting simulation. Daylighting used DELight method in EnergyPlus, which is Radiosity calculation method in calculation daylighting performance. The optimization problem had four objective functions, which are: thermal discomfort during the winter, thermal discomfort during the summer, visual discomfort due to glare, and an inappropriate quantity of illuminance. To perform the optimization, they used the non-dominated sorting genetic algorithm (NSGA-II), implemented in the GenOpt optimization engine through the Java genetic algorithms package, to instruct the EnergyPlus simulation engine. They concluded that in cases of complex optimization problems with many objective functions, their optimization process can represent a valid tool to effectively explore the large number of available building variants. However, their daylighting simulation method Radiosity have limitation related to the accuracy in the light distribution models.

Hou et al. (2017) integrated Grasshopper and simulation tools to design the building envelope. They used a Pareto-optimal solution as a multi-objective optimization (MOO) tool to obtain the best solutions in the design of the building envelope. Three objectives were used in this study, which are: minimizing the total annual space loads, minimizing the total envelope costs, and maximizing UDI₁₀₀₋₂₀₀₀ value. In their analysis, they used a railway station hall as an example to demonstrate that the MOO is a promising way to obtain the optimum solution in façade fenestrations design.

2.8.4. Summary

In summary, building design is a complicated task that seeks to balance various,

opposing building design parameters and constraints. Recently, simulation-based building energy/environment optimization has shown itself to be a promising approach to solve complex design problems with single-objective or multi-objective optimization. Most of the previous studies used meta-heuristic search algorithms (e.g., GA, NSGA-II, and PSO) and implementation tools (i.e., Galapagos, GenOpt, and modeFRONTIER) applied to building optimization problems.

In general, all the studies have shown that optimization algorithms can be successful at finding high performing daylighting or thermal design solutions given multiple design constraints. However, some of the studies did not consider the interactions between daylighting and thermal energy consumption. In addition, although many of the previous studies provided a computational simulation and optimization system to solve the building design problems, they may not have provided suggestions for architects in the preliminary design process.

Therefore, this proposed study will use the GAs and NSGA-II algorithm as an optimization method to find the optimal design factors. Since Rhino and Grasshopper have friendly interfaces for visual tracking of the modeling process, the proposed work will use Rhino and Grasshopper tools to combine the simulation and optimization data flow.

2.9. Design Strategies

Knowledge about how to apply daylighting design strategies plays an important role in the architecture design. It not only affects the building form, function, and

environment design, but it also affects the visual and thermal comfort, which can also affect the overall energy efficiency. In general, when optimizing to design strategies, one needs to consider different types of design strategies that include: daylighting systems, building shape and orientation, window size and placement, building façade, and shading systems.

2.9.1. Daylighting systems

Traditional windows may give rise to uneven daylighting in a room. In some cases, the portion of the room at a distance from the window may appear dark and gloomy, while the perimeter areas near the window are excessively bright. Innovative daylighting systems have been designed to even-out these effects, and thus improve the effectiveness of natural light as a source of illumination for building interiors. Innovative daylighting systems include: light shelves, prismatic glazing, mirrored louvres, and prismatic film system, and Mirrored Louvres.

2.9.1.1. Light shelves (External or Internal)

Light shelves are horizontal solid fixtures positioned at right angles to either the outside or the inside or both sides of a window (Aiziewood, 1993). The upper surface of the shelf is coated with a white or reflective covering (Figure 2.6), which helps reflect both direct and diffuse sunlight into the room (Aiziewood, 1993). External light shelves can be viewed as shading devices that block the direct sunlight. However, they usually do not able to block all direct sunlight.

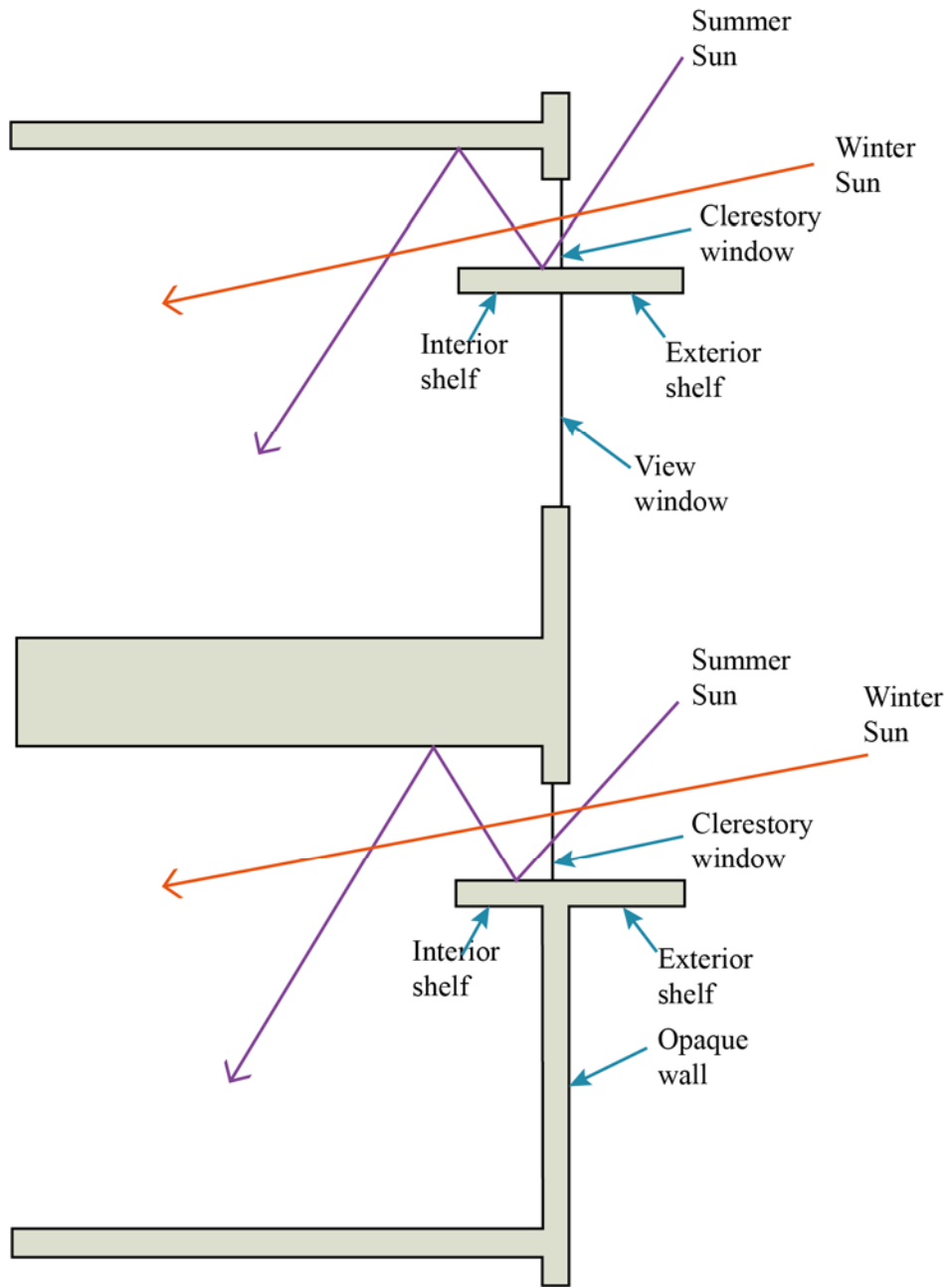


Figure 2.6 Types of Light Shelf and Their Operation (Source: Adapted from (Littlefair, 1990))

Because the light shelf has the internal and external parts, it can both block the direct sun from the window directly below the shade and help introduce sunlight deep

into a room. However, it is not easy to find a balance between how much light to block at the front of room and how much light to direct into the rear of room. There are many variables involved in the daylighting performance of light shelves, which include: building orientation, building geometry, shelf mounting height, materials, and the climate conditions.

2.9.1.2. Prismatic glazing (Within a Double Glazing)

Prismatic glazing consists of a series of plastic or glass prisms designed to fit between the two panes of glass of a double glazing unit (Aiziewood, 1993). Prismatic glazing uses refraction or reflection to redistribute daylight and sunlight away from areas close to the window towards areas further into the room that are away from the window (Figure 2.7) (Aiziewood, 1993). °

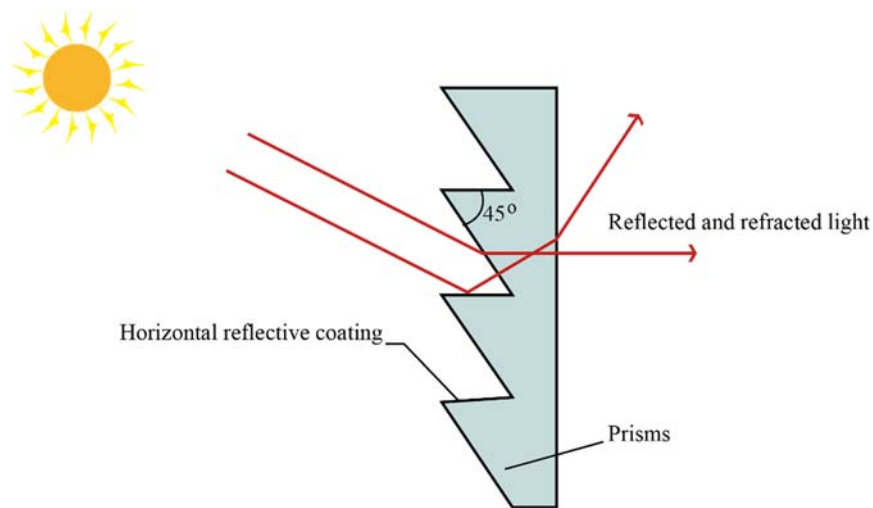


Figure 2.7 Prismatic Glazing (Source: Adapted from (Aiziewood, 1993))

2.9.1.3. Mirrored Louvers (Within a Double Glazing)

Mirrored louvers consist of a number of fixed reflective louvers enclosed within

a double-glazed unit, with each louver having three faces (Figure 2.8) (Aiziewood, 1993). Each face of the louver is designed to either reflect incoming sunlight inside or back outside, depending on the solar altitude (Aiziewood, 1993).

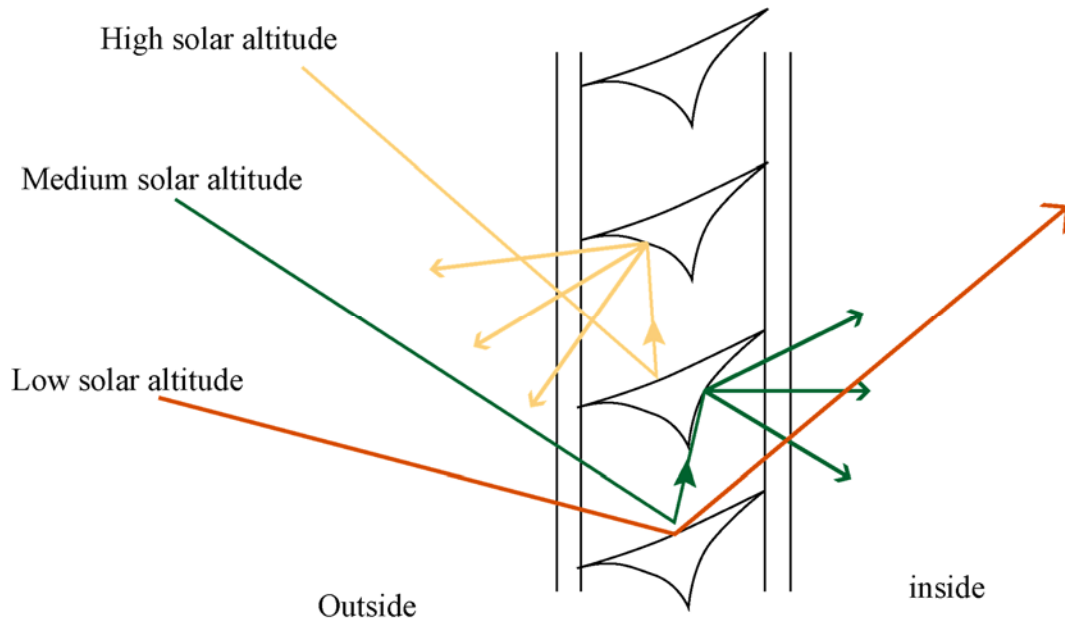


Figure 2.8 Mirrored Louvres (Source: Adapted from (Aiziewood, 1993))

2.9.2. Building Shape and Orientation

Building shape and orientation can also affect the daylighting and thermal efficiency of the external building envelopes. Therefore, the proper building shape and orientation are the primary elements in the design of architectural daylighting to provide a building with natural daylighting and visual comfort. In addition, building shape and orientation determine the amounts of heat transfer through the building envelope, which ultimately affects the cooling and heating load consumption. Several of the previous studies have reviewed the impact of building orientation and building shape, which include: Tuhus-Dubrow and Krarti (2010), Lobaccaro et al. (2012), and Lin et al. (2016).

Tuhus-Dubrow and Krarti (2010) developed and applied a simulation– optimization tool to optimize building shape and building envelope features in five different climate zones. They coupled a genetic algorithm to a building energy simulation engine to select optimal values from a comprehensive list of parameters associated with the envelope to minimize life-cycle cost for residential buildings. The building shapes investigated included: rectangle, L-shaped, T-shaped, cross-shaped, U-shaped, H-shaped, and trapezoid (Figure 2.9). The results of the optimization indicated rectangular and trapezoidal shaped buildings consistently had the best performance (i.e., the lowest life-cycle cost) across five different climates.

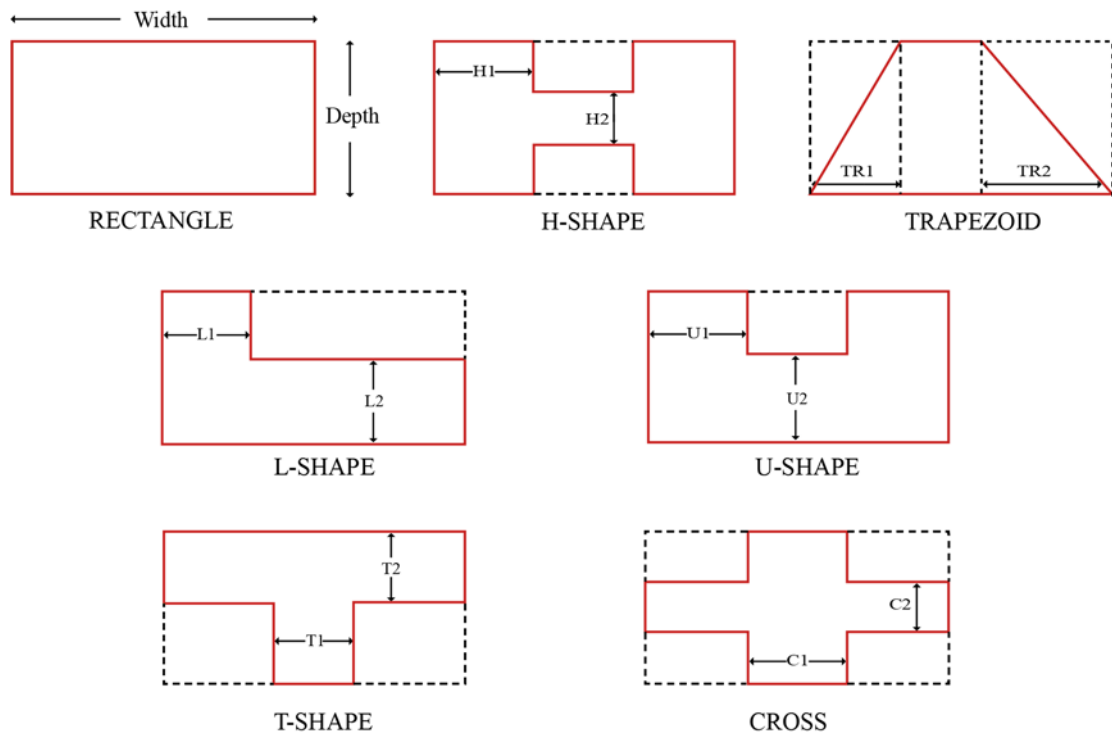


Figure 2.9 Building Shape (Source: Adapted from (Tuhus-Dubrow and Krarti, 2010))

Lobaccaro et al. (2012) optimized the geometry of a building in order to

maximize the annual solar radiation exposure on façades. They researched parametric geometric transformations of the building volume and transformations of façade surfaces to find the best areas on the façade surfaces to install solar systems (i.e., photovoltaic panels). The Grasshopper software was used to iteratively review parametric model façade surfaces to evaluate the solar radiation of different geometric transformations. In this analysis, Radiance/Daysim were used to perform the dynamic solar simulation. The overall goal was to provide guidelines for the assessment of solar potential in existing urban areas.

Lin et al. (2016) developed an office envelope energy performance and configuration model that was based on an envelope energy load equation. This model used the Tabu search optimizer (Chelouah and Siarry, 2000) to minimize the envelope construction cost and still obtain the requirements of a green building (i.e., lower energy consumption). The optimized envelope configurations involved: construction materials, sunshade types, sunshade lengths, window numbers, and window lengths. Their analysis used fifty-four decision variables to generate $2.38 \times 1050 = 2499$ possible designs of a building envelope. The optimal design reduced the total envelope construction cost by 41% compared to the original design.

In summary, finding the optimal configuration of building shape and orientation is not an easy task when one seeks to minimize the annual energy consumption across different climates. The previous studies have shown that the building shape and orientation can be optimized based on the lighting or thermal energy efficiency by using optimization methods. However, not all of the previous research considered the

daylighting effect, the lighting energy consumption, and the visual comfort of the spaces under study. In addition, the previous studies also did not provide practical design strategies for architects to use for the overall the design of building shape and orientation.

2.9.3. Window size and placement

The sizing and placement of windows have a significant effect on the environmental behavior of a building, which includes the energy use for heating, cooling, and lighting. The building location, window material, orientation, and function of a building all affect the optimal design of the window size and placement. Larger window sizes on the South façade will introduce more solar radiation through the window, which reduces the heating load in the winter. However, when not properly designed, larger windows can cause overheating in summer that increases the cooling load. For lighting, there is an increase in daylighting availability as the window sizes increase, which leads to less electricity consumption for supplemental lighting. However, larger windows can lead to glare conditions with reduced visual comfort.

Supplemental or artificial lighting will also affect the cooling and heating loads in a building. Less artificial lighting leads to lower internal heat gains in the building that can increase heating loads during the winter. However, in the summer, the cooling loads will be decreased as the supplemental lighting load decreases. In general, window positions in daylighting systems can be divided into two main categories: sidelights and toplights.

2.9.3.1. Sidelights

Sidelights are regarded as one of the most important building components that are acknowledged for their considerable effects on both energy consumption and indoor environment. There are a number of research articles that have been conducted into sidelight size and placement, which include: Caldas and Norford (2002), Shan (2014), Mangkuto et al. (2016), Goia et al. (Goia, 2016; Goia et al., 2013), Acosta et al. (Acosta et al., 2016; Acosta, Munoz, et al., 2015), and Pellegrino et al. (2017).

Caldas and Norford (2002) tested how window size changes affected the thermal and lighting performance in a building. In their work, they obtained the optimal sizing and placement of windows in a building to optimize its lighting, heating, and cooling performance by using the DOE-2 to do thermal and daylighting simulation. To accomplish this, they varied the window size from 0.3 to 2.4 m using discrete steps of 0.3 m, and they used Genetic Algorithms (Gas) to obtain the optimal size of each window on each orientation based on the calculated optimum annual lighting and thermal energy consumption. For the cooling dominated zone of Phoenix, they concluded that large windows with a North orientation (2.1*2.1 m) that utilized the available daylighting could be maximized without incurring high solar heat gains in the summer. For the East and South orientations, a medium size window (1.2*1.5 m) provided the best balance between admitting useful daylighting and winter solar gains and preventing too much solar gain in the summer. Smaller windows were chosen for West orientations (1.2*0.9 m) since it is the worst orientation in terms of summer overheating. For a cold climate, like Chicago, they determined the optimal window sizes

varied significantly from the Phoenix solutions. In a cold climate, due to the extreme winter conditions, the North window size was reduced to a minimum (0.3*0.3 m). In contrast, the South window size increased (1.8*1.5 m) because of useful benefits of increasing solar gains in the winter. Finally, the East window size remained similar (1.2*1.5 m), and the West window size was reduced to a horizontal strip (2.4*0.3 m) that allowed for some daylighting but prevented excessive heat loss.

Shan (2014) also proposed a methodology to find the optimal building façade design for minimizing the total energy load using a Genetic Algorithm. In this study, the dimension of the window grid and the spacing and depth of shading system were the optimization variables. In addition, the South façade had a window with vertical and horizontal shading fins. This study also used DAYSIM to calculate the internal loads due to the artificial lights, which were controlled On/Off based on a threshold of 500 lux. These internal loads were transferred to TRNSYS to account for the lighting operation in the energy simulation. However, this study only focused on minimizing the energy loads. The study did not consider the impact of the shading devices design on visual comfort. In addition, the window location within the façade was also not considered in the daylighting performance.

Mangkuto et al. (2016) studied a simple building in a tropical climate to investigate the daylighting criteria influence in optimizing the design of the window-to-wall ratio (WWR), orientation, and interior wall reflection. The design variables were: the WWR, which was varied from 30% to 80% in intervals of 10%; the reflectance of the interior walls that were varied from 0.4 to 0.8 in intervals of 0.1; and the four major

orientations of the window. They used DAYSIM to perform the annual daylighting analysis, and they applied six daylighting performance indicators to obtain the optimum solutions using a graphical optimization that used Pareto fronts. They concluded that the optimum solution resulted in a combination of a WWR of about 30%, a wall reflectance of 0.8, and a South orientation. In addition, the graphical optimization method enabled direct observation of the inter-relationship between the performance indicators.

However, this study had limitations, which include the fact that the windows were all centered in the exterior wall and the thermal performance was not be considered.

Goia et al. (2013) integrated thermal-lighting simulations to find the optimal percent of a transparent percentage in a façade module (i.e., optimal WWR value) for a low-energy office building in Frankfurt, Germany. The aim of this study was to minimize the total energy demand of the building, which included heating load demand, cooling load demand and lighting energy demand. In this study, the façade module was composed of two surfaces: a transparent portion and an opaque portion. They performed this study on the four orientations, using three office-building types with different HVAC system efficiencies. The results showed that, regardless of the orientation and area of the façade, the optimal configuration was achieved when the percent transparency was between 35% and 45% of the total façade module area.

In a continuation of the previous study in 2013, Goia (2016) analyzed the optimal window-to-wall ratio (WWR) in four European climates for an office building with the aim of minimizing the energy used for heating, cooling, and lighting. The results indicated that the ideal WWR values were found in the range 0.30-0.45. In addition, they

found that only the South-oriented façades required WWR values outside this range in very cold or very hot climates. For example, in Oslo, Norway, which is a cold climate, the South-oriented façade required a 0.5-0.6 WWR range. In contrast, in Athens and Rome, which are warm climates, the required WWR range of South façades is from 0.2 to 0.35. However, both of Goia's studies (Goia, 2016; Goia et al., 2013) used the EnergyPlus program for the daylighting simulation (split-flux), which split-flux has limitations in the calculation of the daylighting performance.

Acosta et al. (2015) determined rules-of-thumb for window design based on an analysis of daylight factors under overcast sky conditions. The analysis of the daylight factors was carried out using simulation program Daylight Visualizer 2.6 (VELUX, 2019), which calculates luminous distribution using the ray-tracing process. In this study, the shape, size, and position of the windows were tested. They concluded that square windows produce daylight factors slightly higher than those obtained with horizontal windows and noticeably higher than those measured with vertical windows, which considered the same proportion of the openings. In their study, they concluded that the windows in the upper position allowed higher luminance at the back of the room than those in locations that were centered in the façade. However, this study only considered the daylighting factor as a criterion to evaluate the daylighting performance of the window. Therefore, there is a need to evaluate window performance based on dynamic daylighting indexes, visual comfort, thermal comfort, and whole-building energy consumption.

In a follow-on study, Acosta et al. (Acosta et al., 2016) evaluated the variation of

dynamic daylighting metrics in accordance with the window sizes, positions of the opening, and the reflectance of the inner surfaces of the room. In this study, they used the DAYSIM (Reinhart, 2010) tool to evaluate the daylighting performance, with a daylight autonomy (DA) of 250 lux for the daylighting metric. They concluded that all window shapes produce similar values of daylight autonomy at the central axis. However, horizontal windows produced a more uniform illumination, and were more effective in energy savings than other shapes of openings. Based on the variable-sized openings, all windows produced enough illuminance to meet the threshold in the area close to the window. However, their study showed the window size is not relevant for energy saving in the area near the façade. They concluded that windows located higher up in the external wall resulted in higher illuminance at the back of the room than those in locations centered in the façade.

Pellegrino et al. (2017) studied a broad range of possible building configurations of office buildings in Turin, Italy. In their study, numerical simulations were carried out with DAYSIM combined with EnergyPlus to ensure the best performance in both the daylighting and thermal analysis. The metric used in this study for the daylighting analysis was the Spatial Daylight Autonomy (sDA300, 50%). In the study they used DAYSIM to calculate the sDA, and hourly schedules of the status of all lighting and shading groups. As a next step, the lighting and shading schedules were used as input for the energy simulation using EnergyPlus. The results included the sDA and the energy demand for lighting, heating and cooling. The variables considered in the comprehensive study were: the geographic location and the local climate, the room orientation, the room

geometry in terms of room depth (RD), the window sizes (expressed as window-to-wall ratio - WWR), the optical properties of the glass, the external obstruction from nearby buildings of different heights, and the presence of blinds. They concluded that optimizing daylighting can lead to a reduction in the total energy demand of an office. However, they did not consider the visual comfort.

In conclusion, not all the previous studies considered the influence of window placement in the exterior wall (i.e., central in the wall, top portion of the wall, or toward the vertical edges of the wall). In addition, some of previous work did not analysis how the daylighting affects the building thermal performance. Thus, there is a need to analyze daylighting spaces using a sophisticated daylighting and thermal simulation tools to analyze the window placement and location in the both daylighting and thermal performances. In addition, more effective methods need to be proposed to determine how the design of window placement and size affects the building performance. More importantly, the criteria of the window design should be provided for designers and architects based on daylighting and thermal performance.

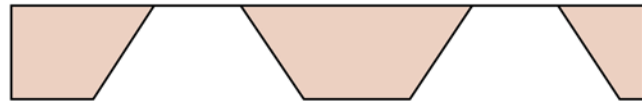
2.9.3.2. Toplights

Toplights have substantial potential for energy conservation in auxiliary lighting during daylight hours. Toplights may affect the interior heat gains and losses that ultimately affect the heating and cooling loads. Therefore, the toplight design needs to consider aperture size, orientation, electric lighting control, and the local climate. Typically, there are four types of toplighting strategies, which include: horizontal skylights; horizontal skylights with splayed wells; vertical opening roof monitors, and

tilted opening roof monitors (Figure 2.10). The reflector shapes of monitor skylights can also be designed as rectangular, slanted, sawtooth, and curved (Figure 2.11).



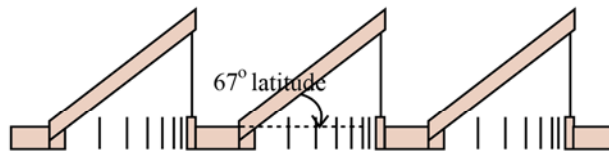
(a) Horizontal skylights with vertical wells and diffuse glazing



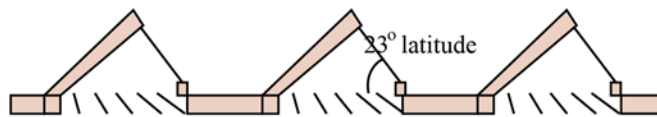
(b) Horizontal skylights with splayed wells and diffuse glazing



(c) Vertical roof monitors facing north and clear glazing
Vertical roof monitors facing south and diffuse glazing



(d) Vertical roof monitors facing south with sunlight diffusing baffles and clear glazing



(e) Tilted roof monitors facing south with sunlight diffusing baffles and clear glazing

Figure 2.10 The Main Types of Skylights (Source: Adapted from (Yoon et al., 2008))

In 2008, the U.S. Department of Energy conducted research (Yoon et al., 2008)

into the energy efficiency of different top-lighting configurations in different climates. This study examined the impacts of eight different toplighting strategies and glazing types on the total annual energy loads for a prototypical open in an office space situated in five different climates. The study combined the lighting simulation program DAYSIM and energy simulation program DOE2.1E to obtain an estimation of annual lighting, cooling, heating consumption. The study showed that different toplighting strategies that were designed to meet a 2% daylight factor can save overall building energy consumption in a variety of climates.

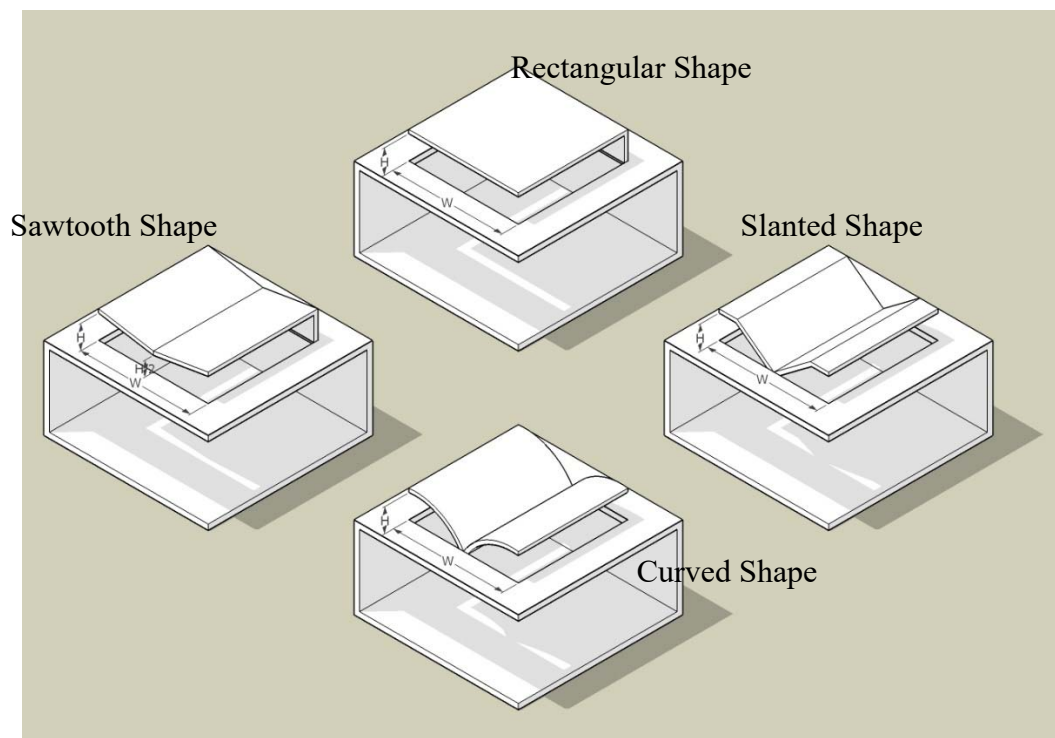


Figure 2.11 Monitor Skylight Reflectors Types: Rectangular, Slanted, Sawtooth or Curved (Source: Adapted from (Acosta,Navarro, et al., 2015))

In another study, Acosta et al. (2012) analyzed the correct height/width ratio of the monitor skylight (lightscoop) reflector for maximizing lighting inside a room under

overcast sky conditions. They used the Lightscape 3.2¹⁰ (Maamari et al., 2002) and the DAYSIM 3.1 simulation programs to analyze the different skylight models. This study analyzed nine rooms with lightscoops of different dimensions but with same interior reflection surfaces (Figure 2.12 and 2.13). They also varied the room dimensions from a square room (9 x 9 meter) to a rectangular room (6 x 12 or 12 x 6 meter) with height varying from 3, 4.5, 6 meters. They concluded that a rectangular monitor skylight with a 4:3 height:width ratio reflector obtained the highest daylight factors.

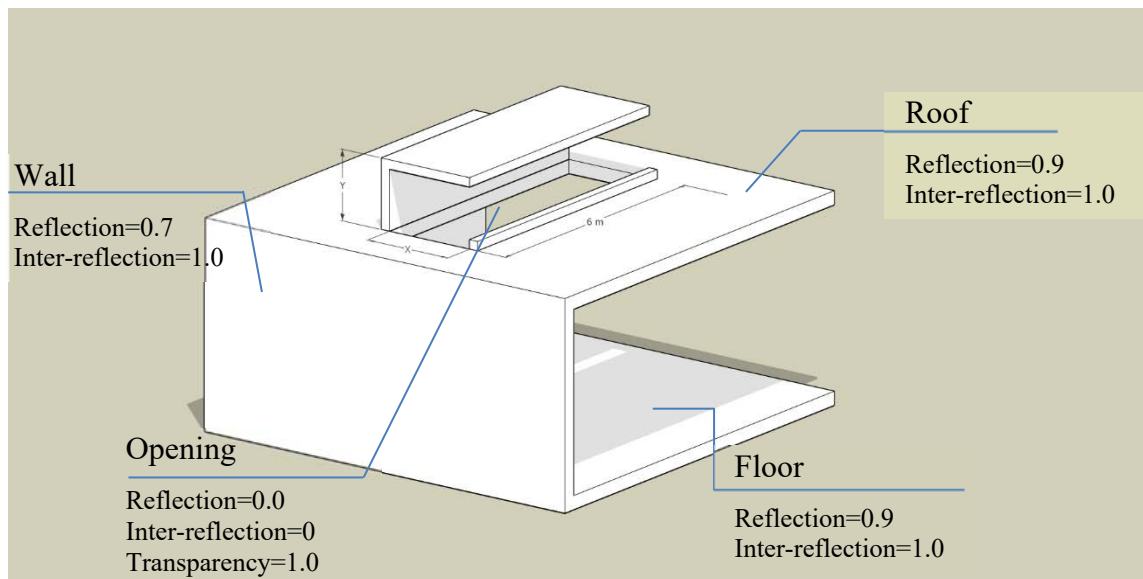


Figure 2.12 Initial Calculation Model of Lightscoops (Source: Adapted from (Acosta et al., 2012))

¹⁰ Lightscape 3.2 calculates luminous distribution using the Radiosity method. Lightscape is a lighting and visualization application that uses both Radiosity and ray-tracing algorithms, with the Radiosity method used for the quantitative results.

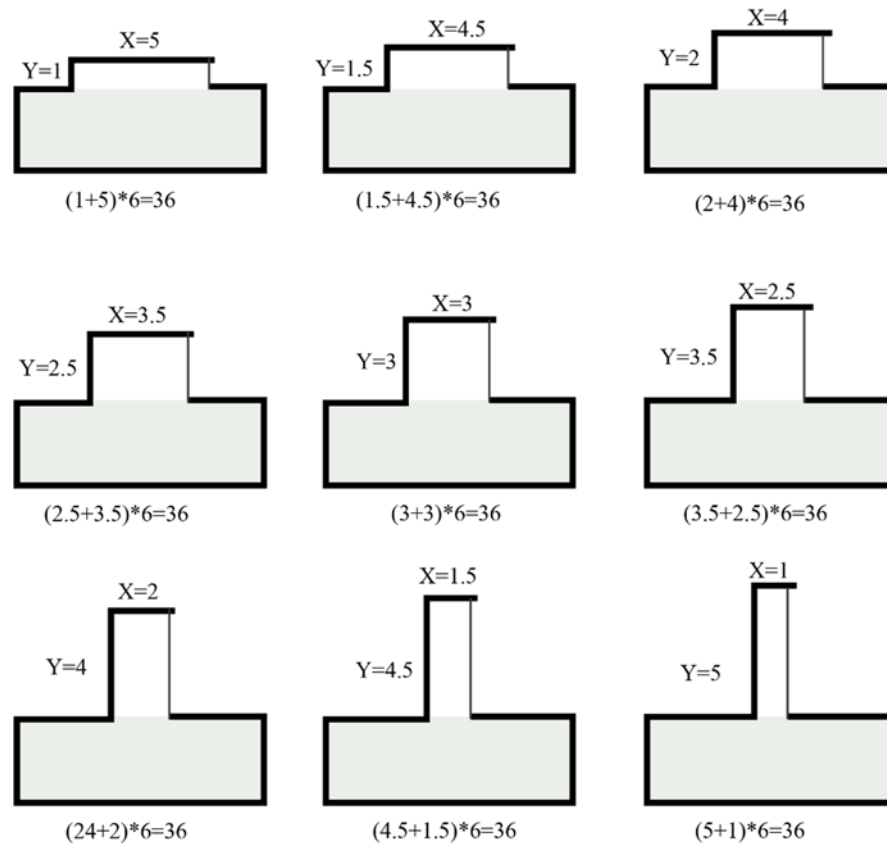


Figure 2.13 Nine Different Lightscoops with Same Reflector Surface (Source: Adapted from (Acosta et al., 2012))

Later, Acosta et al. (2013) studied and compared three different reflector shapes for monitor skylights: rectangular, curved, and sawtooth. Their aim was to determine a suitable shape for monitor skylights to obtain the highest daylight factors. To perform the analysis, they conducted simulation in three different sizes of floor plan include: a square room (9 x 9 meters), a rectangular room (12 x 6 meters), a rectangular room (6 x 12 meters). They used the Lightscape 3.2 software to simulate the daylight factor to find out the optimum shapes of the monitor skylights. They concluded that a curved shaped monitor skylight had the highest daylight factors, while the sawtooth shape produced the

lowest daylight factors.

Acosta (Acosta, Navarro, et al., 2015) also studied the proportions and shapes for monitor skylights to find the maximum illuminance on a work plane. Like the previous two studies, all the simulations were conducted using the Lightscape 3.2 software under the overcast sky conditions. In their study, the daylight factor was used as the criterion to evaluate the performance of the different shapes of monitor skylights. The reflector shapes for the skylight were: rectangular, slanted, sawtooth, and curved. In addition, other variables included different height/width ratios of the vertical and roof openings. The study found that the monitor skylights with a height/width ration 1:1 had the highest average daylight factors, regardless of the reflector shape.

Motamedi and Liedl (2017) proposed an algorithm for Grasshopper program to find the optimal skylight design for an office building. They applied Radiance and EnergyPlus as the daylight and thermal simulations respectively, which were embedded in the Ladybug & Honeybee (Roudsari, 2016) tools for Grasshopper. They coupled the thermal and daylighting simulation and used numeric optimization to find the optimal Skylight Floor area Ratio (SFR) with the minimum annual energy consumption. Their results showed an optimal SFR of 5.5 – 6% for a one-story office building in San Francisco. In addition, they found an energy efficient range of SFR from 3% to a maximum of 14%.

In summary, the previous studies about monitor skylights that were conducted by Acosta only considered the daylighting factor. They did not consider dynamic daylighting matrices, the visual comfort, or the thermal consumption. In addition, the

studies by Acosta did not always consider the impact of daylighting on both visual and thermal performance. The skylight design studied by Motamedi and Liedl (2017) showed a way to use the numeric optimization to find the optimal skylighting floor area ratio (SFR). However, their study only examined uniformly distributed small skylights across the roof, and did not consider the use of larger skylights with equal areas.

2.9.4. Complex Façades Systems

The term Complex Fenestration Systems (CFSs) covers all non-specular transmitting fenestration system components including: layers that provide shading (i.e., fabric shades, louvered blinds, and metal mesh systems); and layers that improve interior daylighting (i.e., prismatic films and mirrored louvered systems) (McNeil et al., 2013). The main types of CFSs are shown in the Figure 2.14 (Andersen and de Boer, 2006), which include: prisms, Laser cut panels, light redirection glass, blinds, and gratings. CFSs are typically used to block direct sunlight entering the interior space, or enhance the overall interior illuminance by redirecting the sunlight into the remote parts of the space. Since the CFSs require a detailed description of directional optical properties, CFSs cannot be evaluated using conventional daylighting and thermal analysis methods.

To simulate the solar heat gain through CFSs, the analysis procedures must determine how the radiation is reflected back from the CFSs (i.e., bidirectional reflectance distribution function (BRDF)), or transmitted through the system (bidirectional transmittance distribution function (BTDF)). The previous work in this area includes: Klems (Klems, 1993, 1994), McNeil et al. (2013), Molina et al. (2015),

Vera et al. (2016), and Bustamante et al. (2017).

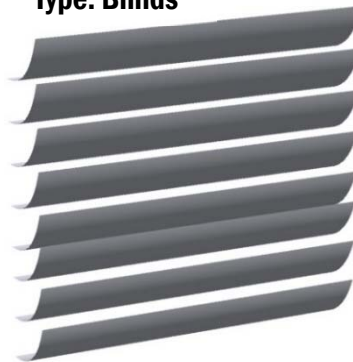
Type: Laser cut panel



Key Parameters:

- Index of refraction
- Thickness of panel
- Distance of cuts
- Angle of cuts

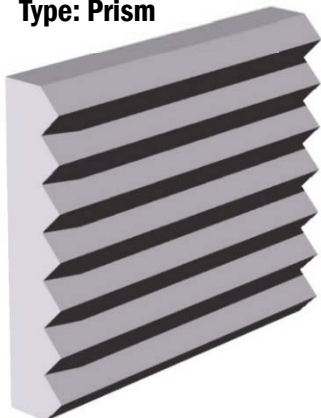
Type: Blinds



Key Parameters

- Specular and diffuse reflection
- Slat curvature
- Distance and number of slats
- Slats incline

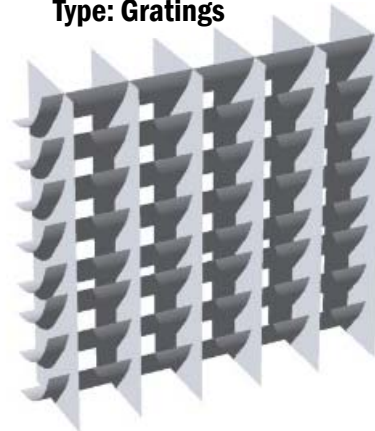
Type: Prism



Key Parameters:

- Index of refraction
- Thickness
- Angle of prism elements

Type: Gratings



Key Parameters

- Specular and diffuse
- Distance of grating slats (H&V)
- Incline of grating slats

Figure 2.14 Selection of CFS-Models Currently Supported by the FHG-IBP CFS-Sample Generator with Key Configuration Parameters (Source: Adapted from (Andersen and de Boer, 2006))

Klems (Klems, 1993, 1994) proposed an efficient calculation method that use Bi-directional Scattering Distribution Functions (BSDF) datasets, which were the combination of BTDF and BRDF, to model solar heat gains for CFSs (Figure 2.18). The BSDF expresses the light scattered by a surface and distributed for all incoming incident directions, which can properly describe the solar and optical performance of CFSs. In this way, the BSDF data provides a method to more accurately calculate the light-scattering properties of CFS. In 2010, BSDFs were added to Radiance to track lighting contributions from a window (Saxena et al., 2010; Ward et al., 2011). This new BSDF method in Radiance is called the three-phase method, which separates the light transport between the sky patches and the illuminance sensor points into three phases: exterior transport, fenestration transmission and interior transport (McNeil and Lee, 2013; Saxena et al., 2010; Ward et al., 2011).

McNeil et al. (2013) described the use of the open-source Radiance software tool, genBSDF, to assess the energy performance of complex fenestration systems (CFS). The genBSDF is a Radiance-based program whose capabilities include generating the bidirectional solar properties of CFS. This tool can generate BSDF datasets for CFSs of any arbitrary geometry. In the study, they described the fundamentals of BSDF conventions and the ray-tracing algorithm, they also validated datasets produced by genBSDF with four cases: air (100% specular transmission); a Lambertian diffuser with 50% transmittance; mirrored blinds; and micro-perforated shades. The output BSDF data produced by genBSDF can be viewed as an input file for daylighting simulation tools in Radiance and thermal simulation tools in EnergyPlus to

analysis the daylighting and thermal performance. In this way, the genBSDF combined with other simulation tool provides users with an accurate method to solve the CFS design problems.

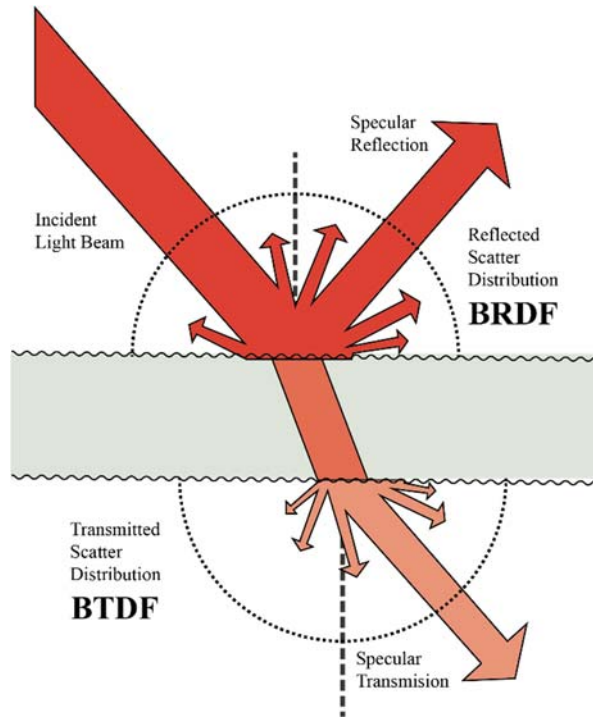


Figure 2.15 Bi-directional Scattering Distribution Function (BSDF) Showing the two Components Bi-directional Reflected Distribution Function (BRDF) and Bi-directional Transmittance Distribution Function (BTDF) (Source: Adapted from (BSDF, n.d.))

Molina et al. (Molina et al., 2015) evaluated the capability of the genBSDF to assess the solar bidirectional properties of CFSs. They used genBSDF to calculate the solar BSDFs of 16 different cases of a venetian blinds by varying the materials (i.e., different solar optical properties) and the slope angle of the slats. They compared the results generated by genBSDF with the Radiosity-based program WINDOW (LBNL, 2017). They concluded that the genBSDF was more precise than the WINDOW program

when it was used to assess the solar bidirectional properties of CFSs.

Vera et al. (2016) proposed an optimization method to integrated lighting and thermal simulation at the design stage of buildings that incorporates CFSs. In the study, they used an office in San Fransisco as an example to show that their methodology was flexible enough to simulate the CFSs.

Later in 2017, Vera et al. (2017) studied a fixed exterior CFS component of offices located in Montreal, which was a set of horizontal, opaque, curved, and perforated louvers. In their optimization, the design variables were the percentage of perforations, the tilt angle, and the spacing of the louvers. The objective functions were the building energy performance as well as metrics related to visual comfort. Both of these two studies used genBSDF to obtain the BSDFs of each combination of CFS design variables. In the study, they showed each BSDF generated in genBSDF must be assembled for each window glazing to obtain the BSDF of the entire fenestration system and solar absorption of each layer. To accomplish this, the BSDF generated in genBSDF was imported into WINDOW 7 (LBNL, 2017) as a shading layer to generate the BSDF of the entire CFSs. Next, all the BSDF data were then integrated into the control strategy using the mkSchedule¹¹ software, which generated the hourly annual schedule with the CFS position and the power fraction of the luminaires. The schedule was then connected to EnergyPlus and Radiance for the energy and lighting simulations. The GenOpt

¹¹ mkSchedule is a tool that integrates the thermal and lighting analyses in a space (Vera et al., 2016). This program implements the method using control sensors of McNeil to generate the annual schedule for the louver position of a movable CFS and the power fraction of controlled luminaries (McNeil et al., 2013; McNeil and Lee, 2013).

optimization engine with the hybrid PSO-HJ algorithm was coupled to mkSchedule, Radiance and EnergyPlus to select the improved performance results. They concluded that the optimization of a CFS must include an analysis of visual comfort because optimal energy performance metrics must include an acceptable visual comfort for the occupants.

Bustamante et al. (2017) evaluated the daylighting and thermal performance of movable CFSs. They tried to reduce the energy consumption while ensuring acceptable visual comfort by integrating energy and lighting simulation. They used the same method as Vera et al. (2016, 2017) to simulate the CFSs performance. In their analysis, the CFS control strategy also used the mkSchedule software to generate a schedule for the CFS position and the luminaires' power fraction. The generated schedule was also connected to EnergyPlus and Radiance for energy and lighting simulation. They used an office space with two different movable CFSs (i.e., movable venetian blinds and perforated curved louvers) and controlled dimmed luminaires in four cities. The four studied cities are Montreal, Canada; Boulder, USA; Miami, USA; and Santiago, Chile. Their work demonstrated how the mkSchedule tool helped to make improved decisions about the shading and control strategies of CFSs to deliver acceptable visual comfort and minimize annual energy consumption.

In summary, the previous studies provided methods to simulate CFSs. They validated the tool genBSDF to assess the solar-optical properties to obtain the BSDFs of each combination of CFS design variables. The BSDF generated in genBSDF was imported into the WINDOW software as a shading layer to generate the BSDF data of

the entire CFSs. Later, The BSDF files were exported to the mkSchedule software with control algorithms to generate the hourly annual schedules with the CFS and the power fraction of the luminaires. The annual schedules were then connected to EnergyPlus and Radiance program for the energy and lighting simulations. However, their combined analysis process is complex and requires data processing that goes well beyond the reach of practicing architects. For example, the process of generating the BSDF data file of entail CFSs is a time-consuming process that require tedious programming skills. In addition, the control algorithms in mkSchedule are defined using Lua¹² scripts, which are not widely used by practicing Architects. Finally, the control in mkSchedule can be based on weather file information or on the output of daylighting simulations, but it cannot be based on thermal parameters.

2.9.5. Shading Devices

Shading systems can control the penetration of direct sunlight and optimize the distribution of natural daylight in a building. When designed properly shading system can have the potential to save a significant portion of the annual energy consumed for cooling and lighting, while minimizing any heating load penalties. Various types of shades have been developed to minimize direct sunlight and maximize daylighting. Shading devices mainly consist of three types based on their position, which include: external shading, internal shading, and the shading between the glass panes of a multi-

¹² Lua is an open-source lightweight, multi-paradigm programming language designed primarily for embedded systems and clients (“Lua”, 2017).

pane window. Shading devices can also be divided into two categories: static and dynamic shades based on their performance.

2.9.5.1. Static Shading Devices

Static shading devices are simple, affordable, and easy to implement daylighting systems. However, static shading devices are limited to the amount of direct sunlight they can block due to the changes of the solar angle and sky conditions. Different types of static shading are presenting in Figure 2.16. The shading types include: overhangs, horizontal louvers, vertical louvers, light-shelves, blind systems, side fins, and combinations of shades. There are many previous studies about static shading systems, including: David et al. (2011), Rapone and Saro (2012), Manzan (2014), González and Fiorito (2015), and Khoroshiltseva et al. (2016).

David et al. (2011) assessed the efficiency of different types of solar shades by comparing the thermal and daylighting performance. To accomplish this, they used EnergyPlus to simulate both the thermal and daylighting conditions to find a balance between effective solar protection and a suitable level of natural lighting. In their work, they used a shading coefficient, cooling load demand, daylight autonomy, and useful daylight illuminance as indexes for rating the performance of different types of external shades, such as: overhangs, rectangular side fins, triangular side fins, and louvers. These four indices were applied to compare the energy and visual behavior of the shading devices. The results showed that the use of the proposed indices gave correct advice for designer to choose the best shading type and sized the shading accordingly.

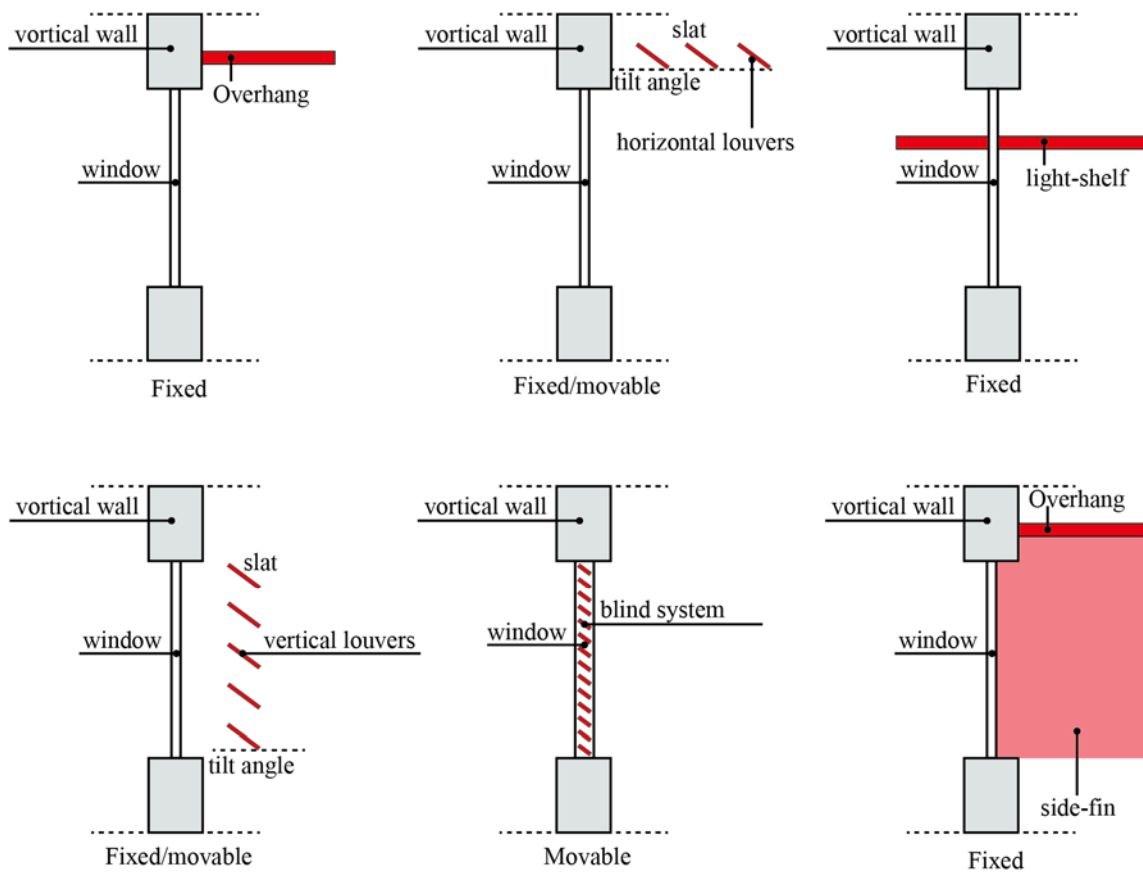


Figure 2.16 Main Shading Type (Source: Adapted from (Bellia et al., 2014))

Rapone and Saro (2012) used the Particle Swarm Optimization (PSO) to find the optimal value of the envelope features based on the energy performance simulated by the EnergyPlus program. They studied typical curtain wall façades with horizontal louvers for an office building in London, England. They tried to obtain the optimal combinations of the types of glazing installed, window-to-wall-ratio, depth and spacing of the louvers, which lead to the minimum amount of carbon emissions required based on delivering the desired indoor lighting conditions (500 lux) in the office. They also provided a method to find near optimal solutions in a shading design using the PSO algorithm.

Manzan (2014) studied an office with a South-facing window to find the optimal shading designs. In this study, the shading device consisted of two large horizontal flat panels that were inclined on its horizontal axis. The design variables were the height, width, and slope of the flat panels, as well as the distance of each panel from the window. This study used DAYSIM (Reinhart, 2010; Reinhart, 2017) to calculate the electricity required for artificial illumination. After DAYSIM was run, the hourly electricity load was transferred to the ESP-r simulation¹³ as an internal heat gain to simulate the energy consumption for heating and cooling the space. In addition to DAYSIM and ESP-r Manzan used the modeFRONTIER (Poles et al., 2008) tool with the non-dominated sorting genetic algorithm (NSGA-II) for optimization. However, their optimization focused only on minimizing the energy consumption without considering the visual comfort or thermal comfort of the office.

González and Fiorito (2015) proposed a method to achieve optimal external shading design based on the daylight and energy performance metrics calculated with the DIVA software (Reinhart et al., 2011) and Galapagos software (Rutten, 2007). In this study, they also used horizontal louvers as shading devices. The design variables were the depth, slope angle, and number of louvers. The cost functions were the energy consumption and CO2 emissions. In this study, they compared the optimum results to cases without shading and cases with traditional shadings (i.e., external metallic louvers

¹³ ESP-r is a building performance analysis tool that can be used for a wide variety of analysis. ESP-r integrates different individual analysis to provide an integrated solution (Clarke et al., 1998). ESP-r can be linked with the RADIANCE simulation tool to perform daylighting simulation (Clarke et al., 1998).

and horizontal overhangs). Although the study evaluated Daylight Autonomy (DA) and Useful Daylight Illuminance (UDI) for the optimum solution, the daylighting metrics were not part of the cost function used in the optimization process.

Khoroshiltseva et al. (2016) developed a multi-objective optimization of external shading devices for an apartment. The goal of this work was to increase indoor thermal comfort and reduce annual energy consumption. To accomplish this, they designed shading devices for two South-facing windows and two West-facing windows, and used optimization tools with smart search algorithms that included a Pareto front (Balling et al., 1999) to find the appropriate shading device. According to the size of the windows, the West and South overhangs were fixed equal to 0.525 m and 0.7595 m respectively, and all lateral fins were equal to 0.6 m. The area of the shading device was the sum of the areas of all the elements of the device (fins and overhangs) surrounding the windows. The results found that the best solutions were shading devices with an area equal to 7.84 m². In addition, their solution provided a 20.2% reduction in overheating. However, it caused a 16% increase in overall energy consumption.

2.9.5.2. Dynamic Shading Devices

Dynamic Shading systems, similar to static shading systems, can provide shading, redirect daylight deeper into the space, improve visual comfort, and reduce glare. Dynamic shading systems alter the shading tilt angle and position based on the solar elevation angle, sky conditions, and occupant comfort preferences. Dynamic window shading technologies often use conventional components such as louvers, venetian blinds, and shades that can be located internally, externally or in between glass

panes (Lee et al., 1998). The movement of the shading device to block the entry of direct solar radiation through the window can prevent overheating or glare. However, the movement can cause reduced user satisfaction and a reduced levels of interior illuminance. Thus, the control algorithms for the dynamic shading movement are very important. The control algorithms should control the movement of the shading device to not only enhance the visual and thermal comfort, but also to substantially reduce the energy usage of the building. There have been a number of studies that have investigated the issues of dynamic shading system, including: Firląg et al. (2015), Skarning et al. (2017), Shen and Tzempelikos (2017), and Choi et al. (2015, 2017).

Firląg et al. (2015) analyzed the influence of control algorithms for dynamic windows on energy consumption. They developed and compared five different control algorithms, which include: Heating/Cooling (i.e., the shade position is up when heating on and is down when cooling on), Simple Rules (i.e., shade is up when the external temperature exceeds 17 °C, otherwise it is down), Perfect Citizen (i.e., if interior room temperature is higher than the cooling set point of 26 °C, the shading is on, or if it is lower than the heating set point 21 °C, the shading is down), Heat Flow, and a Predictive Weather Forecast. In the analysis, they used EnergyPlus to perform the energy simulation. The control algorithms were set in the Energy Management System (EMS)¹⁴ in EnergyPlus, which controlled the shading to be either completely up or completely

¹⁴ The Energy Management System (EMS) in EnergyPlus is a system of computer-aided tools used by operators of electric utility grids to monitor, control, and optimize the performance of the generation and/or transmission system (“Energy Management System”, 2016).

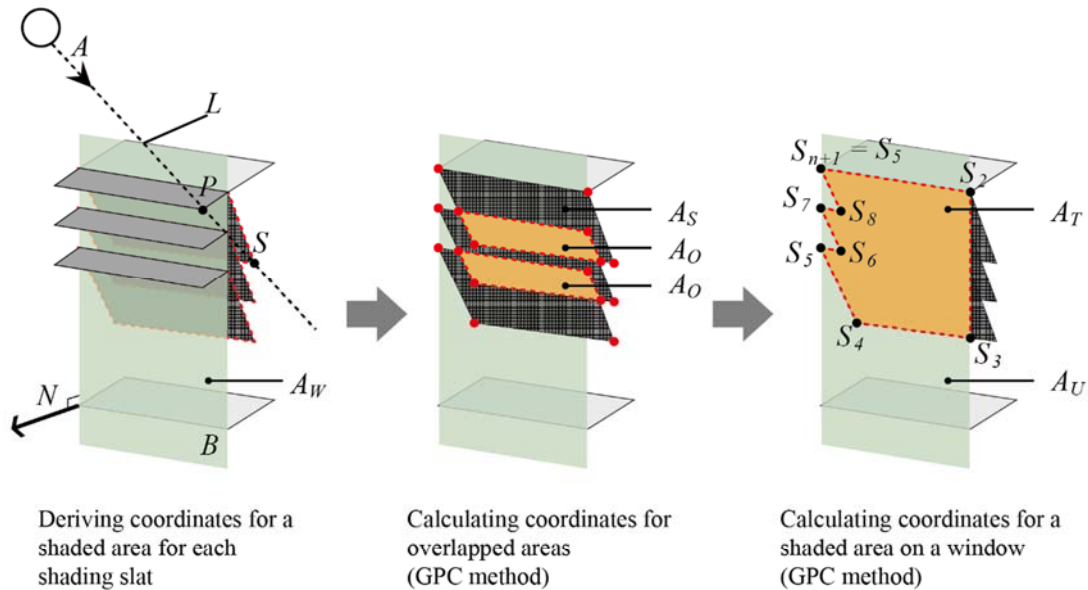
down. They used the WINDOW 7 (LBNL, 2017) program to generate a Bi-directional Scattering Distribution Function (BSDF) file, which describe the optical performance of the dynamic shading systems. These BSDF files were exported to EnergyPlus using the IDF file format to calculate the thermal performance. They compared the total annual energy usage of: no shade, always shaded, half shade, and five automated control algorithms, and found that the use of the automated shading with the proposed control algorithms reduced the site energy use in the range of 11.6–13.0%. In addition, they found the energy usage differences between the five control algorithms were very small. Overall, the best energy performance results were from the perfect citizen-controlled algorithm.

Skarning et al. (2017) investigated dynamic shading compared to solar control coated glazing in well-insulated residential buildings. They considered the transmittances of light and solar for the different shading strategies. They used a loft room with a sloped roof with windows in near zero-energy homes in Rome and Copenhagen, Netherland, to compare energy, daylighting, and thermal comfort for various combinations of window size and glazing properties, with or without a dynamic shading. EnergyPlus was used to simulation the annual energy consumption. They used the Adaptive Thermal Comfort model from EN 15251 (CEN, 2007) for the thermal comfort evaluation. In addition, the daylighting autonomy (DA) was used for evaluation of daylighting performance using the simulation tool DAYSIM. The dynamic shading device was an external roller shade that was activated when the outdoor air temperatures exceeded 18 °C or the total diffuse and direct solar irradiation on the window was above

300 W/m². The results showed that without dynamic shading the lowest heating demand was obtained with the highest possible SHGC (0.48 in Copenhagen and 0.42 in Roma). The heating and daylighting demand using dynamic shading could be replaced by either increasing the SHGC by 0.3 or by the use of 10% larger glazing-to-floor ratios without shading. They concluded that the dynamic shading had no advantages over well-designed permanent glazing solutions for daylighting and that it did not improve the optimum space heating demand of the loft room. They recommended using the solar-control coating rather than dynamic shading devices. However, this study had limitations. First, they did not consider glare. Second, they only tested two cases in a heating dominated climate. Third, they only considered residential buildings.

Shen and Tzempelikos (2017) proposed a simplified model-based control strategy for roller shades. They controlled the roller shading movement to intermediate positions to maximize daylight utilization while avoiding visual discomfort. Their control algorithm involved two steps to prevent direct sunlight from falling on the work plan area and then to protect the space from excessive indoor illuminances (2000 lx). They implemented this shading control strategy in full-scale test offices in Lafayette, Indiana, USA, for different sky conditions and sun angles, during a period of several months. The results showed that the shading control strategy improved energy savings from 50 - 75% compared to a base case with no lighting controls. In addition, the control strategy was also implemented in an integrated daylighting and thermal model to investigate the annual performance for different locations and orientations. They concluded that the synchronized control method could be applied to any shading, glazing

properties, locations, orientation, room configuration, and multiple exterior façades equipped with roller shades to accomplish significant energy savings when integrated with efficient lighting.



A Direction vector of the sun	N Normal vector of plane B	A_U Unshaded area of glazing
L Straight line of \vec{AP}	B Plane of the facade	A_S Shaded area of each slat
P Point on shading elements	A_W Glazed area	A_O Overlapped area
S Point on shaded areas	A_T Total shaded area of glazing	S_i Point on total shaded areas

Figure 2.17 Shaded Area Calculation Process Using the Polygon Method (Source: Adapted from (Choi et al., 2015))

Choi et al. (2015) introduced a dynamic calculation method for deriving shaded fractions of irregular shapes and movement changes with kinetic façades. They used the planar-polygon method (Feito et al., 1995) to calculate the shaded fractions (F_s) by considering the position of sun, climate data, the shading device shapes, and the movement of shading devices. In the method, the shaded area is formed as the shape of the shading elements is projected onto the glazing by the solar rays. They used three

steps to calculate the shaded area (Figure 2.17). First, the planar-polygon method calculated the projection shape of shades onto a plane by connecting the projected coordinates with lines or curved lines. Second, the General Polygon Clipper (GPC)¹⁵ (Murta, 2017) was used to calculate the coordinates of overlapped area of two or more polygons for exclusion. Third, the overlapped area was then subtracted from sum of the shaded area on the window. The range of movement directions was divided into n steps of equivalent intervals to account for movements of the shading elements. The shaded fraction (F_s) estimation equation has movement steps (M_n), which are used as a variable to operate the movement of shading devices in order to simplify the complex calculation process. The results showed that the estimation equation can estimate the shaded fraction relatively accurately. To demonstrate this method, they implemented a calculation tool for calculating the shaded fraction for kinetic façades. This shaded fraction, with movement steps, can be applied into whole-building thermal simulations to improve daylighting and thermal performance of buildings.

Choi et al. (2017) also conducted a whole-building simulation and experimental study of dynamic shading devices to test the shaded fraction and movement steps control algorithm method they proposed in 2015. In a similar fashion as the previous work, the shaded fraction was calculated using the planar-polygon method that calculated the precise shaded area on a window according to the solar angle and the geometrical shapes of various shading devices for each time step. They proposed three goals to control the

¹⁵ The General Polygon Clipper (GPC) is a software library providing for computing the results of clipping operations on sets of polygons (Murta, 2017).

dynamic shading devices, which are: Mode 1 for energy conservation; Mode 2 for glare protection and energy conservation; and Mode 3 for glare protection, illuminance satisfaction, and energy conservation. In this study, they used the new shading calculation tools to generation the shaded fraction (F_s) corresponding to the movement steps (M_n) of dynamic shading devices based on the local weather, solar angle, building information, and shading device geometry. The shaded fraction file (F_s and M_n) was then imported into the energy simulation tool and the daylighting simulation tool for calculating the energy use, glare, and illumination levels. They obtained an optimal movement step (M_n) for the shading device at each hour according to the three goals of the control modes. They confirmed the three control algorithms for the shading device that were derived from simulations in a life-sized mock-up office building. The experimental study showed that the shaded fraction control algorithm could provide users with options for controlling the movable shading device on a building according to various operation goals.

2.9.5.3. Summary

In summary, for the static shading devices, the previous studies tried to find optimal shading designs based on the daylighting and thermal performance of the room being shaded. However, these did not consider the dynamic daylighting metrics, such as sDA+ASE to evaluate the daylighting performance. More importantly, the previous studies did not consider the use of the glare indices and thermal comfort indices to provide a more comfortable interior environment.

Regarding dynamic shading devices, the previous studies proposed two methods to simulate the dynamic shades. The first method is to simulate the dynamic shading system using the BSDF data, which is similar with the CFS simulation methods. The second method is to generate shaded fraction (Fs) corresponding to the movement steps (Mn) file of the dynamic shading devices based on the local weather, solar angle, building information, and shading device geometry. The shaded fraction file and the movement steps (Fs and Mn) can be imported into an energy simulation tool and into a daylighting simulation tool for calculating the energy use, glare, and illumination levels. Several control strategies have been proposed to control the movement of shading to improve the thermal and visual performance. However, due to the different comfort preferences and activities of different individuals, there are challenges to implementing a flexible control system to obtain the optimum energy savings, thermal comfort, and visual comfort. Furthermore, since dynamic systems typically utilize sensitive and delicate components that will increase the cost of system and maintenance fees, there is a need to investigate the potential of using other design strategies to replace or supplement the dynamic shading that have lower costs.

2.10. Overall Summary of the Literature Review

This literature review surveyed the previous work on: daylighting performance indicators, glare indexes, thermal comfort models, daylighting simulation methods and tools, different energy simulation tools, parametric modeling tools, optimization algorithms and tools, and design strategies. It also provided information on the strengths,

capabilities and the shortcomings of each tool, different methods, and design strategies.

The following are the findings from this literature review:

1. In the previous studies, several shortcomings were identified. For example, not all the studies considered both thermal and visual comfort for optimal design. In addition, dynamic daylighting performance indexes (sDA+ASE) were seldom used to evaluate the daylighting environment in design strategies. The use of sDA+ASE indicators and glare matrices provides a more accurate criterion to evaluate the daylighting performance. Finally, for the thermal performance, the use of ASHRAE 55-2017 Standard with an adaptive thermal comfort model, suggests a more sophisticated method to evaluate the indoor thermal environment.

2. Based on the previous works, the Daylight Factor methods do not accurately predict the illumination levels at a point on a plane for a time varying sky luminance distribution. In addition, the Daylight Factor method does not accurately predict illumination levels directly from the sun (Tsangrassoulis and Bourdakis, 2003). In contrast, Daylight Coefficient (DC) methods can be used to calculate a time series of illuminances and luminances in buildings accurately (Tsangrassoulis and Bourdakis, 2003). Finally, a climate-based DC method can be used to calculate the annual dynamic daylight performance metrics such as daylight autonomies (DA) and useful daylight illuminances (UDI) (Nabil and Mardaljevic, 2005).

3. RADIANCE-based daylighting simulation tools are the most accurate daylighting simulation tools that are climate-based; such tools use the ray-tracing and Daylighting Coefficient methods for predicting indoor illumination levels. Table 2-4

shows a comparative analysis (i.e., their strengths and limitations) of the different daylight simulation tools presently available.

4. There are several combined simulation tools that can both simulate daylighting and thermal performance to analyze the impact of both on the energy performance of the building, such as: DOE-2 (Winkelmann, 1983); eQuest (Hirsch, 2006), and EnergyPlus (Crawley et al., 2000). However, the daylighting calculation methods they employ are limited. For example, DOE-2 and eQUEST (DOE-2.2) use limited sky models and employ the split-flux method calculation for Internal Reflected Component (IRC) that only predicts the illumination levels at two points in a zone for certain kinds of room configurations. In contrast, EnergyPlus offers four different sky models, and offers both the Split-flux and Radiosity methods for calculating IRC.

5. Tools that only perform daylighting simulation, such as RADIANCE and DAYSIM that use the backward ray-tracing method to calculate the internal reflection can calculate more accurate daylighting results and simulate more complicated shading devices. However, such tools cannot directly simulate the impact of daylight on building energy consumption.

6. There have been many attempts to couple advanced thermal and daylighting simulation tools to achieve better results. Since these coupled simulation methods provide an improved analysis over tools with less accurate analysis methods. There is a need to use coupled methods to better simulate the performance of buildings incorporating daylighting strategies. All of the previous studies showed that integrating more advanced daylighting analysis into DOE-2 or EnergyPlus enables projects to be

more accurate in their assessment of the overall energy benefits of a daylighting design. Of all the coupled daylighting and thermal simulation tools, DIVA 4.0 and EnergyPlus for Grasshopper not only can simulate the more accurate daylighting performance, but can also automatically transfer the daylighting results into the thermal simulation. More importantly, the DIVA model in grasshopper can be used as a parametric model, which can easily provide rapid analysis of multiple optimal daylighting design strategies. Therefore, this research uses a coupled simulation using DIVA 4.0 and EnergyPlus for Grasshopper to simulate the daylighting and energy performance.

7. Since building design analysis is a complicated task that must counter-balance various parameters and constraints, simulation-based optimization is a promising approach to solve complex design problems with single-objective or multi-objective methods. The most widely-used meta-heuristic search algorithms (e.g., GA, NSGA-II, and PSO) and its implement tools (e.g., Galapagos, GenOpt, and modeFRONTIER) are the most promising techniques to apply to complex building optimization problems.

8. There are many studies that have researched window size and placement in both sidelight and toplight applications. However, these studies did not always consider the influence of the window placement within the wall or roof (i.e., position of the window in the exterior wall or roof), nor they did not analyze how the daylighting affects the thermal performance. One study conducted by Acosta, Munoz, et al. (2015) studied window size and placement based on the analysis of the daylight factor under overcast sky conditions. They concluded that square windows in the center of the wall produced daylight factors slightly higher than those obtained with horizontal windows

and noticeably higher than those measured with vertical windows, considering the same surface area of the openings. Studies showed windows in the upper position allow higher luminance at the back of the room versus those in locations centered in the exterior wall.

9. For the monitor skylight designs, the most relevant studies were conducted by Acosta (Acosta,Munoz, et al., 2015; Acosta et al., 2013; Acosta,Navarro, et al., 2015; Acosta et al., 2012). Unfortunately, these studies only considered the daylighting factor. They did not consider dynamic daylighting matrices, the visual comfort, and thermal consumption. In addition, the studies did not always consider the impact of daylighting on both visual and thermal performance.

10. The previous studies provide a method to evaluate CFSs performance. They also validated the genBSDF tool to assess the solar-optical properties to obtain the BSDFs of each combination of CFS's design variables. In the previous studies, the BSDF generated in genBSDF was imported into the WINDOW software as a shading layer to generate the BSDF data of the entire CFSs. Later, The BSDF files were exported to a control tool (i.e., modeFRONTIER or mkSchedule) with control algorithms to generate the hourly annual schedules with the CFS position and the power fraction of the luminaires required to maintain a predetermine illuminance level. The annual schedules were then connected to EnergyPlus and Radiance for the thermal energy and lighting simulations.

11. For the dynamic shading, the previous studies proposed two methods to simulate the dynamic shading. The first method was to simulate the dynamic shading system using the BSDF data, which is quite similar with the CFSs simulation methods.

The second was to generate a shaded fraction (F_s) corresponding to the movement steps (M_n) file of dynamic shading devices based on the local weather, solar angle, building information, and shading device geometry. The shaded fraction file (F_s and M_n) is then imported into the energy simulation tool and the daylighting simulation tool for calculating the energy use, glare, and illumination levels.

2.11. Issues Identified

The previous studies covered daylighting and thermal simulations, single-objective optimizations, multi-objective optimizations, as well as the building design strategies (i.e., building shape and orientation, window size and placement, complex fenestration system, static shading devices, and dynamic shading). However, there were many issues that were identified below:

- 1, Radiance mainly has three main limitations when used for daylighting simulation, which made an optimization process extremely time consuming. Radiance is a very time-consuming climate-based daylighting simulation program. In order to obtain high accuracy annual daylighting results, the Radiance runtime would be more than one hour, which makes an optimization process extremely time consuming. In addition, Radiance annual daylighting simulation results can have a huge difference in rendering runtime. Unfortunately, this can be a problem since the low-quality preset rendering has the lowest sDA and highest lighting energy. This issue makes it is impossible to use the low quality preset in daylighting optimization to save the runtime.

2. Although the previous literature used coupled daylighting and thermal simulation methods to analyze the daylighting impact on the overall building energy usage, the data exchange between the different simulation programs is not fully automatic, nor is it well-documented.

3. In addition, coupled simulation methods were seldom used by the previous studies to develop the optimal design decisions that included daylighting strategies. Therefore, there is a need to further analyze and classify the capabilities of different design simulation tools to obtain better understand how improved building energy simulation methods can adequately address daylighting. To accomplish this, improved simulation programs will be used to analyze building façade design strategies to provide the most accurate guidance to architects to help them better select the best combination of architectural features (i.e., building shape, size, orientation, window placement, daylighting, utilization, heating/cooling loads, etc.). These coupled simulations can be contracted to the less-accurate combined simulation to determine the design in daylighting strategies.

4. The previous studies have shown that Multi-Objective Optimization (MOO) is needed to make design decisions. Such MOO can be analyzed with either the weighted sum function or Pareto front function. However, both techniques have advantages and disadvantages. The Pareto front solution focuses on exploiting the diversity of many different solutions, but often suffers from calculation inefficiency. In contrast, weighted sum methods are more efficient to implement. However, weighted sum methods require

prior knowledge of two or more objective functions, and often do not provide information about how the method compromises between the objectives.

5. Previous studies have shown that optimization algorithms are successful at finding high performing daylighting or thermal design solutions. They might provide a computational simulation and optimization system to solve the design problems. However, many of these previous studies did not provide general suggestions for architects during the preliminary design process.

6. Many studies have investigated the window size and placement issues. However, most of the previous studies did not consider the influence of window placement within the wall. Only a few analyzed how the daylighting affects the thermal performance. Therefore, there is a need to use the most accurate daylighting tool, coupled to the thermal simulation tools to better analyze window placement and location in regards to the both daylighting and thermal performance. In addition, a more effective method needs to be proposed to better determine how the design of window size and placement affects the building performance. Finally, such coupled daylighting and thermal simulation program should provide feedback to designers and architects based on daylighting and thermal performance.

7. In one of the previous studies, Caldas and Norford (2002) used Genetic Algorithms (GAs) (Goldberg, 1989) combined with the DOE2.1e simulation program to calculate the thermal and daylighting analysis to better inform the architectural design practice. In this analysis, feedback loops between architecture design decisions and the environmental impact (i.e., energy consumption) were used to inform specific designs.

However, there were limitations in the simulation process used in this study that were not fully explained. First is the fact that all the windows in the simulations were centered in the middle of each façade, which does not reflect all types of daylighting strategies related to window locations (Reinhart and Stein, 2014). Second, no supporting documentation was provided to help the reader with details about the simulation (e.g., the placement of the daylight sensors within the zone, etc.). Third, they did not consider the visual and thermal comfort. Therefore, there is a need to reinvestigate the daylighting strategies in this research using a more sophisticated daylighting analysis that can analyze off-center placement of fenestration, and daylighting strategies such as light-shelves based on the visual and thermal comfort. In addition, such an effort needs to be well-documented so that can learn from the study.

8. The methods of simulation the CFSs and dynamic shading system using the BSDF data involves several simulation tools. However, the process of the generation the BSDF dataset file of entail CFSs is a time-consuming process that is not easily used. In addition, manually transferring the data from one tool to another is time consuming and error-prone. For example, the control algorithms in the mkSchedule program are defined using Lua scripts, which is not widely used by practicing Architects. In addition, although the control in mkSchedule can be based on weather file information or on the output of daylighting simulations, but it cannot be based on thermal parameters.

9. Finally, several control strategies have been proposed to better control the movement of shading to improve the thermal and visual performance of the simulated space (i.e., dynamic shading). However, due to the different comfort preferences and

activities of individuals, there are challenges in implementing a flexible control system to obtain the optimum energy saving, thermal comfort, and visual comfort. Furthermore, since dynamic systems typically utilize sensitive and delicate components that will increase the cost of system and maintenance fee, there is a need to investigate the potential of using other design strategies to replace the dynamic shadings and reduce overall costs.

3. METHODOLOGY

3.1. Overview

This chapter discusses the research methodology used in this study. The flow chart in Figure 3.1 shows the steps in the methodology. All simulations of this study are conducted on a commodity personal laptop embedded with an Intel i7-8650U processor with 4 cores @ 2.11 GHz and 16GB RAM.

The methodology is composed of five tasks:

1) reproduce the office models used by Caldas and Norford (2002) to obtain the building simulation parameters used in their study;

2) build a combined daylighting + thermal simulation that uses Radiance (DIVA) and EnergyPlus (Ladybug & Honeybee) through the Grasshopper interface. Develop and test a prototype for the combined daylighting + thermal simulation by comparing the combined simulation methods of DOE-2 + Split-Flux, EnergyPlus + Split-Flux, EnergyPlus + Radiosity, and EnergyPlus + Radiance;

3) develop an improved Radiance annual daylighting simulation method that produces acceptable results while minimizing run time.

4) develop a window design plugin in grasshopper using Python script. This window plugin can generate over thousands different window designs with different sizes and locations that can be used in optimization.

5) apply window design plugin in parametric modeling with Multi-Objective Optimization for window size and placement to determine the best design for North, South, East, and West orientations. Radiance connect to EnergyPlus to perform the

combined daylighting + thermal simulation. The sDA, ASE, lighting electricity use, cooling load, and heating load are the objectives of the optimization.

After finishing all five tasks, a guide will be proposed for architects/engineers to help determine proper window size and placement on a façade that reduces energy use while maintain acceptable indoor environment quality.

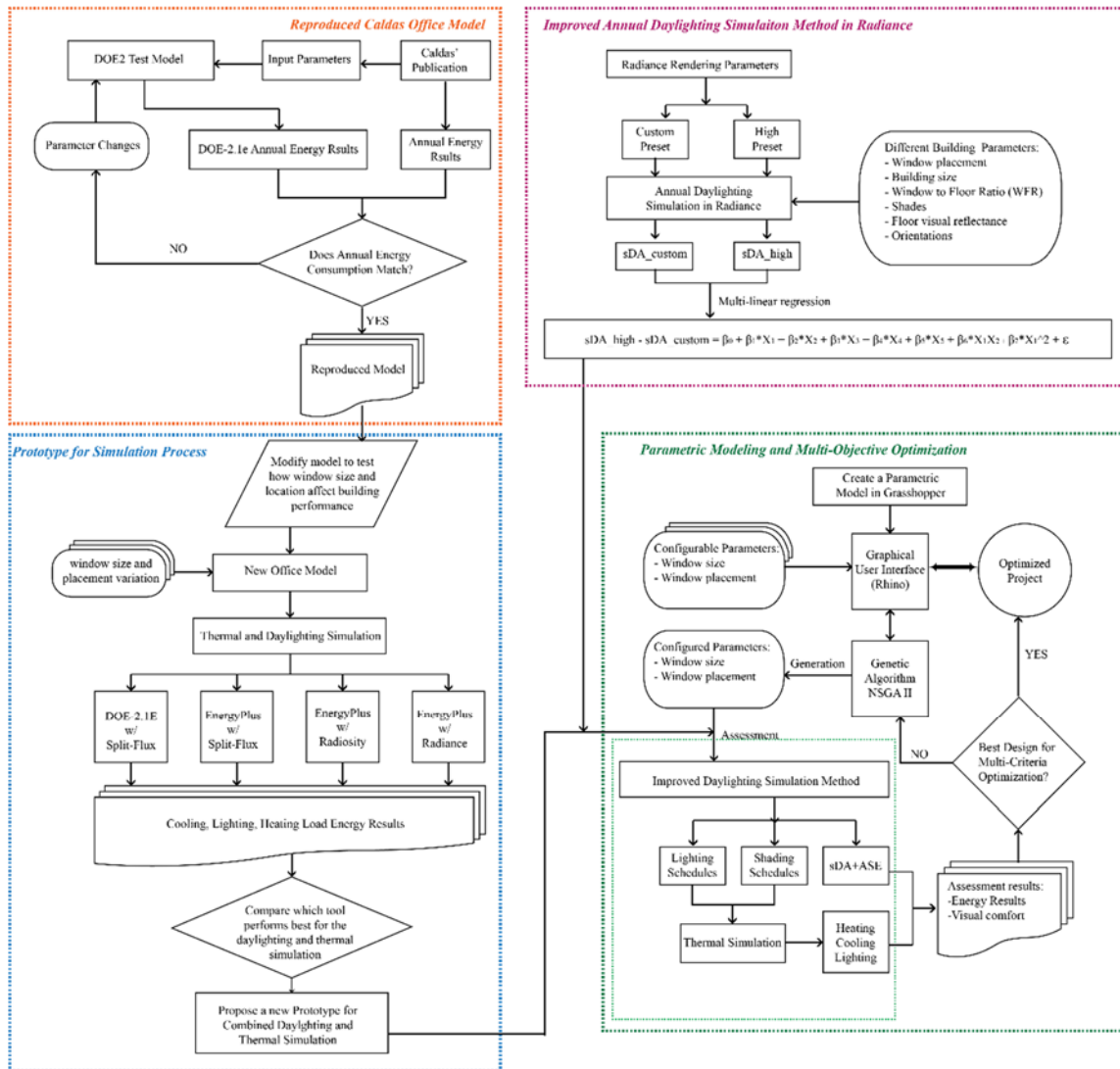


Figure 3.1 Overview of Research Methodology

3.2. Reproduce the Caldas Office Model Using Empirical Testing

Figure 3.2 shows the tasks required to reproduce the Caldas office model using empirical testing to determine input parameters. First, the DOE2.1e sample model RUN_3A is used as a beginning model of DOE-2 test model. Second, the parameters inputs in the RUN_3A model are changed according to the paper of Caldas and Norford (2002), and the relevant information from paper's references Sullivan et al. (1987) and Sullivan et al. (1992). Third, the annual energy results are obtained from the DOE2.1e, and the simulated annual energy results will compare with the annual energy results published in Caldas and Norford paper. Finally, the input parameters in DOE2.1e model are modified and changed by the empirically-determined tests until it produced the same annual energy use listed in the Caldas publication.

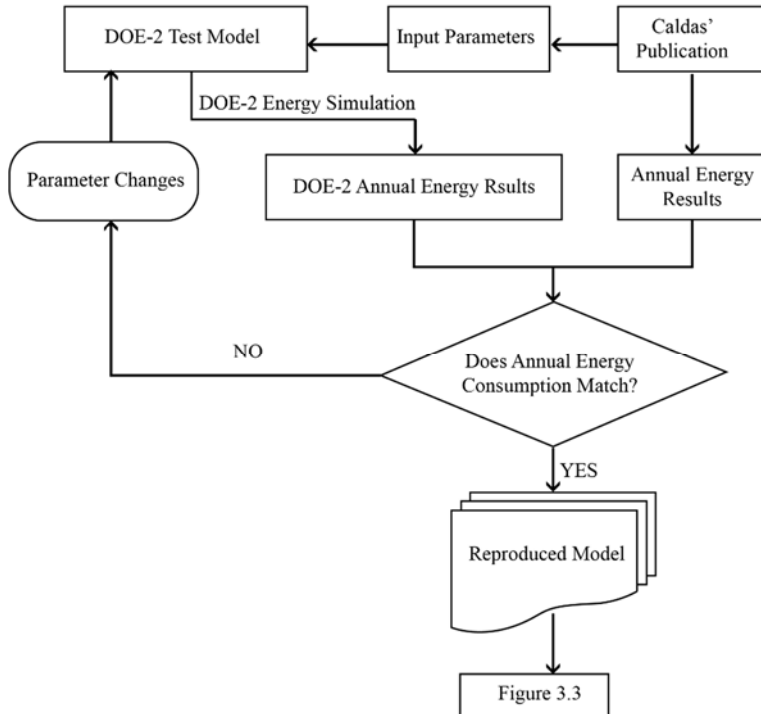


Figure 3.2: Reproduced Office Model

3.3. Propose Prototype for the Simulation Process and Tools

The proposed building will be changed to a single zone open-plan space. Figure 3.3 shows the steps for the proposed new prototype for the simulation process and tools.

First, in order to test the effect of window sizes and placements, the Caldas model was modified. In the new model, only one exterior wall has windows, the other three walls, roof, and floor are set to have no heat transfer (i.e., adiabatic). The window size, wall insulation, and window properties follow ASHRAE Standard 90.1-2016.

Second, the new office model with different window sizes and placements (but with same window area) will be tested and compared the simulation results from different tools, which include DOE2.1e + Split-Flux, EnergyPlus + Split-Flux, EnergyPlus + Radiosity, and EnergyPlus + Radiance.

In these testes, the combined EnergyPlus and Radiance simulation will be connected using the Grasshopper interface. In this combined method, the Radiance model conducts the daylighting simulation to obtain the more accurate results (i.e., lighting and shading schedules). Later, the results will be shared with the energy simulation tool EnergyPlus to obtain more accurate lighting, heating and cooling consumption.

Finally, in the methodology, the results from different simulation tools within different window models will be compared, and a prototype will be proposed for the combined daylighting + thermal simulation method.

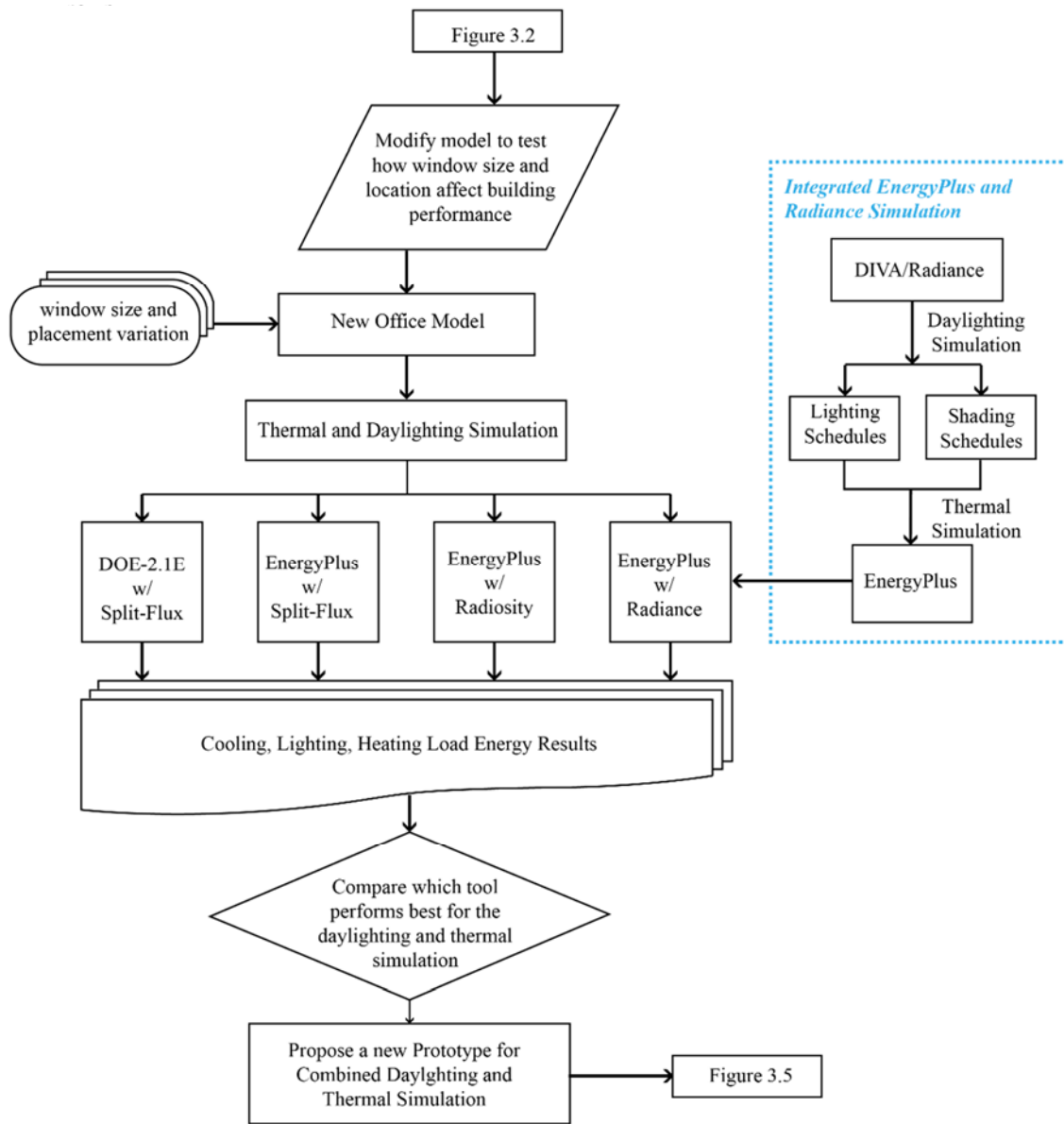


Figure 3.3: Proposed prototype for simulation process and tools (Source: (Li and Haberl, 2020))

3.4. Propose an Improved Radiance Annual Daylighting Simulation Method

In addition to comparing daylighting analysis method, this study also had to resolve issues with the Radiance daylighting simulation because Radiance takes a very long rendering runtime to obtain relative accurate results. In Radiance, the annual

daylighting simulation results can have a huge difference with different rendering times. This is because the more accurate results need a much longer rendering runtime (i.e., more than one hour), which makes a daylighting optimization process extremely time consuming. Therefore, a reasonable Radiance runtime is crucial in an optimization design.

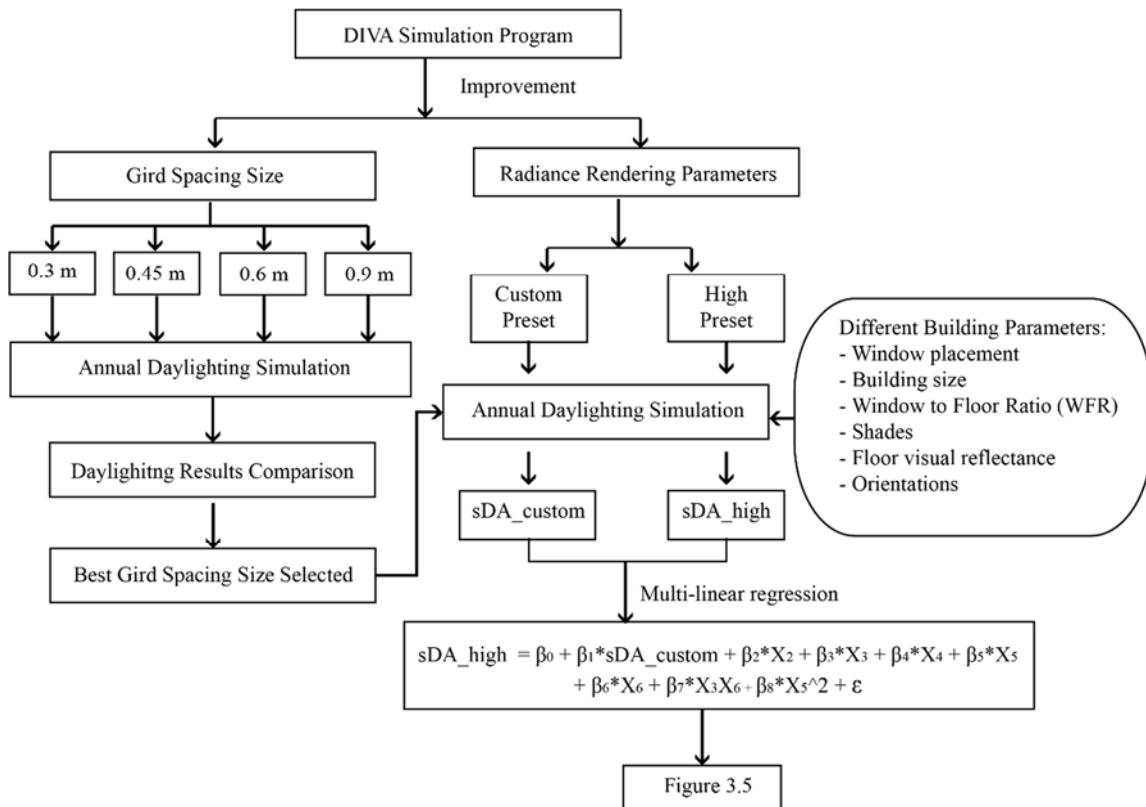


Figure 3.4: Improved Annual Daylighting Simulation Method in DIVA (Radiance)

To resolve this issue, this study proposes an improved Radiance simulation method for the daylighting optimization (Figure 3.4). In the new method, the Radiance rendering parameters were carefully reviewed and customized to reduce the runtime. Then, the annual daylighting results of the customized preset and the high-quality preset

will be compared and analyzed to develop correlations between custom preset and high-quality preset. In this way, sDA was corrected by using multi-linear regression Model.

The process is list below:

- 1) DIVA (Radiance) for Grasshopper will be used for the annual daylighting simulation;
- 2) Radiance rendering parameters were customized to reduce the Radiance runtime. This custom preset only needs 30 seconds to obtain the annual daylighting results. However, the results from this custom preset are less accurate than the high-quality preset in DIVA. Unfortunately, the high-quality preset can cost 1 hour or more in each daylighting simulation run to obtain the accurate annual daylighting results.
- 3) A series of sensitive tests with different office model sizes, window sizes, window locations, floor visual reflectance, building orientations, and shades were conducted to find the correlation between the custom preset and the high-quality preset.
- 4) The annual daylighting simulation results from both custom preset and high-quality preset were compared. A multi-linear regression model was used to correct the sDA daylighting results from the custom preset based on the results from high-quality preset in Radiance rendering.
- 5) The corrected sDA is one of the daylighting optimization objectives. In this analysis, a sDA below 55% was not consider accepted.

- 6) The lighting energy from custom preset was around 20% higher than the results from the high-quality preset. But the lighting energy will not be corrected. This is because the lighting energy profiles for the custom preset versus the high-quality preset were not significantly different.
- 7) In the analysis, the ASE is not affected by the changes in the Radiance runtime. This is because the ASE is calculated with only the direct sunlight.
- 8) The corrected sDA, ASE, and lighting energy will be the criteria of the multi-objective optimization in the daylighting analysis.

3.5. Parametric Modeling and Optimization

In order to find the best solution for a window design, a parametric study will be used. In the study, parametric modeling with the proposed daylighting and thermal simulation prototype from Section 4.3 (Figure 3.3) is used to generate the optimal window design. The improved DIVA (Radiance) simulation method from Section 3.4 (Figure 3.4) is used as the daylighting simulation in the optimization process. The parametric modeling and optimization simulation process is shown in Figure 3.5.

First, Grasshopper software will be used to build the parametric model. This model will use window size, window placement, and window shades as configurable parameters.

Second, a Genetic Algorithm will be used to generate the model with the configured parameters (i.e., window size, window placement, and window shades).

Third, the proposed analysis will use a runtime improved Radiance simulation

method for the daylighting optimization. The sDA, ASE, and lighting energy will be the criteria used for the multi-objective optimization in daylighting analysis.

Fourth, the daylighting simulation results (i.e., lighting schedules) will be connected to the thermal performance to perform the thermal optimization. The process lists below:

- 1) The results (i.e., lighting and shading schedules) generated by DIVA will be shared with the energy simulation tool (i.e., EnergyPlus) to obtain a more accurate heating and cooling consumption based on the thermal comfort model;
- 2) The dynamic daylighting metrics sDA+ASE, annual lighting energy use, cooling and heating load use will be compared and evaluated to obtain the optimum daylighting and thermal performance results.

Fifth, a Multi-Criteria Optimization will be conducted to help select the optimal window designs.

Finally, the results of the optimal, multi-criteria analysis will then be used to develop a framework for a daylighting design guideline for window size and placement for architects.

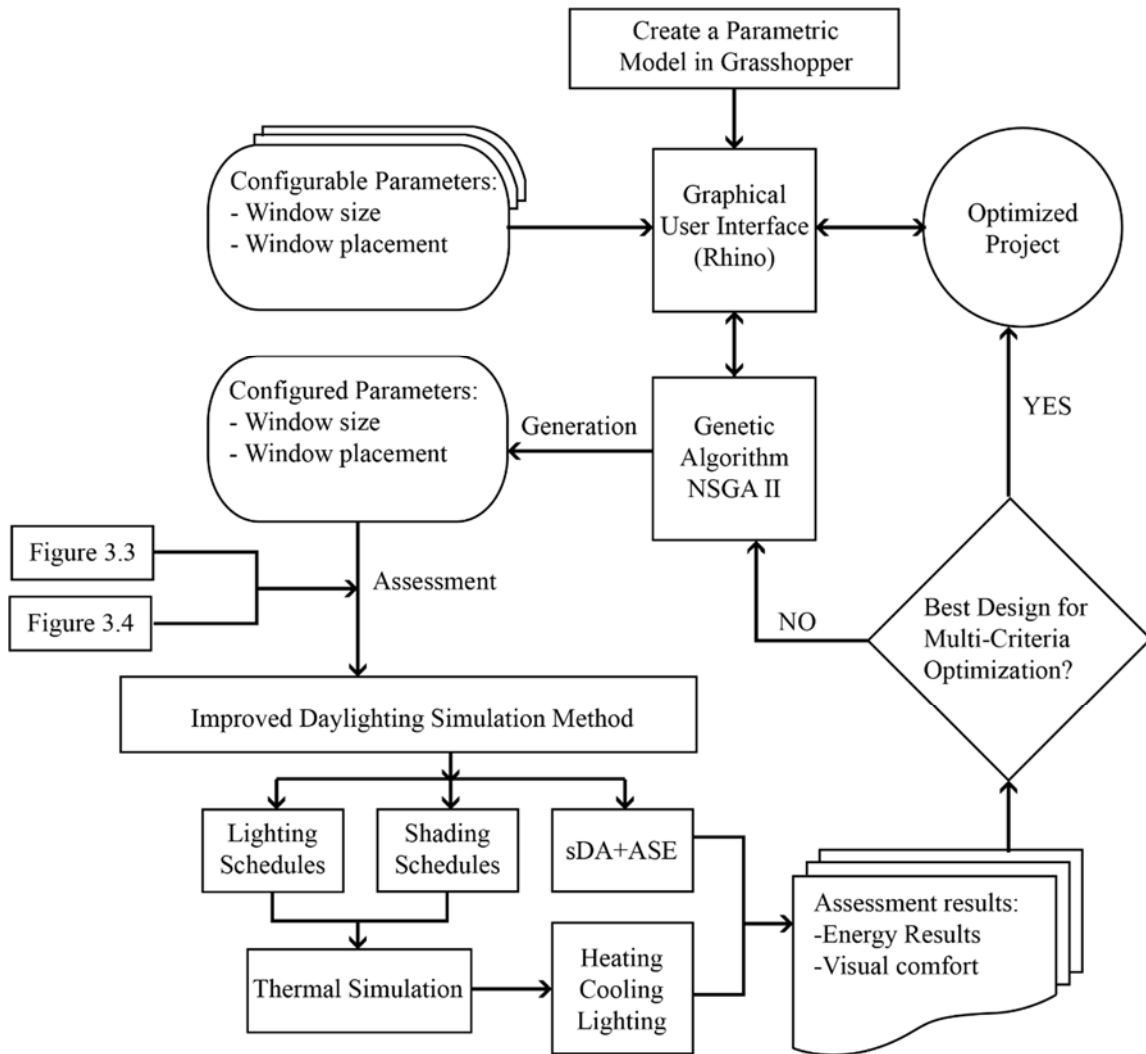


Figure 3.5 Parametric Modeling and Optimization Simulation

4. RESULTS OF THE COMBINING DAYLIGHTING AND THERMAL SIMULATION¹⁶

This chapter includes the results in three sections: Part I: 4.1. Build the simulation model. Part II: Proposed a prototype for the daylighting and thermal simulation process. Part III: Summary of the findings.

4.1. Build the Simulation Model

This section discusses the tasks required to build the simulation model. This study reproduces the Caldas model to better understand how to build an improved model. After analysis and testing the reproduced model, the improved office simulation model is proposed.

4.1.1. Caldas Office Model

Unfortunately, in the Caldas model (Caldas, 2001; Caldas and Norford, 2002), only a few building simulation input parameters were listed. Therefore, the remainder of the parameters for her model had to be determined by empirical testing to see which parameters gave the best statistical fit to match the published results. In her study, the office module consisted of a square 30.5 x 30.5 meter core zone, surrounded by four identical perimeter zones, which were 30.3 x 4.6 meters. The perimeter zone was divided into 10 office spaces of equal size of 3.1*4.6 meters for each orientation (Figure 4.1). The reference point for the daylighting calculation was located 3.1 meters from the

¹⁶ A part of this chapter is reprinted with permission from “Research on Guidelines for Window Design Strategies in High Performance Office Buildings” by Li, Q and J. Haberl. 2020. Proceedings of the 2020 Building Performance Analysis Conference and SimBuild, 447–454, Copyright © 2020. ASHRAE (www.ashrae.org).

window, at desk height (0.76 meter). The required horizontal illuminance at this point is 540 lx. The window glazing was selected as double pane with a layer of spectrally selective glass, with a shading coefficient of 0.34, and visual transmittance of 0.41. The climate used was Phoenix, Arizona. The remaining building parameters were determined by the reference listed in the previous DOE2.1e optimization study by R. Sullivan (Sullivan et al., 1987; Sullivan et al., 1992). Table 4-1 provides a list of the empirically determined office building parameters. The heating, cooling, lighting, and equipment schedules were assumed to be Monday through Friday from 8:00 am to 6:00 pm.

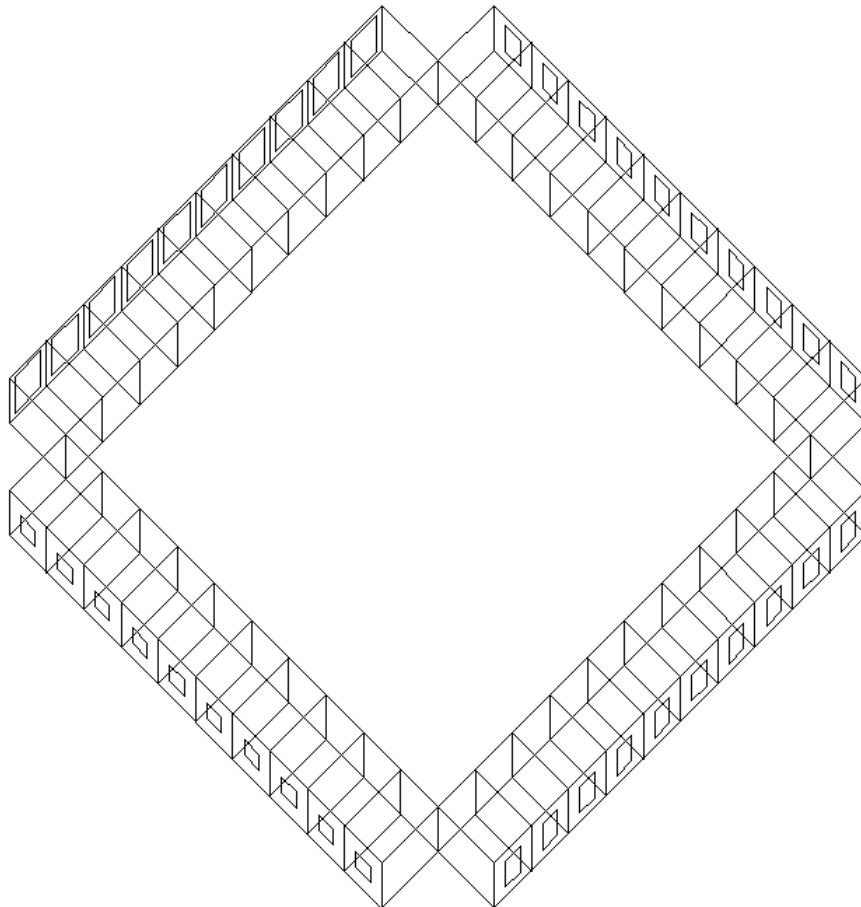


Figure 4.1: The Office Model in DOE2.1e (Source: Adapted from (Caldas and Norford, 2002))

Table 4-1: Empirically Determined Office Building Parameters in the Caldas Model

	I-P	Units	S-I	Units
Core Zone Length/Width	100.0	ft	30.5	m
Perimeter Zone Length	100.0	ft	30.5	m
Perimeter Zone Width	15.0	ft	4.6	m
Desk Height	2.5	ft	0.8	m
Height	8.5	ft	2.6	m
Core Zone Area	10000.0	ft ²	930.3	m ²
Core Zone Volume	85000.0	ft ³	2409.3	m ³
Perimeter Zone Area/Zone	1500.0	ft ²	140.3	m ²
Perimeter Zone Volume/Zone	12750.0	ft ³	363.4	m ³
Shading Coefficient	0.34		0.34	
Visual Transmittance	0.41		0.41	
Roof U-Factor	0.024	Btu/h-ft ² -°F	0.137	W/m ² C°
Floor U-Factor	0.024	Btu/h-ft ² -°F	0.137	W/m ² C°
Exterior Wall U-Factor	0.050	Btu/h-ft ² -°F	0.288	W/m ² C°
Glazing	Double pane		Double pane	
Glazing U-Factor	0.550	Btu/h-ft ² -F°	3.078	W/m ² C°
Daylighting Control	continuous		continuous	
Depth of Sensor from Window	10.0	ft	3.1	m
Horizontal Illuminance	50	fc	538	lux
Lighting Power Density	1.5	w/ft ²	16.1	w/m ²
Equipment Power Density	0.4	w/ft ²	4.3	w/m ²
Thermostat Setpoints	72.0	F°	22.2	C°
Thermostat Setpoints	78.0	F°	25.6	C°
Unoccupied Hour	63.0	F°	17.2	C°
Unoccupied Hour	90.0	F°	32.2	C°
Outside Air Per Zone	5.00	CFM	2.23	M ³ /S
Air Infiltration Fixed at	0.6	ACH	0.6	ACH
Air Flow Rate	0.70	CFM/ft ²	0.03	M ³ /S.m ²

4.1.2. Empirical Testing of Input Parameters

Since the Caldas study had many unknown building simulation inputs, the DOE2.1e sample file “Run_3A” was used as a starting model to match Caldas published energy results by empirically testing. Table 4-2 is a list of each simulation run and includes the parameter has been changed. Table 4-3 lists all the input parameters in the

DOE2.1e daylighting and thermal simulation that were used to match the results listed in Caldas (Caldas, 2001; Caldas and Norford, 2002). The image shown in Figure 4.1 is DOE2.1e model that was used. The daylighting reference points in the different zones are shown in Figure 4.2.

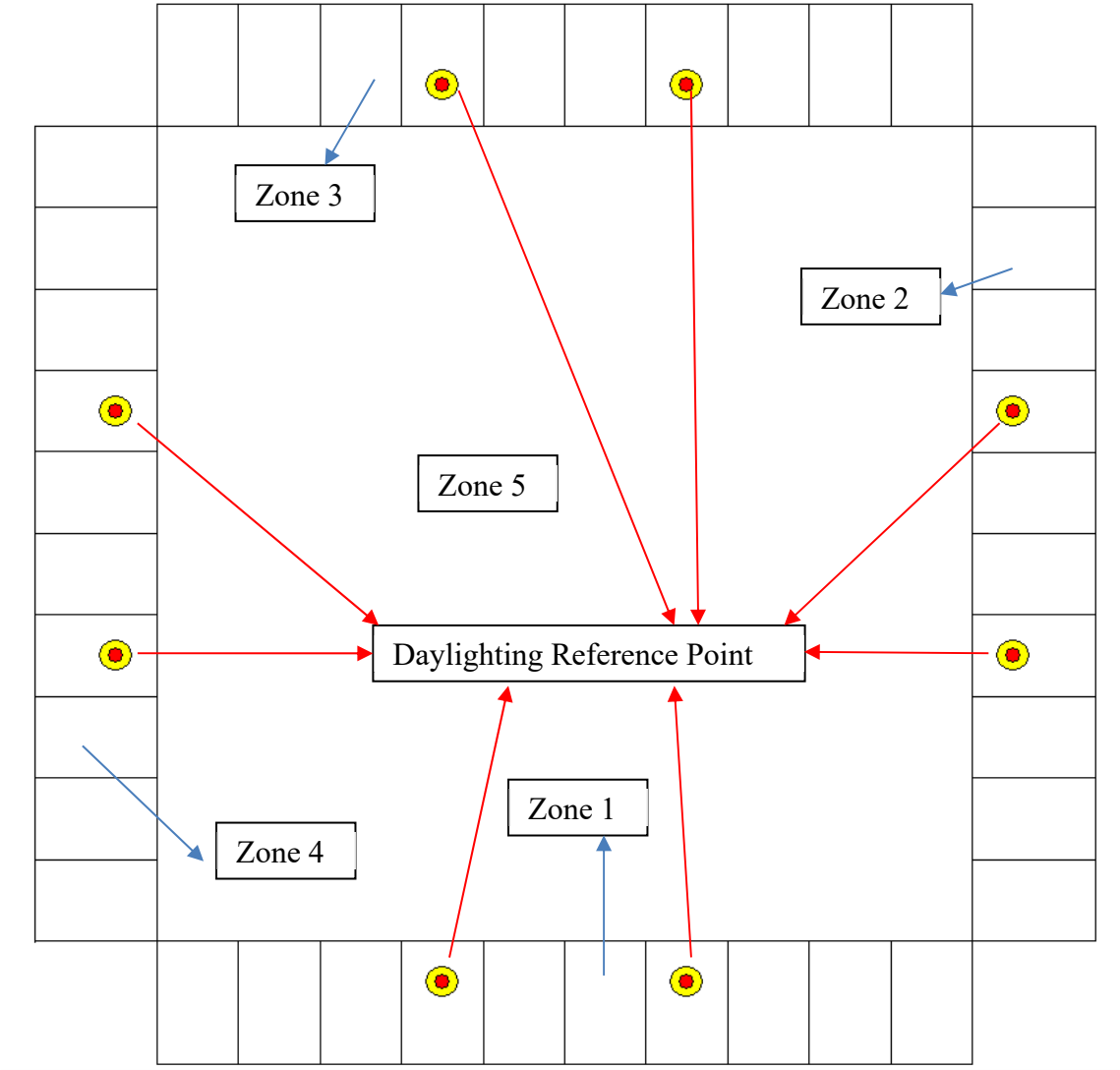


Figure 4.2: Daylighting Reference Points in the Four Perimeter Zones.

Table 4-2: Parameter Change List

Runs	Key Modifications in each run
RUN_3A	Original Model in DOE-2 Sample
Test_1	Caldas Model Dimension Window Case 1 in Phoenix
Test_2	Removed Overhangs
Test_3	Azimuth Changed from 30 degrees to 0 degrees
Test_4	Removed Plenum and Changed the Return-Air-Path from Plenum to Direct
Test_5	Removed Doors
Test_6	Changed Design-Heating-Temperature from 70 to 72 °F
Test_7	Changed Design-Cooling-Temperature from 76 to 78 °F
Test_8	Changed Unoccupied Design-Heat-T from 55 to 62 °F
Test_9	Changed Unoccupied Design-Cool-T from 99 to 90 °F
Test_10	Changed Outside Air Per Zone from 0.4 to 5 CFM
Test_11	Changed Thermostat-Type from Reverse-Action to Proportional
Test_12	Changed Floor U-Factor from 0.05 to 0.02 Btu/h-ft ² -°F
Test_13	Changed Roof U-Factor from 0.048 to 0.024 Btu/h-ft ² -°F
Test_14	Changed Wall U-Factor from 0.069 to 0.05 Btu/h-ft ² -°F
Test_15	Changed floor weight from 70 lb/ft ² to concrete Mass floor
Test_16	Changed glazing U-Factor from 0.3823 to 0.55 Btu/h-ft ² -°F
Test_17	Changed shading coefficient from 0.426 to 0.34 Btu/h-ft ² -°F
Test_18	Changed glass visual transmittance from NONE to 0.41
Test_19	Changed window frame from NONE to YES
Test_20	Changed infiltration rate from 0.25 to 0.6 ACH
Test_21	Changed GND reflection from 0 to 0.2
Test_22	Changed lighting power density from 1.2 to 1.5 W/sqft
Test_23	Changed equipment power density from 0.8 to 0.5 W/sqft
Test_24	Changed Fan Schedule
Test_25	Changed Heating Schedule
Test_26	Changed Cooling Schedule
Test_27	Changed Lighting Schedule
Test_28	Changed Equipment Schedule
Test_29	Changed infiltration Schedule
Test_30	Added interior shading Schedule
Test_31	Added Daylighting simulation Dr. Caldas' Model
Test_32	Remove the interior shading in Window Case 1
Test_33	Window Case 2 in Phoenix
Test_34	Window Case 3 in Phoenix
Test_35	Window Case 4 in Phoenix
Test_36	Window Case 5 in Phoenix

Table 4-3: Simulation Procedure for the Office Model

	Project						System									Construction											
	# of zones	Area ft2	Window-Wall-Ratio	Overhang On Doors	Azimuth	Plenum	Return-Air-Path	Doors	Change system	Design-Heat-T	Design-Cool-T	Unoccupied Design-Heat-T	Unoccupied Design-Cool-T	Outside-Air/Zone CFM	Thermostat-Type	Floor U-Factor	Roof U-Factor	Wall U-Factor	Roof Absorp-tance	Wall Absorp-tance	Floor-Weight	Glazing U-factor	Shading Coef	Glass Vis-Trans	Window Frame	Infiltration ACH	GND Reflec.
RUN 3A	5	5000	NA	YES	30	Plenum	Plenum	Two	VAVS	70	76	55	99	0.4	Reverse-Action	0.05	0.048	0.069	0.7	0.7	70	0.3823	0.426	None	None	0.25	0
Test 1	5	10014	16.02%	YES	30	Plenum	Plenum	Two	VAVS	70	76	55	99	0.4	Reverse-Action	0.05	0.048	0.069	0.7	0.7	70	0.3823	0.426	None	None	0.25	0
Test 2	5	10014	16.02%	NO	30	Plenum	Plenum	Two	VAVS	70	76	55	99	0.4	Reverse-Action	0.05	0.048	0.069	0.7	0.7	70	0.3823	0.426	None	None	0.25	0
Test 3	5	10014	16.02%	NO	0	Plenum	Plenum	Two	VAVS	70	76	55	99	0.4	Reverse-Action	0.05	0.048	0.069	0.7	0.7	70	0.3823	0.426	None	None	0.25	0
Test 4	5	10014	16.02%	NO	0	Removed	Direct	Two	VAVS	70	76	55	99	0.4	Reverse-Action	0.05	0.048	0.069	0.7	0.7	70	0.3823	0.426	None	None	0.25	0
Test 5	5	10014	16.02%	NO	0	Removed	Direct	N	VAVS	70	76	55	99	0.4	Reverse-Action	0.05	0.048	0.069	0.7	0.7	70	0.3823	0.426	None	None	0.25	0
Test 6	5	10014	16.02%	NO	0	Removed	Direct	N	VAVS	72	78	55	99	0.4	Reverse-Action	0.05	0.048	0.069	0.7	0.7	70	0.3823	0.426	None	None	0.25	0
Test 7	5	10014	16.02%	NO	0	Removed	Direct	N	VAVS	72	78	55	99	0.4	Reverse-Action	0.05	0.048	0.069	0.7	0.7	70	0.3823	0.426	None	None	0.25	0
Test 8	5	10014	16.02%	NO	0	Removed	Direct	N	VAVS	72	78	60	99	0.4	Reverse-Action	0.05	0.048	0.069	0.7	0.7	70	0.3823	0.426	None	None	0.25	0
Test 9	5	10014	16.02%	NO	0	Removed	Direct	N	VAVS	72	78	60	90	0.4	Reverse-Action	0.05	0.048	0.069	0.7	0.7	70	0.3823	0.426	None	None	0.25	0
Test 10	5	10014	16.02%	NO	0	Removed	Direct	N	VAVS	72	78	60	90	5	Reverse-Action	0.05	0.048	0.069	0.7	0.7	70	0.3823	0.426	None	None	0.25	0
Test 11	5	10014	16.02%	NO	0	Removed	Direct	N	VAVS	72	78	60	90	5	Proportional	0.05	0.048	0.069	0.7	0.7	70	0.3823	0.426	None	None	0.25	0
Test 12	5	10014	16.02%	NO	0	Removed	Direct	N	VAVS	72	78	60	90	5	Proportional	0.02	0.048	0.069	0.7	0.7	70	0.3823	0.426	None	None	0.25	0
Test 13	5	10014	16.02%	NO	0	Removed	Direct	N	VAVS	72	78	60	90	5	Proportional	0.02	0.024	0.069	0.7	0.7	70	0.3823	0.426	None	None	0.25	0
Test 14	5	10014	16.02%	NO	0	Removed	Direct	N	VAVS	72	78	60	90	5	Proportional	0.02	0.024	0.05	0.7	0.7	70	0.3823	0.426	None	None	0.25	0
Test 15	5	10014	16.02%	NO	0	Removed	Direct	N	VAVS	72	78	60	90	5	Proportional	0.02	0.024	0.05	0.7	0.7	MASS	0.3823	0.426	None	None	0.25	0
Test 16	5	10014	16.02%	NO	0	Removed	Direct	N	VAVS	72	78	60	90	5	Proportional	0.02	0.024	0.05	0.7	0.7	MASS	0.55	0.34	0.41	None	0.25	0
Test 17	5	10014	16.02%	NO	0	Removed	Direct	N	VAVS	72	78	60	90	5	Proportional	0.02	0.024	0.05	0.7	0.7	MASS	0.55	0.34	0.41	None	0.25	0
Test 18	5	10014	16.02%	NO	0	Removed	Direct	N	VAVS	72	78	60	90	5	Proportional	0.02	0.024	0.05	0.7	0.7	MASS	0.55	0.34	0.41	None	0.25	0
Test 19	5	10014	16.02%	NO	0	Removed	Direct	N	VAVS	72	78	60	90	5	Proportional	0.02	0.024	0.05	0.7	0.7	MASS	0.55	0.34	0.41	YES	0.25	0
Test 20	5	10014	16.02%	NO	0	Removed	Direct	N	VAVS	72	78	60	90	5	Proportional	0.02	0.024	0.05	0.7	0.7	MASS	0.55	0.34	0.41	YES	0.6	0
Test 21	5	10014	16.02%	NO	0	Removed	Direct	N	VAVS	72	78	60	90	5	Proportional	0.02	0.024	0.05	0.7	0.7	MASS	0.55	0.34	0.41	YES	0.6	0.2
Test 22	5	10014	16.02%	NO	0	Removed	Direct	N	VAVS	72	78	60	90	5	Proportional	0.02	0.024	0.05	0.7	0.7	MASS	0.55	0.34	0.41	YES	0.6	0.2
Test 23	5	10014	16.02%	NO	0	Removed	Direct	N	VAVS	72	78	60	90	5	Proportional	0.02	0.024	0.05	0.7	0.7	MASS	0.55	0.34	0.41	YES	0.6	0.2
Test 24	5	10014	16.02%	NO	0	Removed	Direct	N	VAVS	72	78	60	90	5	Proportional	0.02	0.024	0.05	0.7	0.7	MASS	0.55	0.34	0.41	YES	0.6	0.2
Test 25	5	10014	16.02%	NO	0	Removed	Direct	N	VAVS	72	78	60	90	5	Proportional	0.02	0.024	0.05	0.7	0.7	MASS	0.55	0.34	0.41	YES	0.6	0.2
Test 26	5	10014	16.02%	NO	0	Removed	Direct	N	VAVS	72	78	60	90	5	Proportional	0.02	0.024	0.05	0.7	0.7	MASS	0.55	0.34	0.41	YES	0.6	0.2
Test 27	5	10014	16.02%	NO	0	Removed	Direct	N	VAVS	72	78	60	90	5	Proportional	0.02	0.024	0.05	0.7	0.7	MASS	0.55	0.34	0.41	YES	0.6	0.2
Test 28	5	10014	16.02%	NO	0	Removed	Direct	N	VAVS	72	78	60	90	5	Proportional	0.02	0.024	0.05	0.7	0.7	MASS	0.55	0.34	0.41	YES	0.6	0.2
Test 29	5	10014	16.02%	NO	0	Removed	Direct	N	VAVS	72	78	60	90	5	Proportional	0.02	0.024	0.05	0.7	0.7	MASS	0.55	0.34	0.41	YES	0.6	0.2
Test 30	5	10014	16.02%	NO	0	Removed	Direct	N	VAVS	72	78	60	90	5	Proportional	0.02	0.024	0.05	0.7	0.7	MASS	0.55	0.34	0.41	YES	0.6	0.2
Test 31	5	10014	16.02%	NO	0	Removed	Direct	N	VAVS	72	78	60	90	5	Proportional	0.02	0.024	0.05	0.7	0.7	MASS	0.55	0.34	0.41	YES	0.6	0.2
Test 32	5	10014	16.02%	NO	0	Removed	Direct	N	VAVS	72	78	60	90	5	Proportional	0.02	0.024	0.05	0.7	0.7	MASS	0.55	0.34	0.41	YES	0.6	0.2
Test 33	5	10014	15.95%	NO	0	Removed	Direct	N	VAVS	72	78	60	90	5	Proportional	0.02	0.024	0.05	0.7	0.7	MASS	0.55	0.34	0.41	YES	0.6	0.2
Test 34	5	10014	16.84%	NO	0	Removed	Direct	N	VAVS	72	78	60	90	5	Proportional	0.02	0.024	0.05	0.7	0.7	MASS	0.55	0.34	0.41	YES	0.6	0.2
Test 35	5	10014	14.92%	NO	0	Removed	Direct	N	VAVS	72	78	60	90	5	Proportional	0.02	0.024	0.05	0.7	0.7	MASS	0.55	0.34	0.41	YES	0.6	0.2
Test 36	5	10014	17.95%	NO	0	Removed	Direct	N	VAVS	72	78	60	90	5	Proportional	0.02	0.024	0.05	0.7	0.7	MASS	0.55	0.34	0.41	YES	0.6	0.2

Table 4-3: Simulation Procedure for the Office Model (Continued)

	Internal Gain		Schedule							Daylighting								
	Lighting (w/sqft)	Equipment (w/sqft)	Fan	Heating	Cooling	Lighting	Equipment	Infiltration	Interior shading	Visible Daylight Transmittance	Daylighting	LIGHT-SET-POINT1	LIGHT-SET-POINT1	Control System	MIN-POWER-FRAC	MIN-LIGHT-FRAC	MAX-GLARE	INSIDE-VIS-REFL
RUN 3A	1.2	0.8	Schedule	Schedule	Schedule	Schedule	Schedule	Schedule	None	N/A	N/A	N/A	N/A	N/A	N/A	N/A	N/A	N/A
Test 1	1.2	0.8	Schedule	Schedule	Schedule	Schedule	Schedule	Schedule	None	N/A	N/A	N/A	N/A	N/A	N/A	N/A	N/A	N/A
Test 2	1.2	0.8	Schedule	Schedule	Schedule	Schedule	Schedule	Schedule	None	N/A	N/A	N/A	N/A	N/A	N/A	N/A	N/A	N/A
Test 3	1.2	0.8	Schedule	Schedule	Schedule	Schedule	Schedule	Schedule	None	N/A	N/A	N/A	N/A	N/A	N/A	N/A	N/A	N/A
Test 4	1.2	0.8	Schedule	Schedule	Schedule	Schedule	Schedule	Schedule	None	N/A	N/A	N/A	N/A	N/A	N/A	N/A	N/A	N/A
Test 5	1.2	0.8	Schedule	Schedule	Schedule	Schedule	Schedule	Schedule	None	N/A	N/A	N/A	N/A	N/A	N/A	N/A	N/A	N/A
Test 6	1.2	0.8	Schedule	Schedule	Schedule	Schedule	Schedule	Schedule	None	N/A	N/A	N/A	N/A	N/A	N/A	N/A	N/A	N/A
Test 7	1.2	0.8	Schedule	Schedule	Schedule	Schedule	Schedule	Schedule	None	N/A	N/A	N/A	N/A	N/A	N/A	N/A	N/A	N/A
Test 8	1.2	0.8	Schedule	Schedule	Schedule	Schedule	Schedule	Schedule	None	N/A	N/A	N/A	N/A	N/A	N/A	N/A	N/A	N/A
Test 9	1.2	0.8	Schedule	Schedule	Schedule	Schedule	Schedule	Schedule	None	N/A	N/A	N/A	N/A	N/A	N/A	N/A	N/A	N/A
Test 10	1.2	0.8	Schedule	Schedule	Schedule	Schedule	Schedule	Schedule	None	N/A	N/A	N/A	N/A	N/A	N/A	N/A	N/A	N/A
Test 11	1.2	0.8	Schedule	Schedule	Schedule	Schedule	Schedule	Schedule	None	N/A	N/A	N/A	N/A	N/A	N/A	N/A	N/A	N/A
Test 12	1.2	0.8	Schedule	Schedule	Schedule	Schedule	Schedule	Schedule	None	N/A	N/A	N/A	N/A	N/A	N/A	N/A	N/A	N/A
Test 13	1.2	0.8	Schedule	Schedule	Schedule	Schedule	Schedule	Schedule	None	N/A	N/A	N/A	N/A	N/A	N/A	N/A	N/A	N/A
Test 14	1.2	0.8	Schedule	Schedule	Schedule	Schedule	Schedule	Schedule	None	N/A	N/A	N/A	N/A	N/A	N/A	N/A	N/A	N/A
Test 15	1.2	0.8	Schedule	Schedule	Schedule	Schedule	Schedule	Schedule	None	N/A	N/A	N/A	N/A	N/A	N/A	N/A	N/A	N/A
Test 16	1.2	0.8	Schedule	Schedule	Schedule	Schedule	Schedule	Schedule	None	N/A	N/A	N/A	N/A	N/A	N/A	N/A	N/A	N/A
Test 17	1.2	0.8	Schedule	Schedule	Schedule	Schedule	Schedule	Schedule	None	N/A	N/A	N/A	N/A	N/A	N/A	N/A	N/A	N/A
Test 18	1.2	0.8	Schedule	Schedule	Schedule	Schedule	Schedule	Schedule	None	N/A	N/A	N/A	N/A	N/A	N/A	N/A	N/A	N/A
Test 19	1.2	0.8	Schedule	Schedule	Schedule	Schedule	Schedule	Schedule	None	N/A	N/A	N/A	N/A	N/A	N/A	N/A	N/A	N/A
Test 20	1.2	0.8	Schedule	Schedule	Schedule	Schedule	Schedule	Schedule	None	N/A	N/A	N/A	N/A	N/A	N/A	N/A	N/A	N/A
Test 21	1.2	0.8	Schedule	Schedule	Schedule	Schedule	Schedule	Schedule	None	N/A	N/A	N/A	N/A	N/A	N/A	N/A	N/A	N/A
Test 22	1.5	0.8	Schedule	Schedule	Schedule	Schedule	Schedule	Schedule	None	N/A	N/A	N/A	N/A	N/A	N/A	N/A	N/A	N/A
Test 23	1.5	0.5	Schedule	Schedule	Schedule	Schedule	Schedule	Schedule	None	N/A	N/A	N/A	N/A	N/A	N/A	N/A	N/A	N/A
Test 24	1.5	0.5	Fan-Sched	Schedule	Schedule	Schedule	Schedule	Schedule	None	N/A	N/A	N/A	N/A	N/A	N/A	N/A	N/A	N/A
Test 25	1.5	0.5	Fan-Sched	Heat-Sched	Schedule	Schedule	Schedule	Schedule	None	N/A	N/A	N/A	N/A	N/A	N/A	N/A	N/A	N/A
Test 26	1.5	0.5	Fan-Sched	Heat-Sched	Cool-Sched	Schedule	Schedule	Schedule	None	N/A	N/A	N/A	N/A	N/A	N/A	N/A	N/A	N/A
Test 27	1.5	0.5	Fan-Sched	Heat-Sched	Cool-Sched	Ligh-Sched	Schedule	Schedule	None	N/A	N/A	N/A	N/A	N/A	N/A	N/A	N/A	N/A
Test 28	1.5	0.5	Fan-Sched	Heat-Sched	Cool-Sched	Ligh-Sched	Equi-Sched	Schedule	None	N/A	N/A	N/A	N/A	N/A	N/A	N/A	N/A	N/A
Test 29	1.5	0.5	Fan-Sched	Heat-Sched	Cool-Sched	Ligh-Sched	Equi-Sched	Infil-Sched	None	N/A	N/A	N/A	N/A	N/A	N/A	N/A	N/A	N/A
Test 30	1.5	0.5	Fan-Sched	Heat-Sched	Cool-Sched	Ligh-Sched	Equi-Sched	Infil-Sched	Shad-Sched	N/A	N/A	N/A	N/A	N/A	N/A	N/A	N/A	N/A
Test 31	1.5	0.5	Fan-Sched	Heat-Sched	Cool-Sched	Ligh-Sched	Equi-Sched	Infil-Sched	Shad-Sched	0.41	YES	50	50	CONTINUOUS	0.1	0.1	25	0.8
Test 32	1.5	0.5	Fan-Sched	Heat-Sched	Cool-Sched	Ligh-Sched	Equi-Sched	Infil-Sched	NONE	0.41	YES	50	50	CONTINUOUS	0.1	0.1	25	0.8
Test 33	1.5	0.5	Fan-Sched	Heat-Sched	Cool-Sched	Ligh-Sched	Equi-Sched	Infil-Sched	NONE	0.41	YES	50	50	CONTINUOUS	0.1	0.1	25	0.8
Test 34	1.5	0.5	Fan-Sched	Heat-Sched	Cool-Sched	Ligh-Sched	Equi-Sched	Infil-Sched	NONE	0.41	YES	50	50	CONTINUOUS	0.1	0.1	25	0.8
Test 35	1.5	0.5	Fan-Sched	Heat-Sched	Cool-Sched	Ligh-Sched	Equi-Sched	Infil-Sched	NONE	0.41	YES	50	50	CONTINUOUS	0.1	0.1	25	0.8
Test 36	1.5	0.5	Fan-Sched	Heat-Sched	Cool-Sched	Ligh-Sched	Equi-Sched	Infil-Sched	NONE	0.41	YES	50	50	CONTINUOUS	0.1	0.1	25	0.8

The purpose of this part of the study was to obtain similar annual energy results as those published by Caldas (Figure 4.3). This figure shows the five test cases with different window sizes in four orientations that was used in Caldas (Caldas, 2001; Caldas and Norford, 2002). Figure 4.4 shows the annual energy consumption from the Caldas model and reproduced model. The results illustrate that an annual energy consumption that was very similar to the values published by Caldas was obtained. Therefore, the process of developing a simulation input file that reproduced Caldas' results was considered successful.

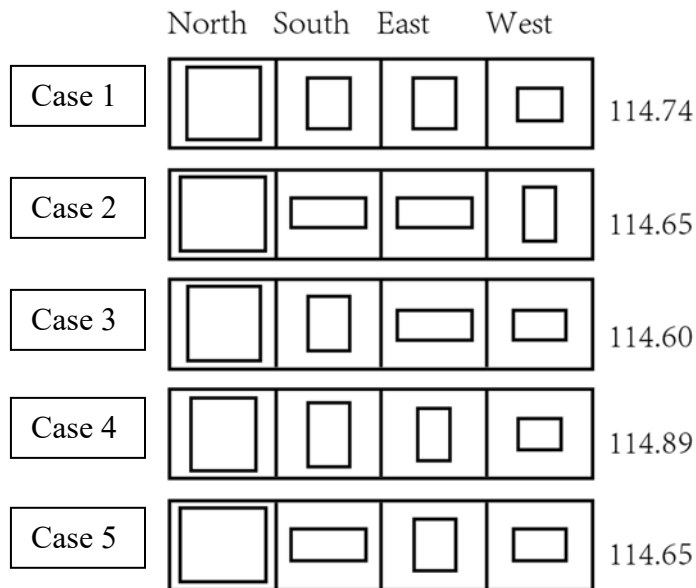


Figure 4.3: Annual Energy Consumption of Five Cases to the Phoenix climate (Source: Adapted from (Caldas and Norford, 2002))

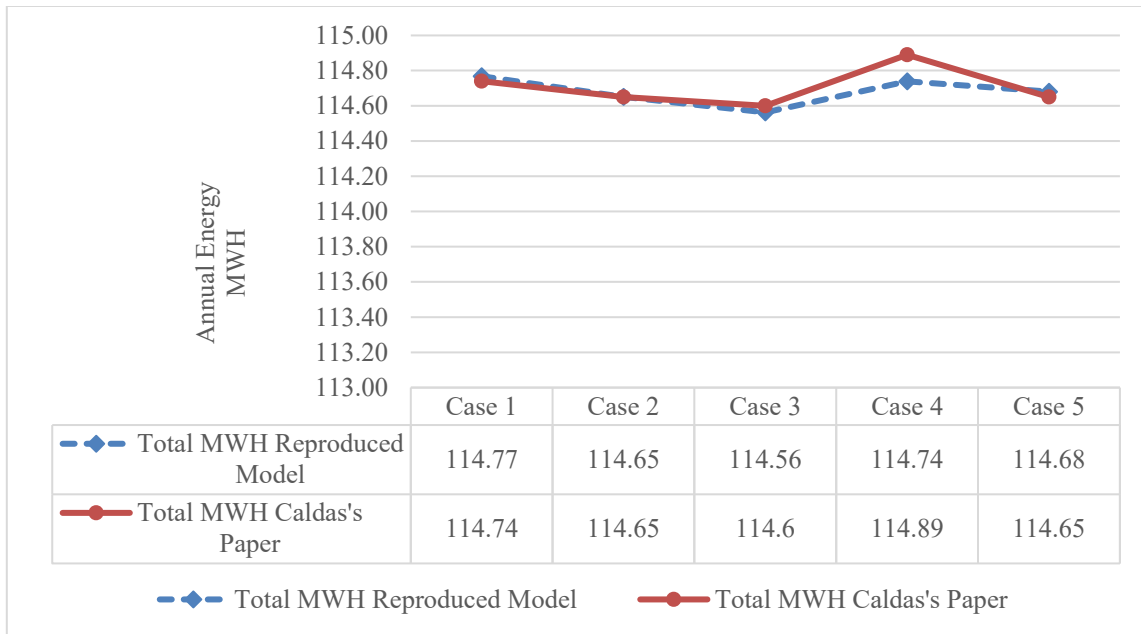


Figure 4.4: Comparison of Total Annual Energy Consumption

4.1.3. Limitations of the Caldas Simulation Model

In the Caldas and Norford (2002) paper, the office building module consisted of a square core zone and four identical perimeter zones surrounding the core zone facing North, South, East, and West. Each perimeter zone was divided into 10 equaled-sized offices. Based on the daylighting simulation rules using the DOE2.1e program, each zone can have a maximum of two daylighting reference points. Therefore, in the Caldas' model, the lighting control was based on the reference points in the perimeter zone with ten small offices, which is not equal to the lighting control on the ten identical single small office zones (Figure 4.5). Therefore, the reference point location difference caused a lighting, heating, and cooling difference. To better understand the window design strategies, this study reduced the model to one single small room with two reference points.

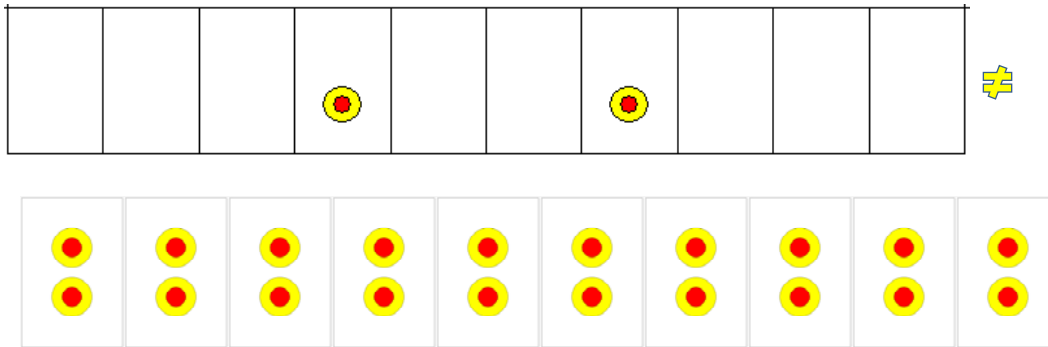


Figure 4.5: Reference Point Location Difference Causes Lighting Control Differences

In addition, this reproduced office model used an air infiltration that was fixed at 0.6 ACH throughout the year, and the roof and floor R-values were set to 40 ft-°F-h/Btu. Unfortunately, all these settings affected the annual cooling and heating consumption. In order to test how the window design strategies effect on the energy consumption, there was a need to minimize the effects of the other parameters on annual energy consumption. Therefore, for an improved model, the air infiltration was equal to zero, and the model reconfigure so that only one side of the wall has windows. The exterior wall had a U-factor of 0.05 Btu/h-ft²-°F. The other three exterior walls, roof, and floor are set to have no heat transfer (i.e., insulation R-value=100 ft-°F-h/Btu).

Finally, in Caldas paper (2002), there were limitations in the simulation process used in her study that were not fully explained. First was that all the windows in the simulations were centered in the middle of each façade, which does not reflect all types of daylighting strategies related to window locations (Reinhart and Stein, 2014). Second, the daylighting calculation method used in DOE-2 is the Split-Flux method, which has limitations in daylighting simulation. Therefore, the following study investigated the

window design strategies using a more sophisticated daylighting analysis that can analyze off-center placement of fenestration. To accomplish this, the study will analyze and compare the results from split-flux, Radiosity, and Radiance daylighting simulation to ascertain the differences in the simulation outputs.

4.1.4. The Improved Office Model

In addition to the above-mentioned limitation, the reproduced model has limitation in testing the window size and placement. For example, the five test cases shown in Figure 4.6 had very similar annual energy consumption, with a difference of only 0.03% to 0.1%. These results are different than those published in Caldas (2002). This is because the original Caldas model had other parameters that impact the cooling and heating load, such as infiltration, floor and roof R-values, outside air per zone, and the system type. Therefore, in this study, all these factors were removed to test the differences of the window design only. To accomplish this, this study made the following changes (Table 4-4):

- 1) the air infiltration was changed from 0.6 to 0;
- 2) The U-factor of exterior walls was set to as 0.05 Btu/h-ft²-°F. The other three exterior walls and floor were changed so the insulation R-value varied from 40 to 100.
- 3) changed the roof insulation R-value from 40 to 100 ft-°F-h/Btu.
- 4) changed Outside Air Per Zone from 5 CFM to 0 CFM;
- 6) changed the assigned-CFM from 0.7 CFM/sqft to “AUTO ADJUST”;
- 7) changed the system from VAV to SUM to eliminate the system effects on

cooling and heating energy use.

All other parameters were kept in the same as the reproduced model.

After modifying these parameters, the improved models were re-simulated. The results are shown in Figure 4.7. Figure 4.6 is shown the energy differences between five reproduced models. The differences between case 2 or 3 or 5 with case 1 are 0.1%, while the energy difference between 4 with case 1 is around 0.03% in reproduced models. In the improved models (Figure 4.7), the energy differences between case 2 or case 3 or case 5 with case 1 are around 0.3%, the energy differences between case 4 with case 1 is around 0.18%. The analysis showed the annual energy consumption of the modified models had a larger difference than the reproduced Caldas models. This increase in the difference in the models helped better identify changes in the annual energy use that were affectable only by the difference in the windows.

Table 4-4: The Parameter changes in order to test the window design strategies

Runs	Parameter Changes	Energy Results (MWH)					Total
		Area Lights	Equip	Heat	Cool	Fan + Pump	
Reproduced Model 1		49.19	17.67	6.39	29.51	12.01	114.77
Change 1	Changed infiltration from 0.6 to 0	49.19	17.67	4.42	29.04	11.75	112.07
Change 2	Changed Floor U-Factor from 0.02 to 0.01	49.19	17.67	3.81	26.28	10.2	107.15
Change 3	Changed Roof U-Factor from 0.02 to 0.01	49.19	17.67	3.72	26.37	10.14	107.09
Change 4	Changed Glazing U-Factor from 0.55 to 0.37	49.19	17.67	2.02	26.31	10.02	105.22
Change 5	Changed Outside Air Per Zone from 5 CFM to 0 CFM	49.19	17.67	1.93	30.30	11.37	110.46
Change 6	Removed zone ASSIGNED-CFM	49.19	17.67	1.67	28.27	11.87	108.67
Change 7	Changed the system from VAV to SUM	49.19	17.67	0.82	24.76	5.33	97.77

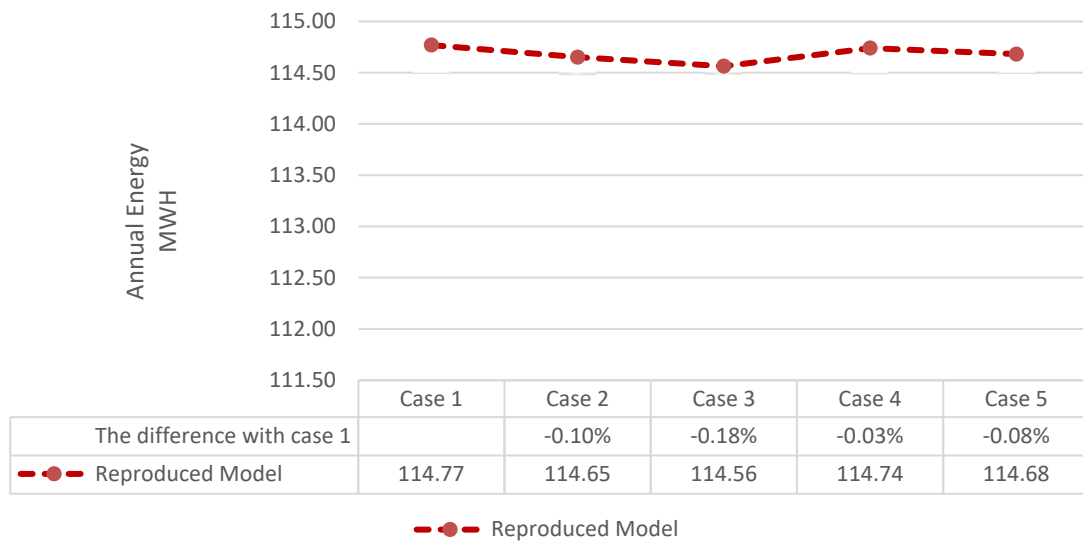


Figure 4.6: The Energy Difference of the Five Reproduced Models

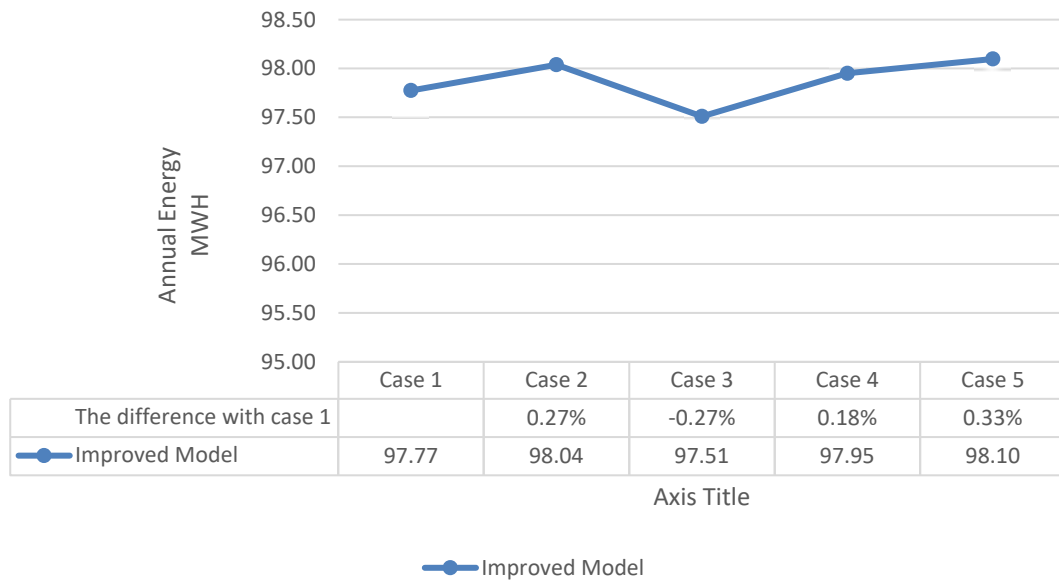


Figure 4.7: The Energy Difference of the Five Improved Models

In summary, the current analysis provided improved models that help magnify the differences to the annual energy use due only to differences in the windows. This

was accomplished by removing the effect of other parameters on the annual heating and cooling load use (e.g., infiltration, floor and roof R-values, outside air per zone, and the system type). In this way, the changes due to window size and placement had a larger percent difference on the heating and cooling consumption. Therefore, in the remaining analysis in this research, the infiltration and outside air were set to 0, the roof and floor R-value were set to 100 ft-°F-h/Btu, and the system type was set to be an ideal system (i.e., system=sum).

4.2. Propose a Prototype for the Daylighting and Thermal Simulation Process

The previous research illustrated three types of daylighting simulation methods, which are: Split-Flux, Radiosity, and Radiance. In this study, an office model with different window sizes and placements (but with same window area) were tested to compare the results from different tools. The purpose of this analysis is to test simulation abilities of different integrated thermal and daylighting simulation methods, which are DOE2.1e with Split-Flux, EnergyPlus with Split-Flux, EnergyPlus with Radiosity, and EnergyPlus with Radiance. The simulation results (i.e., cooling, heating, and lighting energy) will be compared to help develop a prototype for improved simulation tools of an integrated thermal and daylighting environment.

For the office model, in this study, a small office model with the dimension of 10X15X8.5 ft will be studied.

4.2.1. Small Size Office Model

The dimensions of the small size office model are listed in Table 4-5. In this study, the six types of window designs with the same window area were selected to test the window design strategies. The six window designs are shown in Figure 4.8. In all the window types, the window area is 30 ft². Window model 1 is located at the center of the wall. Window model 2 is located at the top of the wall. Window 3 is located at the bottom of the wall. Window model 4 is divided into two windows, and these two windows are located at the two sides of the wall. Window model 5 also has two windows, one window is at top of the wall, the other is located on the left of the wall. Window model 6 has three windows, one window is at the top of the wall, the other two windows are located on the two sides of the wall. All the dimensions are shown in Figure 4.8.

The reference points are at the one third and two third depth of the room (Figure 4.9).

Table 4-5: The small size office model dimension

	I-P	Units	S-I	Units
Length	10.0	ft	3.0	m
Width	15.0	ft	4.6	m
Height	8.5	ft	2.6	m
Window Area	30.0	ft ²	2.79	m ²
Reference Point	2.5	ft	0.8	m
Zone Area	150.0	ft ²	13.9	m ²
Zone Volume	1275.0	ft ³	36.1	m ³

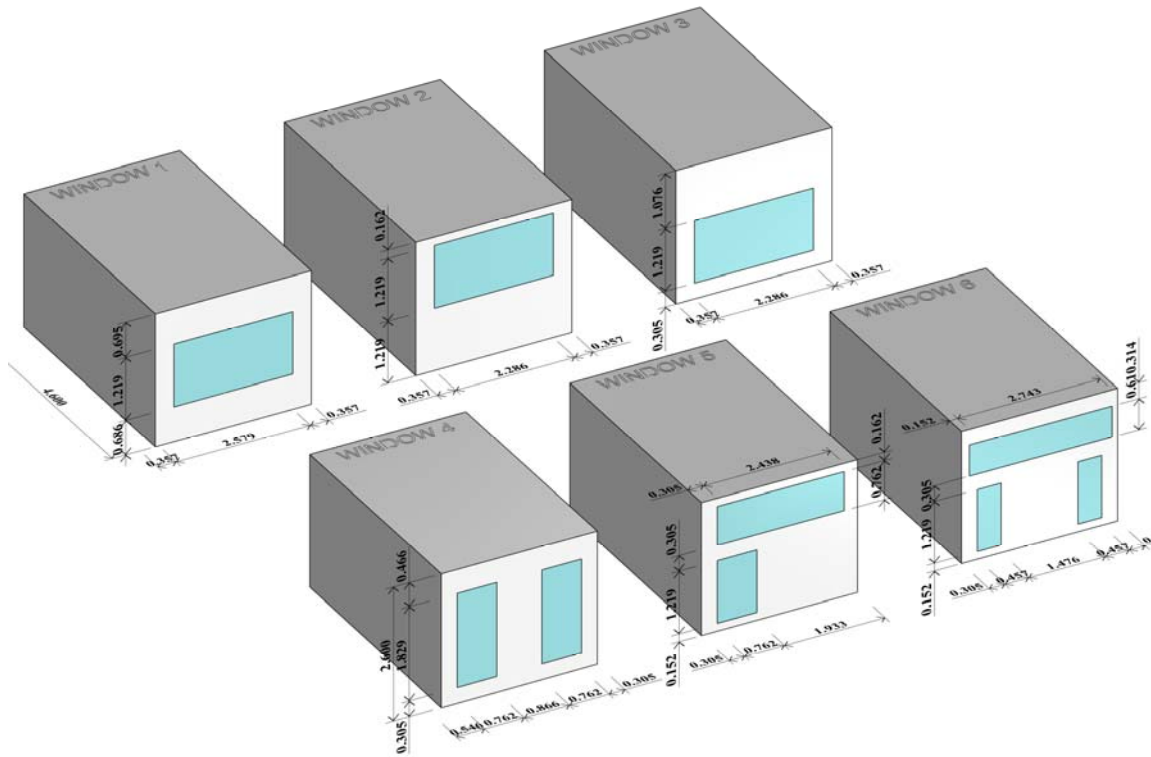


Figure 4.8: Six Different Window Models with the Same Window Area (Source: (Li and Haberl, 2020))

4.2.2. Match Models in DOE-2 and EnergyPlus

In this study, the DOE-2 and EnergyPlus were used for daylighting and thermal simulation. In order to match DOE-2 and EnergyPlus, the Split-Flux method was selected for daylighting simulation. The daylighting reference points were set at a distance of one third and two thirds the depth of the center of the room (Figure 4.9). The reference points have a height of 0.762 m above the floor. The location of the simulation is in Phoenix, Arizona. The other settings are same as the improved office model in the previous section. There is only one exterior wall with window openings; the three other

walls are adiabatic walls (R-value=100). The results of the simulation considered only the cooling, heating, and lighting annual energy use.

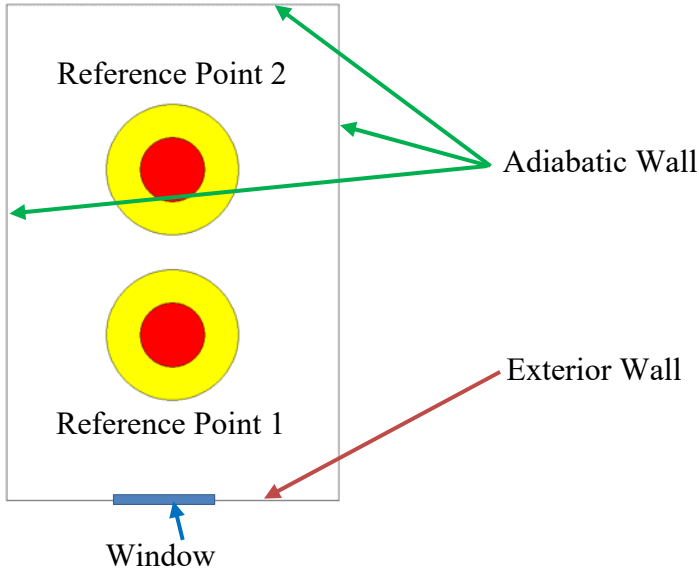


Figure 4.9: Reference Points in Small Office Room

In the analysis, the DOE-2 and EnergyPlus input parameters were kept the same as improved office model. In order to match the envelope properties of the two simulation programs, the lighting and equipment were turned-off. In addition, the cooling and heating schedules were changed from being on only during the weekdays to always on. The lighting schedule and occupancy schedule were set to be the same, which is fully on from 8 am to 6 pm daily for all days of the week. Finally, the simulation did not have occupants.

Unfortunately, DOE-2 and EnergyPlus have very different simulations for slab-on-grade floor types. DOE-2 used Winkelmann's slab-on-grade model (Winkelmann, 1998) for modeling the slab-on-grade heat transfer. Winkelmann's slab-on-grade model

assumes that the heat transfer occurs mainly in the exposed perimeter of the floor slab instead of using the U-value of the entire floor (Andolsun et al., 2012). However, EnergyPlus used a more complex slab model (Bahnfleth, 1989; Clements, 2004) that calculates monthly ground temperatures for single zone slab-on-grade buildings using a 3-D numerical analysis. Therefore, the floor type in this study was set as Slab in the preprocessor program of EnergyPlus that pre-calculates monthly ground temperatures for a single zone slab-on-grade buildings using a 3-D numerical analysis a horizontal exterior wall that is exposed to the ambient environment instead of slab-on-grade. The construction U-factor of DOE-2 and EnergyPlus list in Table 4-6.

Table 4-6: The Construction Material Values in DOE-2 and EnergyPlus

	DOE-2		EnergyPlus	
	Unit SI		Unit IP	
Roof U-factor	0.01	Btu/h.ft ² .F	0.056	W/m ² -K
Floor U-factor	0.01	Btu/h.ft ² .F	0.056	W/m ² -K
Exterior Wall U-factor	0.05	Btu/h.ft ² .F	0.284	W/m ² -K
Adiabatic Wall U-factor	0.01	Btu/h.ft ² .F	0.056	W/m ² -K

The basic window system in DOE-2 is the Transmittance Absorbance Reflectance (TAR) window model that relies on an older polynomial model (Reilly et al., 1995; Winkelmann et al., 1993a). The TAR window model cannot compare directly with NFRC-certified fenestration systems in EnergyPlus. EnergyPlus uses a Multi-Layer Window (MLW) model. In addition, DOE-2 uses a Shading Coefficient (SC) for the fenestration system. However, the Shading Coefficient could not represent the whole fenestration system and only covers the glass. Therefore, the DOE-2 TAR window system needs to be changed to an MLW to compare with EnergyPlus. In ASHRAE

Research Project 1588-RP Huang et al. (2019) developed a computerized tool to help select a real-world fenestration system that best matches a given target SHGC and U-factor.

In this study, the tool from the ASHRAE Research Project 1588-RP ((Huang et al., 2019)) was used to suggest a MLW model that matched a given DOE-2 TAR window model. Then, the MLW model was loaded into the DOE-2 window library to simulate the energy consumption. The results (i.e., such as cooling and heating load) in DOE-2 with different window system model were then compared with EnergyPlus model. In this way, the wall and window models in DOE-2 and Energy were compared.

The five different windows were selected from the 1993 DOE-2 library (Table 4-7) with both single pane window and double pane windows selected and tested. The locations in this study was Phoenix, Arizona and Chicago, Illinois. Based on the ASHRAE Standard 90.1-2016, the window properties in Phoenix are: maximum U-factor is 0.54, maximum SHGC is 0.25; while window properties in Chicago are: maximum U-factor is 0.38, maximum SHGC is 0.38. Therefore, the multi-layer window-type-code 2637 in DOE-2 library was selected for Chicago, the window-type-code 2668 was selected for Phoenix.

Table 4-7: Selected Target Windows from DOE-2 library (Winkelmann et al., 1993b)

	Glass-Type-Code	Glazing U-factor (W/(m ² ·K))	Glazing U-factor (Btu/(h·ft ² ·F))	SC	SHGC	Visual Transmittance
Single-pane, clear	1000	6.31	1.11	1.00	0.86	0.90
Single-pane, tint	1203	6.17	1.09	0.71	0.61	0.75
Double-pane, clear	2000	3.23	0.57	0.88	0.76	0.81
Double-pane, low-e-1	2611	1.99	0.35	0.85	0.73	0.74
Double-pane, low-e-2	2637	1.78	0.31	0.43	0.37	0.44
Double-pane, low-e-3	2668	1.32	0.23	0.32	0.28	0.41

In Table 4-8, the ASHRAE 1588-RP tool ((Huang et al., 2019) provides a match for the single-pane clear and double pane clear window. However, the low-E windows, the ASHRAE 1588 tool recommends a multi-layer window that has a difference in the U-factor and Visual Transmittance (VT) values compared with the target DOE-2 TAR window in Table 4-8. The MLW model in EnergyPlus matched well with the DOE-2 target TAR windows properties.

Table 4-8: Simulation window output parameters

	DOE-2 Transmittance Absorbance Reflectance (TAR) window model			DOE-2 Multi-Layer Window (MLW) model			EnergyPlus Multi-Layer Window (MLW) model		
	U-factor (W/(m2-K))	SHGC	VT	U-factor (W/(m2-K))	SHGC	VT	U-factor (W/(m2-K))	SHGC	VT
Single-pane, clear	6.34	0.86	0.90	6.47	0.81	0.90	6.36	0.86	0.90
Single-pane, tinted	6.21	0.61	0.75	6.34	0.47	0.65	6.17	0.61	0.75
Double-pane, clear	3.29	0.77	0.81	3.30	0.74	0.82	3.12	0.76	0.81
Double-pane, low-e-1	2.03	0.74	0.74	2.84	0.73	0.82	2.05	0.74	0.74
Double-pane, low-e-2	1.81	0.37	0.44	1.74	0.37	0.73	1.80	0.37	0.44
Double-pane, low-e-3	1.34	0.28	0.41	1.69	0.29	0.57	1.34	0.28	0.41

In this study, the DOE-2 cooling and heating loads energy were obtained from the System Monthly Loads Summary (SS-A) reports of DOE-2 when system “SUM” was assigned to the test houses as the “system-type”. In EnergyPlus, cooling and heating loads were obtained from the “Zone Ideal Loads Zone Sensible Heating load” and “Zone Ideal Load Zone Sensible Cooling load” reports of EnergyPlus when the “ZoneHVAC: Ideal-Loads-Air-System” was used.

Besides the window parameters listed in Table 4-8, all other input parameters listed in Table 4-9. The output results also list in Table 4-9.

Table 4-9: The input parameters and output in DOE-2 and EnergyPlus

Parameters		DOE-2	EnergyPlus
Input Parameters	Length	10 ft	3.0 m
	Width	15 ft	4.6 m
	Height	8.5 ft	2.6 m
	Window area	30 ft ²	2.787 m ²
	Reference point height above floor	2.5 ft	0.762 m
	Zone area	150 ft ²	13.9 m ²
	Volume	1275 ft ³	36.1 m ³
	Roof U-factor	0.01 Btu/h.ft ² .F	0.056 W/m ² -K
	floor U-factor	0.01 Btu/h.ft ² .F	0.056 W/m ² -K
	Exterior wall U-factor	0.05 Btu/h.ft ² .F	0.284 W/m ² -K
	Adiabatic wall U-factor	0.01 Btu/h.ft ² .F	0.056 W/m ² -K
	Floor visible reflectance	0.2	0.2
	Wall visible reflectance	0.7	0.7
	Roof visible reflectance	0.7	0.7
	Lighting power density	0 W/ft ²	0 W/m ²
	Equipment	0 W/ft ²	0 W/m ²
	Illuminance dimming setpoint	50 fc	538 lux
	Occupant People	0 People/ ft ²	0 People/ m ²
	Cooling setpoint	78 F	25.6 °C
	Heating setpoint	72 F	22.2 °C
	Infiltration per zone	0 CFM	0 m ³ /s
	Outside air per zone	0 CFM	0 m ³ /s
Assigned-CFM	Auto Adjust	Auto-size	
System	SUM	Ideal-Loads-Air-System	
Output Results	Lighting energy	BEPS: Lighting	InteriorLights:Electricity
	Cooling Load Energy	SS-A: Cooling	Zone Ideal Load Zone Sensible Cooling load
	Heating Load Energy	SS-A: Heating	Zone Ideal Loads Zone Sensible Heating load

The simulation results in Phoenix are shown in Table 4-10. In the results, the cooling and heating load of the single pane window in both the DOE-2 TAR window model and DOE-2 MLW window model were almost the same. However, the cooling load has an approximate 10% difference in the double-pane windows between DOE-2 TAR window model and DOE-2 MLW model. Comparing the results of the DOE-2 and EnergyPlus simulation, the cooling and heating load differences were around 5%

between the DOE-2 TAR window model and the EnergyPlus MLW window model. In addition, the cooling and heating results difference between DOE-2 MLW and EnergyPlus MLW window model has increased to about 8%.

Table 4-10: Simulation results in Cooling Load Energy and Heating Load Energy

	DOE-2 Transmittance Absorbance Reflectance (TAR) window model		DOE-2 Multi-Layer Window (MLW) model		EnergyPlus Multi-Layer Window (MLW) model	
	Cooling load (MWH)	Heating load (MWH)	Cooling load (MWH)	Heating load (MWH)	Cooling load (MWH)	Heating load (MWH)
Single-pane, clear	3.14	0.01	3.13	0.01	2.97	0.16
Single-pane, tint	2.29	0.02	1.99	0.02	2.33	0.16
Double-pane, clear	2.68	0.00	2.71	0.00	2.60	0.07
Double-pane, low-e-1	2.62	0.00	2.75	0.00	2.51	0.04
Double-pane, low-e-2	1.44	0.00	1.67	0.00	1.50	0.04
Double-pane, low-e-3	1.12	0.00	1.28	0.00	1.25	0.03

Therefore, since DOE-2 MLW window model did not match the results well with the EnergyPlus MLW window model, the following studies will select the DOE-2 TAR window model in DOE-2 energy simulation. From the DOE-2 window library, the Double pane low-E-3 window will be used in the Climate Zone 2 (Phoenix) for the following section studies.

4.2.3. Model Parameters of Window Layout and Placement Designs

Previous section 5.2.2 has matched the façade properties between DOE-2 and EnergyPlus. This section focuses on the analysis of the daylighting and thermal performance with different window 6 window layouts and Placements with the same area (Figure 4.8). in this analysis, the lighting power density was set as 1.11 w/sqft based on ASHRAE standard 90.1-2016. The window U-factor is 1.34 W/(m²-K), SHGC is

0.28, and Visual Transmittance (VT) is 0.41. All the inputs and outputs are listed in

Table 4-11.

Table 4-11: The input parameters and output of the office building (Source: (Li and Haberl, 2020))

	Parameters	DOE-2 (IP)	EnergyPlus (SI)
Input Parameters	Length	10 ft	3.0 m
	Width	15 ft	4.6 m
	Height	8.5 ft	2.6 m
	Window area	30 ft ²	2.787 m ²
	Reference point height above floor	2.5 ft	0.762 m
	Zone area	150 ft ²	13.9 m ²
	Volume	1275 ft ³	36.1 m ³
	Roof U-factor	0.01 Btu/h.ft ² .F	0.056 W/m ² -K
	floor U-factor	0.01 Btu/h.ft ² .F	0.056 W/m ² -K
	Exterior wall U-factor	0.05 Btu/h.ft ² .F	0.284 W/m ² -K
	Adiabatic wall U-factor	0.01 Btu/h.ft ² .F	0.056 W/m ² -K
	Glazing U-factor	0.24 Btu/h.ft ² .F	1.34 W/m ² -K
	SHGC	0.28	0.28
	Visual Transmittance	0.41	0.41
	Floor visible reflectance	0.2	0.2
		0.5	0.5
		0.9	0.9
	Wall visible reflectance	0.7	0.7
	Roof visible reflectance	0.7	0.7
	Lighting power density	1.11 W/ft ²	11.95 W/m ²
	Equipment	0 W/ft ²	0 W/m ²
	Illuminance dimming setpoint	50 fc	538 lux
	Occupant People	0 People/ ft ²	0 People/ m ²
	Cooling setpoint	78 F	25.6 °C
	Heating setpoint	72 F	22.2 °C
	Infiltration per zone	0 CFM	0 m ³ /s
	Outside air per zone	0 CFM	0 m ³ /s
Assigned-CFM	Auto Adjust	Auto-size	
System	SUM	Ideal-Loads-Air-System	
Output Results	Lighting energy	BEPS: Lighting	InteriorLights:Electricity
	Cooling Load Energy	SS-A: Cooling	Zone Ideal Load Zone Sensible Cooling load
	Heating Load Energy	SS-A: Heating	Zone Ideal Loads Zone Sensible Heating load

4.2.4. Daylighting Settings in DIVA

In this study, DIVA V4.0 plug-in for Grasshopper was used for the daylighting simulation. DIVA creates physically accurate renderings using Radiance, and exposes the full complement of Radiance raytracing parameters (Solemma, n.d.-b). Radiance uses the Daylight Coefficient Method, the illuminance values for the skies are usually derived from Typical Meteorological Year (TMY3) weather data for different geographical locations (Reinhart, 2005; Wilcox and Marion, 2008). The TMY3 weather data is in the form of EnergyPlus Weather (EPW) files, which contains hourly Direct-Normal and Diffuse-Horizontal irradiation data (EPW, 2019). The EPW files' irradiance hourly data and geographic coordinates can be employed to create continuous luminance or Radiance-based sky definitions through the Perez Sky Model (Perez et al., 1993). The continuous sky models are then discretized into a matrix format by approximating the celestial hemisphere to a series of luminous patches.

In the DIVA analysis, the grid for the illuminance measurements is above the floor at a 0.76 m height. The grid spacing is 0.3 m. The lighting sensors were set the same as the two DOE-2 reference points, whose X, Y, Z coordinate position are (1.524m, 1.524m, 0.762m) and (1.524m, 3.048m, 0.762m). The lighting control system used was the Photosensor Controlled Dimming. The Photosensor Controlled Dimming assumes the dimming control has perfect knowledge of the illuminance from the daylight in the space, and the dims the light to meet the lighting target from a continuous dimming sensor with a user-defined setpoint. The illuminance setpoint in the simulation of the dimming control was 538 lux. The Radiance rendering quality setting in this

section was set at medium-quality, which produces a relatively accurate result with an acceptable software runtime. The grid and lighting control settings are shown in Figure 4.10. Other parameters are listed in the Table 4-11.

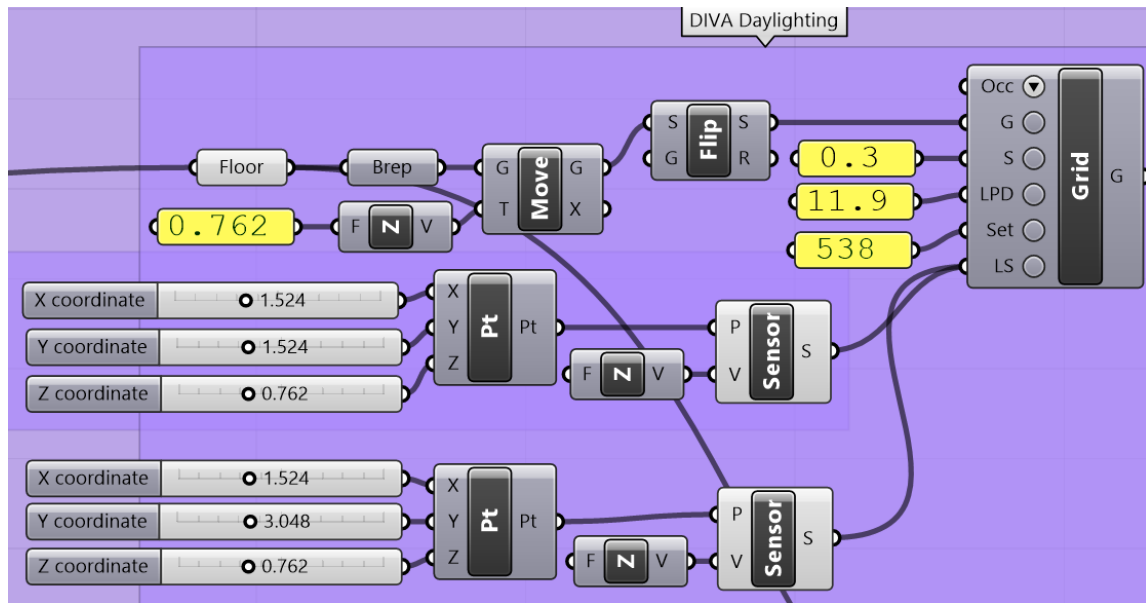


Figure 4.10: The DIVA Daylighting Grid and Lighting Control Setting

The illuminance results from the DIVA analysis are shown in the Figure 4.11. The results show a clear day at 12:00 noon (solar time) on July 24. The illuminance values changed when window location changed. The DIVA simulation used the medium-quality setting in the annual daylighting simulation. Window 2 has more daylight at the back of the room. Window 3 has the least daylight in the back of the room.

In order to test the daylighting sensitivities with the different window designs, the FVR was changed from 0.2 to 0.5/0.9. In this analysis, all other parameters were kept the same.

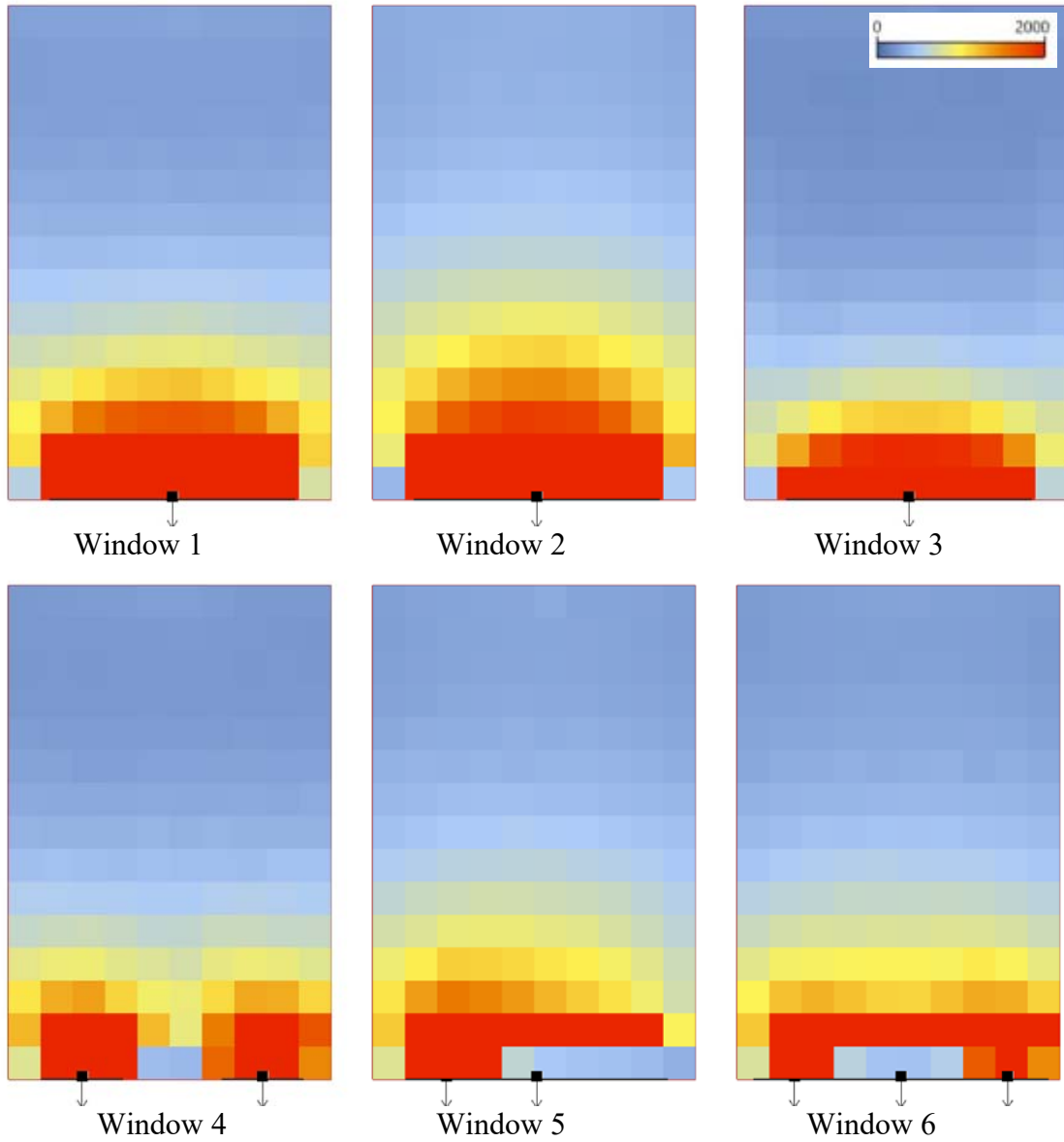
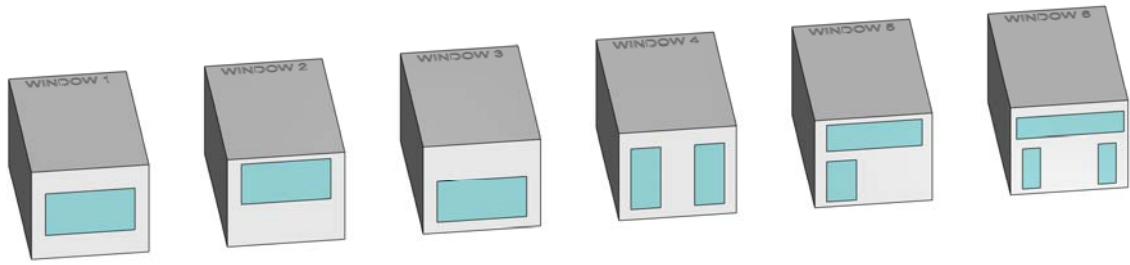


Figure 4.11: Illuminance Map of Six South-Facing Windows at a Solar Time 12:00 noon, July 24 in the Location of Phoenix, AZ. (Floor Visual Reflectance=0.2)

Figure 4.12 shows the illuminance maps when the FVR was set at 0.5, while Figure 4.13 shows the results when the FVR was set to 0.9. From the analysis, it can be concluded that the back part of the room had higher illuminance when the FVR was higher. That is because there was much more reflectance of the daylight when the FVR was increased.

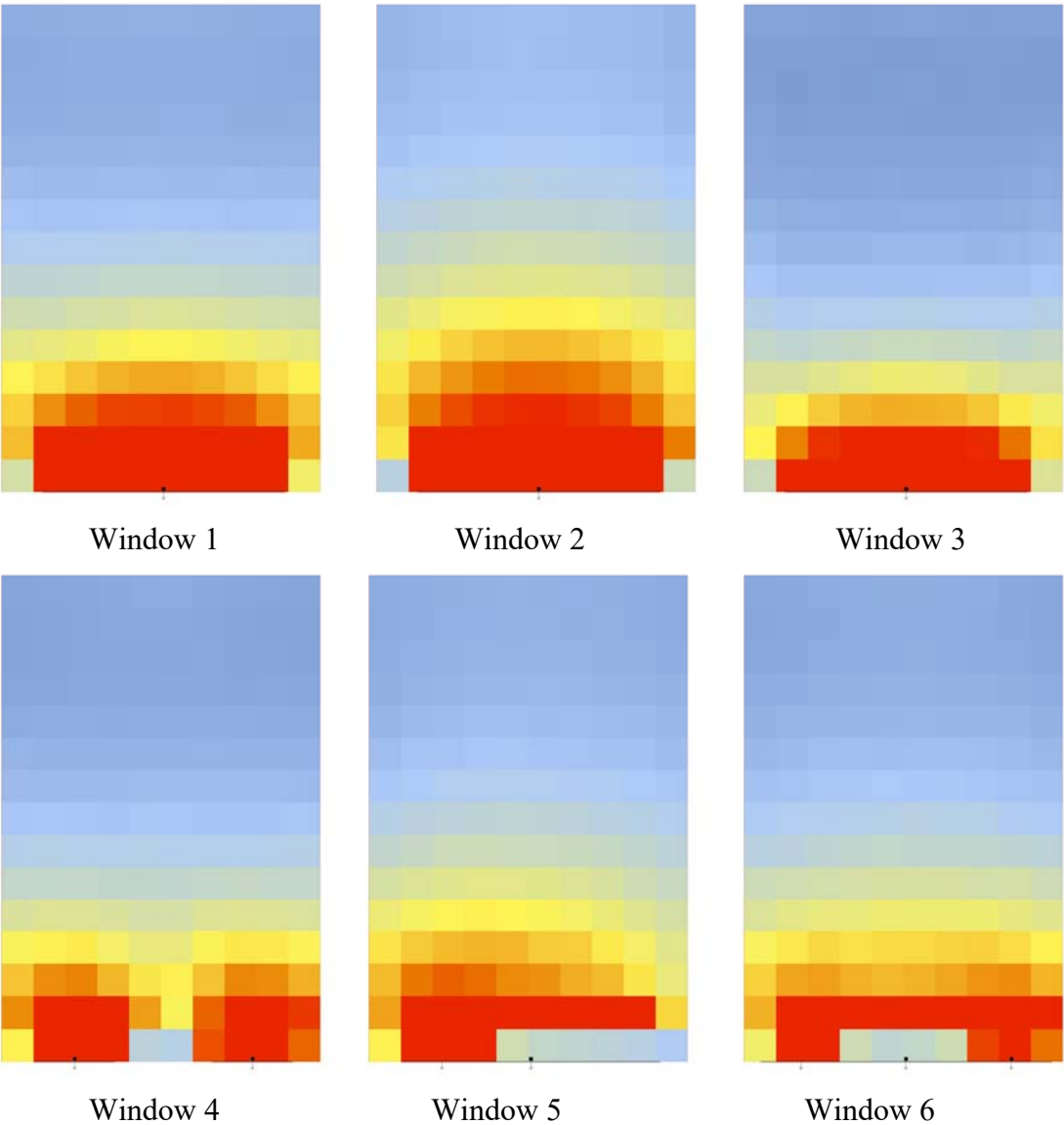


Figure 4.12: Illuminance Map of Six South-Facing Windows at a Solar Time 12:00 noon, July 24 in the Location of Phoenix, AZ. (Floor visual reflectance=0.5)

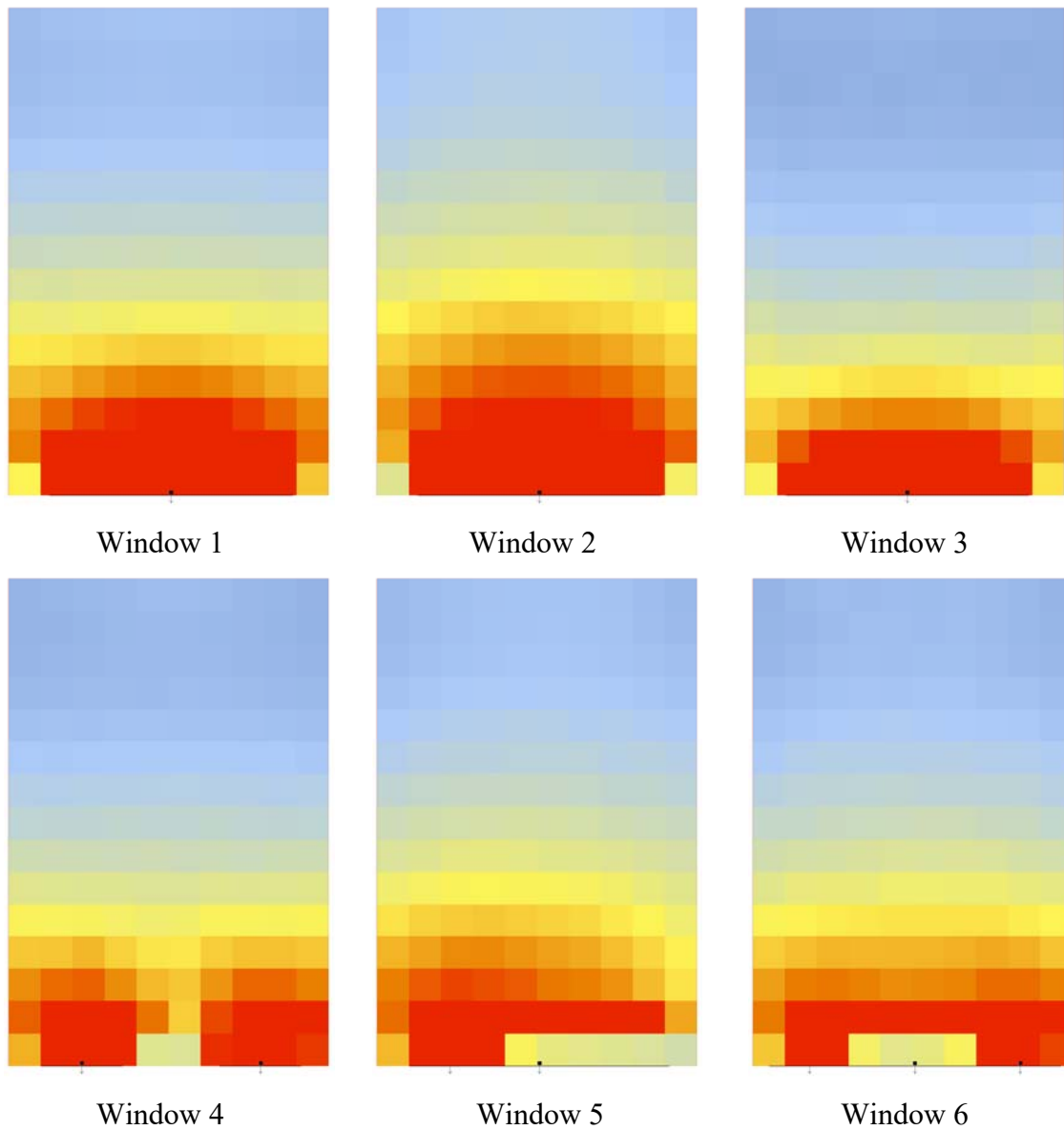


Figure 4.13: Illuminance Map of Six South-Facing Windows at a Solar Time 12:00 noon, July 24 in the Location of Phoenix, AZ. (Floor visual reflectance=0.9)

4.2.5. Combined Daylighting and Thermal Simulation

To combine the daylighting and thermal simulation, the Radiance (DIVA) program was connected with the EnergyPlus (i.e., Ladybug & Honeybee) using the

Rhino & Grasshopper interface. In this analysis, the lighting schedule from the DIVA Photosensor Controlled Dimming system was connected to the EnergyPlus simulation as a lighting input. In this way, EnergyPlus turns-off the daylighting simulation, and instead uses the lighting schedules from the DIVA. Figure 4.14 shows how the lighting schedule for the DIVA daylighting simulation was created. In Figure 4.15, an example of the lighting schedule is shown. This lighting schedule was then connected to the EnergyPlus simulation using the Grasshopper plugin programs Ladybug & Honeybee.

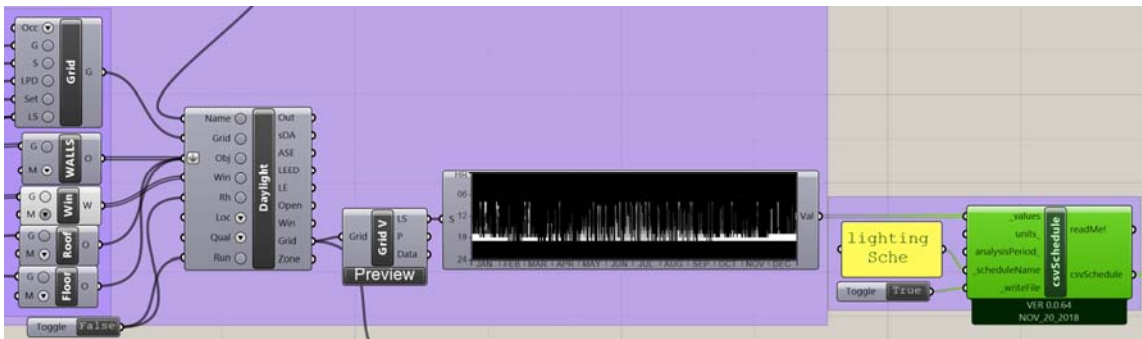


Figure 4.14: The creation of the lighting schedule in DIVA (Solemma, n.d.-a)

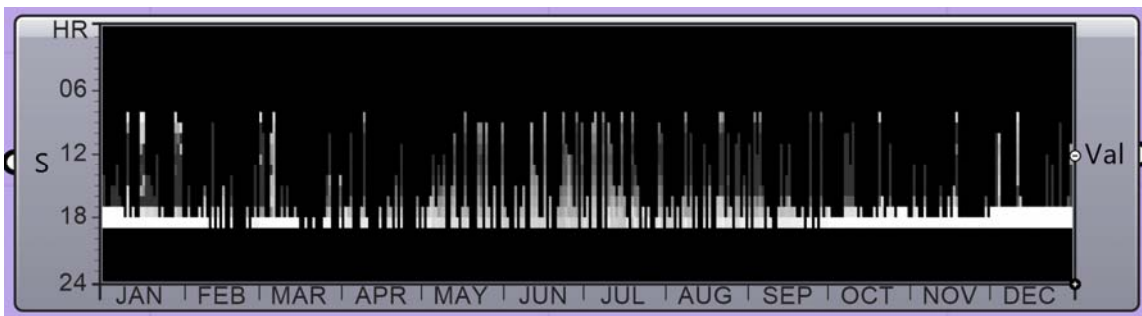


Figure 4.15: A sample of lighting schedule image in DIVA (Solemma, n.d.-a)

The Ladybug & Honeybee plugins from the Grasshopper program used with EnergyPlus, which are written in Python (Rossum, 1995). Unfortunately, the Honeybee

commands in Grasshopper did not have all the setting needed for EnergyPlus. For example, Honeybee did not directly provide the “Ideal-Load-Air-System” that this study needed. In addition, the Honeybee simulation outputs did not have the “Zone Ideal Loads Zone Sensible Heating load” and the “Zone Ideal Load Zone Sensible Cooling load” reports. Therefore, the text string, and text description of the Ideal-Load-Air-System was added as an additional string to be the system string in Honeybee. The simulation outputs were also edited and added using Python in the “runEnergySimulation” command Python Script. The “EpCustomResult” command was edited by the Python script to read the simulation results. This process is shown in Figure 4.16.

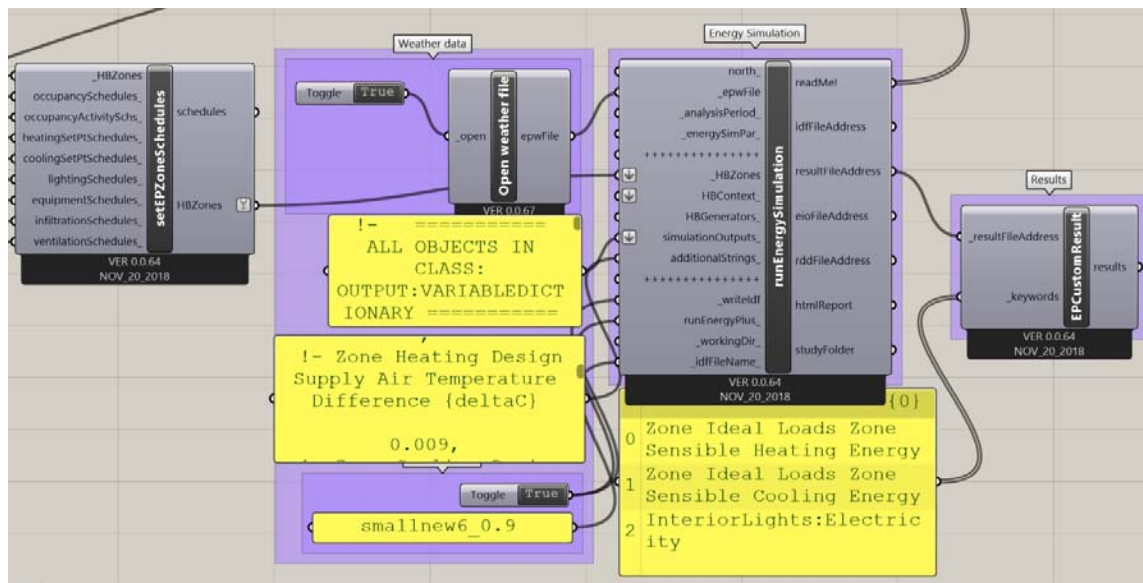


Figure 4.16: Honeybee system and outputs editing in Grasshopper (Solemna, n.d.-a)

4.2.6. Combined Daylighting and Energy Simulation Results

The simulation location of this study is in the hot dry climate zone of Phoenix,

AZ. In this study, four orientations were tested, which are: South, North, East and West, using the simulation parameters listed in Table 4-12. Windows were placed in only one exterior wall. All other walls do not have exterior windows. In the analysis, six window locations were tested with an equivalent window area (Figure 4.8). In this study, there are four combined daylighting and thermal simulation methods were used, which include DOE2.1e+Split-Flux, EnergyPlus+Split-Flux, EnergyPlus+Radiosity, and EnergyPlus+Radiance. The different simulation methods have different simulation runtimes. The DOE2.1e+Split-Flux used the shortest runtime, which only took around 3 seconds to obtain simulation result. EnergyPlus+ Radiosity took around 2 mins to run simulation. There are three different Radiance rendering settings were used for the EnergyPlus+Radiance simulation method, which are low-quality, medium- quality and high-quality settings. The low-quality setting obtains the least accurate results with 10 sec runtimes. The medium-quality setting could obtain relatively correct result with reasonable simulation runtime. The high quality performs the most correct lighting energy use, but it takes more than 1 hour to obtain the simulation result. This study used Radiance daylighting results from medium-quality setting to compare with the results from Split-Flux and Radiosity simulation methods.

Table 4-12: The Simulation Runtimes of Different Simulation Methods

Simulation Program	Runtime	
DOE2.1e+Split-Flux	0.05 mins	
EnergyPlus+Split-Flux	0.15 mins	
EnergyPlus+Radiosity	2.27 mins	
EnergyPlus+Radiance	Low-quality Setting	0.20 mins
	Medium-quality setting	5.00 mins
	High-quality setting	60.00 mins

4.2.6.1. South-Oriented Windows

For the South oriented windows, the importance of the Floor Visual Reflectance (FVR) settings in the daylighting simulation were tested using three different FVR values, which are: 0.2, 0.5, and 0.9.

4.2.6.1.1. Floor Visual Reflectance 0.2

For the lighting electricity use, without daylighting (grey color in Figure 4.17), all six window models have the same high annual lighting energy use¹⁷. After integrating daylighting in the simulation, over 80% of lighting energy was saved. Therefore, there is a huge benefit to use daylighting in saving lighting energy use. Comparing the simulation results with different simulation tools, the DOE2.1e+Split-Flux simulation method and the EnergyPlus+Split-Flux/Radiosity methods obtained similar results for the six window models, which means there were no significant differences in daylighting performance when the window location changes, with the exception the simulation results the window model 3, which had slightly higher lighting energy use compared to other window models.

However, in the EnergyPlus+Radiance simulation results, every window model had different lighting electricity use. The low-quality results in radiance had huge differences with the results from medium and high-quality settings. From Figure 4.17, the results showed that the low-quality results will lead to wrong decision in daylighting

¹⁷ A preliminary analysis of South-oriented windows, which used the medium-quality results from Radiance, was published as a conference paper “Research on Guidelines for Window Design Strategies in High Performance Office Buildings” (Li and Haberl, 2020).

design. The high quality got most correct lighting energy use. The medium-quality setting obtained slightly higher results to the high-quality setting results. In this study, the results from medium-quality setting was used to compare with the results from Split-Flux and Radiosity. Because the medium-quality settings could obtain relatively correct results with reasonable simulation runtime. The results from EnergyPlus+Radiance simulation showed that window model 3 had the highest lighting electricity use, while window 2 has the lowest lighting electricity use. These results show that the simulation results of EnergyPlus + Radiance were more sensitive to the window location changes. From Figure 4.17, for window model 3 and window model 4, the lighting electricity use predicted by EnergyPlus + Radiance was significantly higher than that predicted by DOE2.1e+Split-flux or by EnergyPlus+Split-flux/Radiosity. These differences indicated that only the Radiance daylighting simulation differentiates windows 3 and 4 from the other window models (All windows models 1-6 have equal area). The common characteristic of window 3 and 4 is the larger portion of the window near to the floor (Figure 4.8). When this lower window position is combined with the floor reflectance of 0.2, a large variation in the lighting energy is shown (Figure 4.17) for window model 3 and 4 (to a lesser extent) using the Radiance simulation.

Therefore, compared to Radiance, the Split-Flux and Radiosity daylighting simulation methods over-calculate the illuminance in the interior space when the window is in a low position on the exterior wall. That is because in the Split-Flux method, an empirical formula for calculating the Internal Reflected Component (IRC) is used, which does not consider window position relative to the floor; while in the

Radiosity calculation, the surfaces in the environment are assumed to be perfect (or Lambertian) diffusers, reflectors, or emitters, which are assumed to reflect incident light in all directions with equal intensity. Therefore, the Split-Flux and Radiosity simulation method have limitations for windows with varying window positions.

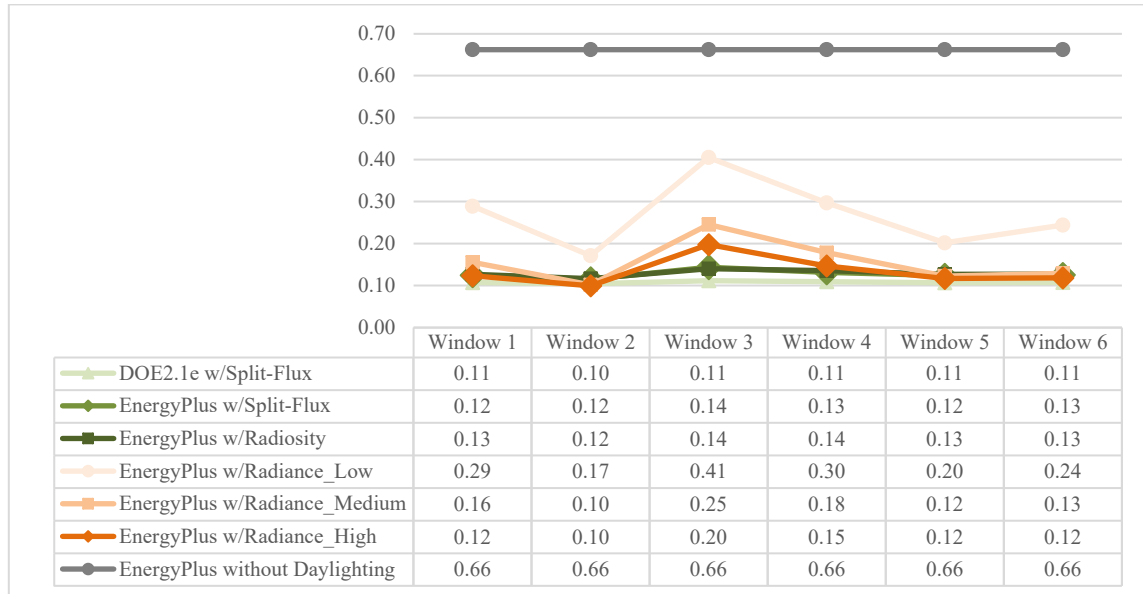


Figure 4.17: Annual Lighting Electricity Use with Floor Visual Reflectance 0.2 (South Facing Window, Phoenix, AZ) (Source: (Li and Haberl, 2020))

Figure 4.18 shows the simulated annual cooling load for Phoenix, AZ. This gray line is the cooling energy results without applying daylighting simulation. The results showed that all six models had similar cooling loads, which means the window location changes will not affect the cooling energy. After connecting daylighting simulation with thermal simulation, the results showed that there was a very large cooling reduction when daylighting techniques were used. Therefore, daylighting helped in reducing cooling energy in a hot climate zone. It can be observed that the results from the EnergyPlus+Split-Flux and the EnergyPlus+Radiosity were almost the same. But the

results from EnergyPlus+Split-Flux/Radiosity and DOE2.1e++Split-Flux have an approximate 9% difference with a higher cooling load predicted by EnergyPlus. This difference is most likely due to the thermal simulation difference between the DOE2.1e and EnergyPlus. Accordingly, the DOE2.1e+Split-Flux and EnergyPlus+Split-Flux/Radiosity obtained very similar lighting energy when window size and location changes were made, and the cooling usage from these simulation methods are almost the same. However, the lighting energy from EnergyPlus+Radiance was significantly different in all six models, thus, the cooling energy use of the six models had the same trends as the lighting energy.

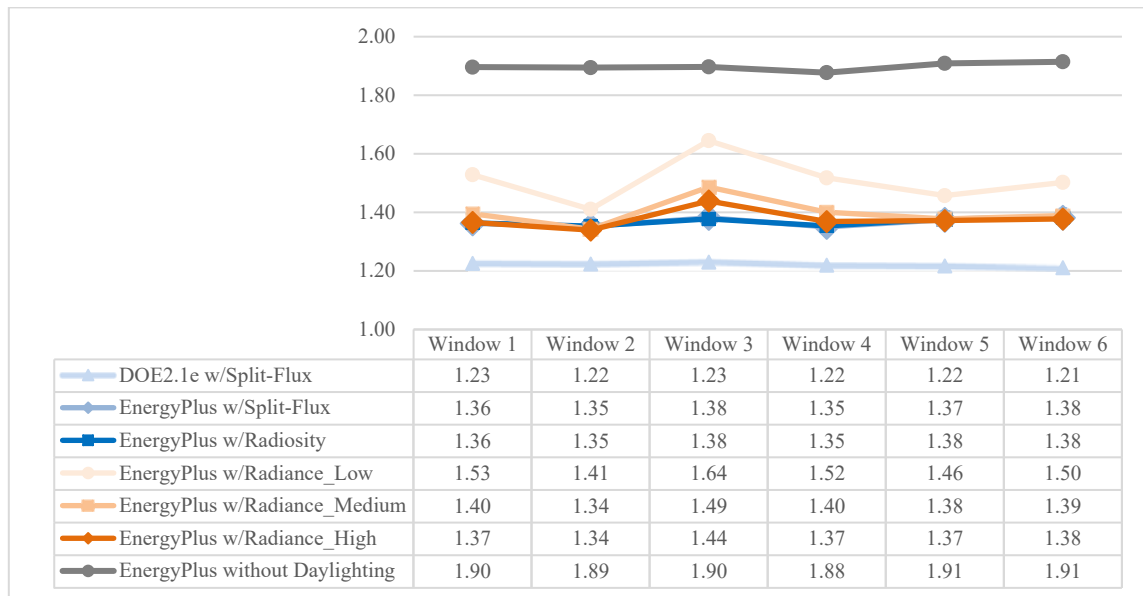


Figure 4.18: Annual Cooling Load Use with the Floor Visual Reflectance 0.2 (South Facing Window, Phoenix, AZ) (Source: (Li and Haberl, 2020))

In the same analysis, the heating load was small (Figure 4.19). This is because the analysis was in a hot climate location (i.e., Phoenix, AZ). In general, the results did not show a sensitivity to the window position. It is interesting to note that DOE2.1e

calculated around “0.0” total annual heating load, whereas all three EnergyPlus simulation methods calculated approximate 0.01 MWH/yr. The heating energy differences between with and without daylighting were very small as well.

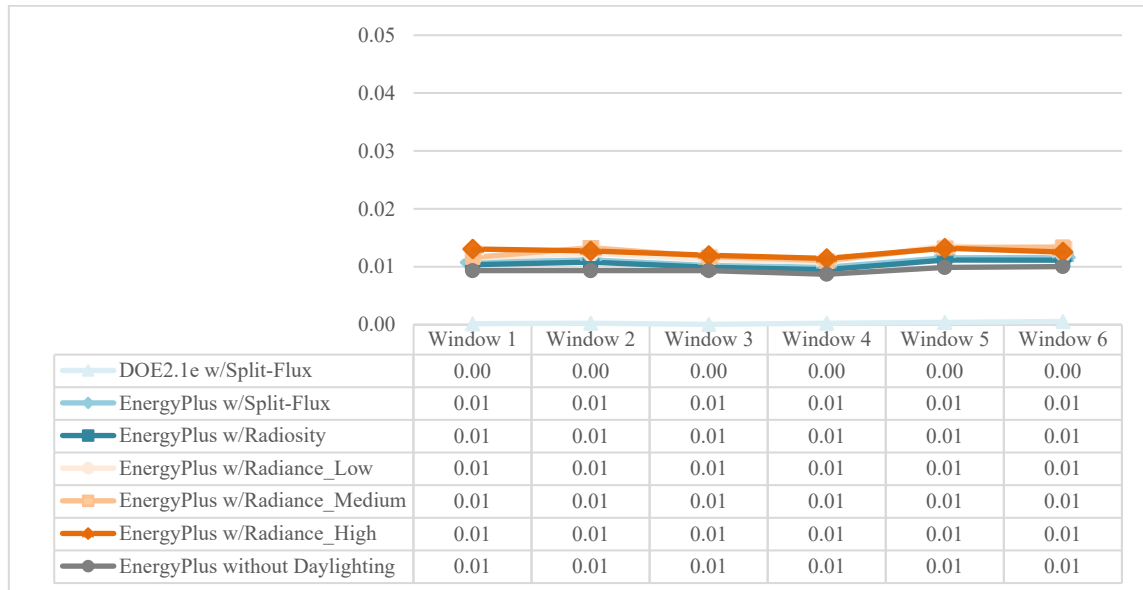


Figure 4.19: Annual Heating Load Use with Floor Visual Reflectance 0.2 (South Facing Window, Phoenix, AZ) (Source: (Li and Haberl, 2020))

4.2.6.1.2. Floor Visual Reflectance 0.5

After changing the floor visual reflectance from 0.2 to 0.5, lighting electricity use (Figure 4.20) decreased, the cooling load (Figure 4.21) also decreased slightly, but the heating load (Figure 4.22) was almost the same. The cooling load decrease is because of the increased daylighting from the increased FVR that decrease the lighting energy use. Unfortunately, the lighting energy decreasing did not impact the heating load because of the hot dry climate location (i.e., Phoenix, AZ, USA). When the simulations were repeated for floor a reflectance of 0.5, the lighting electricity only decreased by a small amount from the results of the DOE2.1e+Split-Flux or EnergyPlus+Split-Flux/Radiosity

simulation methods (Figure 4.20). The results of the combined EnergyPlus+ Radiance simulation method showed that variation in lighting energy of all six windows decreased significantly for the 0.5 floor reflectance when compared to the 0.2 floor reflectance.

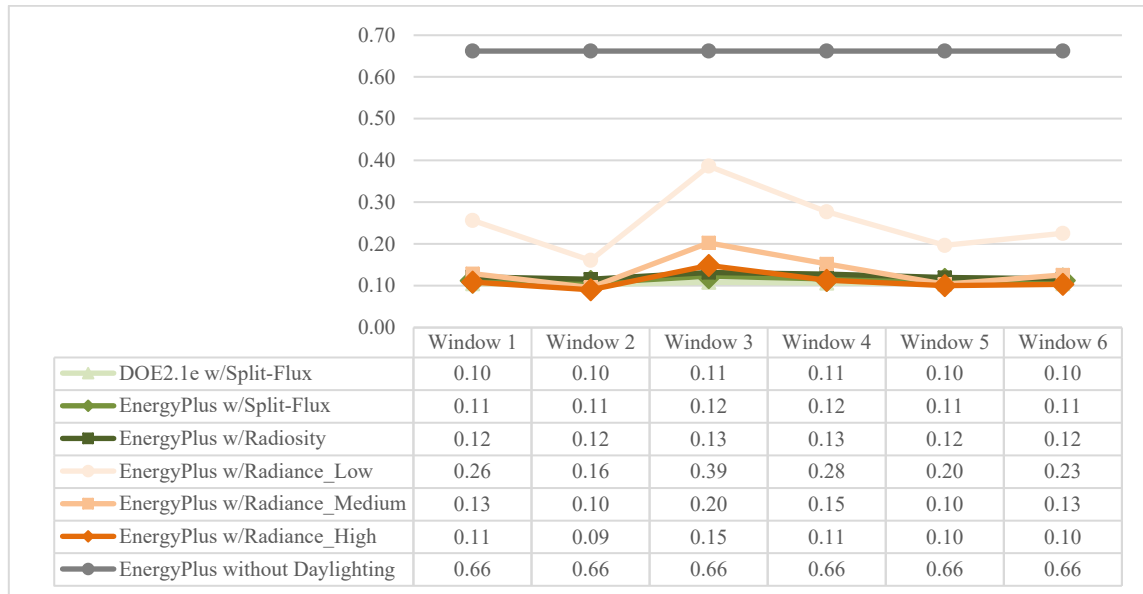


Figure 4.20: Annual Lighting Electricity Use with Floor Visual Reflectance 0.5 (South Facing Window, Phoenix, AZ)

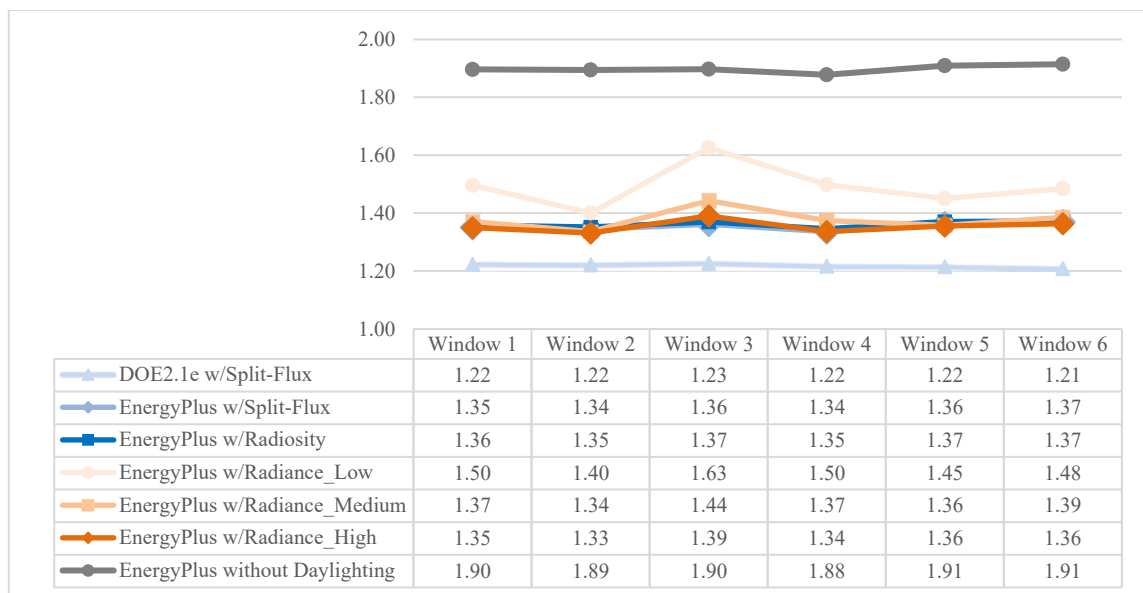


Figure 4.21: Annual Cooling Load Use with Floor Visual Reflectance 0.5 (South Facing Window, Phoenix, AZ)

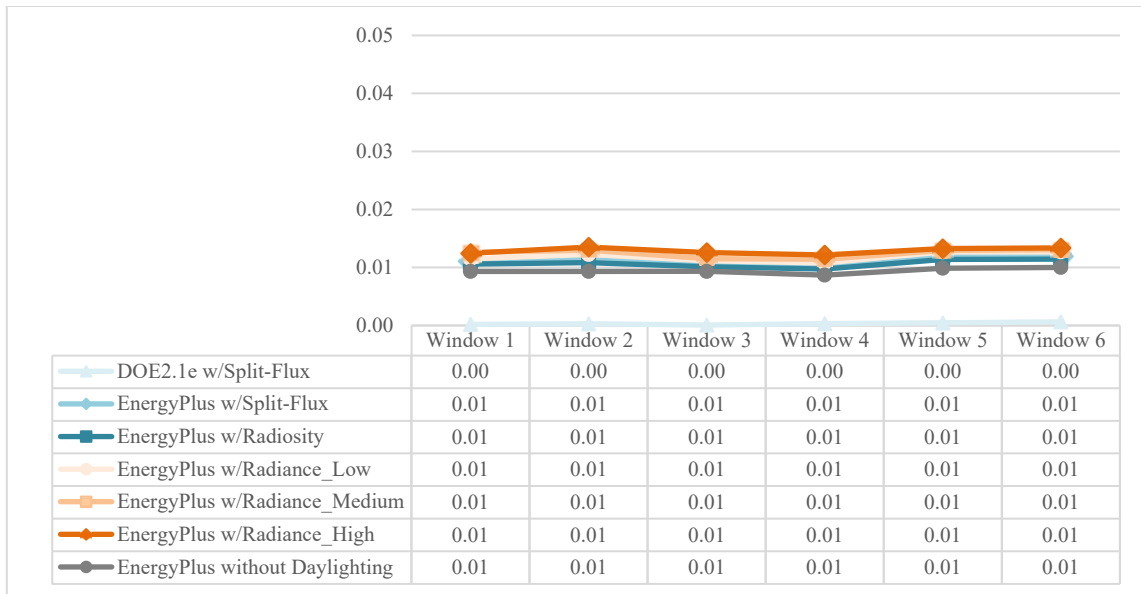


Figure 4.22: Annual Heating Load Use with Floor Visual Reflectance 0.5 (South Facing Window, Phoenix, AZ)

4.2.6.1.3. Floor Visual Reflectance 0.9

When the simulations were repeated for a floor reflectance of 0.9 (Figures 4.23 to 4.25), the results of the annual cooling load (Figure 4.24) and lighting energy usage (Figure 4.23) decreased dramatically in the EnergyPlus+Radiance simulation. In contrast, the annual cooling and lighting energy only dropped very little from the DOE2.1e+Split-Flux and EnergyPlus+Split-Flux/Radiosity simulation. Therefore, the differences in the lighting electricity use decreased for all the combined simulation methods because of the increased FVR. The lighting energy use calculated with the EnergyPlus+Radiance gave very similar results to the value of DOE2.1e+Split-Flux and EnergyPlus+Split-Flux/Radiosity, which had been observed when the floor reflectance was changed from 0.2 to 0.9. For the window model 1, 2, 5, and 6, the Radiance simulation had almost the same lighting energy results with Split-Flux and Radiosity

simulation. Only window model 3 gave higher lighting results from the Radiance simulation versus Split-Flux and Radiosity simulations (Figure 4.23). Therefore, when the interior surfaces were bright, the lighting results using either from Split-Flux or Radiosity or Radiance simulations were almost the same.

The cooling load (Figure 4.24) decrease is because of the increased daylighting, which decreased the lighting energy use. The heating load (Figure 4.25) stayed about the same because it was too small to see the difference.

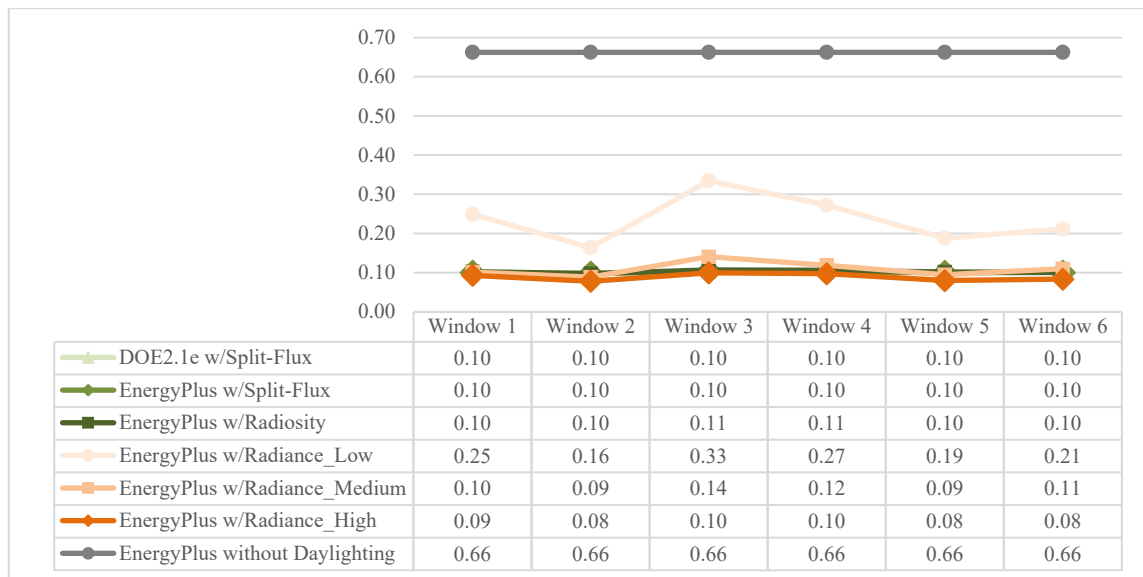


Figure 4.23: Annual Lighting Electricity Use with Floor Visual Reflectance 0.9 (South Facing Window, Phoenix, AZ) (Source: (Li and Haberl, 2020))

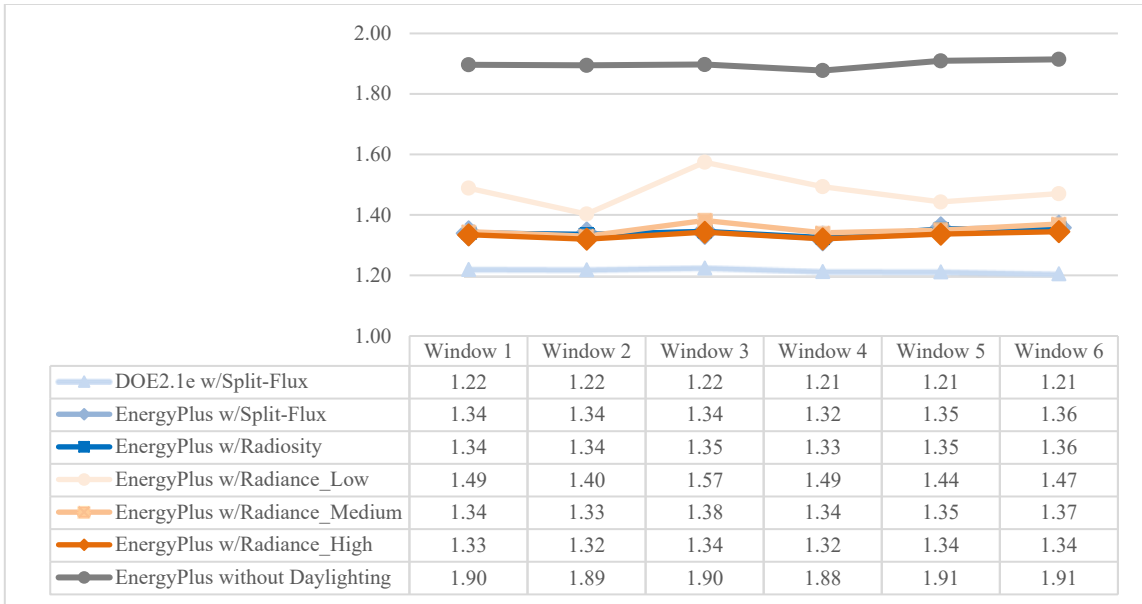


Figure 4.24: Annual Cooling Load Use with Floor Visual Reflectance 0.9 (South Facing Window, Phoenix, AZ) (Source: (Li and Haberl, 2020))

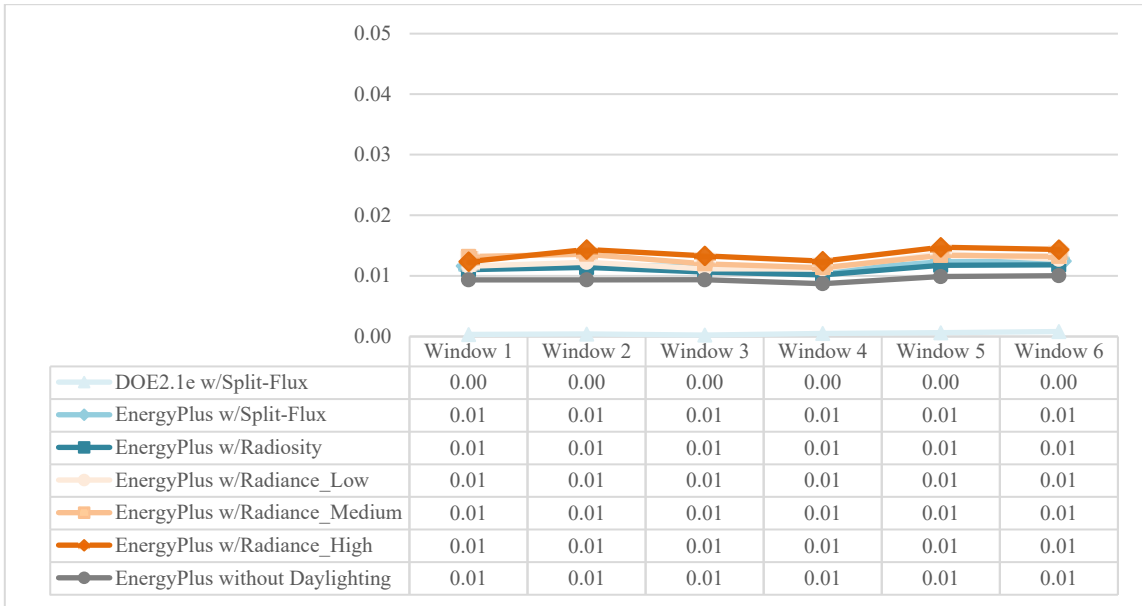


Figure 4.25: Annual Heating Load Use with Floor Visual Reflectance 0.9 (South Facing Window, Phoenix, AZ) (Source: (Li and Haberl, 2020))

4.2.6.2. East-Oriented Windows

For the windows in the East orientation, After integrating daylighting and

thermal simulation, the cooling load (Figure 4.27 - 0.2 FVR, Figure 4.30 - 0.5 FVR, Figure 4.33 - 0.9 FVR) increased as the lighting energy use increased (Figure 4.26 – 0.2 FVR, Figure 4.29 - 0.5 FVR, Figure 4.32 - 0.9 FVR). In a similar fashion as the South-facing windows, the heating load of East-facing windows (Figure 4.28- 0.2 FVR, Figure 4.31- 0.5 FVR, Figure 4.34 - 0.9 FVR) can be ignored in this cooling dominated climate.

For the lighting electricity use in a dark floor (Figure 4.26), like the results of South-facing windows, after integrating daylighting in the simulation, over 80% of lighting energy of East-facing windows was saved. The results of the East-facing window also showed that there were no significant differences in daylighting performance when the window location changes in the daylighting simulations of DOE2.1e+Split-Flux, EnergyPlus+Split-Flux/Radiosity. However, in the EnergyPlus+Radiance simulation results, every window model has a different lighting electricity use. These results imply that the use of the EnergyPlus+Radiance simulation method was more sensitive to the window location changes.

When the simulations were repeated for floor reflectances of 0.5 and 0.9 (Figure 4.29, Figure 4.32), in the lighting results from the DOE2.1e + Split-Flux, and the EnergyPlus + Split-Flux/Radiosity simulations, the lighting electricity use was very similar in all 6 window models. Unlike the South-facing window, the EnergyPlus + Radiance simulation results in the East-facing window produced different lighting electricity use in all six window models. In addition, in the East-facing windows, the lighting electricity use from the EnergyPlus + Radiance simulation (Medium-quality setting) was higher than the results from the DOE2.1e + Split-Flux and the EnergyPlus +

Split-Flux/Radiosity simulation for FVR varying from 0.2 to 0.5 to 0.9. Therefore, the Radiance simulation in the East-facing windows are more sensitive to the window location changes than the South-facing windows when the FVR changed from 0.2 to 0.9.



Figure 4.26: Annual Lighting Energy Use with Floor Visual Reflectance 0.2 (East Facing Window, Phoenix, AZ)

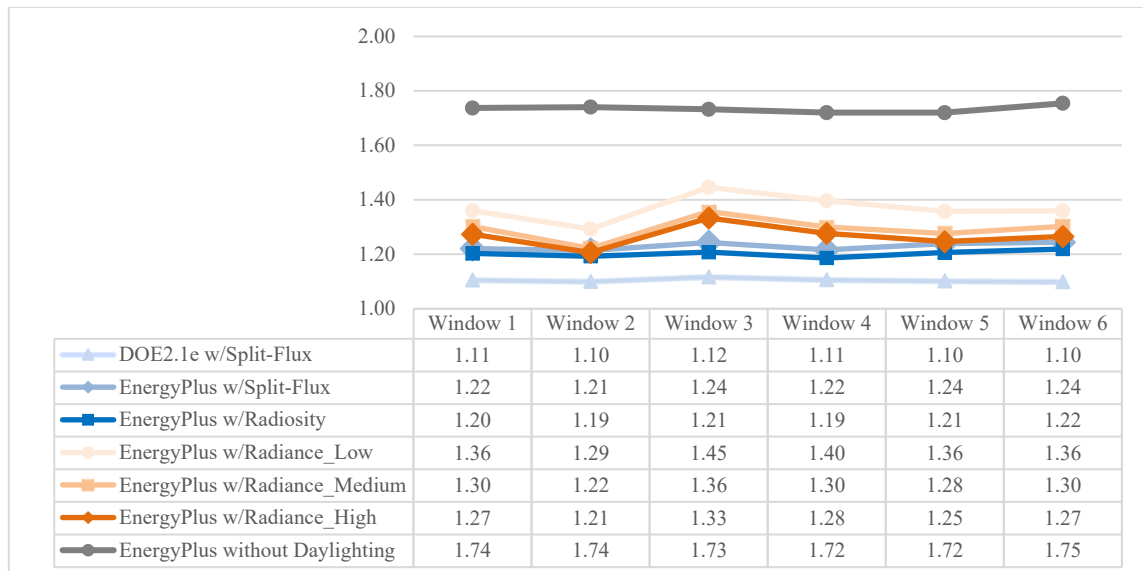


Figure 4.27: Annual Cooling Load Use with Floor Visual Reflectance 0.2 (East Facing Window, Phoenix, AZ)

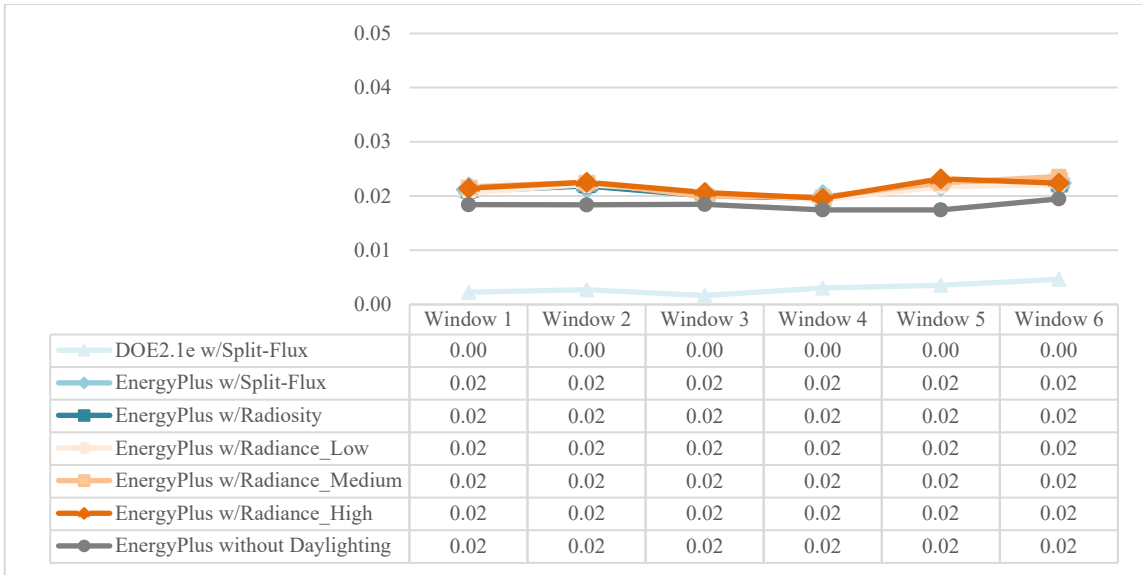


Figure 4.28: Annual Heating Load Use with Floor Visual Reflectance 0.2 (East Facing Window, Phoenix, AZ)

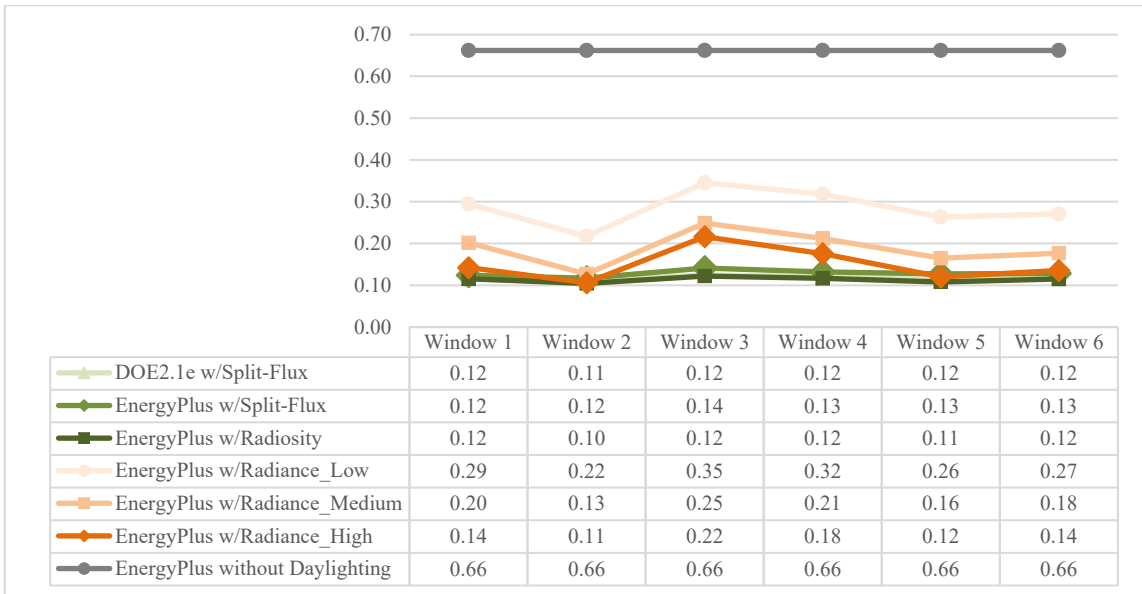


Figure 4.29: Annual Lighting Energy Use with Floor Visual Reflectance 0.5 (East Facing Window, Phoenix, AZ)

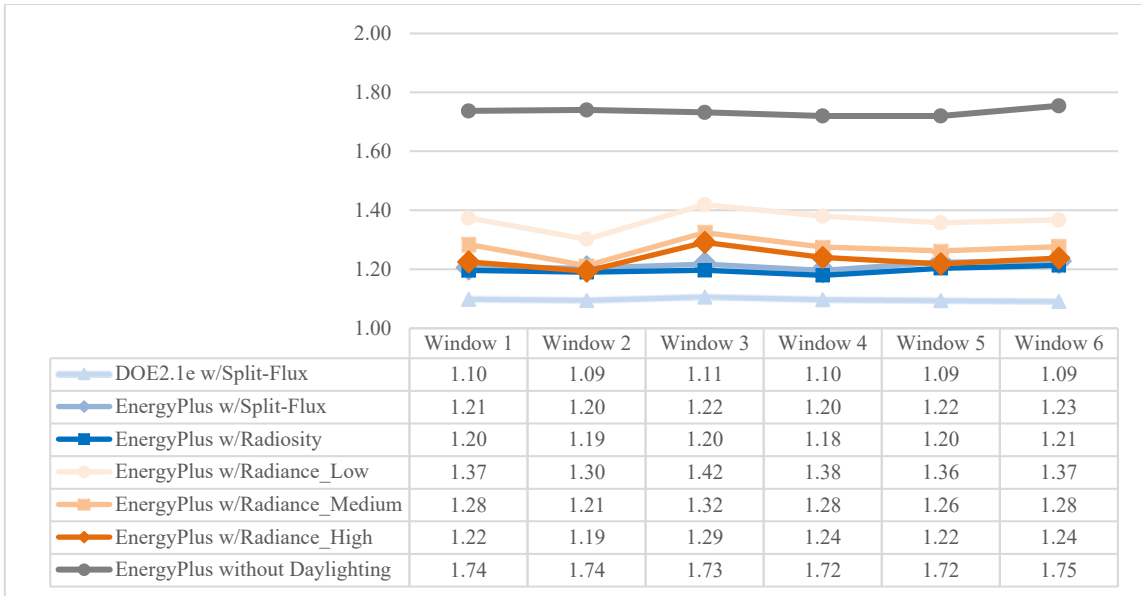


Figure 4.30: Annual Cooling Load Use with Floor Visual Reflectance 0.5 (East Facing Window, Phoenix, AZ)

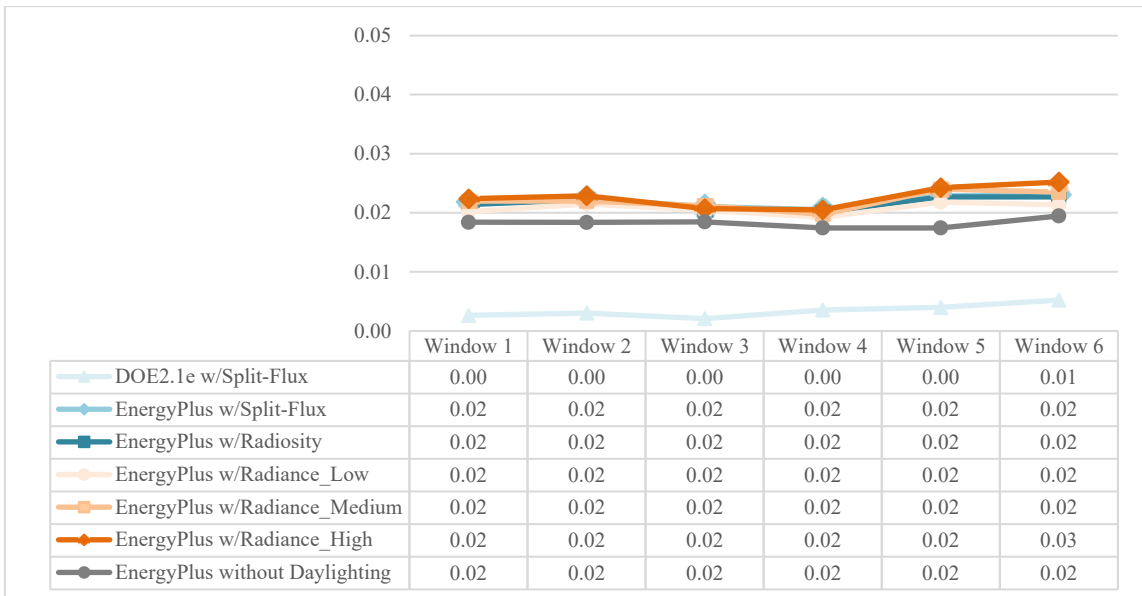


Figure 4.31 Annual Heating Load Use with Floor Visual Reflectance 0.5 (East Facing Window, Phoenix, AZ)

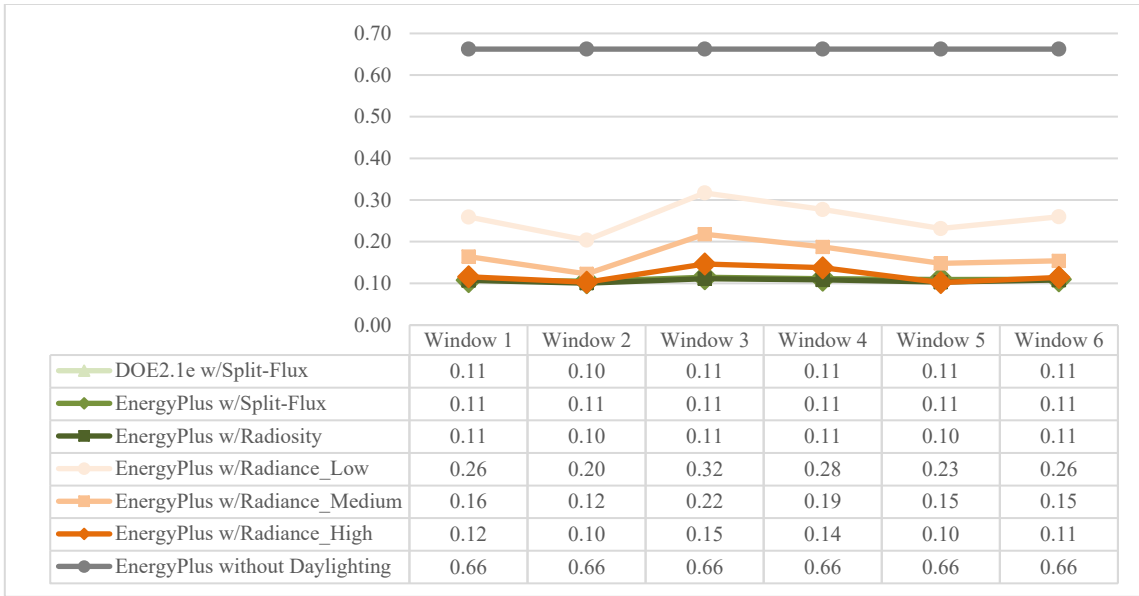


Figure 4.32: Annual Lighting Energy Use with Floor Visual Reflectance 0.9 (East Facing Window, Phoenix, AZ)

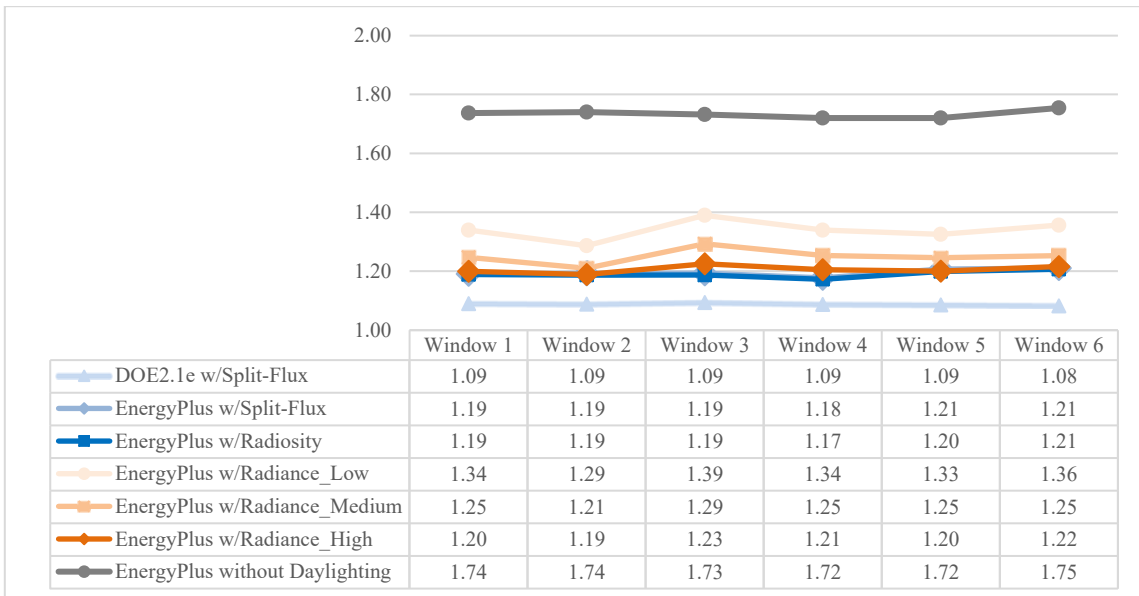


Figure 4.33: Annual Cooling Load Use with Floor Visual Reflectance 0.9 (East Facing Window, Phoenix, AZ)

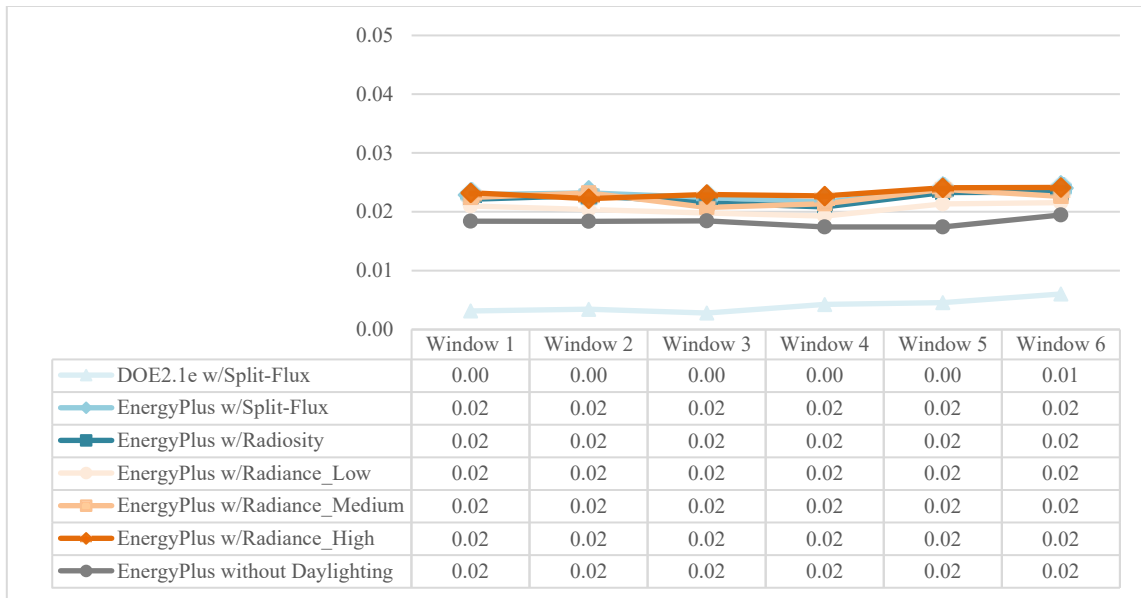


Figure 4.34 Annual Heating Load Use with Floor Visual Reflectance 0.9 (East Facing Window, Phoenix, AZ)

4.2.6.3. North-Oriented Windows

The results of the analysis for the North-oriented windows are shown in the Figure 4.35 to 4.43, the North-oriented windows have very different cooling, heating, and lighting results from the South and East-oriented windows. Without daylighting simulation, the North-oriented window cooling loads (the gray line in Figure 4.36) reduced a half compared to the cooling loads of South and East-facing window. However, the heating load of North-facing windows double compared to South or East facing windows. All the windows had similar cooling and heating results, which means the window location changes will not affect the cooling and energy without daylighting simulation. After integrated the daylighting and thermal simulation, the cooling loads (Figure 4.36 - 0.2 FVR, Figure 4.39 - 0.5 FVR, Figure 4.42 - 0.9 FVR) of the six models had the same trends as the lighting energy (Figure 4.35 - 0.2 FVR, Figure 4.38 - 0.5

FVR, Figure 4.41 - 0.9 FVR), while the heating load (Figure 4.37 - 0.5 FVR, Figure 4.40 - 0.5 FVR, Figure 4.43 - 0.9 FVR) the opposite trends as the lighting energy.

For the lighting electricity use with a FVR of 0.2 (Figure 4.35), the DOE-2.1e+Split-Flux simulation method and the EnergyPlus+Split-Flux/Radiosity methods obtained similar results for all the six window models with a exception of window 3 had slightly higher lighting electricity use than other five window models. However, in the EnergyPlus+Radiance simulation results, every window model had a very different lighting electricity use. More importantly, the lighting energy differences between EnergyPlus+Radiance versus EnergyPlus+Split-Flux/Radiosity methods became larger compared to the lighting results of the South and East-facing windows. For the window models 1, 3, 4, and 6, the lighting electricity use predicted by EnergyPlus+Radiance simulation was significantly higher than result predicted by DOE2.1e+Split-Flux or by the EnergyPlus+Split-flux/Radiosity simulation.

When the simulations were repeated for floor reflectances of 0.5 and 0.9, for the combined simulation methods of the DOE2.1e+Split-Flux and the EnergyPlus+Split-Flux/Radiosity simulation methods, the lighting electricity became exactly the same in all 6 window models (Figure 4.38 and Figure 4.41). However, unlike the South-facing windows, in the North-facing Window models 1, 3, 4, and 6, the lighting electricity difference between Radiance (Medium-quality setting) and Split-Flux/Radiosity simulation did not decrease significantly when the FVR changed from 0.2 to 0.5 to 0.9.

For the North-orientated windows, the lighting results from Radiance have a large difference compared to the results from Split-Flux and Radiosity. Radiance

simulation for the North-facing windows were more sensitive to the window location changes than the South and East-facing windows when the FVR changed from 0.2 to 0.5 to 0.9. This is because the North-facing window only gain the in-direct light and reflected light, and it could not obtain the direct sunlight. Therefore, the Split-Flux and Radiosity simulation over calculate the indirect light compared to the results from a Radiance simulation. In order to obtain the correct window location designs in North orientation, the Radiance simulation tool is suggested to use with the condition of both dark and bright floors.

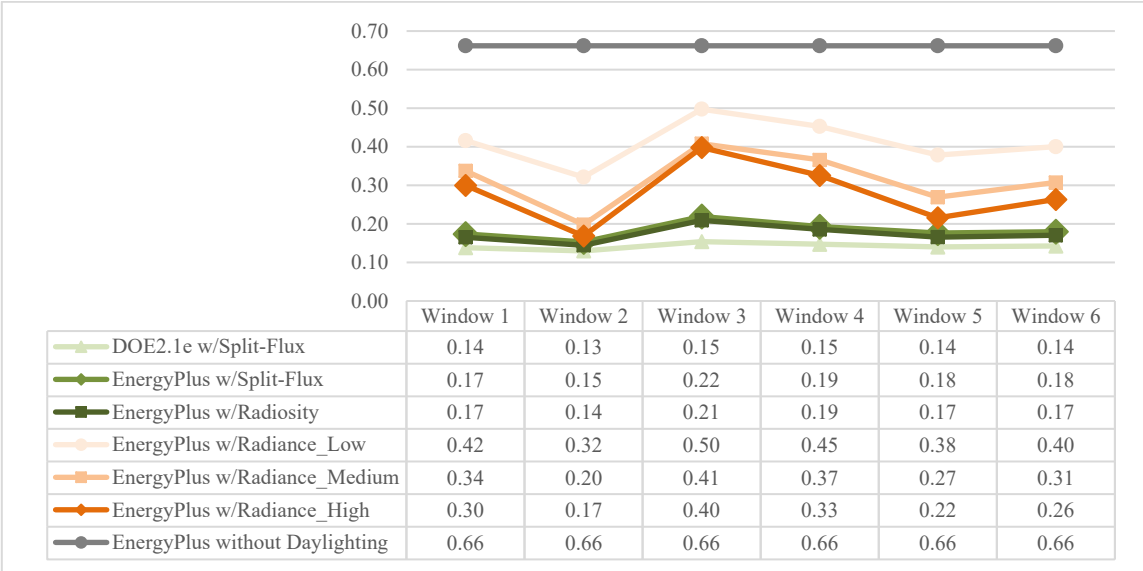


Figure 4.35: Annual Lighting Energy Use with Floor Visual Reflectance 0.2 (North Facing Window, Phoenix, AZ)

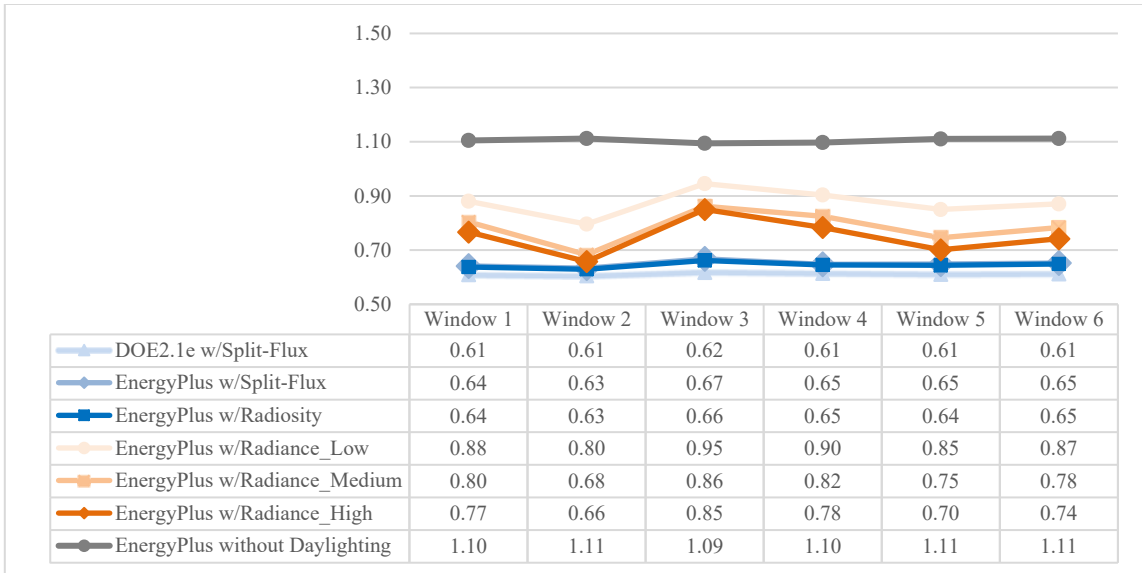


Figure 4.36: Annual Cooling Load Use with Floor Visual Reflectance 0.2 (North Facing Window, Phoenix, AZ)

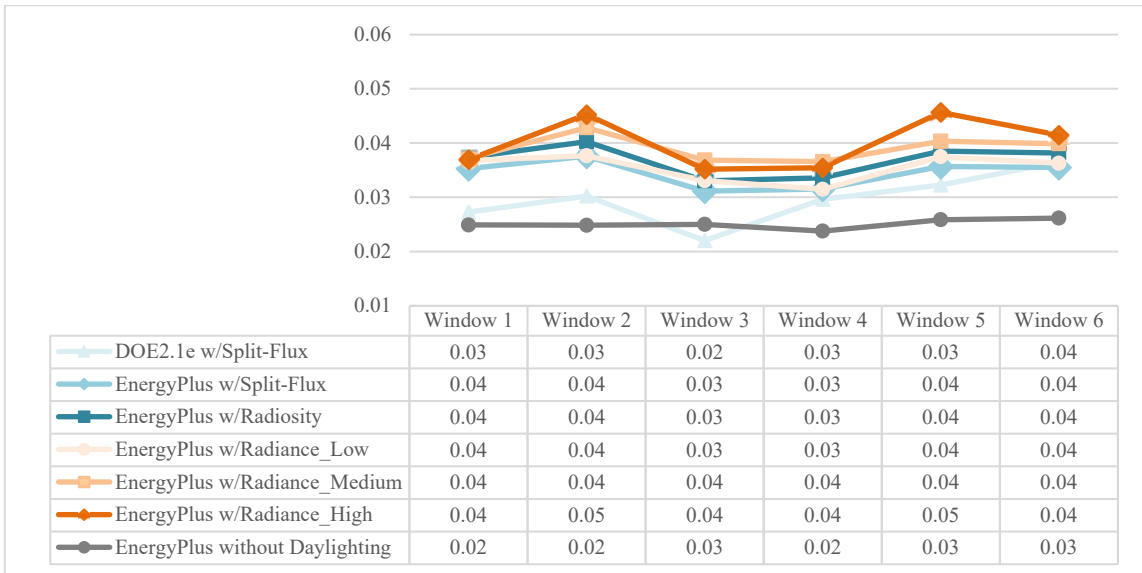


Figure 4.37: Annual Heating Load Use with Floor Visual Reflectance 0.2 (North Facing Window, Phoenix, AZ)

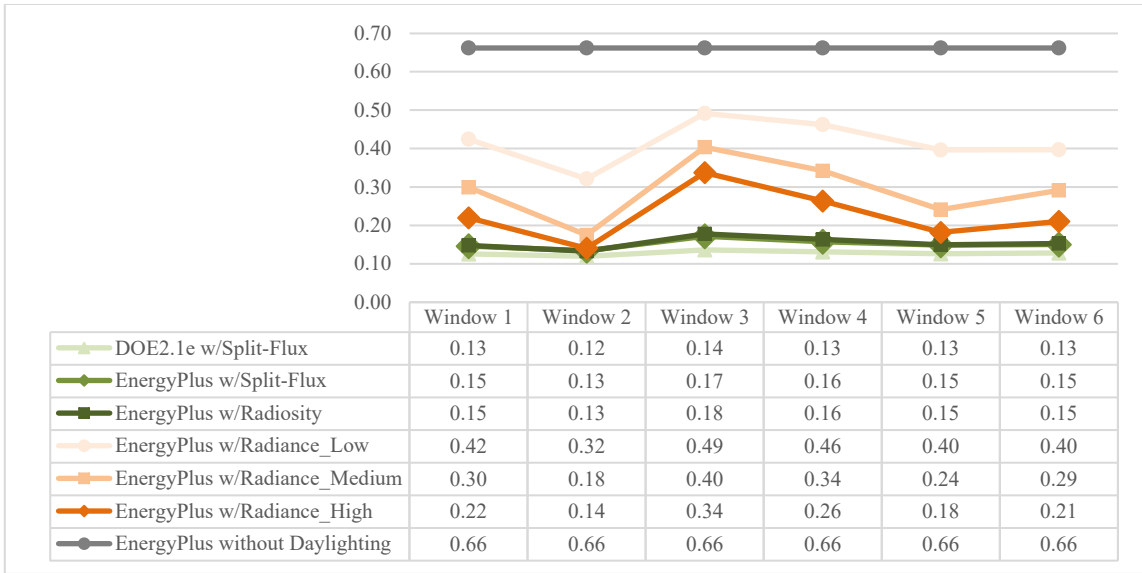


Figure 4.38: Annual Lighting Energy Use with Floor Visual Reflectance 0.5 (North Facing Window, Phoenix, AZ)

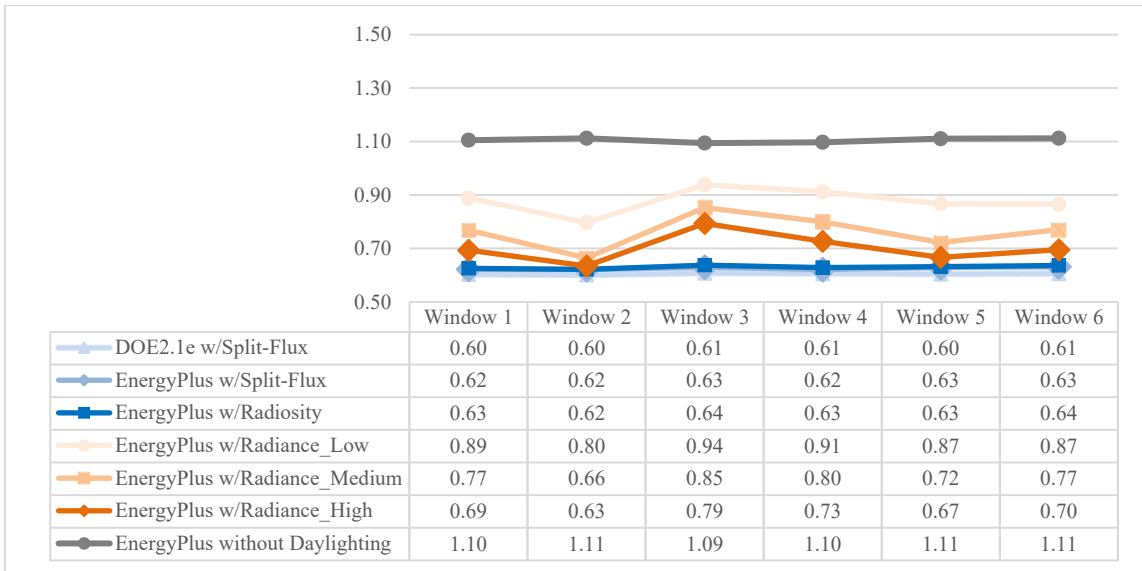


Figure 4.39: Annual Cooling Load Use with Floor Visual Reflectance 0.5 (North Facing Window, Phoenix, AZ)

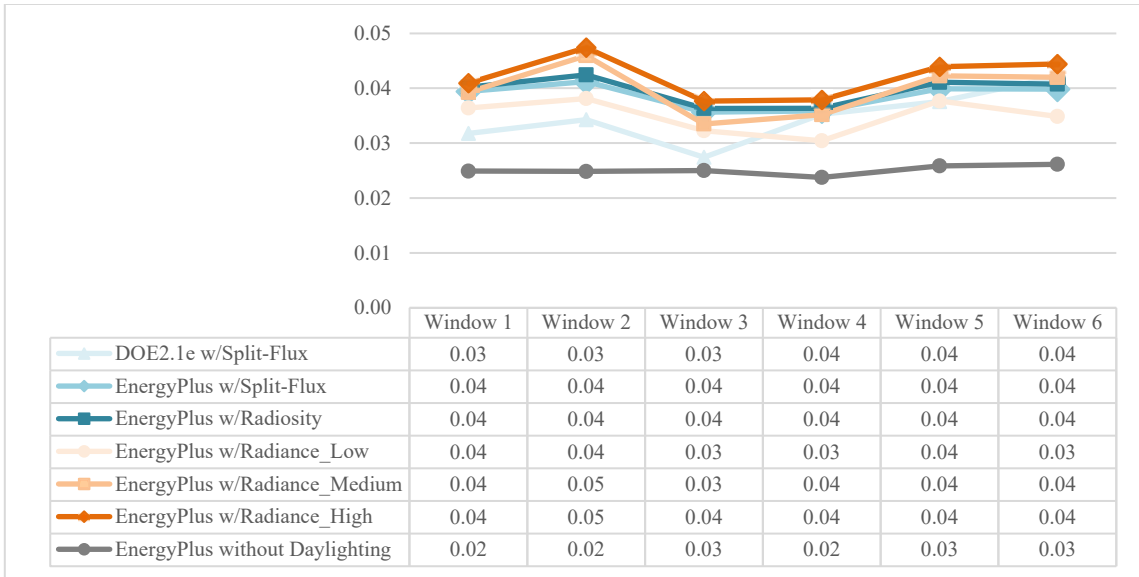


Figure 4.40: Annual Heating Load Use with Floor Visual Reflectance 0.5 (North Facing Window, Phoenix, AZ)

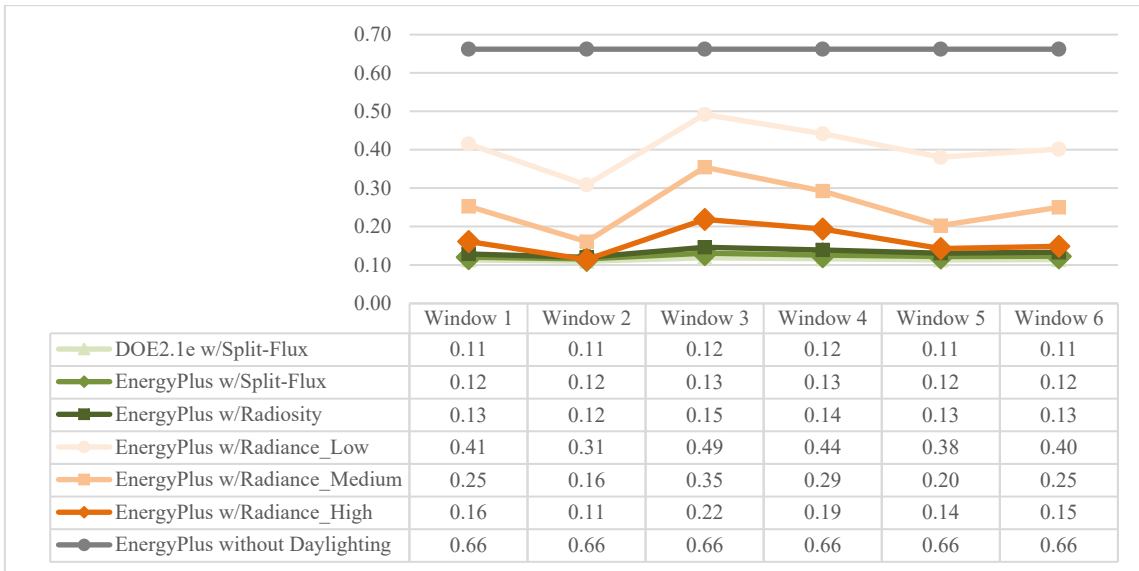


Figure 4.41: Annual Lighting Energy Use with Floor Visual Reflectance 0.9 (North Facing Window, Phoenix, AZ)

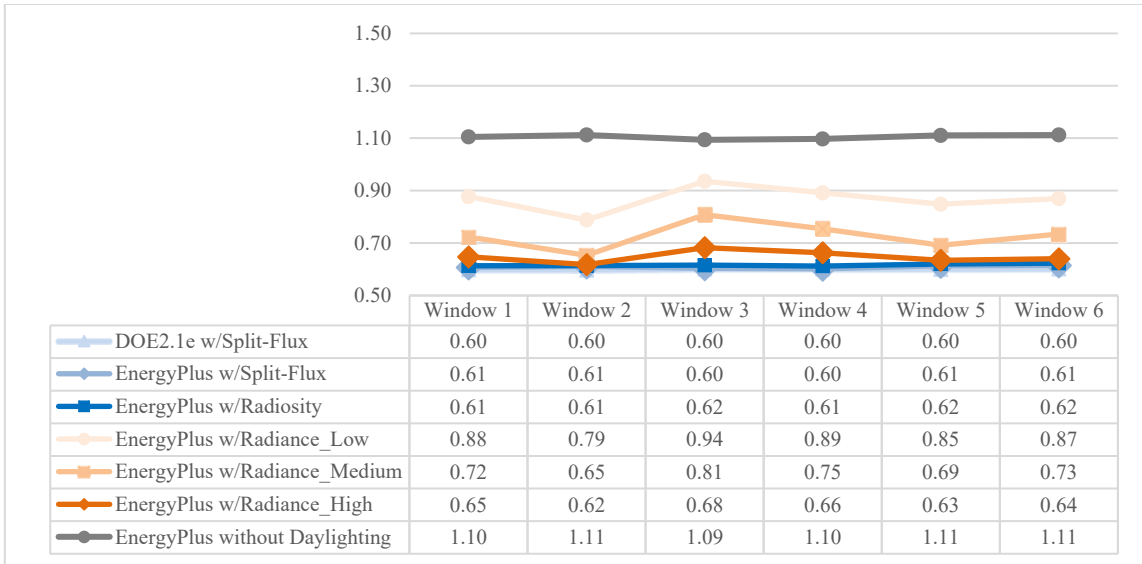


Figure 4.42: Annual Cooling Load Use with Floor Visual Reflectance 0.9 (North Facing Window, Phoenix, AZ)

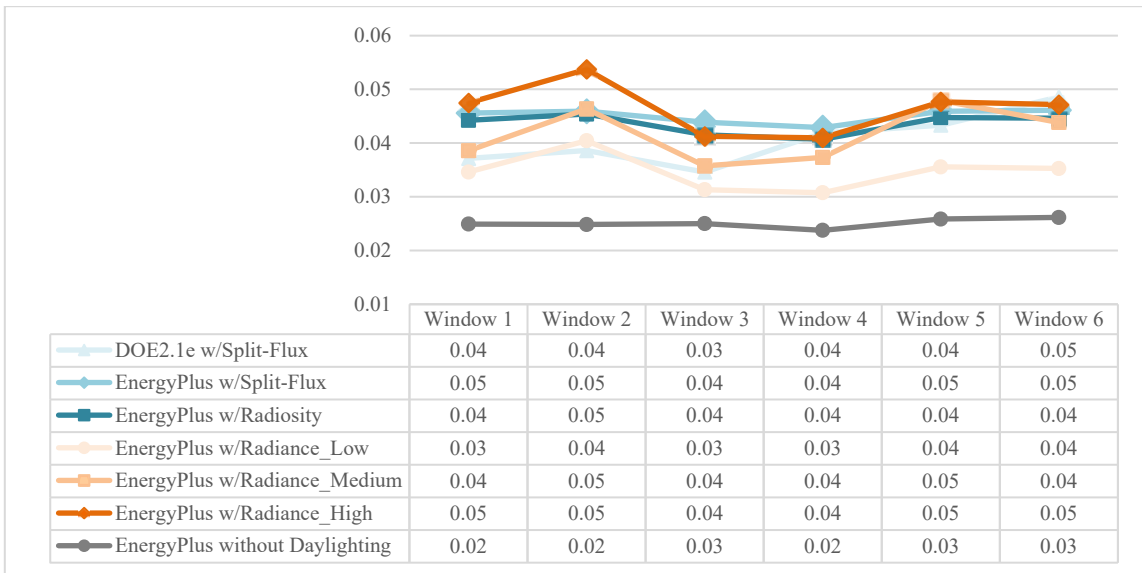


Figure 4.43: Annual Heating Load Use with Floor Visual Reflectance 0.9 (North Facing Window, Phoenix, AZ)

4.2.6.4. West-Oriented Windows

The simulation results of the West-orientated windows are shown in Figure 4.44 to 4.52. In the results, after integrating the daylighting and thermal simulation, the

cooling load (Figure 4.45-FVR 0.2, Figure 4.48-FVR 0.5, Figure 4.51-FVR 0.9) increased as the lighting increased (Figure 4.44-FVR 0.2, Figure 4.47-FVR 0.5, Figure 4.50-FVR 0.9), whereas the heating load (Figure 4.46-FVR 0.2, Figure 4.49-FVR 0.5, Figure 4.52-FVR 0.9) decreased as the lighting energy increased.

Like the East-facing windows, the lighting electricity use with floor visual reflectance 0.2 of West-facing window (Figure 4.44) showed that there were no significant differences in daylighting performance when the window location changed in the daylighting simulations of DOE2.1e+Split-Flux, EnergyPlus+Split-Flux/Radiosity. However, in the EnergyPlus+Radiance simulation results, every window model has different lighting electricity use. In window models 1, 3, 4, and 6, the lighting electricity usage predicted by EnergyPlus+Radiance was significantly higher than the other simulations. These results showed that the EnergyPlus+Radiance simulation method was more sensitive to the window location changes for the West-orientation.

When the simulations were repeated for floor reflectances of 0.5 and 0.9 (Figure 4.47 and Figure 4.50), the calculated lighting electricity use was very similar in all 6 window models from the DOE2.1e+Split-Flux and the EnergyPlus+Split-Flux/Radiosity simulations. Like the East-facing window, the EnergyPlus+Radiance simulation results in West-facing window obtain very different lighting electricity use in all the six window models. In addition, in the West-facing windows, the lighting electricity use of window models (1, 3, 4, and 6) from EnergyPlus+Radiance (Medium-quality setting) simulation were still higher than the results from DOE2.1e+Split-Flux and EnergyPlus+Split-Flux/Radiosity simulation for FVR of 0.2 to 0.5 to 0.9. Therefore, the results showed

that use of EnergyPlus with Radiance provided more sensitivity to the changes of floor reflectances empirically for darker floor. The results of West-orientated window design showed that it is useful to use the Radiance simulation for both dark and bright floors.

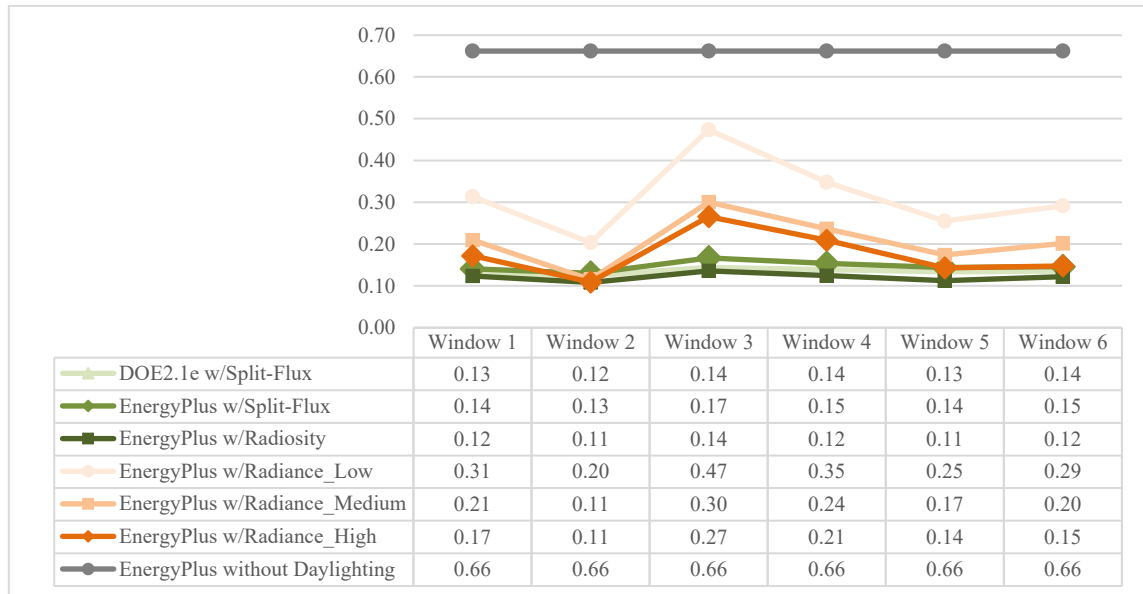


Figure 4.44: Annual Lighting Energy Use with Floor Visual Reflectance 0.2 (West Facing Window, Phoenix, AZ)

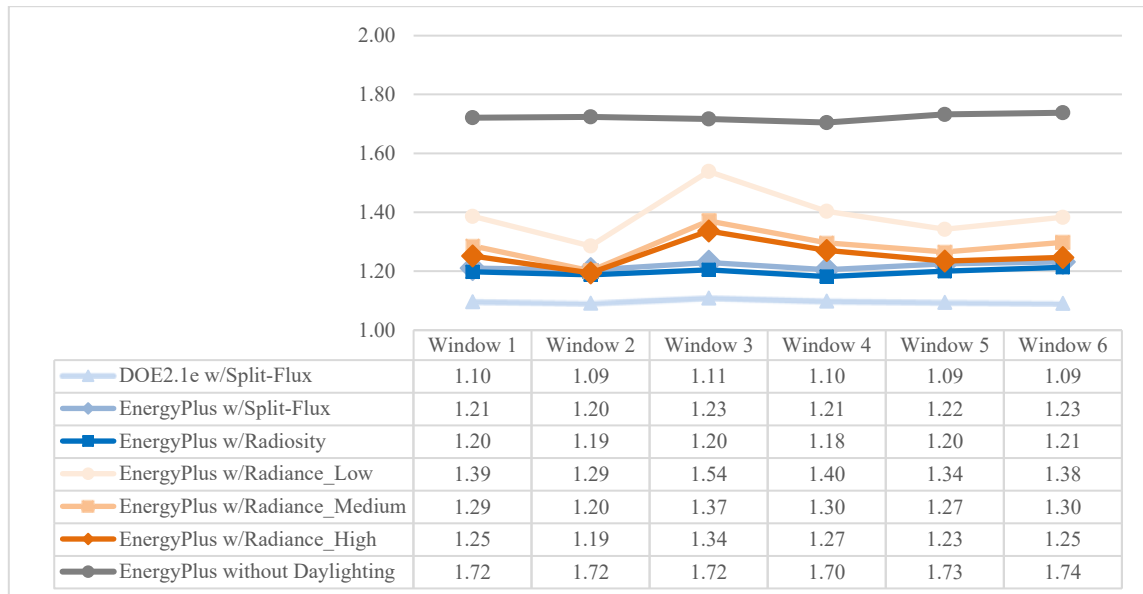


Figure 4.45: Annual Cooling Load Use with Floor Visual Reflectance 0.2 (West Facing Window, Phoenix, AZ)

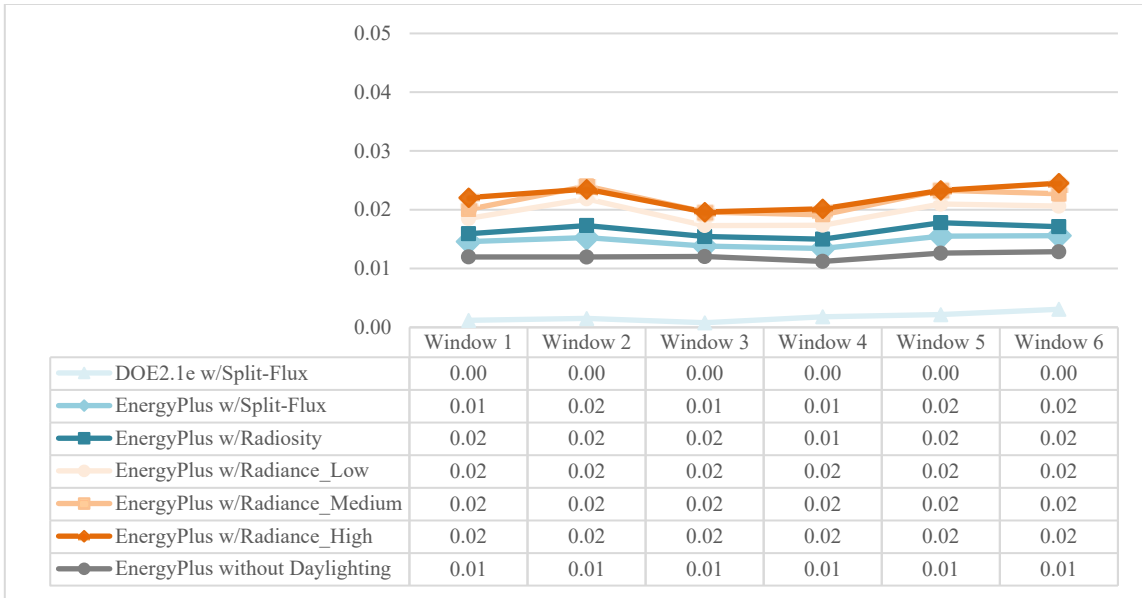


Figure 4.46: Annual Heating Load Use with Floor Visual Reflectance 0.2 (West Facing Window, Phoenix, AZ)

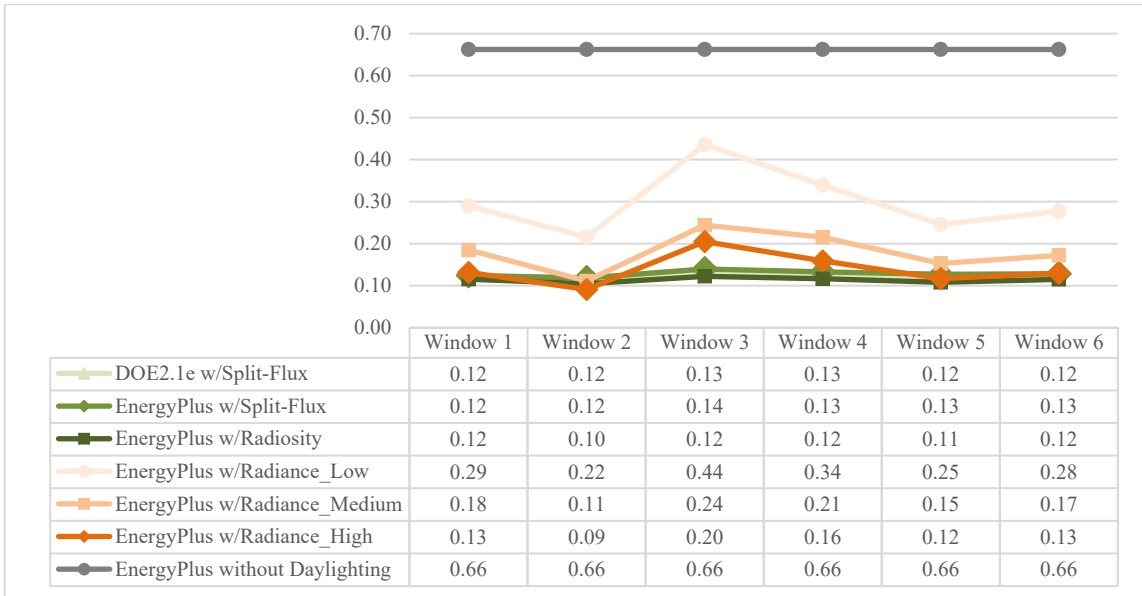


Figure 4.47: Annual Lighting Energy Use with Floor Visual Reflectance 0.5 (West Facing Window, Phoenix, AZ)

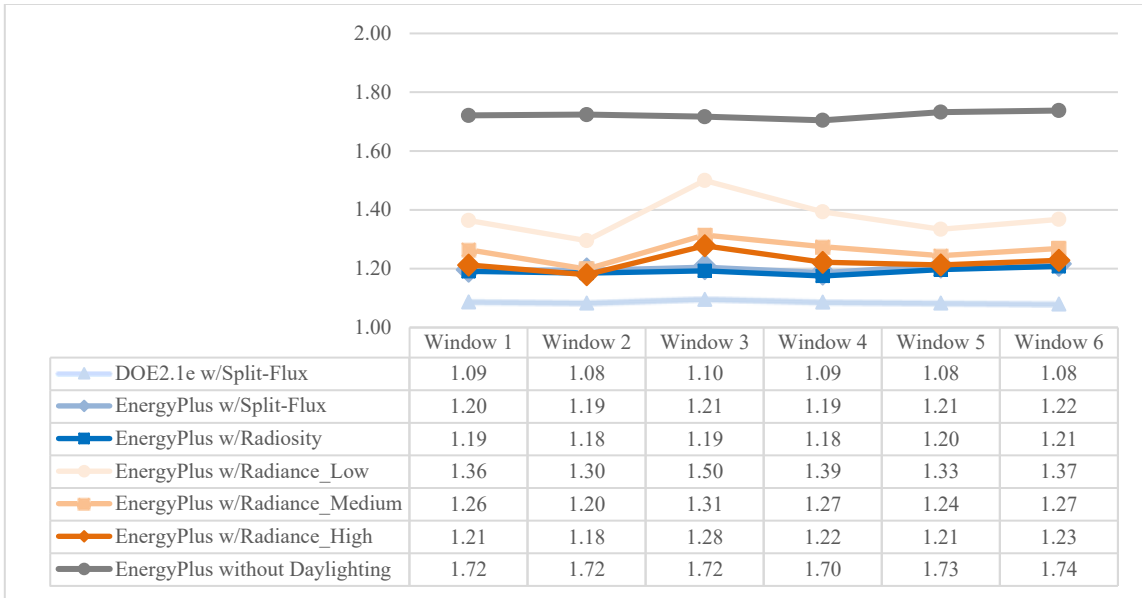


Figure 4.48: Annual Cooling Load Use with Floor Visual Reflectance 0.5 (West Facing Window, Phoenix, AZ)



Figure 4.49: Annual Heating Load Use with Floor Visual Reflectance 0.5 (West Facing Window, Phoenix, AZ)

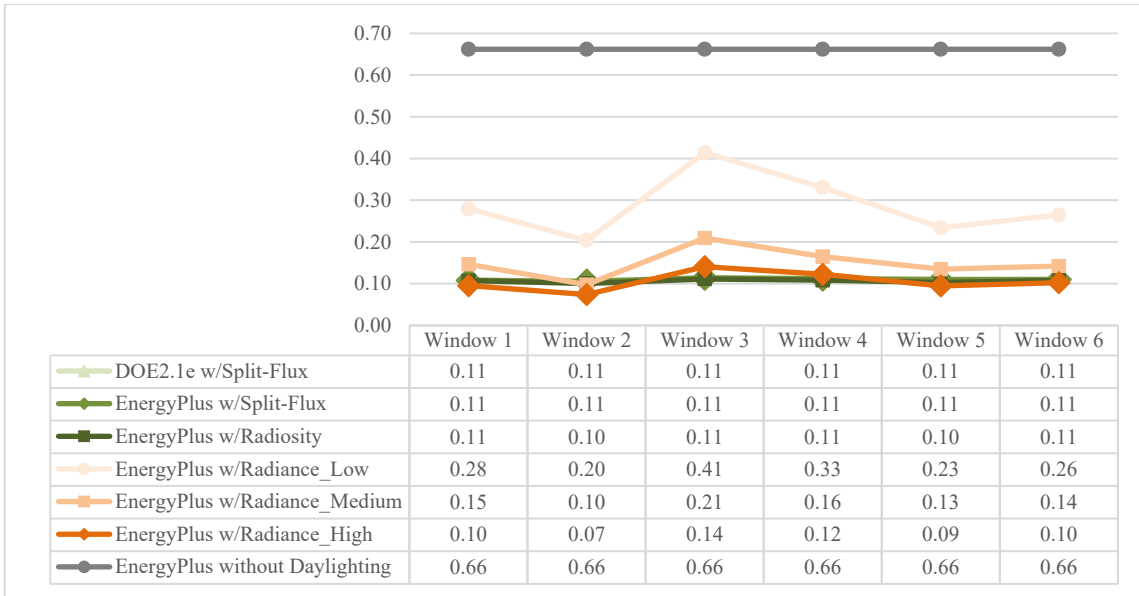


Figure 4.50: Annual Lighting Energy Use with Floor Visual Reflectance 0.9 (West Facing Window, Phoenix, AZ)

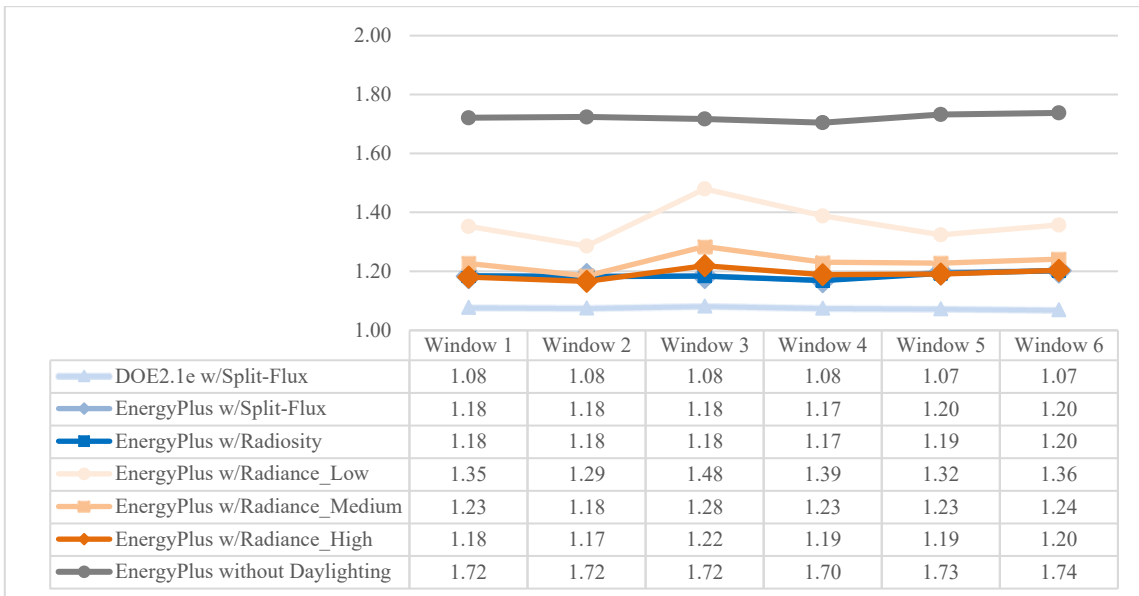


Figure 4.51: Annual Cooling Load Use with Floor Visual Reflectance 0.9 (West Facing Window, Phoenix, AZ)

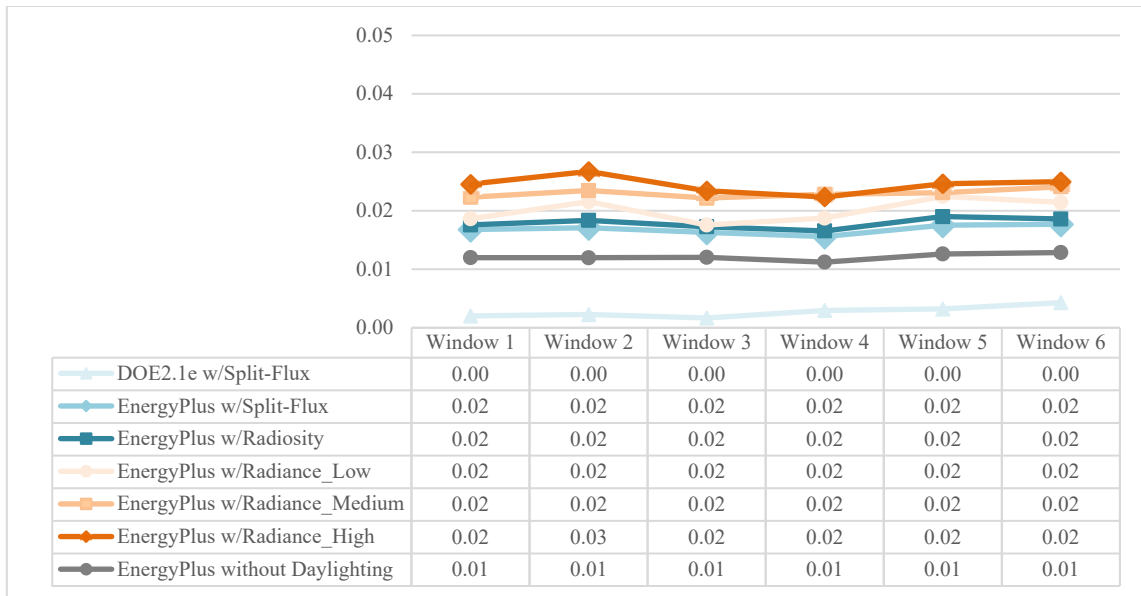


Figure 4.52: Annual Heating Load Use with Floor Visual Reflectance 0.9 (West Facing Window, Phoenix, AZ)

4.2.6.5. Summary

In summary, this section tested six window models using four different combination of daylighting and thermal simulation models, which include DOE2.1e+Split-Flux, EnergyPlus+Split-Flux, EnergyPlus+Radiosity, and EnergyPlus+Radiance. The different simulation methods have different simulation runtimes. The DOE2.1e+Split-Flux take the shortest runtime with few seconds, while EnergyPlus+Radiosity take around 2 mins to run simulation (Table 4-12). The EnergyPlus+Radiance simulation method had three rendering settings, which are low-quality, medium- quality and high-quality settings. The low-quality setting obtains the least accurate results, which will lead to wrong direction of daylighting design. The medium-quality setting could obtain relatively correct result with reasonable simulation runtime. The high quality performs the most correct results, but it takes more than 1 hour

to obtain the simulation result. Therefore, this study used daylighting results from Radiance with medium-quality setting to compare with the results from Split-Flux and Radiosity simulation methods.

The six window models were tested in four orientations (South, North, East, and West) with different Floor Visual Reflectance (FVR) (i.e., 0.2, 0.5, 0.9), in Phoenix, AZ. In this simulation, the wall and roof surface were bright (visual reflectance 0.7). The heating load is too small to be analyzed. Without daylighting simulations, all the windows had similar cooling and heating results, which means the window location changes will not affect the cooling and heating energy. After integrated the daylighting and thermal simulation, the lighting energy and cooling energy decreased dramatically. In addition, the cooling loads of the six models had the same trends as the lighting energy. Therefore, in this cooling-dominated climate zone, reducing the lighting energy use is the important to reduce the total energy use.

For the South-facing windows, when the floor was a dark surface with a visual reflectance 0.2, the EnergyPlus+Radiance simulation resulted in a higher lighting energy use than the lighting results of EnergyPlus+Split-Flux/Radiosity and DOE-2.1e+Split-Flux simulation. In addition, the Radiance simulation is more sensitive to window location changes than the Split-Flux and Radiosity. The results also showed that when the FVR was increased from 0.2 to 0.5/0.9, the lighting energy results from EnergyPlus+Radiance became closer to the results of other simulation methods. From these results it can be concluded that when the interior surfaces of the room are all bright (i.e., reflectance 0.7, 0.8 or 0.9), the lighting results from the Split-Flux, Radiosity, and

Radiance simulations become very similar. The Split-Flux is a relatively simple calculation, which takes seconds to run an annual daylighting simulation versus an analysis with Radiosity that can take around 2.7 minutes to run a daylighting simulation (Table 4-12). However, a Radiance analysis can take around 5 minutes to run a medium-quality annual daylighting simulation with relatively medium accuracy, or more than 60 minutes to run a high accuracy daylighting simulation (Table 4-12), which makes an optimization analysis difficult. Therefore, there is a need for an accurate daylight/thermal analysis tool that runs quickly. In addition, for the South-facing windows, the results show that a DOE-2/eQuest+Split-Flux simulation can be relatively accurate when the interior surfaces are bright, which saves simulation runtime.

For the East-oriented and West-oriented windows, when the simulations were repeated for floor reflectances of 0.2, 0.5 and 0.9, the results also showed that there were no significant differences in daylighting performance when the window location changes in the daylighting simulations of DOE2.1e+Split-Flux or EnergyPlus+Split-Flux/Radiosity. However, in the EnergyPlus+Radiance simulation results, every window model has a different lighting electricity use. Unlike the South-facing window, the EnergyPlus+Radiance simulation in East and West-facing windows always resulted in a higher lighting energy use than the lighting results of EnergyPlus+Split-Flux/Radiosity or DOE2.1e+Split-Flux simulation. Radiance in East and West-facing windows are more sensitive to the window location changes than the South-facing windows when the FVR changed from 0.2 to 0.5 to 0.9. Therefore, for off-center window location designs in the East or West orientations, it is important to use the Radiance simulation tool for either

dark or bright floors.

The North-oriented windows have very different cooling and heating load results from the South and East-oriented windows. The cooling loads reduced a half compared to the cooling loads of South and East-facing window. However, the heating load of North-facing windows double compared to South or East facing windows. For the lighting electricity use with FVR 0.2, the DOE-2.1e+Split-Flux simulation method and the EnergyPlus+Split-Flux/Radiosity methods obtained similar results for all the six window models. However, in the EnergyPlus+Radiance simulation results, every window model had a very different lighting electricity use. More importantly, the lighting energy differences between EnergyPlus+Radiance versus EnergyPlus+Split-Flux/Radiosity methods became larger compared to the lighting results of the South, East, and West-facing windows. When the simulations were repeated for floor reflectances of 0.5 and 0.9, lighting electricity differences between Radiance and Split-Flux/Radiosity simulation did not decrease. For the window models 1, 3, 4, and 6, the lighting electricity use predicted by EnergyPlus+Radiance simulation were significantly higher than result predicted by DOE2.1e+Split-Flux or by the EnergyPlus+Split-flux/Radiosity simulation. Therefore, in a similar fashion as the East and West-orientation, for a window location design in the North orientation, it is useful to use the Radiance simulation tool for either dark or bright floors.

4.2.7. Dynamic Daylighting Metric Analysis

Dynamic daylighting metrics include the spatial Daylight Autonomy (sDA) index

and the Annual Sun Exposure (ASE) index. In order to gain LEED daylighting credit, the interior spaces should achieve a spatial Daylight Autonomy index (sDA_{300 lux / 50% of the annual occupied hours}) of 55% (2pts) or 75% (3pts) with an Annual Sunlight Exposure index (ASE_{1000lx, 250h}) below 10% in all regularly occupied floor areas. Therefore, in order to have a good interior visual environment, the sDA should be larger than 55%, and the ASE should be less than 10%. Unfortunately, the DOE-2+Split-Flux and EnergyPlus+Split-Flux/Radiosity simulation methods do not calculate the ASE and sDA results. Therefore, in this study, the EnergyPlus+Radiance (DIVA) simulation was used to calculate the sDA and ASE results. Tables 4-13 to Table 4-24 showed the dynamic daylighting matrix for the South, East, North, and West orientations with different FVRs (i.e., 0.2, 0.5, 0.9).

4.2.7.1. Dynamic Daylighting Metric in South-Facing Window

In Table 4-13 to 4-15, the sDA increased as the floor visual reflectance increased. However, the ASE was not affected by changes in the floor visual reflectance. This is because the ASE is only related to the direct sunlight. Unfortunately, the ASE for the South-facing window simulations were much higher than 10%. Therefore, the results indicated these South-facing windows may have glare.

Table 4-13: sDA and ASE with Floor Visual Reflectance 0.2 (South-Facing Window, Phoenix, AZ)

	Window 1	Window 2	Window 3	Window 4	Window 5	Window 6
sDA	69.3	100	48	63.3	92.7	78
ASE	40	58	26.7	42	56.7	53.3

Table 4-14: sDA and ASE with Floor Visual Reflectance 0.5 (South-Facing Window, Phoenix, AZ)

	Window 1	Window 2	Window 3	Window 4	Window 5	Window 6
sDA	100	100	62.7	80	100	100
ASE	40	58	26.7	42	56.7	53.3

Table 4-15: sDA and ASE with Floor Visual Reflectance 0.9 (South-Facing Window, Phoenix, AZ)

	Window 1	Window 2	Window 3	Window 4	Window 5	Window 6
sDA	100	100	100	100	100	100
ASE	40	58	26.7	42	56.7	53.3

4.2.7.2. Dynamic Daylighting Metric in East-Facing Window

In Table 4-16 to 4-18, for the East-oriented windows, the sDA were below 55% in the most cases. However, the ASE did not decrease that much compared to South-oriented windows. Therefore, for the same window areas, the East-oriented windows have fewer windows when the $sDA \geq 55$ compared to South oriented window. In addition, all the windows showed glare conditions.

Table 4-16: sDA and ASE with Floor Visual Reflectance 0.2 (East-Facing Window, Phoenix, AZ)

	Window 1	Window 2	Window 3	Window 4	Window 5	Window 6
sDA	52.7	66.7	34	42	49.3	48.7
ASE	35.3	37.3	25.3	34	39.3	36.7

Table 4-17: sDA and ASE with Floor Visual Reflectance 0.5 (East-Facing Window, Phoenix, AZ)

	Window 1	Window 2	Window 3	Window 4	Window 5	Window 6
sDA	53.3	72	40	46	55.3	51.3
ASE	35.3	37.3	25.3	34	39.3	36.7

Table 4-18: sDA and ASE with Floor Visual Reflectance 0.9 (East-Facing Window, Phoenix, AZ)

	Window 1	Window 2	Window 3	Window 4	Window 5	Window 6
sDA	60.7	91.3	46	53.3	62	58.7
ASE	35.3	37.3	25.3	34	39.3	36.7

4.2.7.3. Dynamic Daylighting Metric in North-Facing Window

For the North-facing windows (Table 4-19, Table 4-20, Table 4-21), the ASE was 0 since there is no direct sunlight for the North windows. However, many of the windows' sDA values were below 55%, which is the minimum value for LEED V4 daylighting credit. The maximum sDA in these simulations was window 2 with high floor reflectance. In order to increase the sDA to 75% or above, the options include: 1, increase the window area; 2, increase the visual reflectance; 3, re-run the case with the high-quality Radiance rendering setting. Unfortunately, the third option is a limitation of Radiance, which will be discussed in Section 5.

Table 4-19: sDA and ASE with Floor Visual Reflectance 0.2 (North-Facing Window, Phoenix, AZ)

	Window 1	Window 2	Window 3	Window 4	Window 5	Window 6
sDA	46.7	51.3	32	34.7	36	37.3
ASE	0	0	0	0	0	0

Table 4-20: sDA and ASE with Floor Visual Reflectance 0.5 (North-Facing Window, Phoenix, AZ)

	Window 1	Window 2	Window 3	Window 4	Window 5	Window 6
sDA	46.7	57.3	38.7	46	39.3	40.7
ASE	0	0	0	0	0	0

Table 4-21: sDA and ASE with Floor Visual Reflectance 0.9 (North-Facing Window, Phoenix, AZ)

	Window 1	Window 2	Window 3	Window 4	Window 5	Window 6
sDA	53.3	62.7	40	41.3	46.7	44
ASE	0	0	0	0	0	0

4.2.7.4. Dynamic Daylighting Metric in West-Facing Window

In Table 4-22, Table 4-23, and Table 4-24, for the West-oriented windows, the sDA had lower value compare to the South-oriented window. The ASE for the West-

oriented windows had the similar value with the South-facing Windows. Therefore, the sDA and lighting energy consumption got worse in West-oriented windows.

Table 4-22: sDA and ASE with Floor Visual Reflectance 0.2 (West Facing Window, Phoenix, AZ)

	Window 1	Window 2	Window 3	Window 4	Window 5	Window 6
sDA	58	86	40.7	50	62.7	59.3
ASE	44	52.7	34.7	41.3	42	50

Table 4-23: sDA and ASE with Floor Visual Reflectance 0.5 (West Facing Window, Phoenix, AZ)

	Window 1	Window 2	Window 3	Window 4	Window 5	Window 6
sDA	64.7	98	46.7	57.3	71.3	67.3
ASE	44	52.7	34.7	41.3	42	50

Table 4-24: sDA and ASE with Floor Visual Reflectance 0.9 (West Facing Window, Phoenix, AZ)

	Window 1	Window 2	Window 3	Window 4	Window 5	Window 6
sDA	78.7	100	54.7	65.3	91.3	80
ASE	44	52.7	34.7	41.3	42	50

4.2.7.5. Summary

In summary, the tests that were conducted showed that for a room with the same window areas, the South-facing windows had the highest sDA versus the other orientations. The ASE in South-facing window were much higher than 10%, which caused glare and overheating. In contrast, the East and West orientated windows had lower sDA, but had relatively higher ASE value than the South-facing windows. Finally, the North-facing window had the lowest sDA compared with the other three orientated windows, but the ASE was 0. Therefore, the South-facing window designs are much better for daylighting than East and West-facing windows. Design the window in North façade is the best solutions to avoid glare without shading devices.

The sDA increased as the floor visual reflectance increased. However, the Annual Sun Exposure (ASE) was affected by reflected interior lights, since it is using the direct exposed sunlight for calculation. Without shades, the ASE in the South, East, and West orientated windows are much higher than 10%, which cause glare. Therefore, in order to reduce the ASE to avoid glare, the following daylighting strategies can be used: reduce the window size, change the window orientation, change the window location, and apply shading devices. All these recommend actions agree with many of the previous authors.

4.3. Overall Summary

This section reproduced the Caldas office model, and found limitations in the results. First was the fact that all the windows in the simulations were centered in the middle of each façade, which does not reflect all types of daylighting strategies related to window locations (Reinhart and Stein, 2014). Second, the daylighting calculation method used in DOE-2 is the Split-Flux method, which has limitations in daylighting simulation. Therefore, the following study further investigated the window design strategies using a more sophisticated daylighting analysis that can analyze off-center placements of fenestration. To accomplish this, the study analyzed and compared the results from split-flux, Radiosity, and Radiance daylighting simulations.

This section also provided improved models that help magnify the differences to the annual energy use due only to differences in the windows based on reproduced model. This was accomplished by removing the effect of other parameters on the annual

heating and cooling load use (e.g., infiltration, floor and roof R-values, outside air per zone, and the system type). In this way, the changes due to window size and placement had a larger percent differences on the heating and cooling consumption. Therefore, in the remaining studies of this research, the infiltration and outside air are set to 0, the roof and floor R-value are set to 100 ft-°F-h/Btu (i.e., no heat transfer), and the system type is set to be an ideal system (i.e., DOE2.1e system = SUM).

In this study, an office model with different window sizes and placements (but with same window area) were tested to compare the results from different daylighting simulation tools. The overall purpose of this analysis was to test simulation abilities of different integrated thermal and daylighting simulation methods, which include DOE2.1e+Split-Flux, EnergyPlus+Split-Flux, EnergyPlus+Radiosity, and EnergyPlus+Radiance. The simulation results (i.e., cooling, heating, and lighting energy) will be compared to assist in the development of a prototype for an improved simulation tool using an integrated thermal and daylighting environment. In this analysis, six window models were tested in four orientations (South, North, East, and West) with different floor visual reflectances (i.e., 0.2, 0.5, 0.9). The tested location used for the simulations was in Phoenix, AZ. In this simulation, the wall and roof surface had a modestly bright reflectance (i.e., visual reflectance 0.7).

Phoenix, AZ is a cooling-dominated climate. The heating load is too small to be analyzed. The preliminary results showed that without daylighting simulations, all six windows (i.e., window that had different sizes and placements but with same window area) had similar cooling and heating results, which means the window location changes

will not affect the cooling and heating energy. After integrating the daylighting and thermal simulation, the lighting energy and cooling energy decreased dramatically. In addition, the cooling loads of the six models had the same trends as the lighting energy use. Therefore, in this cooling-dominated climate zone, reducing the lighting energy use contributed significantly to the reduction of the total energy use. In addition, the results showed that the use of a sophisticated daylighting simulation method was critical to obtain more accurate lighting energy results.

For the South-facing windows, when the floor was a dark surface with a visual reflectance 0.2, the EnergyPlus+Radiance simulation resulted in a higher lighting energy use than the lighting results of EnergyPlus+Split-Flux/Radiosity and DOE-2.1e+Split-Flux simulation. In addition, the Radiance simulation was sensitive to window location changes than the Split-Flux and Radiosity. The results also showed that when the FVR was increased from 0.2 to 0.5/0.9, the lighting energy results from EnergyPlus+Radiance became closer to the results of other simulation methods. From these results it can be concluded that when the interior surfaces of the room are all bright (i.e., reflectance 0.7, 0.8 or 0.9), the lighting results from the Split-Flux, Radiosity, and Radiance simulations become very similar. The Split-Flux is a relatively simple calculation, which takes seconds to run an annual daylighting simulation versus an analysis with Radiosity that can take around 2.7 minutes to run a daylighting simulation (Table 4-12), However, a Radiance analysis can take around 5 minutes to run a medium-quality annual daylighting simulation with relatively medium accuracy, or more than 60 minutes to run a high accuracy daylighting simulation (Table 4-12), which makes an optimization analysis

difficult. Therefore, there is a need for an accurate daylight/thermal analysis tool that runs quickly.

For the East-oriented and West-oriented windows, when the simulations were repeated for floor reflectances of 0.2, 0.5 and 0.9, the results also showed that there were no significant differences in daylighting performance when the window location changes in the daylighting simulations of DOE2.1e+Split-Flux or EnergyPlus+Split-Flux/Radiosity. However, in the EnergyPlus+Radiance simulation results, every window model had a different lighting electricity use. Unlike the South-facing window, the EnergyPlus+Radiance simulation in East and West-facing windows always resulted in a higher lighting energy use than the lighting results of EnergyPlus+Split-Flux/Radiosity or DOE2.1e+Split-Flux simulation. The results showed the Radiance in East and West-facing windows were more sensitive to the window location changes than the South-facing windows when the FVR changed from 0.2 to 0.5 to 0.9. Therefore, for off-center window location designs in the East or West orientations, it is important to use the Radiance simulation tool for either dark or bright floors.

The North-oriented windows have very different cooling and heating load results from the South and East-oriented windows. The cooling loads were reduced a half compared to the cooling loads of South and East-facing window. However, the heating load of North-facing windows doubled compared to South or East facing windows. For the lighting electricity use with FVR 0.2, the DOE-2.1e+Split-Flux simulation method and the EnergyPlus+Split-Flux/Radiosity simulation obtained similar results for all six window models. However, in the EnergyPlus+Radiance simulation results, every

window model had a very different lighting electricity use. More importantly, the lighting energy differences between EnergyPlus+Radiance versus EnergyPlus+Split-Flux/Radiosity methods became larger compared to the lighting results of the South, East, and West-facing windows. When the simulations were repeated for floor reflectances of 0.5 and 0.9, the lighting electricity differences between Radiance and Split-Flux/Radiosity simulation did not decrease. For the window models 1, 3, 4, and 6, the lighting electricity use predicted by EnergyPlus+Radiance simulation were significantly higher than result predicted by DOE2.1e+Split-Flux or by the EnergyPlus+Split-flux/Radiosity simulation. Therefore, in a similar fashion as the East and West-orientation, for a window location design in the North orientation, it is useful to use the Radiance simulation tool for either dark or bright floors.

Table 4-25: The Lighting Energy Difference between EnergyPlus+Radiance and EnergyPlus+Split-Flux/Radiosity

Runs	Orientation				Floor Visual Reflect			Lighting Differences in Window Models					
	South	East	North	West	0.2	0.5	0.9	1	2	3	4	5	6
Fig4.19	●				●			■	■	■	■	■	■
Fig4.21	●					●		■	■	■	■	■	■
Fig4.25	●						●	■	■	■	■	■	■
Fig4.28		●			●			■	■	■	■	■	■
Fig4.31		●				●		■	■	■	■	■	■
Fig4.34		●					●	■	■	■	■	■	■
Fig4.37			●		●			■	■	■	■	■	■
Fig4.40			●			●		■	■	■	■	■	■
Fig4.43			●				●	■	■	■	■	■	■
Fig4.46				●	●			■	■	■	■	■	■
Fig4.49				●		●		■	■	■	■	■	■
Fig4.42				●			●	■	■	■	■	■	■

0%-20%
 40%-60%
 60%-80%
 60%-80%
 ≥80

Table 4-25 showed the lighting difference between EnergyPlus+Radiance and

EnergyPlus+split-flux/radiosity. For the North oriented windows, the lighting energy use differences between EnergyPlus+Radiance versus EnergyPlus+Split-Flux/Radiosity methods in windows 1, 3, 4, 5, and 6 were huge, which were more than an 80% difference. For the East and West windows, the lighting differences in windows 1, 3, 4, and 6 were noticeable, which were more than a 60% difference. For the South-facing windows, when the floor was a dark surface with an FVR of 0.2, the EnergyPlus with Radiance had a higher lighting energy use in windows 3 and 4. When the simulations were repeated for an FVR of 0.9, the Radiance simulation had almost the same lighting energy results with Split-Flux and Radiosity simulation. Therefore, in East, North, and West-facing windows, Radiance was more sensitive to the window location changes than the South-facing windows when the floor visual reflectance changed from 0.2 to 0.5 to 0.9. Therefore, for the analysis of window designs in the East, North, and West orientations, it is useful to use the Radiance simulation tool for both dark and bright floors.

In addition, only Radiance can obtain the dynamic daylighting metric Spatial Daylight Autonomy (sDA) and Annual Sun Exposure (ASE). In order to obtain the LEED v4 credits in daylighting for an acceptable interior visual comfort, the sDA should be larger than 55%, and the ASE should be less than 10%. The tests that were conducted showed that for a room with the same window areas, the South-facing windows had the highest sDA versus the other orientations. The ASE in South-facing window were much higher than 10%, which caused glare and overheating. In contrast, the East and West orientated windows had lower sDA, but had relatively higher ASE value than the South-

facing windows. Finally, the North-facing window had the lowest sDA compared with the other three orientated windows, but the ASE was 0. Therefore, the South-facing window designs are much better for daylighting than East and West-facing windows. Design the window in North façade is the best solutions to avoid glare without shading devices.

The sDA increased as the floor visual reflectance increased. However, the Annual Sun Exposure (ASE) was affected by reflected interior lights, since it is using the direct exposed sunlight for calculation. Without shades, the ASE in the South, East, and West orientated windows are much higher than 10%, which cause glare. Therefore, in order to reduce the ASE to avoid glare, the following daylighting strategies can be used: reduce the window size, change the window orientation, change the window location, and apply shading devices. All these recommend actions agree with many of the previous authors.

In summary, the combined daylighting and thermal simulation to reduce the lighting and cooling load is important in cooling dominated climate. A combined EnergyPlus with Radiance simulation method could obtain the most accurate daylighting and thermal performance results. This study connected Radiance and EnergyPlus by using DIVA and Honeybee for Grasshopper, which provided a path to perform optimization in window size and location selection to obtain most energy saving design based on thermal and visual comfort.

5. RESULTS OF THE PARAMETRIC ANALYSIS

This chapter includes the results in four sections: Part I: An improved Radiance daylighting simulation method for optimization; Part II: Window size and placement design plugin in Grasshopper; Part III: Window design optimization process and results for an office model; Part IV: Summary of the findings.

5.1. An Improved Radiance Simulation Method in Optimization

Radiance has three main limitations when used for daylighting simulations. The first limitation is that a Radiance simulation can be a very time-consuming. For example, in order to obtain high accuracy daylighting results, the most accurate Radiance runtime would be more than one hour for one room, which makes an optimization process extremely time consuming, especially if more than one room is being analyzed.

Radiance's rendering parameters have four options: min, fast, accur, and max (Figure 5.1). The "min" value gives the fastest, crudest rendering with least accurate annual daylighting results. The "fast" value gives a reasonably fast rendering. The "accur" value gives a more accurate rendering than the "fast". The "max" value gives the highest accuracy. These settings affect the number of bounces (i.e., reflections) and the number of rays that the Radiance engine will use to calculate a simulation. For example, DIVA performs a daylight analysis using the Rhinoceros and Grasshopper architectural model that incorporates Radiance and DAYSIM. DIVA has four presets for its Radiance rendering parameters, which are: lowest-quality, low-quality, medium-quality, and high-quality. The Figure 5.2 shows the four preset rendering results from DIVA. The lowest-preset is the fastest runtime that gives rough results (5 seconds). However, it yields the

lowest illuminance values for the simulated room. The high-quality preset yielded the most reliable and accurate results. However, the runtime took over one hour to obtain the highest accuracy illuminance.

Param	Description	Min	Fast	Accur	Max	Notes
=====	=====	=====	=====	=====	=====	=====
-ps	pixel sampling rate	16	8	4	1	
-pt	sampling threshold	1	.15	.05	0	
-pj	anti-aliasing jitter	0	.6	.9	1	A
-dj	source jitter	0	0	.7	1	B
-ds	source substructuring	0	.5	.15	.02	
-dt	direct thresholding	1	.5	.05	0	C
-dc	direct certainty	0	.25	.5	1	
-dr	direct relays	0	1	3	6	
-dp	direct pretest density	32	64	512	0	C
-sj	specular jitter	0	.3	.7	1	A
-st	specular threshold	1	.85	.15	0	C
-ab	ambient bounces	0	0	2	8	
-aa	ambient accuracy	.5	.2	.15	0	C
-ar	ambient resolution	8	32	128	0	C
-ad	ambient divisions	0	32	512	4096	
-as	ambient super-samples	0	32	256	1024	
-lr	limit reflection	0	4	8	16	
-lw	limit weight	.05	.01	.002	0	C

NOTES:

- A) This option does not affect the rendering time
- B) This option adversely affects image sampling (ie. use -ps 1)
- C) Maximum value disables optimization and can be very expensive

Figure 5.1: Radiance Reference Rendering Settings (Source from (LBL, 2019))

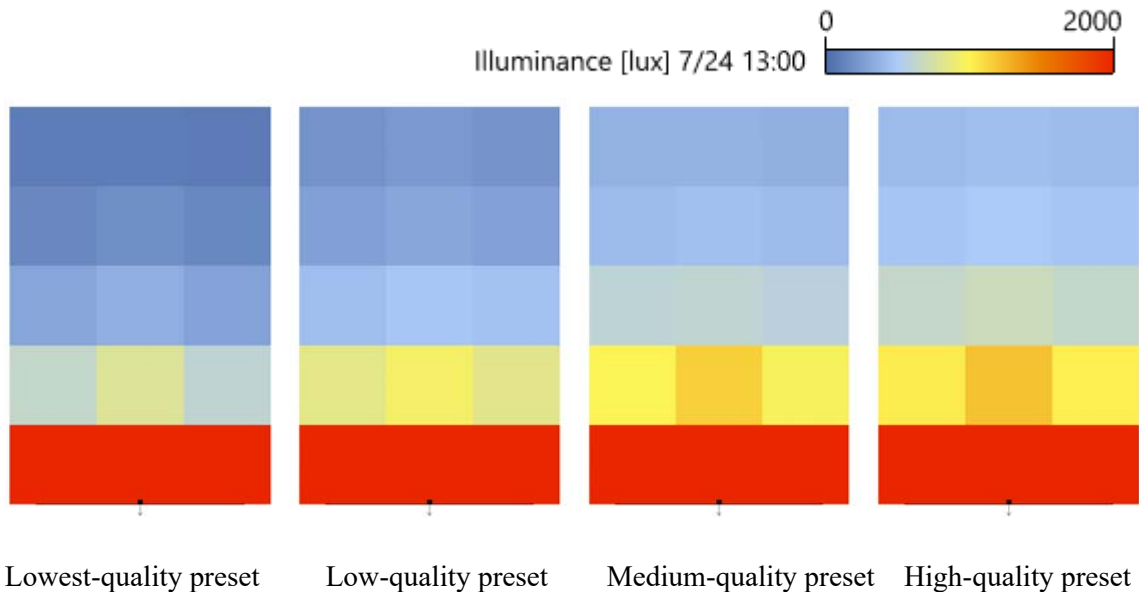


Figure 5.2: The Illuminance Map of the Four Presets in DIVA.

Second, Radiance simulations use a stochastic process to start the rendering for each image (i.e., randomly determined). Therefore, re-running the exact same case can produce a $\pm 5\%$ difference each time using the low-quality rendering simulation. However, the high-quality rendering simulation can reduce the differences between two simulation of the same room. Therefore, higher resolution settings will reduce the variability in the results, but at the expense of longer simulation times.

Third, Radiance annual daylighting simulation results can have a large difference in rendering runtimes. Unfortunately, this can be a problem since the low-quality preset rendering has the lowest sDA and highest lighting energy use. This issue makes it almost impossible to use the low-quality preset in a daylighting optimization to save the runtime due to the inaccurate results. Table 5-1 lists the annual lighting electricity use of different presets in DIVA with the same office model (Note: the simulation parameters are listed in Table 5-2 with a dark floor and bright shades). All simulations are conducted on a commodity personal laptop embedded with an Intel i7-8650U processor with 4 cores @ 2.11 GHz and 16GB RAM.

In this analysis, the high-quality preset required 62 minutes of rendering runtime to obtain the most accurate annual daylighting results, while the medium preset took only 3 minutes to obtain results. The low preset took 0.18 minutes and the lowest preset took only 0.08 minutes (4.8 seconds) to obtain very rough results. The results of the comparison showed that the lighting energy increased as the Radiance rendering runtime decreased, while the sDA decreased as the Radiance rendering runtime decreased. The sDA is a percentage of floor area that receives at least 300 lux for at least 50% of the

annual occupied hours (IESNA, 2012). The ASE (Annual Sun Exposure) measures the percentage of floor area that receives at least 1,000 lux for at least 250 occupied hours per year. ASE only relates to the direct sunlight; it was not affected by the Radiance rendering settings (Table 5-1). With the condition of the ASE below 10%, if the sDA value is larger than 55%, the building could obtain 2 LEED points; or if sDA is larger than 75%, it could obtain 3 LEED points in daylighting credit (USGBC, 2014).

However, in Table 5-1, the sDA in medium, low, and lowest quality settings were less than 75%, while the sDA in high-quality setting were 100%. In addition, the results showed that the building has 3 points in LEED daylighting credit when the simulation setting used the high-quality preset, while it had 2 points when the simulation used medium-quality preset. There was no LEED point under the low-quality and lowest quality presets with the same building. Therefore, an accurate daylighting simulation result (i.e., high-quality preset) must be used in daylighting optimizations to obtain the largest points in LEED daylighting credit. Therefore, there is a need to obtain accurate daylighting results with less simulation runtime.

Table 5-1: The Daylighting Simulation Runtimes and Results with Different Simulation Programs

Simulation Program		Run time	sDA	ASE	LEED Points	Lighting Electricity (kWh)
Radiance (DIVA)	High-quality	62 mins	100.0	2.7	3	106.1
	Medium-quality	4 mins	66.7	2.7	2	139.8
	Low-quality	0.18 mins	6.7	2.7	0	292.4
	Lowest-quality	0.08 mins	0	2.7	0	453.0

In an optimization process, there can be hundreds or thousands of simulations that need to be conducted. Therefore, a reasonable runtime is crucial for a cost-effective

optimization design. As a result, there is a need to reduce the Radiance runtimes to obtain relatively accurate daylighting annual simulation results. One additional place to look for savings in the Radiance runtime is the grid size. The Radiance settings both the for grid spacing and simulation rendering settings influence the annual daylighting results and simulation runtime. Therefore, in order to reduce the Radiance daylighting simulation time and maintain accurate daylighting result, tests on the grid spacing and rendering quality settings were conducted to obtain the best daylighting simulation settings.

5.1.1. Grid Spacing Setting

The grid subdivision in Radiance affects the annual daylighting simulation results. The sDA and ASE calculation grids should be no more than 0.6 meter (2 feet) (USGBC, 2014). Therefore, in this study, different grid spacing sizes (0.30 m, 0.45 m, 0.60 m, 0.9 m) (1.0 ft, 1.5 ft, 2.0 ft, 3.0 ft) were tested to check the accuracy of the annual daylighting simulation. The results of the simulated sDA, ASE, lighting energy, and running time were then compared.

The model parameters are listed in Table 5-2. In this analysis, models with different conditions were tested, which included models without shades, models with bright shades (i.e., reflectance of 0.9), models with a dark floor (i.e., low reflectance of 0.2), and models with a bright floor (i.e., high reflectance). In the analysis, DIVA was used for annual daylighting simulation for all the models. The Radiance rendering setting in this analysis was set to the Medium-quality preset.

Table 5-2: Model Parameters in Daylighting Simulation

Parameters	Value	
Length (m)	3.0	
Width (m)	4.6	
Height (m)	2.6	
Window area (m ²)	2.76	
Reference point height above floor (m)	0.76	
Lighting dimming setpoint (lux)	538	
Lighting Power Density (W/m ²)	11.95	
Glazing U-factor (W/m ² -K)	1.34	
SHGC	0.28	
Visual Transmittance	0.41	
Floor Visible Reflectance	Dark	0.2
	Bright	0.9
Wall Visible Reflectance	0.7	
Roof Visible Reflectance	0.7	
Shading Visible Reflectance	No shades	NA
	Bright	0.9
Rendering quality setting	Medium	

The simulation results of the sDA, ASE and the lighting electricity use are listed in Table 5-3, Table 5-4, and Table 5-5. From the results, the lighting electricity differences between these four grid spacing sizes were almost the same. The sDA have little differences between different spacing sizes for the study conditions of with shades and a dark floor (Table 5-5). However, these differences were not significantly noticeable. In the analysis, the ASE is very different in Table 5-4 and Table 5-5. This is because the ASE in each grid spacing size calculate the average sun exposure hour on different sizes of floor area. Different sized floor area can have very different average sun exposure value in each grid size. More importantly, the results showed that the larger grid spacing size takes less simulation time. For example, the simulation time for model with a grid spacing size 0.3 m (1 ft) is around 6 minutes, while the model with a

spacing size 0.6 m (2 ft) is around 4 minutes. Therefore, in order to save time in daylighting optimization, a spacing size 0.6 m (2 ft) was selected for this study.

Table 5-3: Daylighting Simulation Results with Different Grid Spacing in the Room Condition of No Shades with a Dark Floor

Grid Spacing	sDA	ASE	Lighting Electricity (kwh)	Running time
0.30 m	100	60	97.8	00:05:21
0.45 m	100	60	95.6	00:04:10
0.60 m	100	60	97.6	00:03:59
0.90 m	100	60	98.9	00:03:09

Table 5-4: Daylighting Simulation Results with Different Grid Spacings with the Room Condition of Shades with a Bright Floor

Grid Spacing	sDA	ASE	Lighting Electricity (kwh)	Running time
0.30 m	52.7	2.7	152.5	00:07:25
0.45 m	52.9	0	155.5	00:06:71
0.60 m	52.5	7.5	156.7	00:05:41
0.90 m	53.3	6.7	157.1	00:04:39

Table 5-5: Daylighting Simulation Results with Different Grid Spacings with the Room Condition of Shades with a Dark Floor

Grid Spacing	sDA	ASE	Lighting Electricity (kwh)	Running time
0.30 m	60.7	2.7	144.1	00:06:36
0.45 m	61.4	0	144.7	00:05:45
0.60 m	60	7.5	144.2	00:04:15
0.90 m	66.7	6.7	138.2	00:03:51

5.1.2. Radiance Rendering settings

In DIVA for grasshopper, each preset for the rendering settings can be checked in the "Radiance Parameter" of the annual daylighting simulation command (Figure 5.3). The Radiance rendering parameters in an annual daylighting analysis are -aa, -ab, -ad, -ar, -as, -dr, -ds, -lr, -lw, -dj, -lr, -sj, -st. To achieve the best balance between accuracy and runtime, there was a need to understand how the RADIANCE rendering parameters impact the results. Therefore, this study proposed a customized preset of Radiance

Rendering parameters in DIVA called “Custom” preset to obtain a relatively accurate annual daylighting results with less runtime (30 seconds). The according radiance parameters of the custom preset and the four rendering quality presets of DIVA are listed in Table 5-6.

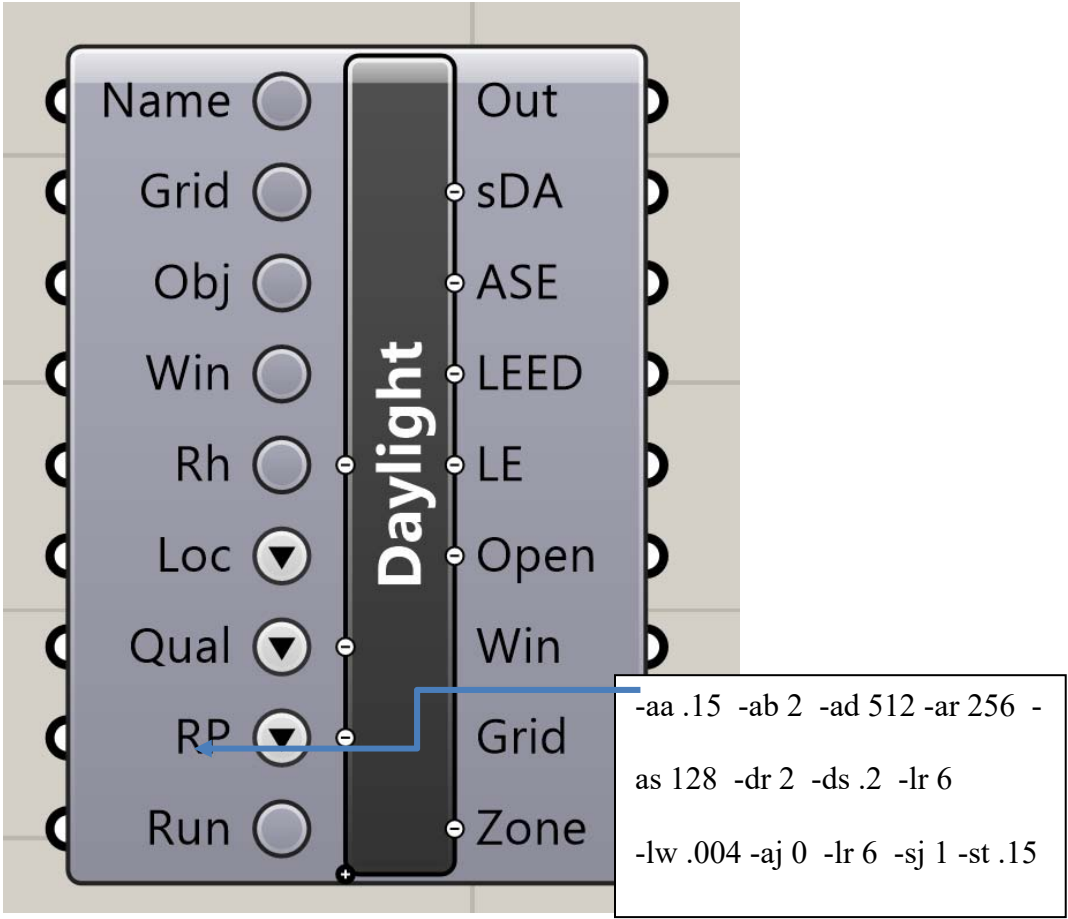


Figure 5.3: Radiance Rendering Setting in DIVA for Grasshopper.

Table 5-6: DIVA presets of the Radiance Rendering Parameters (Solemna, n.d.)

	Lowest	Low	Medium	High	Custom
-aa	0.15	0.15	0.1	0.1	0.15
-ab	1	2	4	7	4
-ad	512	512	1024	4096	512
-ar	256	256	256	512	256
-as	64	128	256	1024	256
-dr	2	2	2	2	2
-ds	0.2	0.2	0.2	0.2	0.2
-lr	6	6	12	12	8
-lw	0.004	0.004	0.004	0.001	0.004
-dj	0	0	0	0	0
-lr	6	6	6	6	8
-sj	1	1	1	1	1
-st	0.15	0.15	0.15	0.15	0.15

The detailed custom preset parameters in Table 5-6 are listed below:

-aa: ambient accuracy was set to 0.15. This value will approximately equal the error from indirect illuminance interpolation. A value of zero implies no interpolation. This setting alone is no guarantee of overall accuracy, since this parameter only controls the indirect irradiance interpolation accuracy (Ward, 2019).

-ab: ambient bounces were set to 4. This is the maximum number of diffuse bounces computed by the indirect calculation. A value of zero implies no indirect calculation (Ward, 2019).

-ad: ambient divisions were set to 512. A value of zero implies no indirect calculation (Ward, 2019).

-ar: ambient resolution set as 256. This number will determine the maximum density of ambient values used in interpolation (Ward, 2019).

-as: ambient super-samples were set to 256. Super-samples are applied only to the ambient divisions which show a significant change (Ward, 2019).

-dr: direct relays set to 2. A value of 0 means that secondary sources will be ignored. A value of 1 means that sources will be made into first generation secondary sources; a value of 2 means that first generation secondary sources will also be made into second generation secondary sources, and so on (Ward, 2019).

-ds: source substructuring was set to 0.2. A light source will be subdivided until the width of each sample area divided by the distance to the illuminated point is below this ratio. This assures accuracy in regions close to large area sources at a slight computational expense. A value of zero turns source subdivision off, sending at most one shadow ray to each light source (Ward, 2019).

-lr: limit reflection was set to 8. Limit reflections set to a maximum of N, if N is a positive integer. If N is zero or negative, then Russian roulette is used for ray termination, and the *-lw* setting (below) must be positive. If N is a negative integer, then this sets the upper limit of reflections past which Russian roulette will be used. In scenes with dielectrics and total internal reflection, a setting of 0 (no limit) may cause a stack overflow (Ward, 2019).

-lw: limit weight of each ray was set to 0.004. During ray-tracing, a record is kept of the estimated contribution a ray would have in the image. If this weight is less than the specified minimum and the *-lr* setting (above) is positive, the ray is not traced. Otherwise, Russian roulette is used to continue rays with a probability equal to the ray weight divided by the given fraction (Ward, 2019).

-dj: direct jittering set to 0. A value of zero gives a smoother but somewhat less accurate rendering. A positive value causes rays to be distributed over each source

sample according to its size, resulting in more accurate penumbras. This option should never be greater than 1 (Ward, 2019).

-sj: specular jitter was set to 1. This option does not affect the rendering time.

-st: specular threshold set to 0.15. The specular threshold is the minimum fraction of reflection or transmission, under which no specular sampling is performed. A value of zero means that highlights will always be sampled by tracing reflected or transmitted rays. A value of one means that specular sampling is never used. Highlights from light sources will always be correct, but reflections from other surfaces will be approximated using an ambient value. A sampling threshold between zero and one offers a compromise between image accuracy and rendering time (Ward, 2019).

5.1.2.1. Daylighting Performance Results Comparison with Different Radiance Rendering Presets

This study used DIVA to perform the annual daylighting simulations to evaluate the different Radiance rendering presets, which include: lowest, low, medium, high, and custom presets (Table 5-6). The office model parameters for the daylighting simulation are listed in Table 5-2. In this analysis, the window-to-wall ratio was 20%. The window visual transmittance was 0.41. The different conditions tested were: a dark floor, a bright floor, and a model with and without shading devices.

The results are listed in Table 5-7. The analysis showed the lighting energy use increased as the Radiance rendering time decreased (Figure 5.4), while sDA was reduced as the Radiance rendering time decreased (Figure 5.5).

Table 5-7: Daylighting Results of Different Preset of Radiance Rendering

Condition	Preset	Runtime	sDA	Lighting Electricity (kWh)
No shades + bright floor	High	60 mins	100	78.8
	Medium	4 mins	100	84.1
	Custom	0.5 mins	100	89.5
	Low	0.18 mins	80	130.2
	Lowest	0.08 mins	46.7	245.8
No shades + dark floor	High	60 mins	100	86.6
	Medium	4 mins	100	94.3
	Custom	0.5 mins	100	106.4
	Low	0.18 mins	66.7	140.1
	Lowest	0.08 mins	46.7	251.4
Shades + bright floor	High	60 mins	100	102.4
	Medium	4 mins	80	136.9
	Custom	0.5 mins	73.3	143.8
	Low	0.18 mins	6.7	290.4
	Lowest	0.08 mins	0	458.5
Shades + dark floor	High	60 mins	100	106.1
	Medium	4 mins	66.7	139.8
	Custom	0.5 mins	60	164.2
	Low	0.18 mins	6.7	292.4
	Lowest	0.08 mins	0	453

In the analysis, the high preset took 60 minutes to obtain the most accurate results. The lowest and low presets spent less than one min to obtain the results. However, the results had large differences compared to the results from the high-quality preset. The lowest-quality and low-quality settings produced the crudest rendering images, which had the much lower illuminance than the high-quality preset. Therefore, the high-quality preset had the highest sDA and lowest lighting electricity, while the lowest-quality preset had the lowest sDA and highest lighting electricity. The simulation runtime from medium preset was 4 minutes, but the differences between medium preset

and high preset were acceptable. The results from custom preset are close to the medium preset. However, the runtime in the medium-preset was 6 times the runtime of the custom preset (30 seconds). Therefore, custom preset was considered an acceptable setting in the Radiance rendering for the use of optimization. However, there is a gap between high-quality preset and custom preset.

In addition, the differences between these five presets increased as the visual reflectance of the floor changed from dark to bright, or the building shades setting changed from without shades to with bright shades. That is because there was more light reflection from the bright surface than from the dark surface.

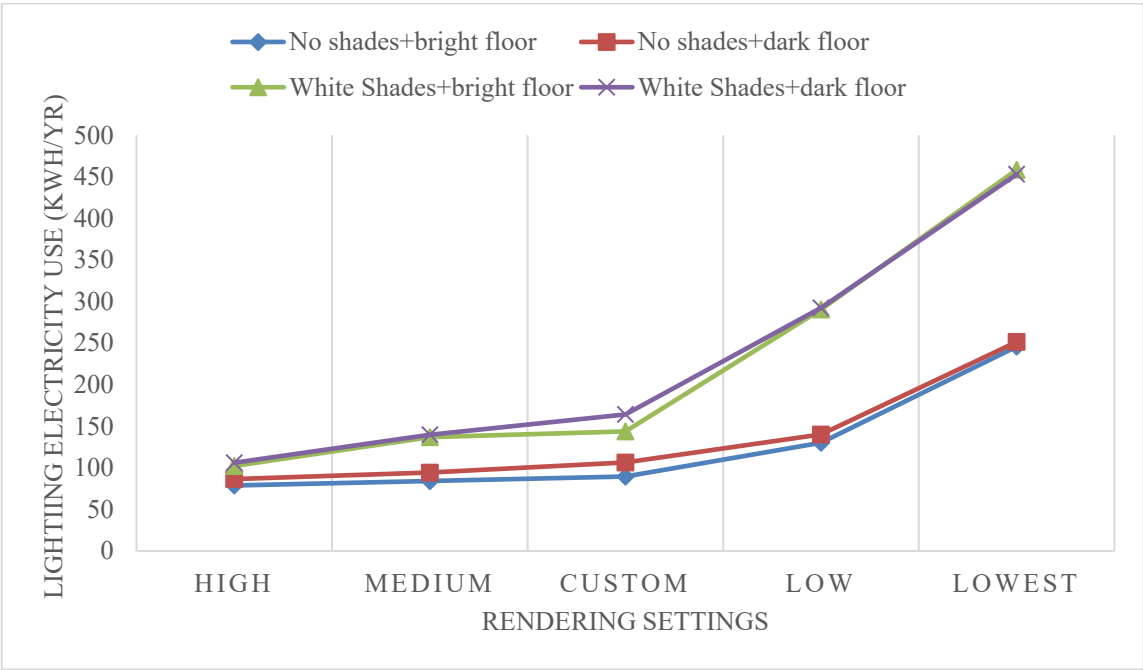


Figure 5.4: The Lighting Energy Changes with Different Rendering Settings

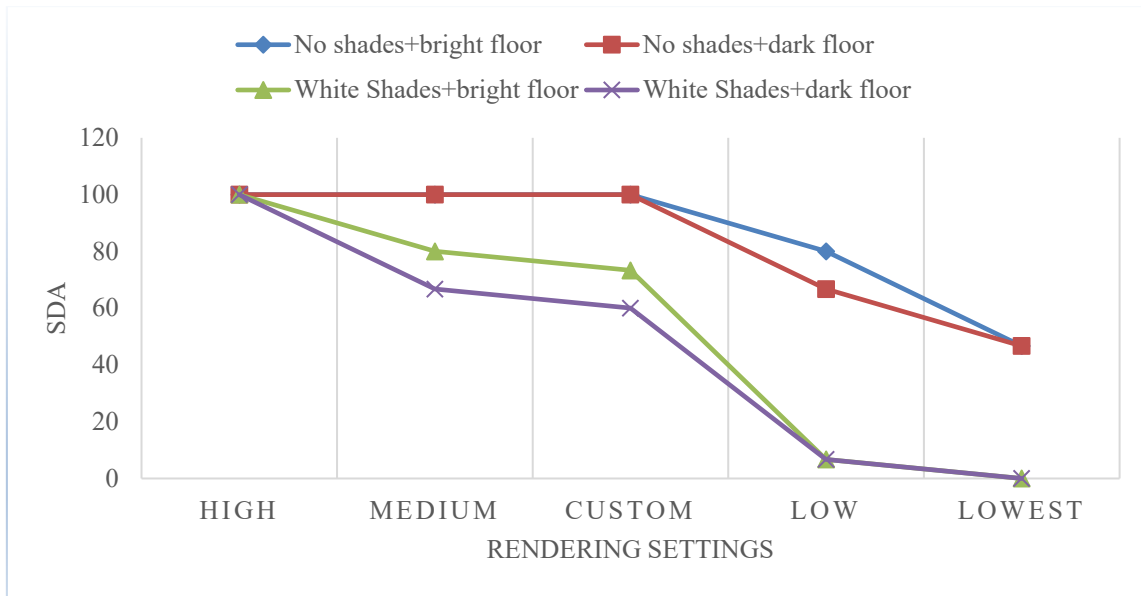


Figure 5.5: The sDA Changes with The Different Rendering Settings

5.1.2.2. The Correlation Between High-Quality Preset with Custom Presets

As mentioned previously, the aim of this study is to use the carefully selected custom preset to optimize a daylighting design to save runtime while providing reasonable accuracy. To accomplish that, there was a need to find a correction between the use of the high-quality preset and the custom preset. To optimize the design, the criteria of daylighting performance are: minimize the lighting electricity use, minimize the Annual Sun Exposure (ASE), and maximize the spatial Daylight Autonomy (sDA). The ASE index describes how much of a space receives too much direct sunlight penetration into the room, which can cause visual discomfort (i.e., glare) or an increase in cooling loads. The results showed that the ASE was the same for all the presets, because the ASE was only related to the direct sunlight. Therefore, there was no need to correct the ASE results. For the lighting energy calculation, the optimization criterion

was to select the lowest value of all the possible design models. Therefore, in the lighting energy criterion, there was a need to perform more tests to check the lighting electricity profile of the different office models in the custom preset and the high-quality preset.

The sDA is the criterion to evaluate the annual useful daylighting in an interior space. In order to obtain a LEED score, the sDA should be larger than 55% or 75% (USGBC, 2014). However, the sDA for a lower quality Radiance rendering setting has a lower value compare to higher rendering setting. Therefore, one goal of this study was to find a correlation between the sDA from a custom preset and the sDA from a high-quality preset. This is useful because once the correlation is known it can be reused in the future daylighting simulations. Therefore, the sDA results from the custom preset can be used to predict the sDA from high-quality preset to save simulation runtime.

5.1.2.2.1. Simulations with Custom Preset and High-Quality Preset

In order to find the correlation between the custom preset and high-quality preset, a series of simulations were conducted with different model conditions, such as different room size, window-to-floor ratios, floor visual reflectances, orientations, window positions, and shades. All daylighting simulation parameters used in these simulations are listed in Table 5-8.

Two office room sizes were selected for this simulation. One is a small room size (3m x 4.6m x 2.6m) (apx. 10ft x 15ft x 8.5ft), another one is medium room size (15m x 6m x 3m) (apx. 49ft x 20ft x 10ft). The window size is also a variable, where the

window-to-floor ratio changed from 3% to 31%. The Floor Visible Reflectance (FVR) used was 0.2 (dark), 0.5 (grey), or 0.9 (bright). The orientations were South (S), East (E), North (N), and West (W). The window positions were divided into four categories: centered, top, down, and mix (Figure 5.6). To distinguish the window position, the exterior wall height was set as z , the z_{mid} is the half height of the exterior wall. Finally, the window height was set as h .

If $(z - z_{mid}) \geq -h/4$, set window position as "top".

Else if $(z + h - z_{mid}) \leq h/4$, set window position as "down".

Otherwise set window position "centered".

For more than one window condition, if all the window locations were the same, then set window position as the same, otherwise set the window position as a "mix" (i.e., the windows have mixed top or down positions).

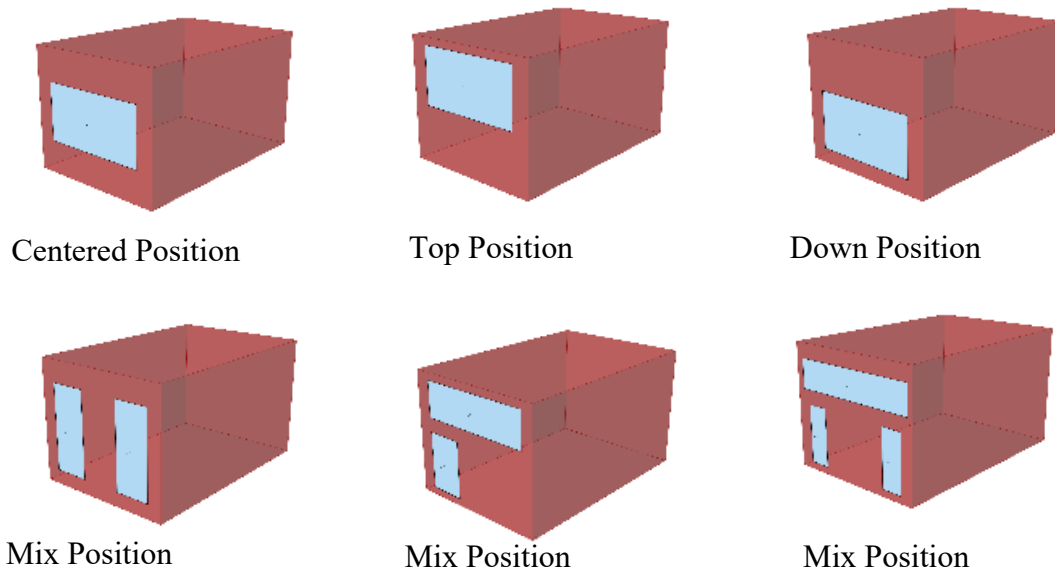
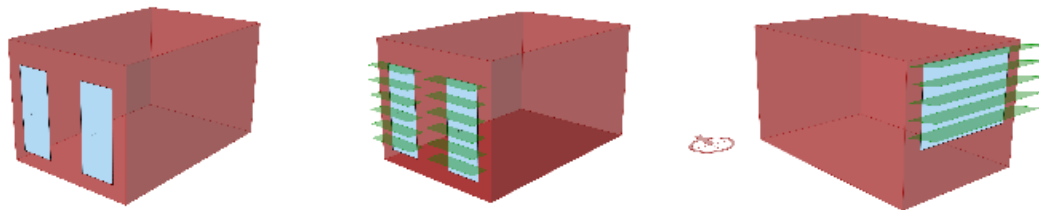


Figure 5.6: Window Positions

Table 5-8: The daylighting simulation parameters and variables

Parameters		Small size room	Medium size room
Length (m)		3.0	15.0
Width (m)		4.6	6.0
Height (m)		2.6	3.0
Window to Floor Ratio		3%-31%	3%-31%
Reference point height above floor (m)		0.762	0.762
Lighting dimming setpoint (lux)		538	538
Lighting Power Density (W/m ²)		11.95	11.95
Glazing U-factor (W/m ² -K)		1.34	1.34
SHGC		0.28	0.28
Visual Transmittance		0.41	0.41
Wall Visible Reflectance		0.7	0.7
Roof Visible Reflectance		0.7	0.7
Floor Visible Reflectance (FVR)	Dark	0.2	0.2
	Grey	0.5	0.5
	Bright	0.9	0.9
Orientation		S,E,N,W	S,E,N,W
Window Position		Centered	Centered
		Top	Top
		Down	Down
		Mix	Mix
Shading Visible Reflectance	No shades	NA	NA
	Bright	0.9	0.9
	Dark	0.3	0.3
Rendering quality setting		High	High
		Custom	Custom

In the analysis, the window shades had three options, which were: no shades, white shades, and dark shades (Figure 5.7). The Radiance rendering quality settings were high and custom.



No Shades

White Shades or Dark Shades

Figure 5.7: Window Shade Examples

5.1.2.2.2. Simulation Results for the Lighting Electricity

In the analysis, a total of 185 simulation runs were conducted. Table A-1 in the Appendix lists the results of all 185 runs. For the lighting energy use, the optimization criterion was selected to be the lowest value of all the possible design models. The results of the small size offices are shown in Figure 5.8, and the results of the medium size office are shown in Figure 5.9. For both the small and medium size office, the lighting energy trends of the different models in the custom preset and the high-quality preset were the same. Therefore, the lowest lighting energy use and the highest lighting energy usage for the high-quality preset and the custom preset result in the same trends. As a result, there was no need to correct the lighting energy results for the custom preset. In such cases for the daylighting optimization, the lowest value will be selected from the custom preset simulations.

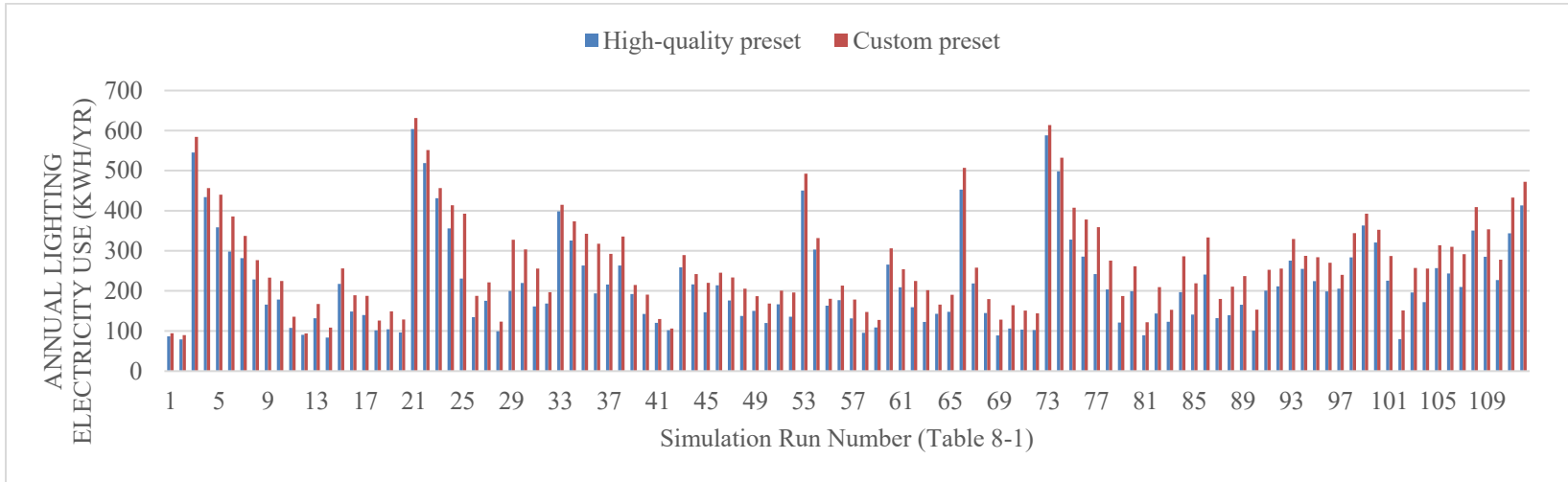


Figure 5.8: Lighting Energy Use in the Small Size Office

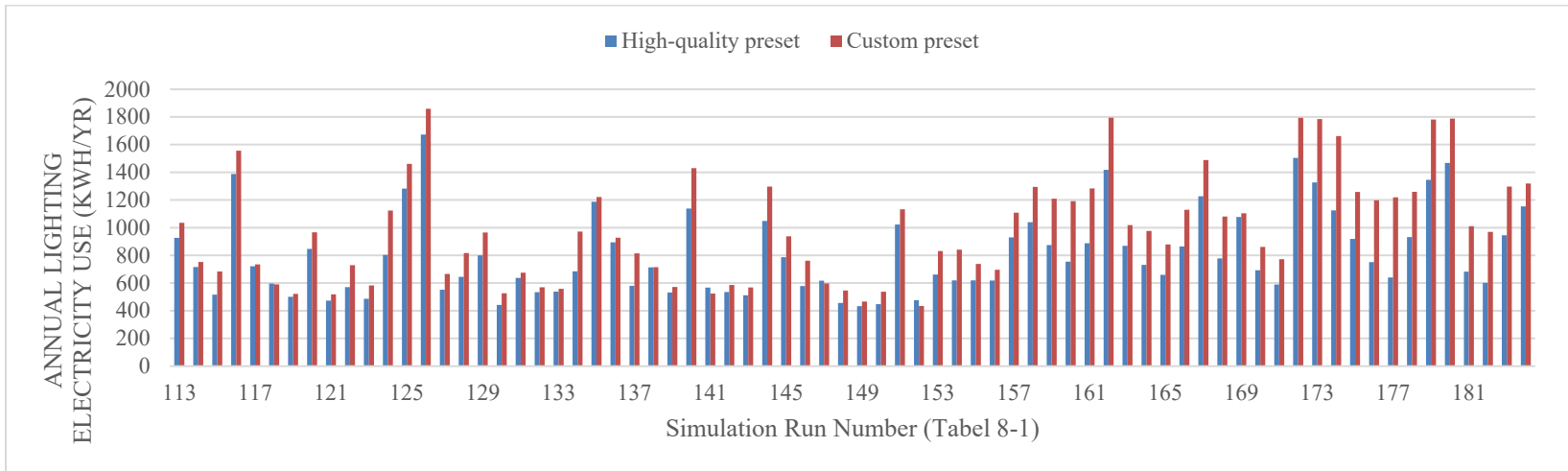


Figure 5.9: Lighting Energy Use in the Medium Size Office

5.1.2.2.3. Correlation Between the sDA_custom and the sDA_high

Figure 5.10 and Figure 5.11 show the sDA results using the high and custom presets of all 185 cases that categorized according to the size of room (i.e., small office or medium office) and with and without shades.

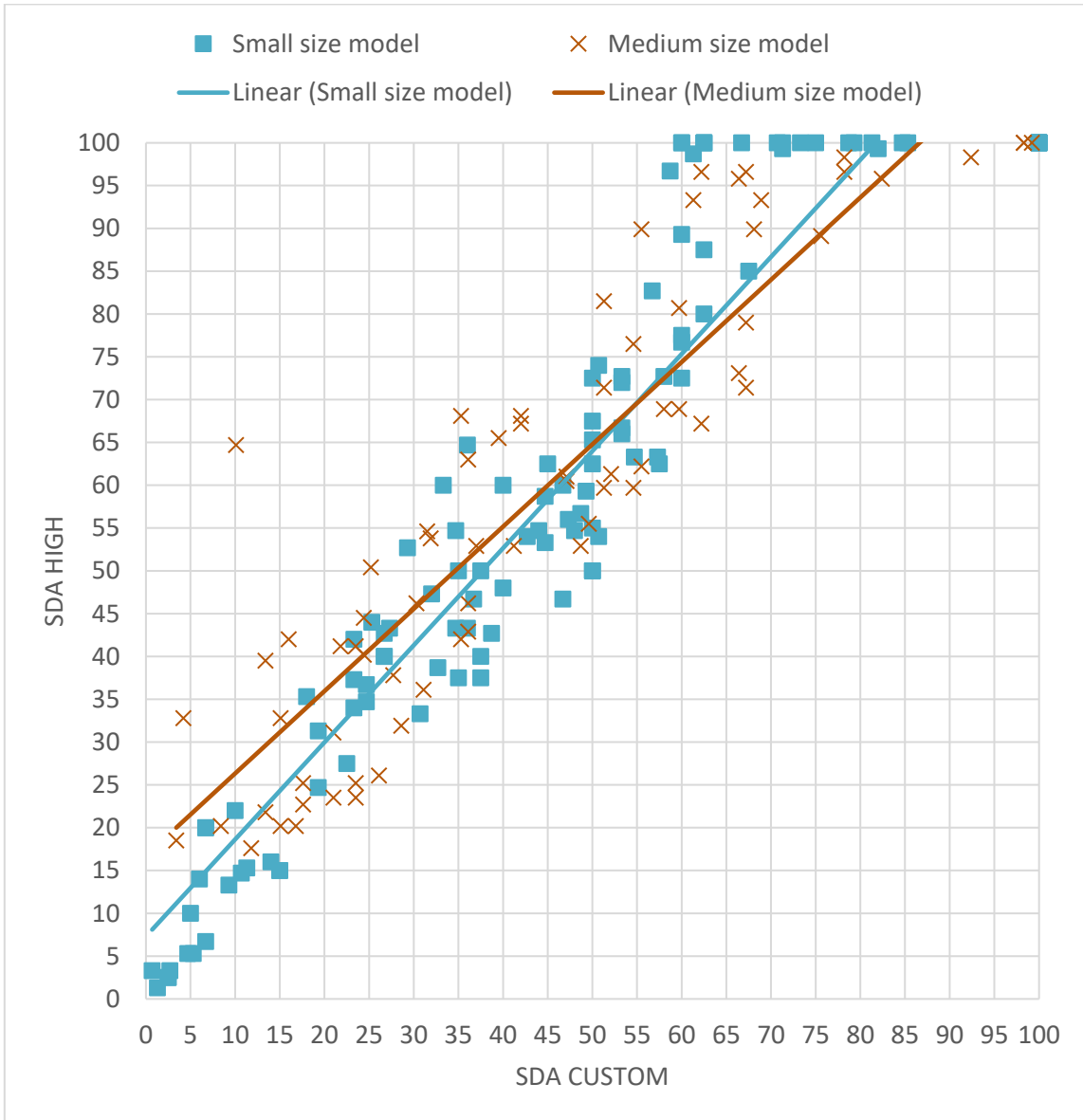


Figure 5.10: The sDA Correlation Between the sDA_custom and the sDA_high in Categories: Small size office and Medium size office

Figure 5.10 shows the categories of Small size office and Medium size office.

The results show that the majority of the simulation results were located within the linear trend shown for both the small and medium size office cases.

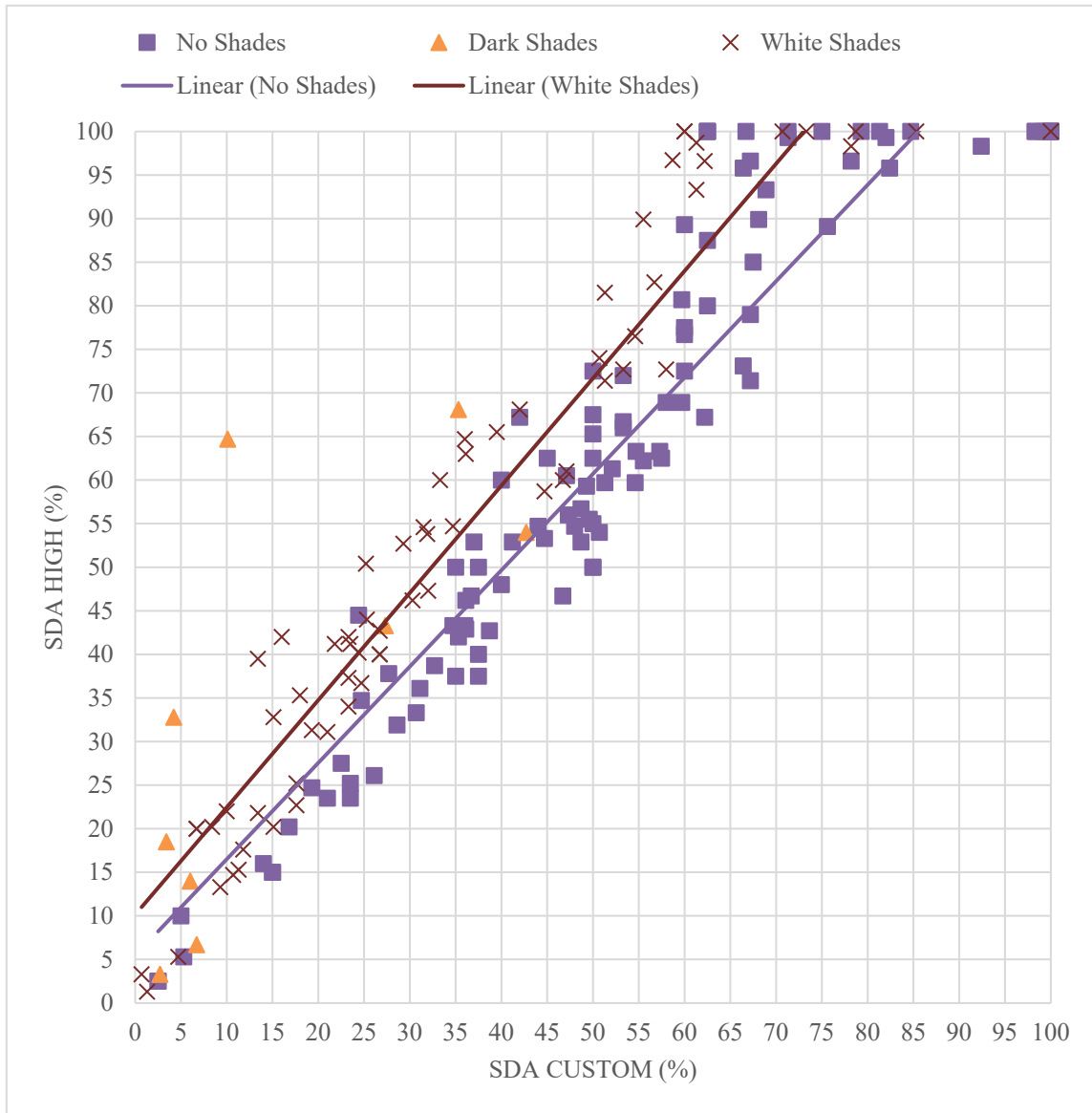


Figure 5.11: The sDA Correlation between the sDA_custom and the sDA_high in Categories: No Shades, Dark Shades, and White Shades

Figure 5.11 shows clear differences in the trends of the categories of No Shades, Dark Shades, and White Shades, with a few points outside of the linear trend. Several of the outliers are the sDA results of the dark shades. For the majority of the simulations, the cases without shades and with shades formed two parallel trend lines (Figure 5.11).

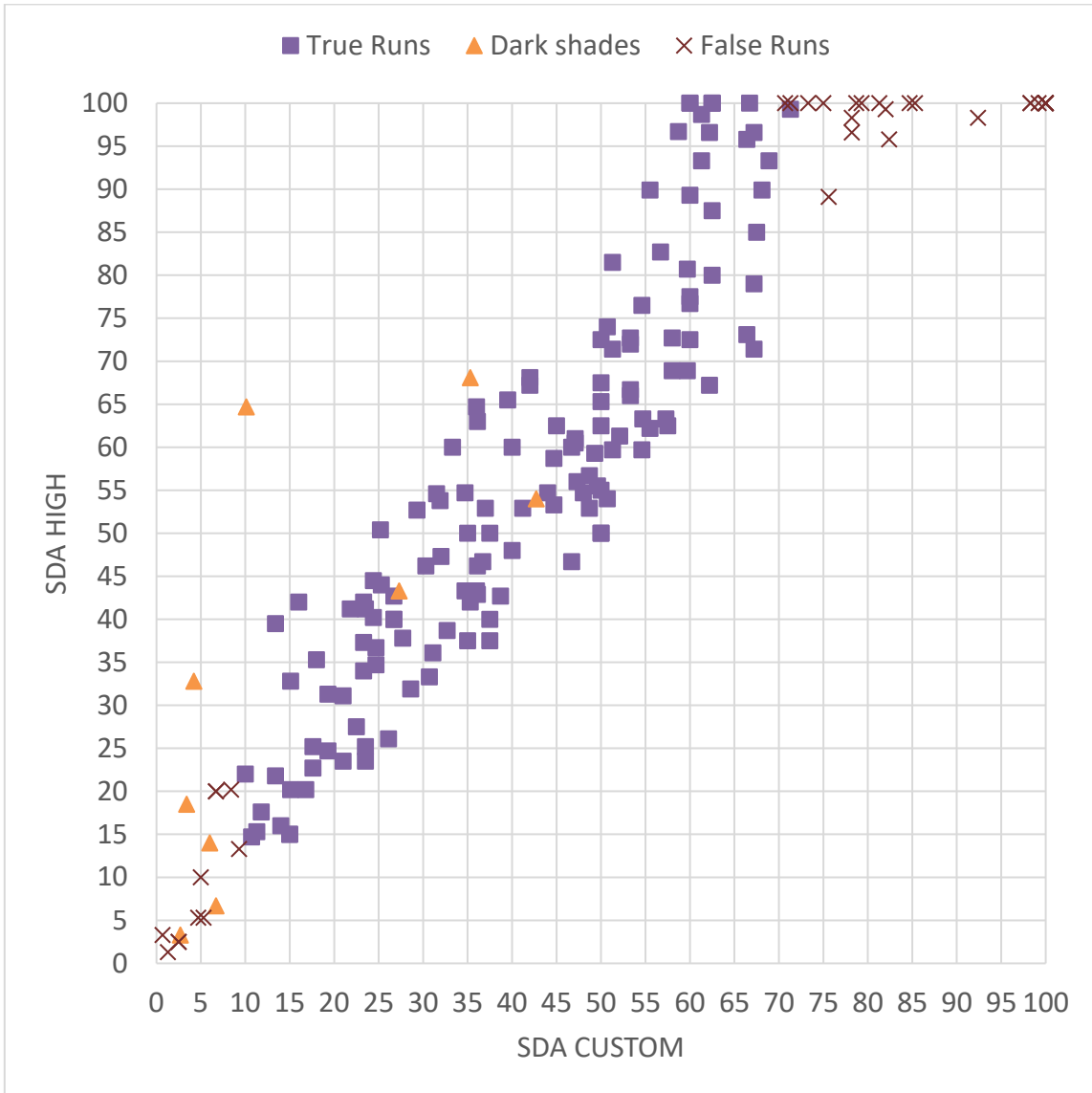


Figure 5.12: The Final True Runs (Purple) Used to Find the sDA Correlation between the sDA_custom and the sDA_high

The sDA is the percentage of floor area that receives at least 300 lux for at least 50% of the annual occupied hours, the maximum value of sDA is 100%. The results showed that when the custom preset sDA was larger than 70%, the high-quality preset sDA reached 100%. Therefore, in order to find the correlation between high-quality preset and the custom preset in sDA results, if the sDA_custom was larger than 70% and the sDA_high equaled 100%, then the simulated cases were removed. In addition, when the sDA_custom was smaller than 10% and larger than 75% cases, they were not considered for the regression. All these cases that were called false runs in Figure 5.12. Dark shades were not considered in this study. Finally, the 139 true simulation runs (purple) were then selected from 185 simulation runs.

The statistical software JMP Pro 14 (SAS, 2019) was used to calculate the correlation between the high-quality preset and custom preset. In the analysis, a multi-linear regression model was used. The dependent variable of the regression model was sDA_{high}. The 139 simulation cases served as the observations. The independent variables are listed in Table 5-9, which include: the sDA_custom, shades, orientations, window position, Window-to-Floor Ratio (WFR), Floor Visual Reflectance (FVR), and building size (small, medium).

$$Y = \beta_0 + \beta_1 * X_1 + \beta_2 * X_2 + \beta_3 * X_3 + \beta_4 * X_4 + \beta_5 * X_5 + \beta_6 * X_6 + \beta_7 * X_7 + \epsilon$$

Equation 5-1

Where:

- Y= sDA_{high}
- X_j = Factor, Predictor; j = 1, 2...p (p = number of factors)
- β₀ = Intercept
- β_j = Coefficients

Table 5-9: Independent Variables

Variables		Levels
X1	sDA_custom	0% - 75%
X2	Shades	No shades=0 ¹⁸
		White shades
X3	Orientation	South
		North
		East
		West=0
X4	Window position	Top
		Centered=0
		Down
		Mix
X5	Window to Floor Ratio (WFR)	2% - 40%
X6	Floor Visual Reflectance (FVR)	0.2
		0.5
		0.9
X7	Building size	Small=0
		Medium

In the single-predictor model, the T-test was used to show the correlation between each independent variable versus the dependent variable. When the P-value was smaller than 0.05, the independent variable was considered significant. Table 5-10 shows that the shades ($p < 0.0001$), WFR ($p = 0.0140$), FVR ($p < 0.0001$), and sDA_custom ($p < 0.001$) had statistically significant linear trends at $p < 0.05$ level. In addition, the window position had a marginally statistically significant linear trend ($p = 0.0834$). However, the building size ($p = 0.9226$) and orientations ($p = 0.9608$) did not have statistically significant linear trends. Therefore, the building size and orientations did not affect the Y response.

¹⁸ Set reference category =0. Reference category makes interpretation of results easier. All the comparisons of the dummy variable are made in relation to its reference category.

Table 5-10: Parameter Estimates of Single Variable

Source	DF	Sum of Squares	F Ratio	Prob > F
Building Size	1	0.3340	0.0095	0.9226
Shades	1	2848.2230	80.7917	<.0001*
Orientations	3	10.4110	0.0984	0.9608
Window Position	3	240.2860	2.2720	0.0834
WFR	1	219.0790	6.2143	0.0140*
FVR	1	2172.5370	61.6254	<.0001*
sDA Custom	1	42508.7650	1205.7890	<.0001*

For multiple regression models, this study used the minimum corrected Akaike Information Criterion (Minimum AICc) to choose the best model in JMP. The Akaike Information Criterion (AIC) is an estimator of out-of-sample prediction error and thereby is a relative quality of statistical models for a given set of data (Aho et al., 2014; Akaike, 1998). Given the collection of models for the data, the AIC estimates the quality of each model, relative to each of the other models. When using the Minimum AICc stopping rule in the stepwise regression, the automatic fits continued until a best model was found, where the best model is the one with a minimum AICc, which was 890.475 (Table 5-11).

Table 5-11: Minimum AICc Stepwise Regression Results

Ste	Parameter	Action	"Sig	Seq SS	RSq	Cp	p	AICc	BIC
1	sDA_custom	Entere	0.000	57991.	0.830	227.	2	1018.	1026.
2	Shades [White shades]	Entere	0.000	4702.8	0.898	85.2	3	949.6	961.0
3	FVR	Entere	0.000	2033.4	0.927	24.8	4	904.9	919.1
4	WFR	Entere	0.002	334.90	0.932	16.5	5	897.6	914.5
5	WFR * WFR	Entere	0.005	270.75	0.936	10.2	6	891.6	911.3
6	FVR * Shades [White	Entere	0.089	97.056	0.937	9.22	7	890.8	913.2
7	Window Position [Top]	Entere	0.117	81.357	0.938	8.72	8	890.5	915.5
8	Window Position [Mix]	Entere	0.136	72.722	0.939	8.48	9	890.4	918.1
9	Window Position	Entere	0.486	15.886	0.939	10	1	892.3	922.5
	Best	Specifi	.	.	0.939	8.48	9	890.4	918.1

Therefore, the variables: sDA_custom shades, Window-to-Floor Ratio (WFR), Floor Visual Reflectance (FVR), WFR*WFR, FVR * Shades [White shades], and Window position were selected for the final model. The final multi-linear regression is shown in Equation 5-2.

$$\begin{aligned}
 sDA_{\text{high}} = & -12.1351 + 1.2249 * sDA_{\text{custom}} \\
 & + 13.4245 * \text{Shades [White shades]} \\
 & + 41.3652 * \text{WFR} \\
 & + 19.3939 * \text{FVR} \\
 & - 1.9254 * \text{WFR}^2 \\
 & - 6.0909 * \text{Shades [White shades]} * \text{FVR} \\
 & + 1.0354 * \text{Window Position [Top]} \\
 & - 3.0621 * \text{Window Position [Down]} \\
 & - 1.9597 * \text{Window Position [Centered]}
 \end{aligned}$$

Equation 5-2

This regression needs to follow conditions list below:

- 1) If the office model has shades, the window shades should be white, (i.e., shades visual reflectance>0.7).
- 2) The wall and roof visual reflectance would between 0.7 to 0.9.
- 3) The maximum predicted sDA_high should not be higher than 100%.
- 4) The simulation location should be limited in Phoenix, AZ
- 5) The room geometry limited to regular sized room, the heigh of the simulation model will be limited to 4 meters. The high-space room needs to do more test.

Table 5-12 shows the correlation between sDA_high and independent variables using the multi-linear regression. The predictors WFR, FVR, sDA_custom, Shades [White shades], and WFR * WFR are significant in this multi-linear regression model with P<0.05. The predictor FVR * Shades [White shades] and Window Positions showed marginally statistically significant trends.

Table 5-12: Associations Between Y Response and Variables from the Multiple Regression Model

Term		Estimate	Std Error	t Ratio	Prob> t
Intercept	Biased	-12.1351	2.9951	-4.05	<.0001*
WFR		41.3652	14.8472	2.79	0.0061*
FVR	Biased	19.3939	2.5178	7.70	<.0001*
sDA_custom		1.22491	0.0431	28.40	<.0001*
Shades [White shades]	Biased	13.4244	1.8624	7.21	<.0001*
WFR*WFR		-1.9254	0.7007	-2.75	0.0069*
FVR*Shades [White shades]	Biased	-6.0908	3.7732	-1.61	0.1089
Window Position [Top]	Biased	1.0354	2.1726	0.48	0.6345
Window Position [Down]	Biased	-3.0621	1.8977	-1.61	0.1091
Window Position [Centered]	Biased	-1.9597	1.5754	-1.24	0.2158
Window Position [Mix]	Zeroed	0	0	.	.
Shades [No shades]	Zeroed	0	0	.	.
FVR*Shades [No shades]	Zeroed	0	0	.	.

Table 5-13: Summary of fit

RSquare	0.939827
RSquare Adj	0.935629
Root Mean Square Error	5.706049
Mean of Response	55.65036
Observations (or Sum Wgts)	139

Table 5-13 shows the statistic results of the multi-linear regression model. The R-square is the statistical measure that represents the proportion of the variance for a dependent variable that is explained by the independent variables in a regression model.

An R-square of 0.940 means approximately a 94.0% of the observed variation in the output variable can be explained by the input variables.

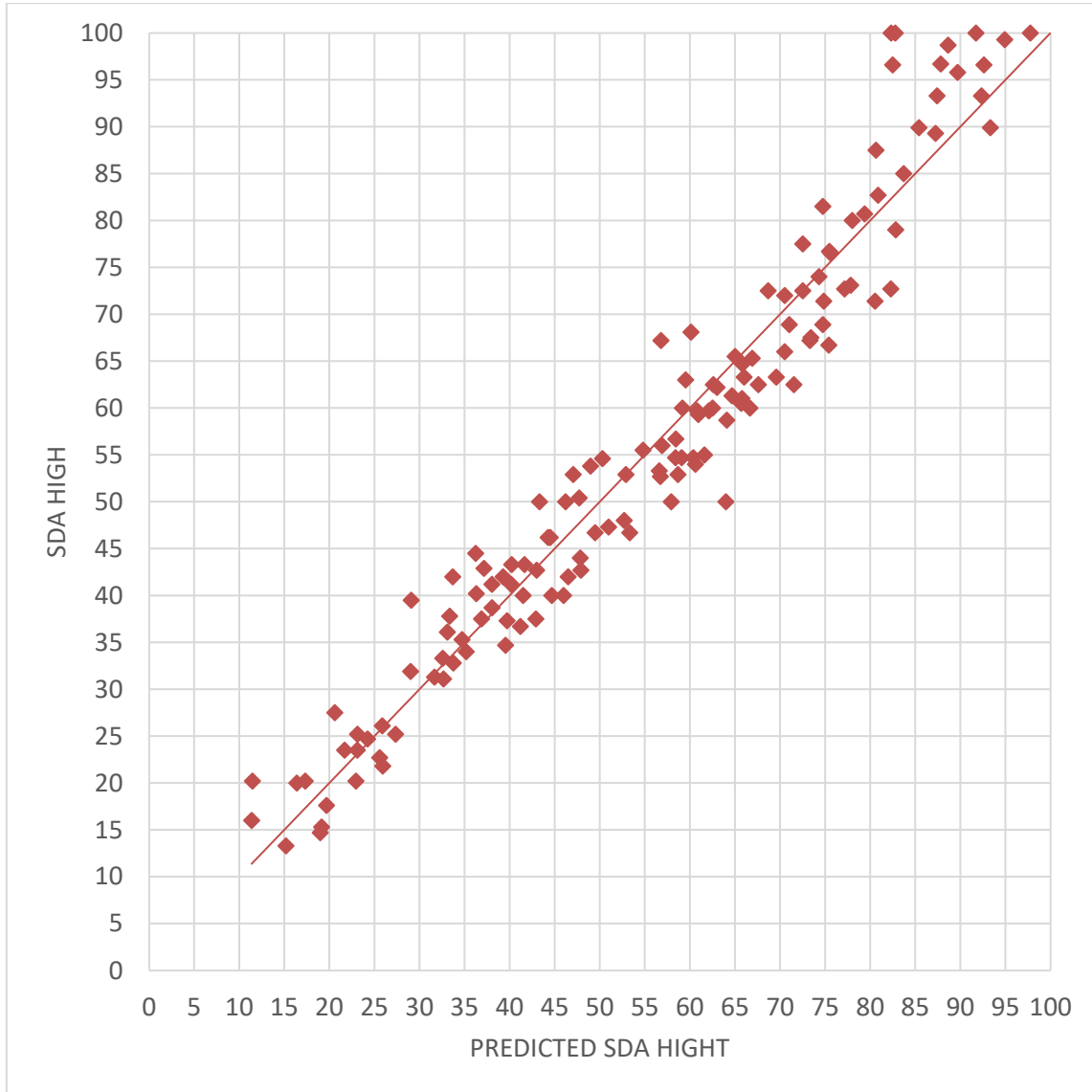


Figure 5.13: Actual Data by Predicted Data Plot

Table A-2 in the Appendix lists the statistical analysis data from the analysis tool JMP Pro 14 (SAS, 2019). The predicted sDA_high value calculated from Equation 5-2 is also listed in Table A-2. The average difference between Predicted sDA_high and

simulated sDA_high was 9.4%, which is an acceptable error in the prediction. The actual sDA_high by predicted sDA_high plot is shown in Figure 5.13.

5.2. Window Size and Placement Design Plugin in Grasshopper

One aim of this study was to use a Genetic Algorithm to help find the optimal window design on the façade. However, generating the thousands of window models for the optimization is a very time-consuming process. Therefore, to resolve this issue, this study created a window design plugin in Grasshopper (Davidson, 2019) that can automatically generate window designs.

The window design plugin was scripted in Python (Langtangen, 2006) (Figure 5.14). The inputs are listed on the left, and the Boolean Toggle is set “True” to run this window design plugin. The input Srf is set as the wall surface that supposed to has windows. The input X and Z are values that divide the wall surface length and height into X and Z units according to “X” and “Z” axis (Figure 5.15). The larger numbers in the X and Z input will generate more possible different window designs. In order to better calculate and design of the window in this plugin, a normalized surface area was used, where the surface area was equal to $X * Z$ ($srf_area = X * Z$). Each normalized unit in the “X” axis: $x_unit = real_wall_length / X$, each normalized unit in the “Z” axis: $z_unit = real_wall_height / Z$ as shown in Figure 5.15. The WWR input is the Window-to-Wall Ratio. The calculated normalized total $window_area = srf_area * WWR$.

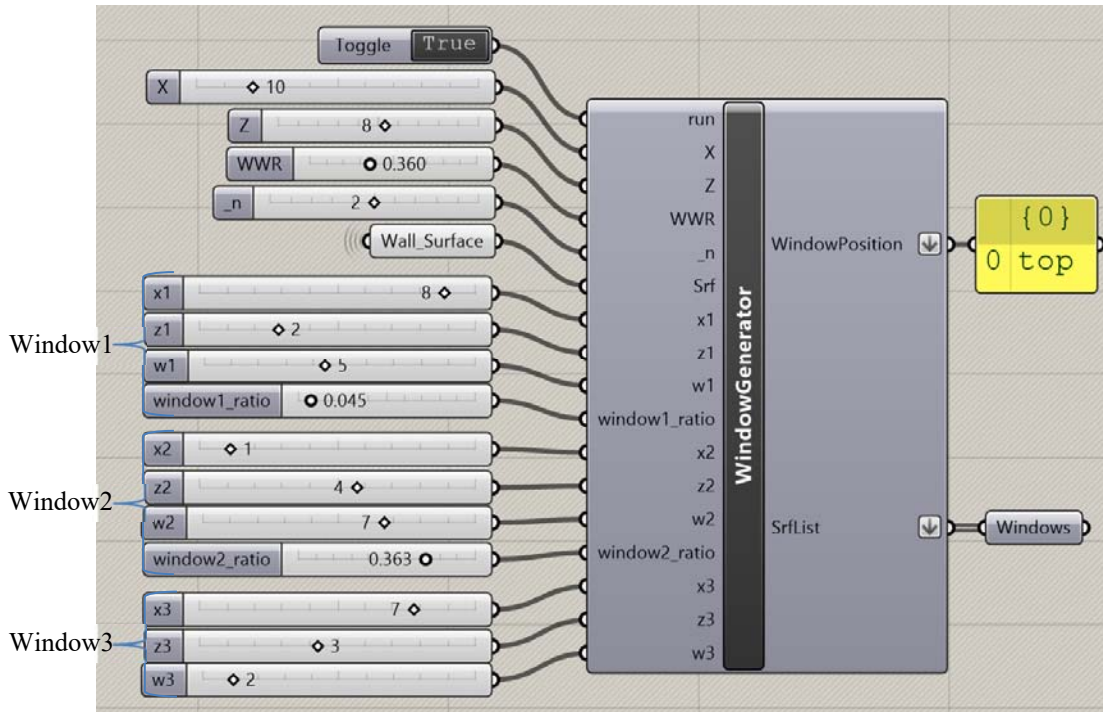


Figure 5.14: Window Design Generator in Grasshopper (Rutten, 2014)

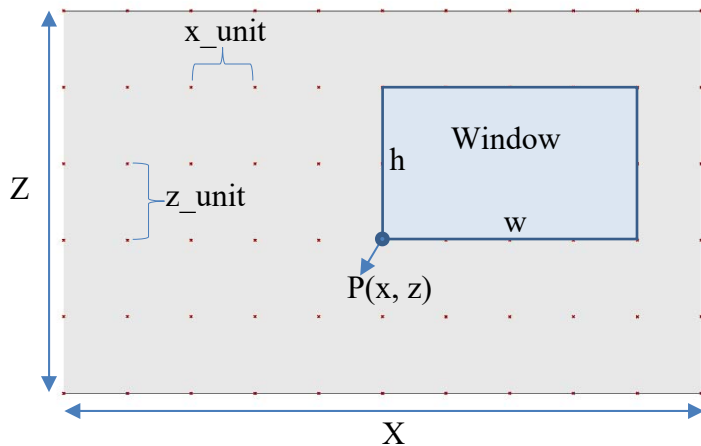


Figure 5.15: Window Parameters on Surface

The input $_n$ equals how many windows were on the wall surface, the number should be 1 or 2 or 3. The inputs x_1 , z_1 , w_1 , $window1_ratio$ are the parameters to the generate window1, while the inputs x_2 , z_2 , w_2 , $window2_ratio$ are the parameters to the

generate window2, and the inputs x_3, z_3, w_3 are the genes to generate window3. If $_n = 1$, only window1 input parameters ($x_1, z_1, w_1, \text{window1_ratio}$) were used, the window2 ($x_2, z_2, w_2, \text{window2_ratio}$) and window3 (x_3, z_3, w_3) input parameters were ignored. If $_n = 2$, the window3 (x_3, z_3, w_3) input parameters were ignored. The window is composed from the four parameters, which are: width (w), window height (h), and window position $P(x, z)$ (Figure 5.15). Therefore, the window genes are: w, h, x, z in the Genetic Algorithm. To generate the window (w, h, x, z) design, the process list below was used:

- 1) the window (w, x, z) are window inputs, the window1 inputs are x_1, z_1, w_1 , window2 inputs are x_2, z_2, w_2 , and the window 3 input are x_3, z_3, w_3 .
- 2) $\text{window1_area} = \text{window_area} * \text{window1_ratio}$. If input “ $_n$ ” = 1, the window1_ratio always equal to 1. Window1 height (h) = $\text{window1_area} / w_1$.
- 3) $\text{window2_area} = \text{window_area} * \text{window2_ratio}$. If input “ $_n$ ” = 2, window2_ratio always equal to $1 - \text{window1_ratio}$ (the input of window2_ratio was ignored). If input “ $_n$ ” = 3, the window2_ratio value gets from input window2_ratio . Window2 height (h) = $\text{window2_area} / w_2$.
- 4) $\text{window3_area} = \text{window_area} * \text{window3_ratio}$. If input “ $_n$ ” = 3, window3_ratio always equal to $1 - \text{window1_ratio} - \text{window2_ratio}$. Window3 height (h) = $\text{window3_area} / w_3$.
- 5) If the generated window surface is out of the wall surface boundaries, the window area will be reduced by removing the part of the window surface that

outside the wall surface boundaries. Therefore, the window genes (w, h, x, z)

followed the rule below:

if $(x + w) > X$: set width (w) = $X - x$

if $(z + h) > Z$: height (h) = $Z - z$

- 6) If the window1, window2, and window3 are overlapped, then set them as a Boolean union surface (Figure 5.16). Therefore, the total window areas were reduced.

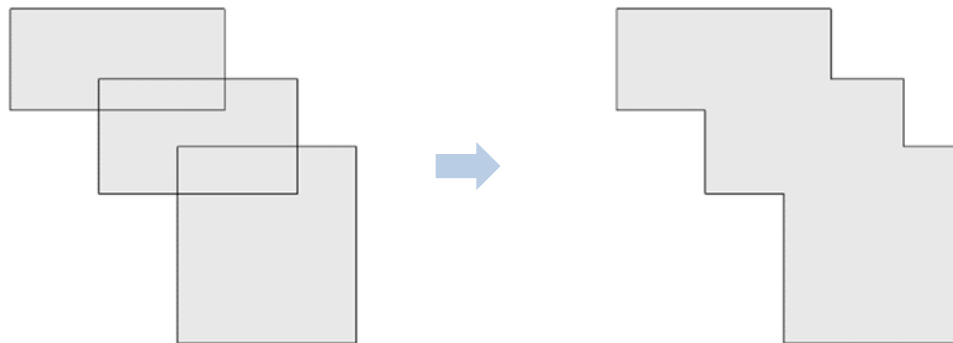


Figure 5.16: Overlapped Windows Change to a Boolean Union Window

- 7) Finally, transform the normalized window parameters (x, z, w, h) into real parameters (x_r, z_r, w_r, h_r) on the wall surface:

$$x_r = x * x_unit,$$

$$z_r = z * z_unit)$$

$$w_r = w * x_unit$$

$$h_r = h * z_unit$$

$$real_window = (x_r, z_r, w_r, h_r), \text{ window position } P_real = (x_r, z_r).$$

The output WindowDesign is the result of generated window, which can be one, two, or three windows depends on the input `_n`.

The output WindowPosition is the generation position of the window with reference to the to the wall surface. This output result is for correcting the sDA value when use the `custom_preset` in Radiance rendering parameter in DIVA. The window position rules set below:

For one window:

$z_mid = wall_surface_real_height / 2$

if $(z - z_mid) \geq -h/4$, set window position as "top",

else if $(z + h - z_mid) \leq h/4$, set window position as "down",

else set window position "centered".

For more than one window:

if all window locations are the same, set the window position as the same,

else if one window area is 70% larger than the others, set the window

position as the largest window position.

else set window position as "mix".

5.3. Window Design Optimization Process and Results in Office Models

This study used the Octopus program (Vierlinger, n.d.) to select the optimal window design on an office facade. Octopus is a plug-in in the grasshopper program for applying multi-objective evolutionary algorithm to parametric design. It can search for many goals at once, producing a range of optimized trade-off solutions between each

goal. Octopus is based on the Galapagos User Interface (Rutten, 2017), which uses a Genetic Algorithm for optimization. The office model input parameters and output setting are listed in Table 5-14. The simulated location is in Phoenix, AZ, USA.

Table 5-14: The Input Parameters and Output Setting for Simualtion

	Parameters	Unit	Settings
Input Parameters	Length	m	3.0
	Width	m	4.6
	Height	m	2.6
	Reference point height above floor	m	0.762
	Zone area	m ²	45.7
	Volume	m ³	388.6
	Roof U-factor	W/m ² -K	0.056
	floor U-factor	W/m ² -K	0.056
	Exterior wall U-factor	W/m ² -K	0.284
	Adiabatic wall U-factor	W/m ² -K	0.056
	Glazing U-factor	W/m ² -K	1.34
	SHGC		0.28
	Visual Transmittance		0.41
	Floor visible reflectance		0.2
	Wall visible reflectance		0.7
	Roof visible reflectance		0.7
	Lighting power density	W/m ²	11.95
	Equipment	W/ m ²	0
	Illuminance dimming setpoint	lux	538
	Occupant People	People/ m ²	0
	Rendering quality setting		Custom-Preset
	Cooling setpoint	°C	25.6
	Heating setpoint	°C	22.2
	Infiltration per zone	m ³ /s-m ²	0
	Outside air per zone	CFM	0
	Assigned-CFM	CFM	Auto-size
System		Ideal-Loads-Air-System	
Output Results from EnergyPlus	Lighting energy	MWH	InteriorLights:Electricity
	Cooling Load Energy	MWH	Zone Ideal Load Zone Sensible Cooling load
	Heating Load Energy	MWH	Zone Ideal Loads Zone Sensible Heating load
Output Results from DIVA	ASE	%	Annual Daylighting Simulation
	sDA	%	Annual Daylighting Simulation

In this study, the genes for optimization were connected to the Genome of the Octopus (Figure 5.17), which include the number of windows ($_n$), window 1 parameters (x_1 , z_1 , w_1 , window1_ratio), window 2 genes (x_2 , z_2 , w_2 , window2_ratio), and window 3 genes (x_3 , z_3 , w_3). All of these parameters are explained in the Section 5.2. In the analysis, the maximum Window-to-Wall Ratio (WWR) was 36%. The solutions in this study were the generated window surfaces.

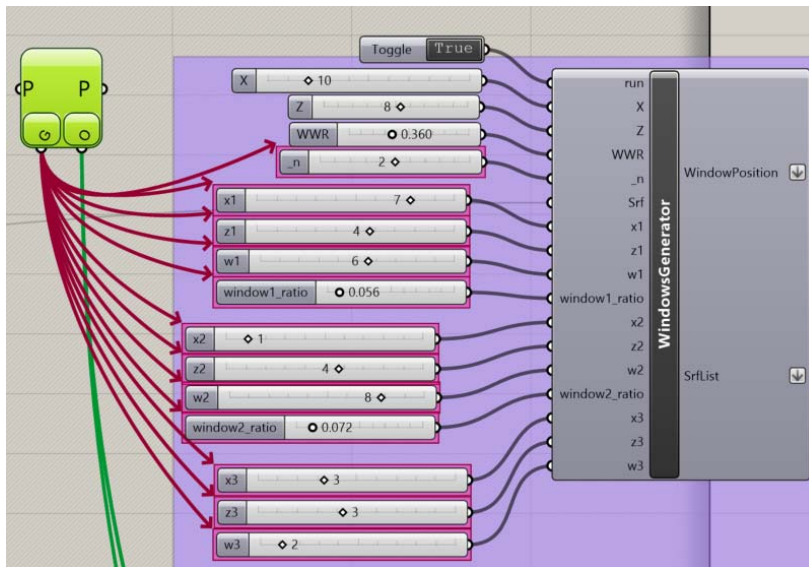


Figure 5.17: The Genes Used for Selecting

The objectives of the optimization are the ASE, sDA, and the energy usage (heating + cooling + lighting). The results are shown in the 3-D in a space rectangular coordinate system shown in Figure 5.18. The optimal solutions should be close to the origin point (i.e., within the red cube zone in Figure 5.18). The ASE is a simulated result from the daylighting analysis, the minimal number will be selected in the optimization process. Based on the LEED score, the objective is to obtain a result below 10%. The sDA is another simulated result from the daylighting analysis that is described in Section

5.1.2, and uses Equation 5-2 to correct the sDA value from the “custom-preset”. The maximum value will be selected for the optimization. When connected to the Octopus software, the sDA was multiplied by -1, because Octopus was designed to select the minimal value. In the LEED requirement, the sDA should be larger than 55% or 75%. The energy usage results are from the combined daylighting and thermal simulation, minimal value will be selected. The combined daylighting and thermal simulation method were mentioned in the Section 4.2.5. The energy usage is a weighted value from the lighting electricity use, cooling load, and heating load. Because the cooling and heating are the ideal system loads, a weighted Equation 5-3 was used to combine lighting, cooling, and heating energy use. This equation used a factor as an example to convert system cooling and heating load to cooling and heating electricity consumption.

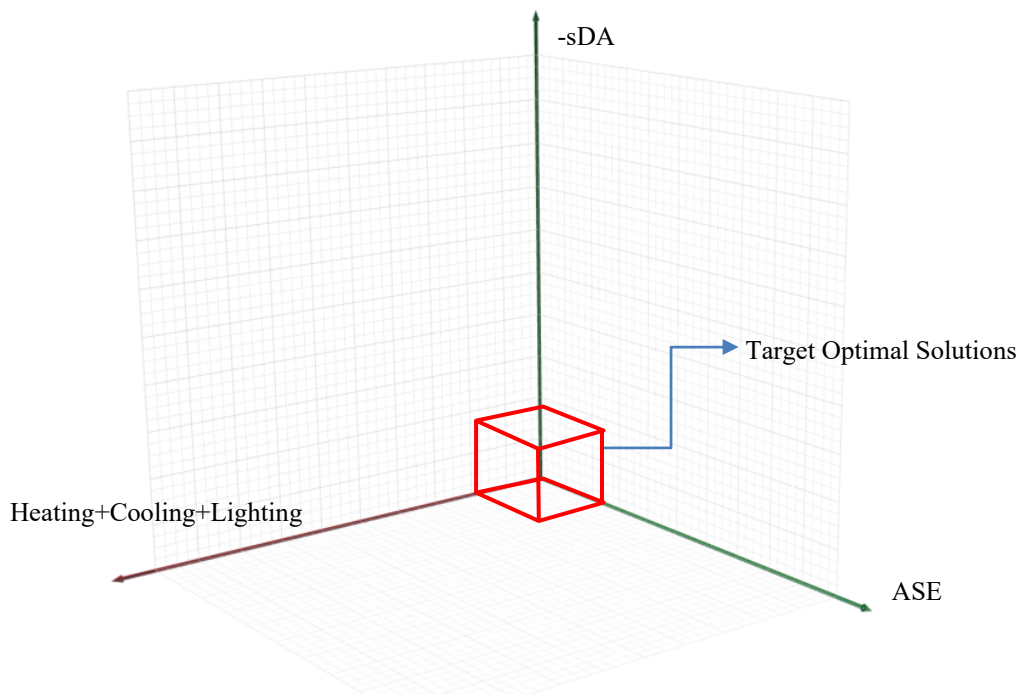
$$\text{Energy Usage} = (\text{cooling load} + \text{heating load})/3 + \text{lighting electricity} \quad \text{Equation 5-3}$$


Figure 5.18: The Objectives of Optimization

5.3.1. The Results for South-Facing Windows

Unfortunately, during certain part of the year for the South-facing windows, there can be significant solar radiation passing through the window into the interior space, which can cause glare. In order to prevent the glare, shade devices were applied in this study. These shades were automatically added based on the generated windows (Figure 5.19). For the shade, overhangs that extend outward horizontally by 0.32 meters were selected. The overhangs were extruded along a horizontal line of the designed window in 0.01 meters on each side. The gap between each overhang is 0.3 meters.

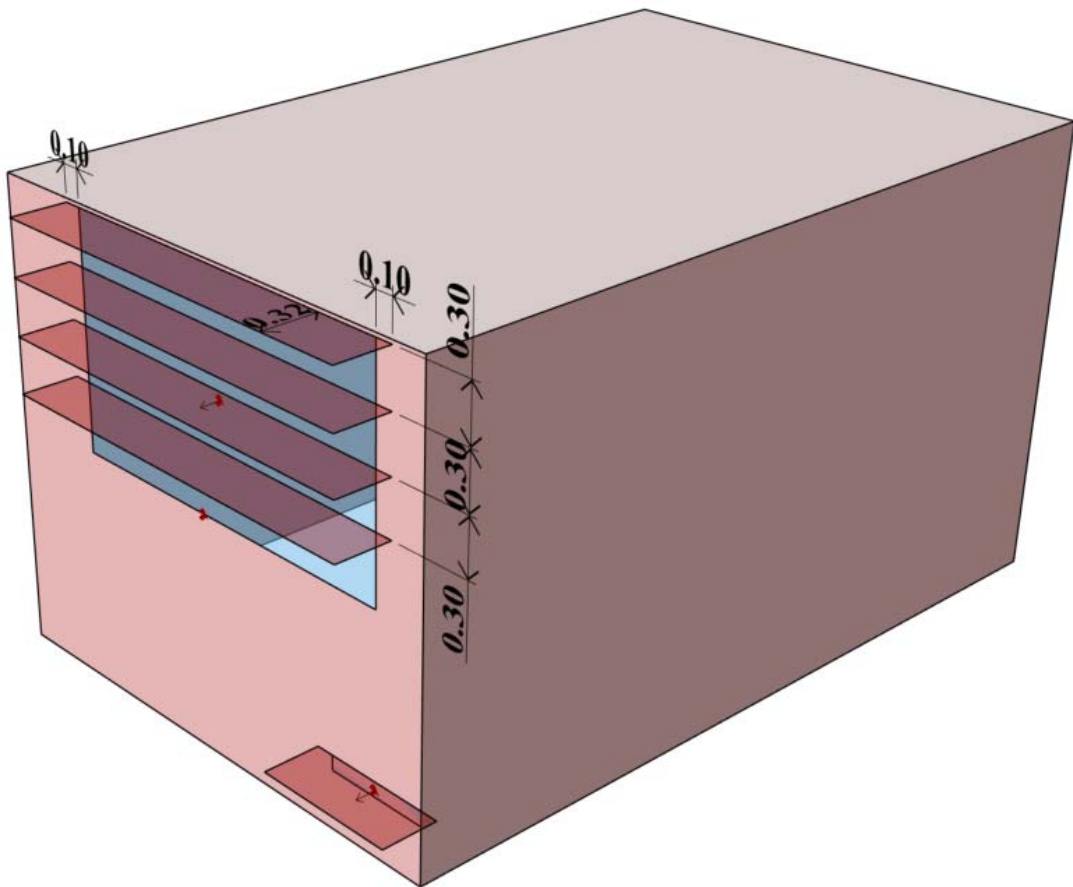


Figure 5.19: Shading Device for South-Oriented Window

The Figure 5.20 showed the results of generation 1 (brown points). The figure shows the majority solutions are far from the target optimal zone (red box in Figure 5.18). These solutions had relatively low sDAs and high energy consumptions. The later generations (generation 5 to generation 40) are shown in Figure 5.21 to Figure 5.28, which brown points represent the current generation points, the green points represent the previous generation points in each figure. This sequence shows that the solutions are gradually closing toward the optimal zone after starting at generation 1. The majority of the solutions in generation 40 are in the desired zone (Figure 5.28).

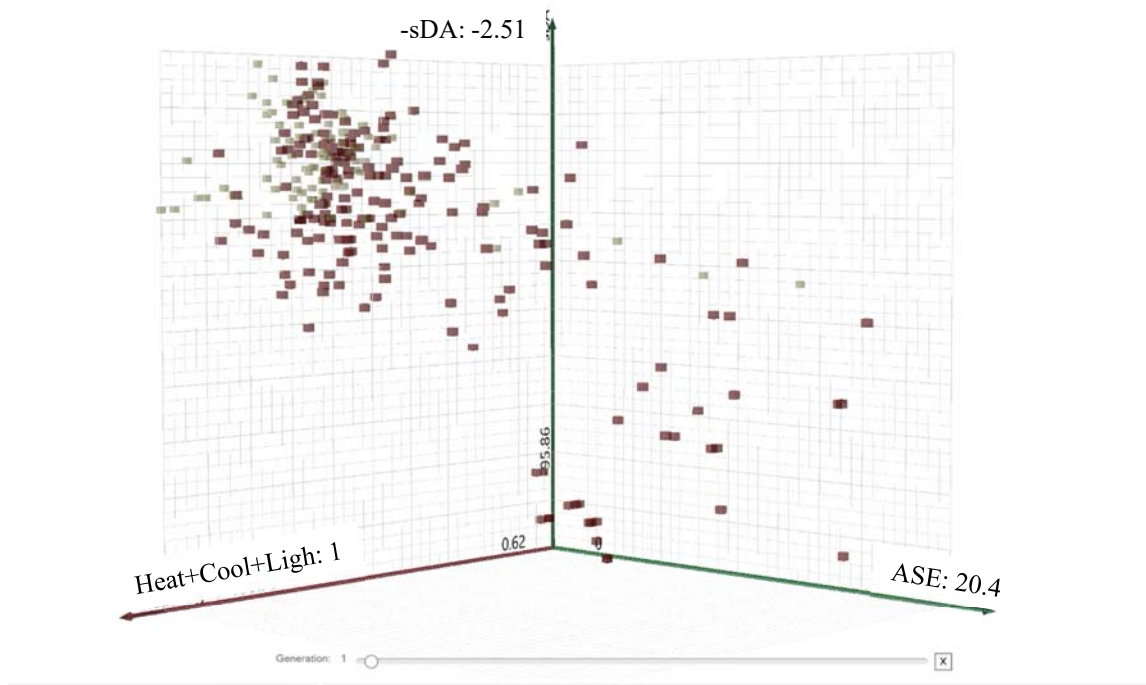


Figure 5.20: Generation 1

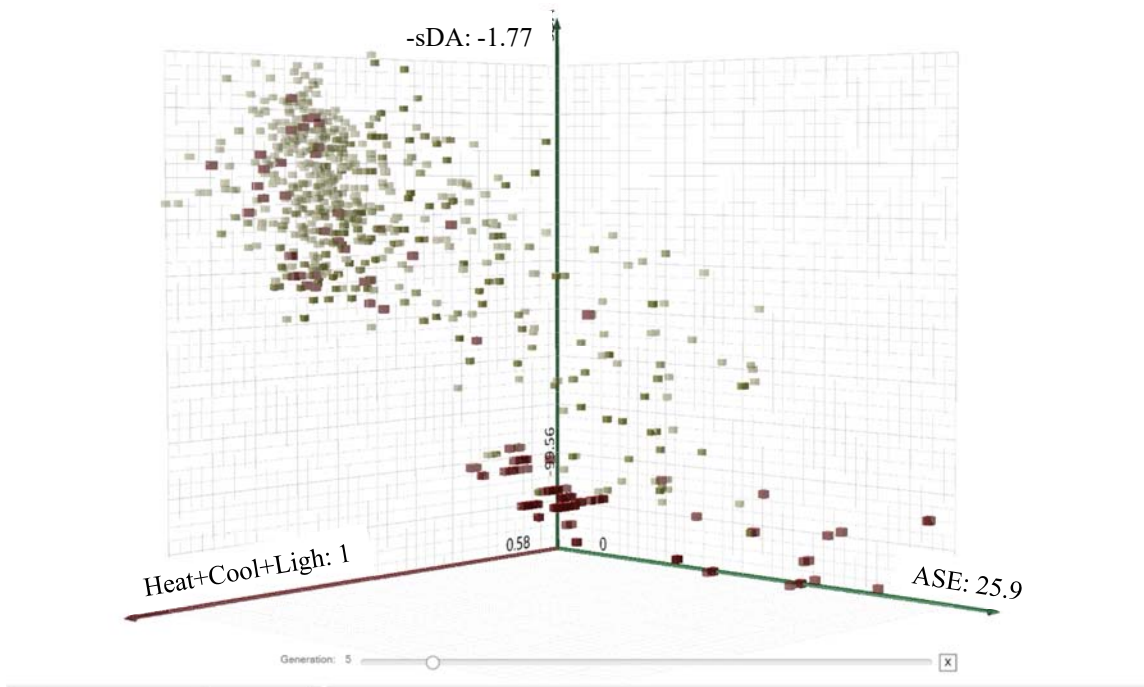


Figure 5.21: Generation 5 (Brown Points are Generation 5; The Green Points are the Previous Generations)

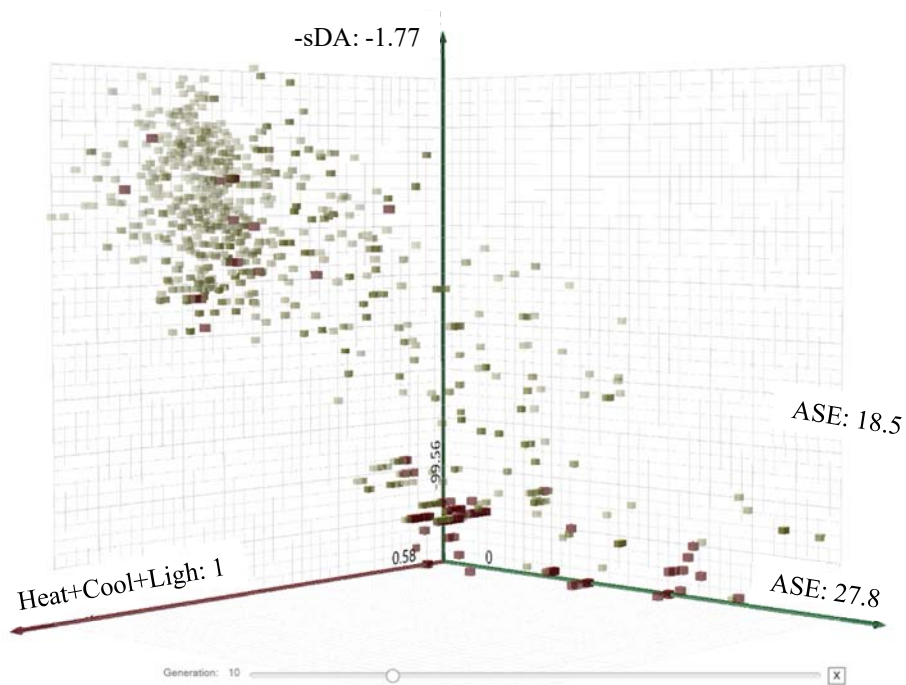


Figure 5.22: Generation 10 (Brown Points are Generation 10; The Green Points are the Previous Generations)

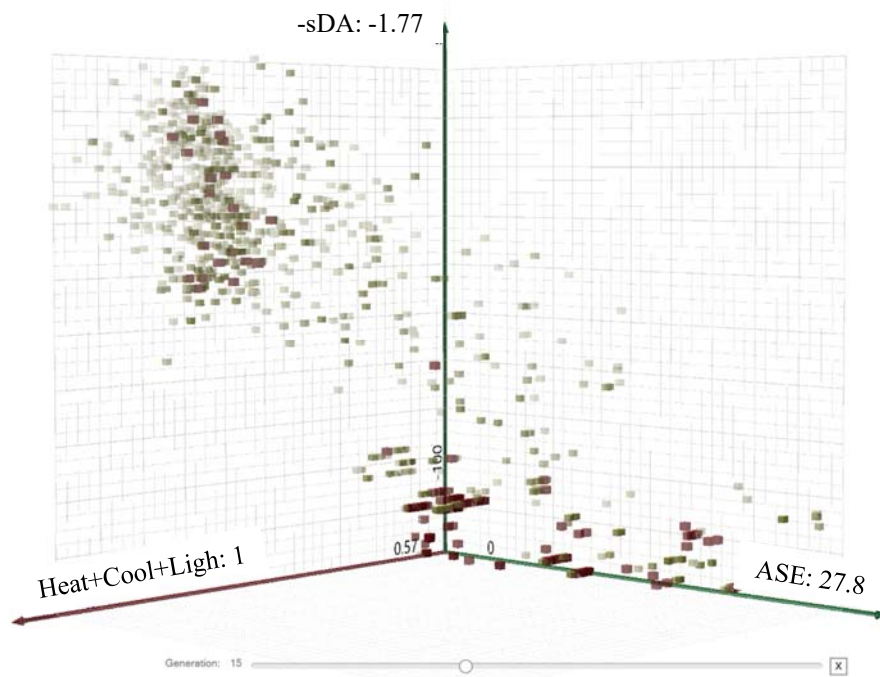


Figure 5.23: Generation 15 (Brown Points are Generation 15; The Green Points are the Previous Generations)

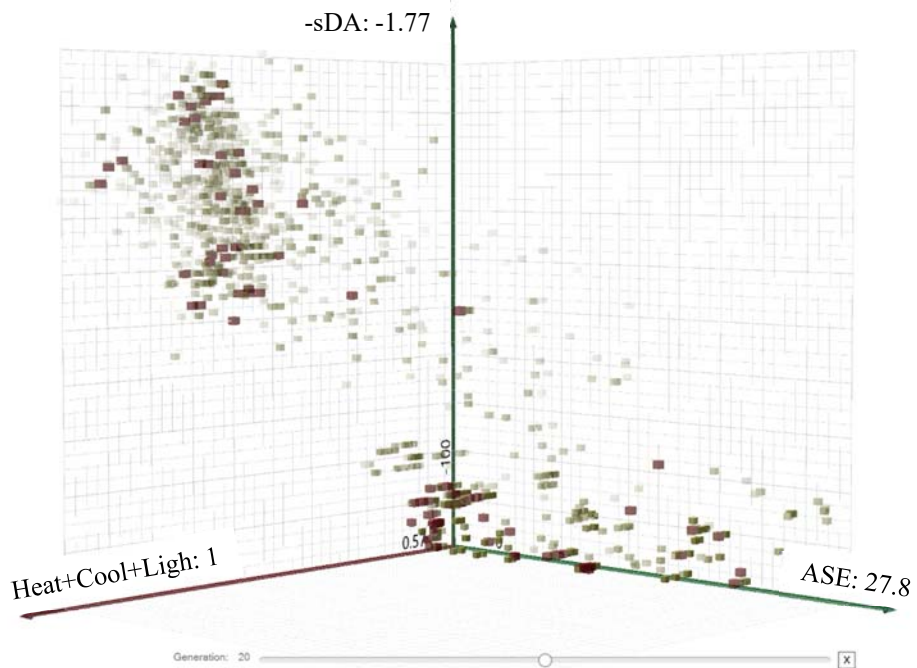


Figure 5.24: Generation 20 (Brown Points are Generation 20; The Green Points are the Previous Generations)

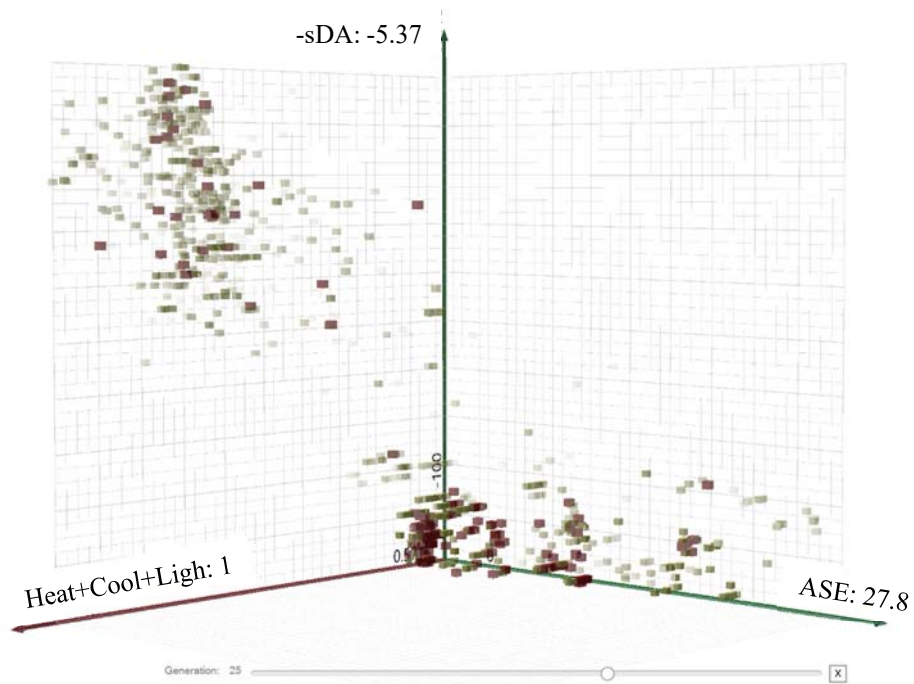


Figure 5.25: Generation 25 (Brown Points are Generation 25; The Green Points are the Previous Generations)

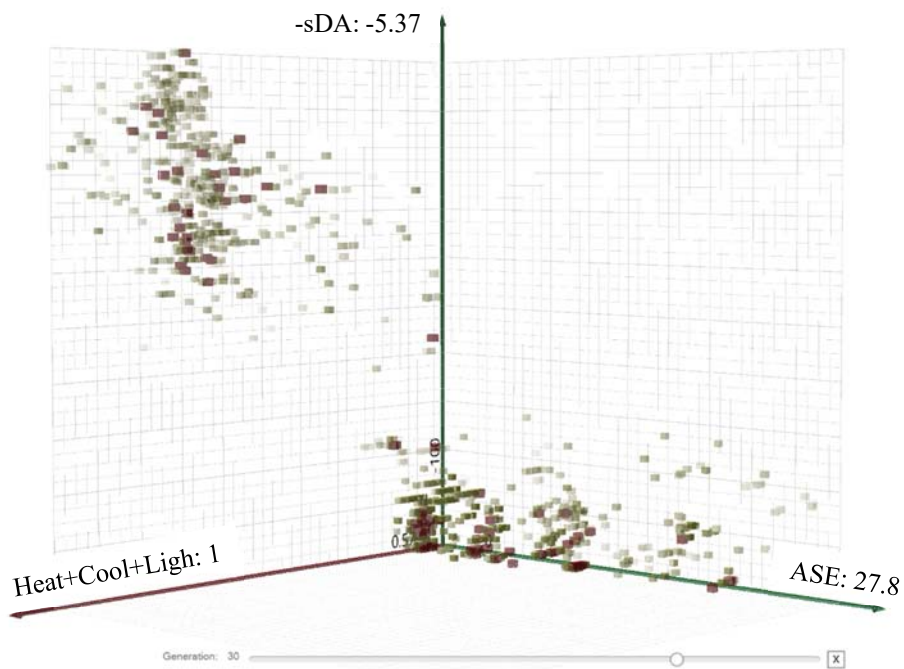


Figure 5.26: Generation 30 (Brown Points are the Generation 30; The Green Points are the Previous Generations)

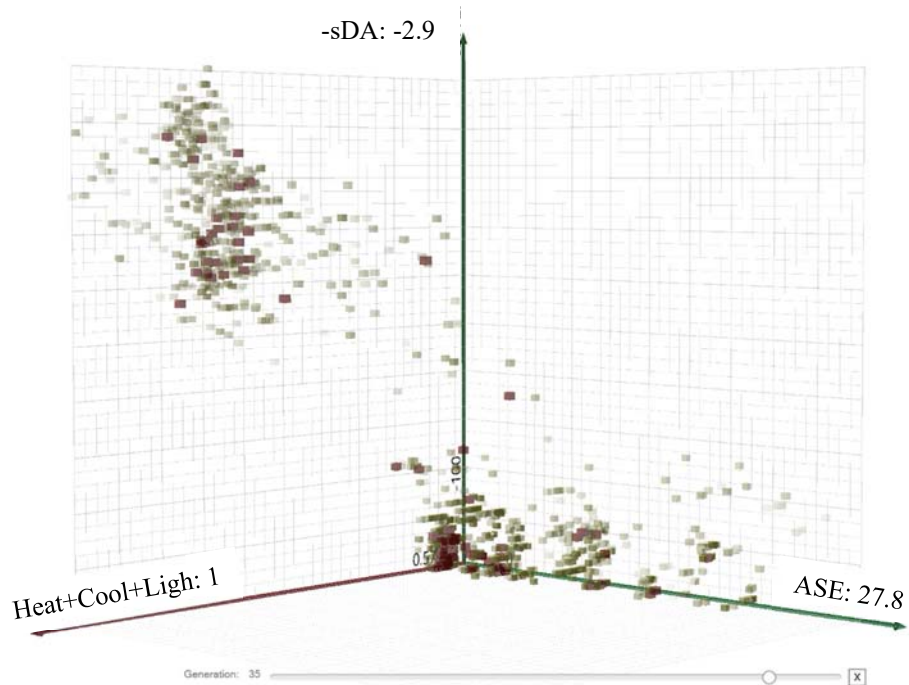


Figure 5.27: Generation 35 (Brown Points are Generation 35; The Green Points are the Previous Generations)

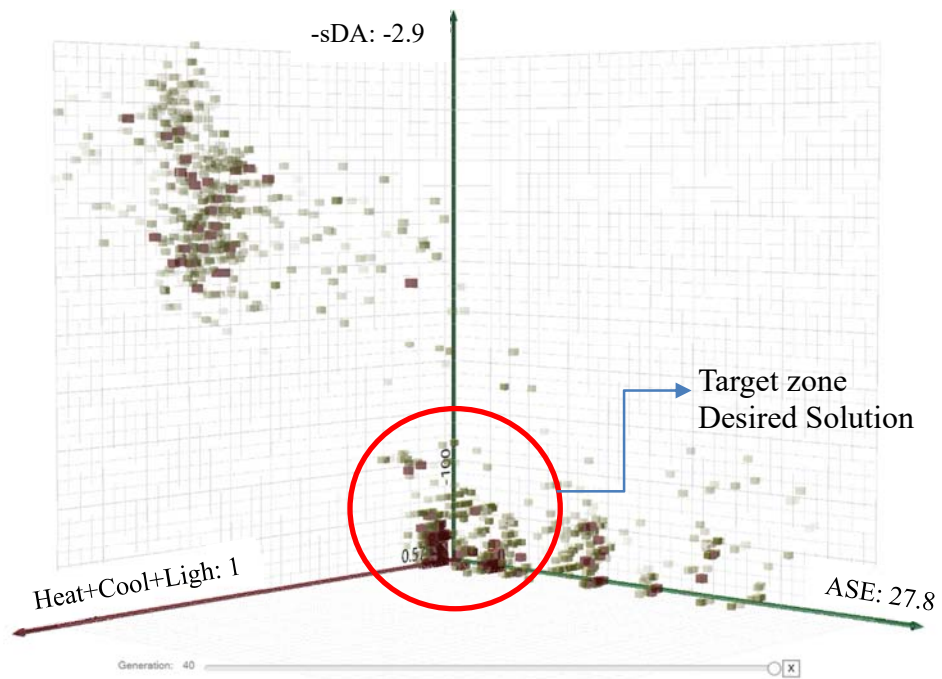


Figure 5.28: Generation 40 (Brown Points are Generation 40; The Green Points are the Previous Generations)

The optimal designs located in target zone (red circle in Figure 5.28) for the South orientation are listed in Table 5-15, where the maximum sDA was 100%, and minimal annual energy use was 0.59 MWH. The results showed the majority of the optimal window designs were located at the top position of the wall. In general, the top position of the windows (case 1 to 7 in Table 5-15) had the lowest energy use, smaller window-to-wall ratios, and maximum sDA. The top position window case 1 with a WWR of 28% could obtain three points in LEED daylighting credit. However, for the center positioned windows (case 8 to 11) and the low positioned windows (case 14, 15, 16), the WWR must be the maximum value of 36% to reach the optimal results to obtain three points in LEED daylighting credit. In addition, the results showed the top position window had the smallest annual energy use compared to other window positions. The annual energy use in the top position windows could be 20% lower than the results of the windows in the centered or down position (i.e., the energy difference between case 6 and case 15).

However, this current software of window design has a limitation to generate and place a very small sized window on the wall surface (Table 5-15). The small window may not want in practical building design.

Table 5-15: Optimal Designs of South-Facing Windows

Case	Position		WWR %	sDA %	ASE %	Energy MWH
1	Top		28	75	9	0.65
2	Top		30	77	3.7	0.62
3	Top		31	91	1.9	0.61
4	Top		33	86	1.9	0.6

Table 5-15: Optimal Designs of South-Facing Windows (Continued)

Case	Position		WWR %	sDA %	ASE %	Energy MWH
5	Top		34	94	0	0.62
6	Top		35	93	3.7	0.59
7	Top		35	100	1.9	0.6
8	Center		36	80	10	0.67

Table 5-15: Optimal Designs of South-Facing Windows (Continued)

Case	Position		WWR %	sDA %	ASE %	Energy MWH
9	Center		36	80	10	0.68
10	Center		36	79	3.7	0.67
11	Center		36	83	0	0.67
12	Mix		36	94	0	0.65

Table 5-15: Optimal Designs of South-Facing Windows (Continued)

Case	Position		WWR %	sDA %	ASE %	Energy MWH
13	Mix		33	84	5.6	0.66
14	Down		36	78	1.9	0.69
15	Down		36	77	1.9	0.71
16	Down		36	78	0	0.68

5.3.2. The Results for East-Facing Windows

For the East-facing windows, the shading devices are different from the South-facing windows. Due to the East-facing windows have more direct sunlight in the morning, the overhangs were extruded along a horizontal line of the window in 0.02 meter on each side (Figure 5.29). Other East-oriented shades settings are same as the South-facing window shades.

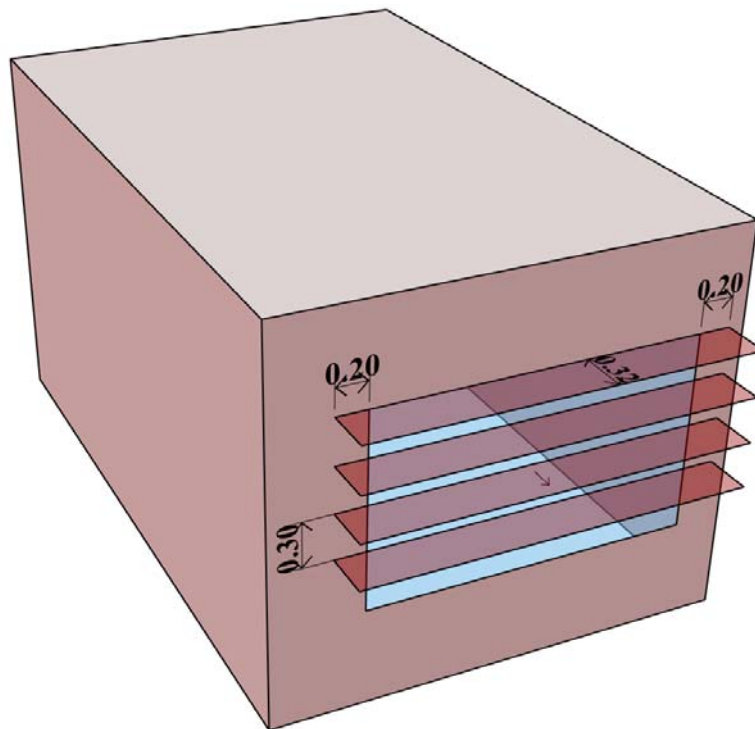


Figure 5.29: Shading Device for East-Oriented Windows

In this part of the analysis, 40 generations were used to calculate the optimal analysis as shown in Figure 5.30. In a similar fashion as the previous analysis, the results for the East-facing window showed that the minimal annual energy use was 0.62, and

the maximum sDA was 77%. However, when the sDA was higher than 75%, the ASE was higher than 10%, which are not acceptable for LEED requirements. Therefore, the majority of the optimal East-facing window designs can only obtain 2 LEED points. In general, the East-facing windows had a lower sDA, a higher ASE, and a higher energy consumption than the South-facing windows with the same window area.

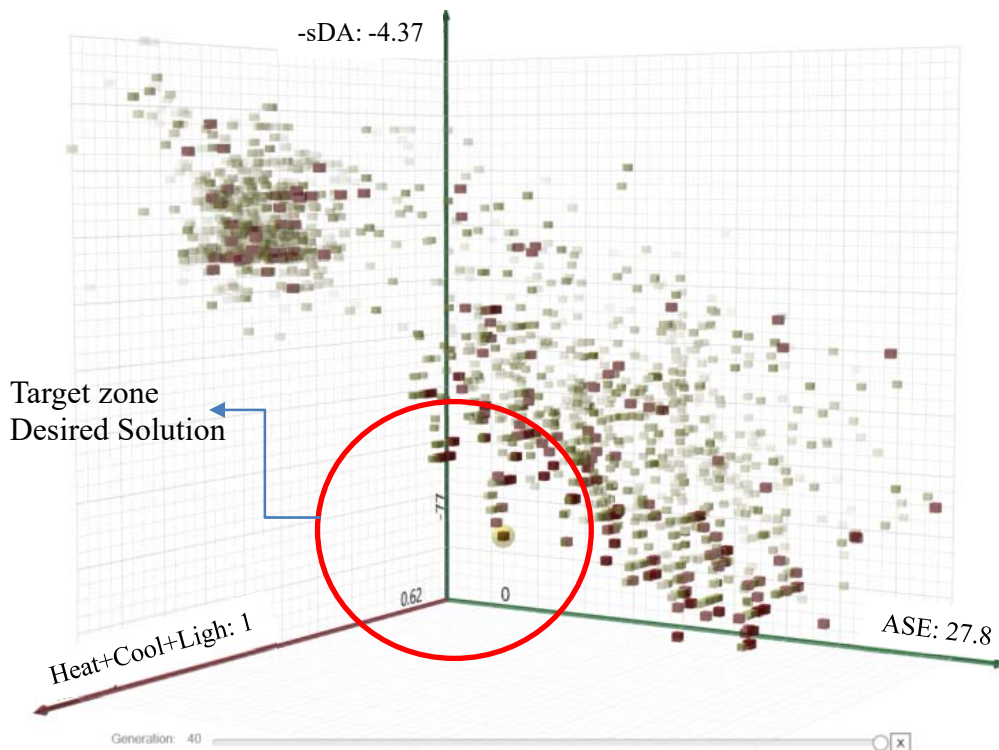


Figure 5.30: 40 Generation Results of East-Facing Window Designs

There are several optimal solutions in the target zone (red circle in Figure 5.30) in the East-facing windows was shown in Table 5-16. In the analysis, the criteria for LEED daylighting credit was used. In order to obtain 2 LEED points, the ASE should be below 10%, and sDA should be larger than 55%. The analysis showed that the majority of the optimal window designs were located at the top position of the wall. The top

positioned window designs cases 17 through 20 had lower lighting energy and higher sDA than the centered and mixed positioned windows (cases 21, 22, 23). Surprisingly, there were no windows selected that were located at the bottom of the wall that could obtain two LEED scores. The analysis showed the top window positions had higher sDA results and lower energy consumption than the center and mix position windows.

Table 5-16: The Optimal Designs of East-Facing Windows

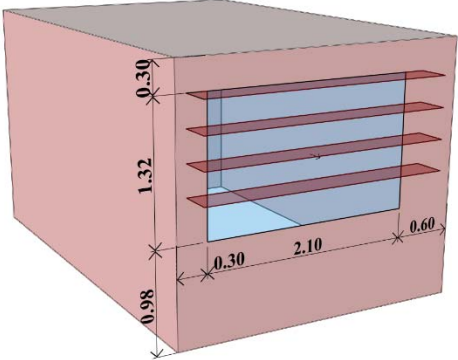
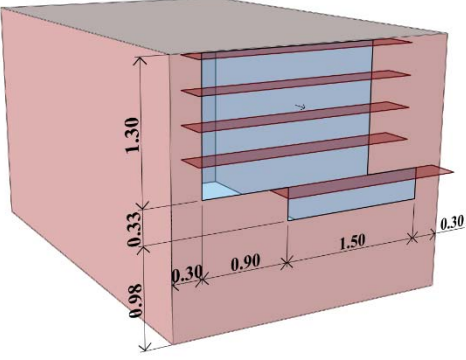
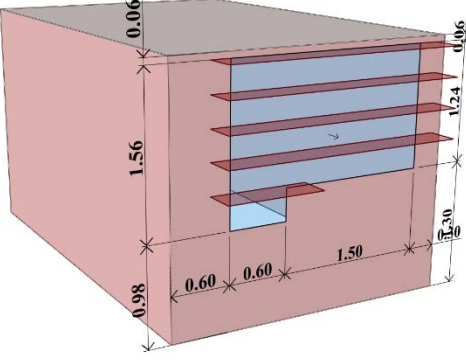
Case	Position		WWR %	sDA %	ASE %	Energy MWH
17	Top		35.6	66	5.6	0.67
18	Top		36	68	10	0.66
19	Top		35.8	55	10	0.64

Table 5-16: The Optimal Designs of East-Facing Windows (Continued)

Case	Position		WWR %	sDA %	ASE %	Energy MWH
20	Top		36	55	5.6	0.66
21	Mix		36	62	10	0.68
22	Mix		36	62	5.6	0.69
23	Center		35	57	9.3	0.72

5.3.3. The Results for West-Facing Windows

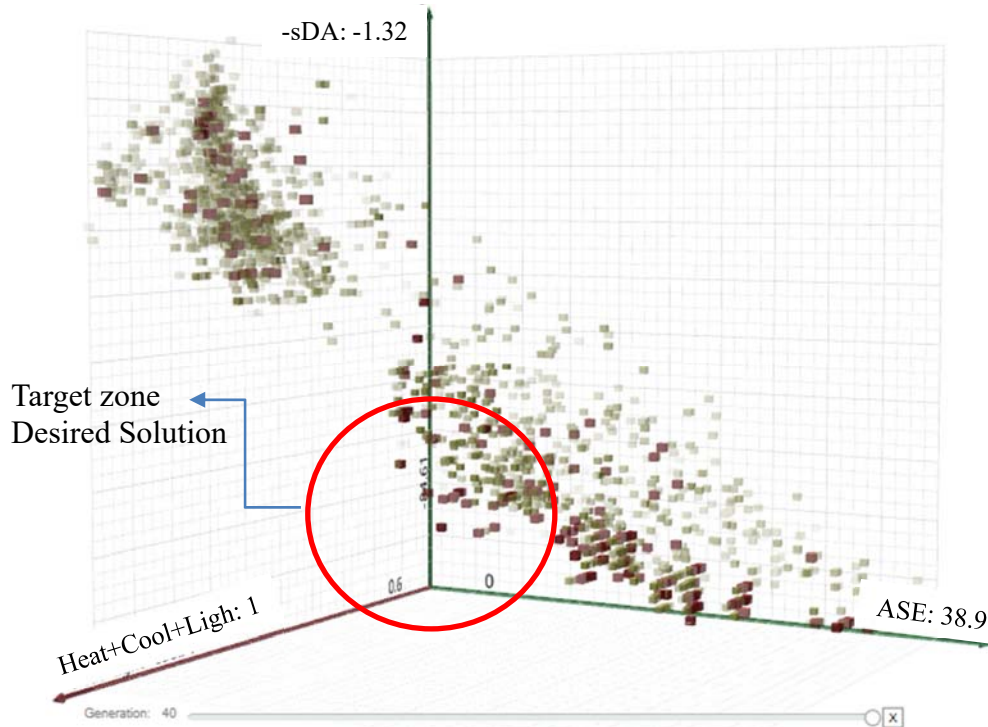


Figure 5.31: 40 Generation Results of West-Facing Window Designs.

The results showed that the window shades in West-facing windows were the same as the East-facing windows. The results of the analysis with 40 generations are shown in Figure 5.31. The results for the West-facing window showed that the minimal annual energy use was 0.6, and the maximum sDA was 84%. However, when the sDA was higher than 84%, and the ASE was higher than 10%, it did not fulfill the LEED requirements.

Some of the top positioned West-facing windows (case 24 and case 25) could obtain 3 LEED points, which had better results than East-facing windows. Some of the

optimal window design solutions (red circle in Figure 5.31) are shown in Table 5-16.

The results indicate that the windows in the top position had a higher LEED score and a lower annual energy usage than other window locations (case 27 to 29). Compared to the South-facing windows, the West-facing windows needed to have a larger window-to-wall ratio to obtain the high sDA and LEED credits.

Table 5-17: The Optimal Designs of West-Facing Windows

Cases	Position		WWR %	sDA %	ASE %	Energy MWH
24	Top		34	75	1.9	0.63
25	Top		35	80	10	0.64
26	Top		36	66	9.3	0.65

Table 5-17: The Optimal Designs of West-Facing Windows (Continued)

Cases	Position		WWR %	sDA %	ASE %	Energy MWH
27	Mix		35.6	70	7.4	0.65
28	Mix		34	69	10	0.67
29	Mix		33.4	67	9.3	0.63

5.3.4. The Results for North-Facing Windows

For the North facing windows, there was no glare from the direct sunlight, thus, the ASE will always be 0. Therefore, the objectives were only the sDA and the annual

energy use (cooling + heating + lighting). The results from an analysis with 40 generations are shown in Figure 5.32. The results showed that the maximum value of sDA was 85%. The minimal annual energy use was 0.43, which is much lower than the energy use of the other three orientations. Table 5-18 shows some optimal window designs for the North façade that are located in the target zone in Figure 5.32. The top positioned window designs (Case 31, 32, 33 in Table 5-18) had three LEED points. The centered and mix positioned window designs (case 34 to 38 in Table 5-18) could only obtain 2 LEED points. In the analysis, the top positioned windows had a higher sDA and a lower energy consumption than other window positions.

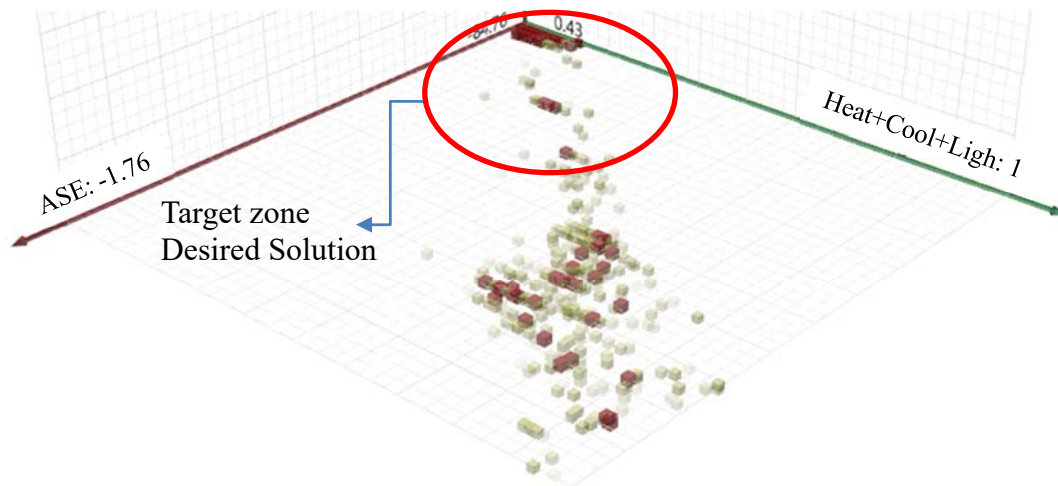


Figure 5.32: 40 Generation Results of North-Facing Window Designs

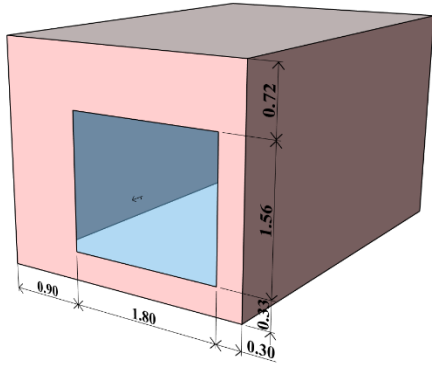
Table 5-18: The Optimal Designs of West-Facing Windows

Cases	Position		WWR %	sDA %	ASE %	Energy MWH
30	Top		31.6	69	0	0.53
31	Top		36	81	0	0.47
32	Top		36	81	0	0.45
33	Top		36	78.6	0	0.51

Table 5-18: The Optimal Designs of West-Facing Windows (Continued)

Cases	Position		WWR %	sDA %	ASE %	Energy MWH
34	Mix		36	62	0	0.55
35	Mix		36	59	0	0.69
36	Center		30	67.6	0	0.6
37	Center		33	62	0	0.64

Table 5-18: The Optimal Designs of West-Facing Windows (Continued)

Cases	Position		WWR %	sDA %	ASE %	Energy MWH
38	Down		36	56.6	0	0.66

5.4. Summary

This section discussed the development and application of an improved Radiance simulation analysis. In this analysis a Grasshopper plugin was created to design window size and placement in an exterior wall. Later, this window design program was used to obtain optimal window designs in an office building.

The results showed that Radiance had limitations in rendering runtime and accuracy of the daylighting simulate results. Therefore, this study proposed an improved daylighting simulation method that produces accurate results while minimizing Radiance simulation runtime. The results showed that a reasonable runtime and accurate simulation results were crucial in daylighting optimization when using the lighting electricity, Annual Sun Exposure (ASE), and spatial Daylight Autonomy (sDA) as optimization criteria. This study also analyzed changes to the grid spacing and Radiance rendering quality setting to reduce the Radiance simulation runtime and yet maintain an accurate daylighting result.

This study analyzed the grid spacing settings in DIVA. To accomplish this, four grid spacing sizes (0.3 m, 0.45 m, 0.6 m, 0.9 m) were tested in an annual daylighting simulation. The results of the sDA, ASE, lighting energy, and running time were then compared. The results show that the daylighting results between the spacing sizes 0.3 m, 0.45 m, 0.6 m, and 0.9 m were not significantly different. However, the larger grid spacing size uses less simulation time. Therefore, the spacing size of 0.6 m was selected in this study to save the simulation runtime.

This study demonstrated the use of a new customized Radiance rendering parameters (called custom preset) in DIVA to simulate the annual daylighting. This custom preset only took 30 seconds to obtain annual daylighting results, while the most accurate preset (high-quality preset) in DIVA takes over one hour to complete the simulation. This study conducted 185 simulations with different building conditions to find the correlation between custom preset and high-quality preset. The study showed the ASE results were not be affected by the Radiance rendering setting changes, because the ASE was only related to the direct sunlight penetrating through the window. Therefore, there was no need to correct the ASE results.

For the lighting electricity results, the optimization criteria for the lighting energy selected the lowest value in all the possible design models. In this study, the lighting energy profile of different office models in the custom preset and the high-quality preset were the same. The lowest lighting energy use and highest lighting energy usage in high-quality preset and custom preset used the same models. For the daylighting optimization,

the lowest value was selected from the custom preset simulations. Therefore, there was no need to correct the lighting energy results in the custom preset.

For the sDA results, a sDA result larger than 55% or 75% was needed for LEED daylighting credit. The statistical software JMP Pro 14 was used to calculate the correlation between high-quality preset and custom preset. The results showed a high accuracy annual daylighting result could be predicted by the simulation results from the custom preset using the multi-linear regression Equation 5-2. The predictors WFR, FVR, sDA_custom, Shades [White shades], and WFR * WFR were significant in this multi-linear regression model ($P < 0.05$). The predictor FVR * Shades [White shades] and Window Positions showed marginally statistically significant linear trends. The R-square of this regression model was 0.940, which means approximately 94.0% of the observed variation in the output variable can be explained by the input variables. The average difference between the Predicted sDA_high and simulated sDA_high was 9.4%, which is an acceptable error in prediction. However, this regression needs to follow conditions list below:

- 1) If the office model has shades, the window shades should be white, (i.e., shades visual reflectance > 0.7).
- 2) The wall and roof visual reflectance would be between 0.7 to 0.9.
- 3) The maximum predicted sDA_high should not be higher than 100%.
- 4) The simulation location should be limited in Phoenix, AZ
- 5) The room geometry limited to regular sized room, the height of the simulation model will be limited to 4 meters. The high-space room needs to do more test.

The current work created a window design plugin in Grasshopper (Davidson, 2019) that can automatically generate window designs. Based on varying the user input Window-to-Wall Ratio (WWR), wall surface, number of windows, window1 input parameters, window2 input parameters, and window3 input parameters, thousands of window models were generated for the optimization. The outputs of this window design plugin software were generated window surfaces and the window position in the exterior wall surface (such as top, down, centered, and mixed positions).

The Octopus software in Grasshopper was used to select the optimal window design based on the daylighting and thermal performance. The objectives of the optimization were the ASE, sDA, and the energy usage (heating + cooling + lighting). The ASE was the simulated result from the daylighting analysis, the minimal number will be selected in the optimization process. The sDA is another simulated result from the daylighting analysis that is described in Section 5.1.2, and used Equation 5-2 to correct the sDA value from the “custom-preset”. In this analysis, the maximum value was selected for the optimization. In the energy usage results from the combined daylighting and thermal simulation, the minimal value was then selected.

In the results of window design optimization, the optimal design for the South-oriented window showed that the maximum sDA was 100%, and the minimal annual energy use was 0.59 mWh/yr. The optimal designs were able to obtain three LEED points. The results showed the majority optimal window designs were located at the top position of the wall. The top position windows had the lowest energy use, the smallest window-to-wall ratio, and the maximum sDA. For example, in the top positioned

windows, it was easier to obtain 3 LEED points when the WWR were equal or higher than 28%. However, for the center and lower positions, the WWR had to a maximum value of 36% to obtain 3 LEED points. In addition, the results showed the top position window had the smallest annual energy use compared to other window positions. The annual energy use in the top position windows reached up to 20% lower than the centered and lower position windows.

For the East-oriented windows, the majority of the generated optimal East-facing window designs that were generated can only obtain 2 LEED points. Compared to South-facing windows, the East-facing windows had higher ASE, and lower sDA results. The results for the East-facing window showed that the minimal annual energy use was 0.62 mWh/yr, which was higher than the energy use of the South-facing windows. In addition, the analysis showed that the majority of the optimal window designs were located at the top position of the wall. Surprisingly, there were no windows located at the bottom of the wall that could obtain two LEED points. The analysis showed the top window positions had higher sDA results and lower energy consumption than the center position windows.

The West-facing windows had improved simulation results versus the East-facing windows. The results showed that some of the West-facing windows could obtain three LEED points in daylighting. In addition, the annual energy use in West-facing windows were smaller than the results of East-facing windows. The optimal West-facing windows design indicated that the windows in the top position satisfied the LEED daylighting credit and had lower annual energy usage than other window positions.

Compared to the South-facing windows, the West-facing windows needed to have a larger window-to-wall ratio to obtain the a higher sDA.

The analysis showed the North-facing window did not have the direct sunlight. Therefore, the ASE was always zero. As a result, the objectives for the North-oriented windows were then limited to optimizing the sDA and the annual energy usage. The results showed that the maximum value of sDA was 85%. The minimal annual energy use was 0.43, which was much lower than the energy use of the other three orientations. In the analysis of the North-facing window, the top positioned windows had the highest sDA and the lowest energy consumption.

In summary, for all the orientations, windows at higher positions had higher sDA and lower energy consumption than other window locations. The windows at the lower position of the wall had the worst optimization results. The results showed that the top-positioned window could have relatively lower window-to-wall ratio to obtain three LEED points in daylighting credit and lower annual energy use than the other window positions in hot climate zones. Therefore, the results imply the national building energy codes and standards should not give the same credits for all the window locations on an exterior wall.

6. SUMMARY, RESULTS, CONCLUSIONS, AND FUTURE WORK

The results and conclusion of this study are particular to the location of Phoenix, Arizona.

6.1. Summary

This dissertation presents the results of a new optimal window design method for an office by using a combined daylighting and thermal simulation in Phoenix, Arizona. The purpose of this work was to better inform the building window design process in the preliminary design stage for improving building thermal and visual performance.

The major contributions of this work are as follows:

- 1) This study proposed a new office simulation model that helps magnify the differences in the annual energy use due only to differences in the windows based on the results from the reproduced Caldas model (Caldas and Norford, 2002). This study used the new office model to develop and test a new prototype for the combined daylighting+thermal simulation by comparing the combined simulation methods of DOE-2+Split-Flux, EnergyPlus+Split-Flux, EnergyPlus+Radiosity, and EnergyPlus+Radiance. This study also proposed guidelines for how to conduct the combined daylighting and thermal simulation to obtain the accurate results.
- 2) This study developed an improved Radiance simulation method for daylighting optimization. This new method produces accurate annual daylighting results while minimizing run times.

- 3) This study developed a window design plugin in grasshopper using a Python script. This new window design plugin can generate thousands of different window sizes and placement designs.
- 4) The window design plugin with a Multi-Objective Optimization (MOO) tool were applied to the analysis of window size and placement designs. Finally, four optimization studies were conducted for the office model in four orientations (i.e., N, S, E, W). New optimal window design strategies the were then developed that are based on the different orientations in the hot-dry climate of Phoenix, AZ.

6.2. Results

6.2.1. Results from the Combined Daylighting and Thermal Simulation

This study first reproduced the results from Caldas office model to access the new method was working correctly, and then refined and improved the reproduced office model to help magnify the differences to the annual energy use due only to differences in the window designs. The improved office model with six different window designs were tested in four orientations (South, North, East, and West) with different floor visual reflectances (i.e., 0.2, 0.5, 0.9). The major results of this section are as follows:

- 1) The location tested in Phoenix, AZ. Since Phoenix, AZ is a cooling dominated climate, the heating energy use was very small, and the analysis focused on the cooling analysis. The preliminary result showed that without daylighting simulations, all the six window models (i.e., windows that had different sizes and

placements but with same window area) had similar cooling and heating results, which means the window location changes did not significantly affect the cooling and heating energy. After integrated the daylighting and thermal simulation, the lighting energy and cooling energy decreased dramatically. In addition, the cooling loads of the six models had the same trends as the lighting energy.

- 2) For the South-facing windows, when the floor was a dark surface with a visual reflectance 0.2, the EnergyPlus+Radiance simulation resulted in a higher lighting energy use than the lighting results of EnergyPlus+Split-Flux/Radiosity and DOE-2.1e+Split-Flux simulations. The Radiance simulation was also more sensitive to window location changes than the Split-Flux and Radiosity. The results also showed that when the FVR was increased from 0.2 to 0.5 or 0.9, the lighting energy results from EnergyPlus+Radiance became closer to the results of other simulation methods.
- 3) For the East-oriented and West-oriented windows, when the simulations were repeated for floor reflectances of 0.2, 0.5 and 0.9, the results showed that the EnergyPlus+Radiance simulation always resulted in a higher lighting energy use than the lighting results of EnergyPlus+Split-Flux/Radiosity or DOE2.1e+Split-Flux simulation. Radiance results for the East and West-facing windows were more sensitive to the window location changes than the South-facing windows when the FVR changed from 0.2 to 0.5 to 0.9.
- 4) For the East and West windows, the lighting differences in window 1, 3, 4, and 6 were noticeable, which were more than a 60% difference.

- 5) For the North-oriented windows, the lighting energy differences between EnergyPlus+Radiance versus EnergyPlus+Split-Flux/Radiosity methods became larger compared to the lighting results of the South, East, and West-facing windows. The lighting differences between EnergyPlus+Radiance versus EnergyPlus+Split-Flux/Radiosity methods in windows 1, 3, 4, 5, and 6 were larger, which were more than 80% differences. The lighting electricity use predicted by EnergyPlus+Radiance simulation were significantly higher than result predicted by DOE2.1e+Split-Flux or by the EnergyPlus+Split-flux/Radiosity simulation.
- 6) The results showed that there were no significant differences in daylighting performance when the window location changes in the daylighting simulations of Split-Flux or Radiosity.
- 7) In the East, North, and West-facing windows, Radiance was more sensitive to the window location changes than the South-facing windows when the floor visual reflectance changed from 0.2 to 0.5 to 0.9.
- 8) The results showed that different window size and location designs could have very different annual energy consumption results using the combined Radiance+EnergyPlus simulation tool. The results were different from many of the previous studies. For example, some of previous studies always set the window position at the center of the exterior wall, which is not an optimal result in a daylighting window design. In addition, the results showed that changing the window size and position, but keeping the window area the same may reduce or

increase the annual energy use.

6.2.2. Results from Improved Radiance Simulation Method in Optimization

This section proposed a customized Radiance rendering parameters (called custom preset) in DIVA to simulate the annual daylighting to save the runtime. This custom preset only took 30 seconds to obtain annual daylighting results, while the most accurate preset (high-quality preset) in DIVA took over one hour to complete the simulation on a commodity personal laptop embedded with an Intel i7-8650U processor with 4 cores @ 2.11 GHz and 16GB RAM. This study conducted 185 simulations with different building conditions to find the correlation between custom preset and high-quality preset. The major results of this section are as follows:

- 1) The study showed the Annual Sun Exposure (ASE) results were not affected by the Radiance rendering setting changes, because the ASE was only related to the direct sunlight. Therefore, there was no need to correct the ASE results.
- 2) For the lighting electricity results, the optimization criteria in the lighting energy selected the lowest value in all the possible design models. In this study, the lighting energy profile of different office models in the custom preset and the high-quality preset were the same. The lowest lighting energy use and highest lighting energy usage in the high-quality preset and custom preset used the same models. Therefore, there was no need to correct the lighting energy results in the custom preset. For the daylighting optimization, the lowest value was selected from the custom preset simulations.

- 3) For the spatial Daylight Autonomy (sDA) results, the results showed that the high accuracy annual daylighting result could be predicted by the simulation results from the custom preset by multi-linear regression Equation 5-2. The predictors WFR, FVR, sDA_custom, Shades [White shades], and WFR * WFR were significant in this multi-linear regression model ($P < 0.05$). The predictor FVR * Shades [White shades] and Window Positions showed marginally statistically significant linear trends.
- 4) The R-square of the new regression model is 0.940. The average difference between the Predicted sDA_high and simulated sDA_high was 9.4%, which is an acceptable error in prediction.

6.2.3. Results from Window Design Optimization in Office Models

This section created a window design plugin in Grasshopper (Davidson, 2019) that can automatically generate a group of possible window designs. This section also used Octopus (Genetic Algorithm) in Grasshopper to select the optimal window design based on the daylighting and thermal performance. The objectives are the ASE, sDA, and the energy usage (heating + cooling + lighting). The major results of window design optimization are as follows:

- 1) For the South-oriented window, in the top positioned windows, it was easier to obtain three LEED points when the WWR were equal or higher than 28%. However, for the center and lower positions in the exterior wall, the WWR should have a maximum value of 36% to obtain three LEED points.

- 2) In addition, for the South-oriented window, the results showed the top position window had the smallest annual energy use compared to other window positions. The annual energy use in the top position windows reached up to 20% lower than centered and down position windows.
- 3) For the East-oriented windows, the majority of the generated optimal East-facing window designs that were generated could only obtain two LEED points. Compared to the South-facing windows, the East-facing windows had higher ASE, and lower sDA results.
- 4) The results for the East-facing window showed that there were no windows located at the bottom of the wall could obtain two LEED points.
- 5) Compared to South-facing windows, the East-facing windows had higher ASE, and lower sDA results.
- 6) The West-facing windows had a better simulation results than East-facing windows. Some of the West-facing windows could obtain three LEED points. In addition, the annual energy use in West-facing windows were smaller than the results of East-facing windows.
- 7) Compared to the South-facing windows, the West-facing windows needed to have a larger window-to-wall ratio to obtain the high sDA.
- 8) The North-facing window did not have the direct sunlight. Therefore, the ASE was always zero. The objectives for North-oriented windows were then limited to optimize sDA and annual energy usage.

- 9) The results showed that the total energy use in North-facing windows was much lower than the energy use of the other three orientations. The top positioned window designs had three LEED points, while the centered and mix positioned window designs could only obtain 2 LEED points.
- 10) The results showed the majority optimal window designs were located at the top position of the wall. The top position windows had the lowest energy use, smallest window-to-wall ratio, and maximum sDA.
- 11) The top-positioned window could have a relatively lower window-to-wall ratio to obtain 3 LEED points in daylighting credit and lower annual energy use than other window positions in hot climate zones.

6.3. Conclusion

The overall conclusion of this study listed below:

- 1) In the cooling-dominated climate zone, reducing the lighting energy usage contribute to the reduction of the total energy use. In addition, the results showed that the use of a sophisticated daylighting simulation method is critical to obtain more accurate lighting energy results.
- 2) For South-facing windows, the results show that a DOE-2 + Split-Flux and EnergyPlus + Split-Flux/Radiosity simulations can be relatively accurate when all the interior surfaces are bright, which saves simulation runtime.
- 3) For East, North, and West orientations, it is useful to use the Radiance for daylighting simulation for both dark and bright floors.

- 4) This study demonstrated that the statistical multi-linear regression is a useful method to improve the Radiance simulation-based method to obtain relative accurate daylighting results while minimizing the simulation runtime.
- 5) For best window designs, top position windows were suggested because they had the lowest energy use, smallest window-to-wall ratio, and maximum sDA.
- 6) For best window designs, South facing windows were suggested, because they had better performance than East and West-facing windows.
- 7) The West-facing windows had larger LEED points than East-facing windows because the sDA in West-facing windows is larger than the East-facing windows. This is because the spatial Daylight Autonomy (sDA) metrics simulate 10 hours a day between 8:00 am and 6:00 pm, which causes the West-facing windows had longer daylighting hours than East-facing windows. Therefore, there is a bias in LEED in considering daylighting performance in East orientation.
- 8) This study demonstrated improved results compared with the previous studies. This is important since some of the previous studies used the Split-Flux method for the daylighting simulation to find the optimal window design. However, the previous studies showed that all the windows were placed at the center of the facades. This is because the Split-Flux simulation could not calculate the differences in the window location with same window area. This study used a more sophisticated Radiance-based daylighting analysis to analyze off-center placement of fenestration. The results showed that the top-positioned windows

had the highest sDA and the lowest energy consumption, whereas the lower-positioned windows had the opposite results.

- 9) The national building energy codes and standards should not give the same credits for all the window locations of equal area in an exterior wall.

6.4. Future Work

The following work needs to be performed in the future:

- 1) This study only simulated buildings in a cooling dominated climate zones; Future work will need to conduct the simulations for the heating dominated climate zones, and simulations in mild climates.
- 2) The Genetic Algorithm with window generator tool in this study was not an efficient method to find optimal window design. This is because the window placement design is a discrete optimization, even though in this study, the window placements were set as continuous selections (the window placement controlled by variables x and y coordinates). However, this window placement optimization in GA is not real continuous in computers. In addition, this study did 40 generations (4,000 runs) to obtain the optimal results. However, in the later generations, some of the window designs were still far from the optimal target zone, and many of optimal designs were similar. Therefore, there is a need to find more effective optimization method for discrete window placement designs.

- 3) Future work will need to find the most accurate simulation methods to correctly evaluate the integrated daylighting and thermal performance of the Complex Fenestration Systems (CFSs), static shading devices, and the dynamic shading devices, such a tool would also need to be efficient to use on a typical desktop/laptop computer.
- 4) The window design plugin that was created in Grasshopper has one limitation that generated and placed a very small-sized window on the exterior wall surface. Therefore, there is a need to update this window design plugin to fix this limitation.
- 5) This study did not evaluate the effect of surrounding structures such as reflected solar radiation or shading from nearby buildings. Therefore, future studies would need to evaluate this.
- 6) In this study, only static overhangs were tested. Therefore, there is a need to investigate all form of shades, including: static shading, CFSs, and dynamic shading devices to find out if it is more useful to use static shading devices that require less maintenance instead of dynamic shading to deliver optimal energy savings, and maximize daylighting with acceptable visual and thermal comfort, but may require more attention.
- 7) The successful use of the multi-linear regression implies that there should be good success in the development and use of artificial neural network model, or machine learning procedure to assist with the design optimization

REFERENCES

- Acosta, I., Campano, M. Á., & Molina, J. F. (2016). Window design in architecture: Analysis of energy savings for lighting and visual comfort in residential spaces. *Applied Energy*, 168(Supplement C), 493-506.
doi:<https://doi.org/10.1016/j.apenergy.2016.02.005>
- Acosta, I., Munoz, C., Campano, M. A., & Navarro, J. (2015). Analysis of daylight factors and energy saving allowed by windows under overcast sky conditions. *Renewable Energy*, 77(Supplement C), 194-207.
doi:<https://doi.org/10.1016/j.renene.2014.12.017>
- Acosta, I., Navarro, J., & Sendra, J. J. (2013). Daylighting design with lightscoop skylights: Towards an optimization of shape under overcast sky conditions. *Energy and Buildings*, 60(Supplement C), 232-238.
doi:<https://doi.org/10.1016/j.enbuild.2013.01.006>
- Acosta, I., Navarro, J., & Sendra, J. J. (2015). Towards an analysis of the performance of monitor skylights under overcast sky conditions. *Energy and Buildings*, 88(Supplement C), 248-261. doi:<https://doi.org/10.1016/j.enbuild.2014.12.011>
- Acosta, I., Navarro, J., Sendra, J. J., & Esquivias, P. (2012). Daylighting design with lightscoop skylights: Towards an optimization of proportion and spacing under overcast sky conditions. *Energy and Buildings*, 49(Supplement C), 394-401.
doi:<https://doi.org/10.1016/j.enbuild.2012.02.038>

- Aerts, J., van Herwijnen, M., & Stewart, T. (2003). Using simulated annealing and spatial goal programming for solving a multi site land use allocation problem. *IN: Proceedings of Evolutionary multi-criterion optimization*. p. 73-73.
- Aho, K., Derryberry, D., & Peterson, T. (2014). Model selection for ecologists: the worldviews of AIC and BIC. *Ecology*, 95(3), 631-636.
- Aiziewood, M. (1993). Innovative daylighting systems: An experimental evaluation. *Lighting Research and Technology*, 25(4), 141-152.
- Akaike, H. (1998). Information theory and an extension of the maximum likelihood principle *Selected papers of hirotugu akaike* (pp. 199-213): Springer.
- Akashi, Y., Muramatsu, R., & Kanaya, S. (1996). Unified Glare Rating (UGR) and subjective appraisal of discomfort glare. *International Journal of Lighting Research and Technology*, 28(4), 199-206.
- An, J., & Mason, S. (2010). Integrating Advanced Daylight Analysis into Building Energy Analysis. *Proceedings of Simbuild*.
- Andersen, M., & de Boer, J. (2006). Goniophotometry and assessment of bidirectional photometric properties of complex fenestration systems. *Energy and Buildings*, 38(7), 836-848. doi:<http://dx.doi.org/10.1016/j.enbuild.2006.03.009>
- Andolsun, S., Culp, C. H., Haberl, J. S., & Witte, M. J. (2012). EnergyPlus vs DOE-2.1e: The effect of ground coupling on cooling/heating energy requirements of slab-on-grade code houses in four climates of the US. *Energy and Buildings*, 52, 189-206. doi:<https://doi.org/10.1016/j.enbuild.2012.06.012>

Asadi, E., da Silva, M. G., Antunes, C. H., & Dias, L. (2012). A multi-objective optimization model for building retrofit strategies using TRNSYS simulations, GenOpt and MATLAB. *Building and environment*, 56, 370-378.
doi:<http://dx.doi.org/10.1016/j.buildenv.2012.04.005>

Standard ASHRAE. (1981). Standard 55-81. Thermal environmental conditions for human occupancy. Ashrae Inc.

Standard ASHRAE. (2004). Standard 55-2004. Thermal environmental conditions for human occupancy.

Standard ASHRAE. (2010). Standard 55-2010. Thermal environmental conditions for human occupancy. Atlanta USA

Standard ASHRAE. (2013). Standard 55-2013 Thermal environmental conditions for human occupancy.

Standard ASHRAE. (2016). Standard 90.1-2016, Energy standard for buildings except low rise residential buildings.

Handbook ASHRAE. (2017a). 2017 ASHRAE Handbook–Fundamentals. Atlanta, USA

Standard ASHRAE. (2017b). Standard 55-2017 Thermal environmental conditions for human occupancy.

Audet, C., & Dennis Jr, J. E. (2002). Analysis of generalized pattern searches. *SIAM Journal on optimization*, 13(3), 889-903.

- Bahnfleth, W. P. (1989). *Three-dimensional modelling of heat transfer from slab floors*.
CONSTRUCTION ENGINEERING RESEARCH LAB (ARMY) CHAMPAIGN
IL.
- Baker, M. S., & Salem, O. (1990). Modeling complex daylighting with DOE 2.1-C.
DOE-2 user news, 11(1).
- Balling, R. J., Taber, J. T., Brown, M. R., & Day, K. (1999). Multiobjective urban
planning using genetic algorithm. *Journal of urban planning and development*,
125(2), 86-99.
- Bayes, T. (1970). An essay towards solving a problem in the doctrine of chances. *Studies
in the History of Statistics and Probability*, 1, 134-153.
- Bellia, L., Marino, C., Minichiello, F., & Pedace, A. (2014). An Overview on Solar
Shading Systems for Buildings. *Energy Procedia*, 62(Supplement C), 309-317.
doi:<https://doi.org/10.1016/j.egypro.2014.12.392>
- BEopt. (2017) BEopt - Building Energy Optimization. Retrieved September 21, 2017,
Retrieved from <https://beopt.nrel.gov/>
- Bodart, M., & De Herde, A. (2002). Global energy savings in offices buildings by the
use of daylighting. *Energy and Buildings*, 34(5), 421-429.
doi:[http://dx.doi.org/10.1016/S0378-7788\(01\)00117-7](http://dx.doi.org/10.1016/S0378-7788(01)00117-7)
- Bustamante, W., Uribe, D., Vera, S., & Molina, G. (2017). An integrated thermal and
lighting simulation tool to support the design process of complex fenestration
systems for office buildings. *Applied Energy*, 198(Supplement C), 36-48.
doi:<https://doi.org/10.1016/j.apenergy.2017.04.046>

- Caldas, L. (2001). *An evolution-based generative design system: using adaptation to shape architectural form*. Massachusetts Institute of Technology.
- Caldas, L. G., & Norford, L. K. (2002). A design optimization tool based on a genetic algorithm. *Automation in construction*, *11*(2), 173-184.
- Cao, K., Huang, B., Wang, S., & Lin, H. (2012). Sustainable land use optimization using Boundary-based Fast Genetic Algorithm. *Computers, Environment and Urban Systems*, *36*(3), 257-269.
doi:<https://doi.org/10.1016/j.compenvurbsys.2011.08.001>
- Carlucci, S., Cattarin, G., Causone, F., & Pagliano, L. (2015). Multi-objective optimization of a nearly zero-energy building based on thermal and visual discomfort minimization using a non-dominated sorting genetic algorithm (NSGA-II). *Energy and Buildings*, *104*(Supplement C), 378-394.
doi:<https://doi.org/10.1016/j.enbuild.2015.06.064>
- Standard CEN. (2007). EN 15251:2007. Indoor environmental input parameters for design and assessment of energy performance of buildings addressing indoor air quality, thermal environment, lighting and acoustics. Brussels, Belgium
- Choi, S.-J., Lee, D.-S., & Jo, J.-H. (2017). Lighting and cooling energy assessment of multi-purpose control strategies for external movable shading devices by using shaded fraction. *Energy and Buildings*, *150*(Supplement C), 328-338.
doi:<https://doi.org/10.1016/j.enbuild.2017.06.030>

- Choi, S., Lee, D., Lee, B., Koo, S., & Jo, J. (2015). Calculation method of Shaded Ratio according to Shading Operations for Kinetic Façade. *IN: Proceedings of Proceedings of the ISHVAC-COBEE Conference, Tianjin, China.* p. 12-15.
- Chopra, A. (2012). *Introduction to google sketchup*: John Wiley & Sons.
- Christensen, C., Horowitz, S., Givler, T., Courtney, A., & Barker, G. (2005). BEopt: software for identifying optimal building designs on the path to zero net energy. *IN: Proceedings of Proceedings of ISES 2005 Solar World Congress, Orlando, FL, USA.*
- CIE. (1973). Standardisation of luminance distribution on clear skies. *Pub. CIE No. 22, TC-4.2.*
- CIE. (1995). Natural daylight, Official recommendation. . *Compte Rendu, CIE 13th Session, Committee E-13.12, vol. II, parts 13–12, II–IV&35–37.*
- CIE, S. (2003). 2003 Spatial Distribution of Daylight-CIE Standard General Sky.
- Clarke, J. (1996). The Esp-r system: advances in simulation modeling. *Building Services Journal pp27–9.*
- Clarke, J. A., Hensen, J., & Janak, M. (1998). Integrated building simulation: state-of-the-art. *Proceedings Indoor Climate of Buildings.—SI: sn.*
- Clements, E. D. (2004). *Three dimensional foundation heat transfer modules for whole-building energy analysis.* Pennsylvania State University.
- Coley, D. A., & Schukat, S. (2002). Low-energy design: combining computer-based optimisation and human judgement. *Building and environment, 37(12), 1241-1247.* doi:[https://doi.org/10.1016/S0360-1323\(01\)00106-8](https://doi.org/10.1016/S0360-1323(01)00106-8)

- Crabb, J., Murdoch, N., & Penman, J. (1987). A simplified thermal response model. *Building Services Engineering Research and Technology*, 8(1), 13-19.
- Crawley, D. B., Hand, J. W., Kummert, M., & Griffith, B. T. (2008). Contrasting the capabilities of building energy performance simulation programs. *Building and environment*, 43(4), 661-673.
- Crawley, D. B., Pedersen, C. O., Lawrie, L. K., & Winkelmann, F. C. (2000). EnergyPlus: energy simulation program. *ASHRAE journal*, 42(4), 49.
- Darula, S., & Kittler, R. (2002). CIE general sky standard defining luminance distributions. *Proceedings eSim*, 11-13.
- David, M., Donn, M., Garde, F., & Lenoir, A. (2011). Assessment of the thermal and visual efficiency of solar shades. *Building and environment*, 46(7), 1489-1496. doi:<http://dx.doi.org/10.1016/j.buildenv.2011.01.022>
- Davidson, S. (2019). *Grasshopper-Algorithmic modelling for Rhino software version 0.9077*. Retrieved 4/17/2019, from <https://www.grasshopper3d.com/>.
- Deb, K. (2001). *Multi-objective optimization using evolutionary algorithms* (Vol. 16): John Wiley & Sons.
- Deb, K., Pratap, A., Agarwal, S., & Meyarivan, T. (2002). A fast and elitist multiobjective genetic algorithm: NSGA-II. *IEEE transactions on evolutionary computation*, 6(2), 182-197.
- Degertekin, S. O., Saka, M. P., & Hayalioglu, M. S. (2008). Optimal load and resistance factor design of geometrically nonlinear steel space frames via tabu search and

- genetic algorithm. *Engineering Structures*, 30(1), 197-205.
doi:<http://dx.doi.org/10.1016/j.engstruct.2007.03.014>
- Delgarm, N., Sajadi, B., Delgarm, S., & Kowsary, F. (2016). A novel approach for the simulation-based optimization of the buildings energy consumption using NSGA-II: Case study in Iran. *Energy and Buildings*, 127, 552-560.
doi:<http://dx.doi.org/10.1016/j.enbuild.2016.05.052>
- DiLaura, D., Houser, K. W., Mistrick, R. G., & Steffy, G. R. (2011). The Lighting Handbook 10th Edition: Reference and Application. *Illuminating Engineering Society of North America*, 120.
- Documentation, D. (2006). DesignBuilder User Manual, Version 1.2. UK: *DesignBuilder Software Limited*.
- Eastman, C., Teicholz, P., Sacks, R., & Liston, K. (2011). *BIM handbook: A guide to building information modeling for owners, managers, designers, engineers and contractors*: John Wiley & Sons.
- Eberhart, R., & Kennedy, J. (1995). A new optimizer using particle swarm theory. IN: *Proceedings of Micro Machine and Human Science, 1995. MHS'95., Proceedings of the Sixth International Symposium on*. p. 39-43.
- Einhorn, H. (1979). Discomfort glare: a formula to bridge differences. *Lighting Research & Technology*, 11(2), 90-94.
- Ellis, P. G., Strand, R. K., & Baumgartner, K. T. (2004). *Simulation of tubular daylighting devices and daylighting shelves in ENERGYPLUS*. Paper presented at the IBPSA-USA National Conference, Boulder, CO.

- Energy, D. (2018). Energyplus V8. 9.0 Engineering Reference. *US Department of Energy: Washington, DC, USA.*
- EPW. (2019) Energy Plus Weather (EPW). Retrieved October 01, 2019, Retrieved from <https://energyplus.net/weather>
- Fanger, P. O. (1970). Thermal comfort. Analysis and applications in environmental engineering. *Thermal comfort. Analysis and applications in environmental engineering.*
- Fanger, P. O. (1986). *Thermal environment—Human requirements* (Vol. 6).
- Feito, F., Torres, J. C., & Urena, A. (1995). Orientation, simplicity, and inclusion test for planar polygons. *Computers & Graphics, 19*(4), 595-600.
- Firlag, S., Yazdanian, M., Curcija, C., Kohler, C., Vidanovic, S., Hart, R., & Czarnecki, S. (2015). Control algorithms for dynamic windows for residential buildings. *Energy and Buildings, 109*(Supplement C), 157-173.
doi:<https://doi.org/10.1016/j.enbuild.2015.09.069>
- Fonseca, C. M., & Fleming, P. J. (1993). Genetic Algorithms for Multiobjective Optimization: Formulation Discussion and Generalization. *IN: Proceedings of ICGA. Vol. 93, p. 416-423.*
- Futrell, B. J., Ozelkan, E. C., & Brentrup, D. (2015). Bi-objective optimization of building enclosure design for thermal and lighting performance. *Building and environment, 92*(Supplement C), 591-602.
doi:<https://doi.org/10.1016/j.buildenv.2015.03.039>

- Gagge, A. P., Fobelets, A., & Berglund, L. (1986). A standard predictive Index of human reponse to thermal enviroment. *Transactions/American Society of Heating, Refrigerating and Air-Conditioning Engineers*, 92(2B), 709-731.
- Geebelen, B., van der Voorden, M., & Neuckermans, H. (2005). Fast and accurate simulation of long-term daylight availability using the radiosity method. *Lighting Research and Technology*, 37(4), 295-310.
- Ghaffarianhoseini, A., Tookey, J., Ghaffarianhoseini, A., Naismith, N., Azhar, S., Efimova, O., & Raahemifar, K. (2017). Building Information Modelling (BIM) uptake: Clear benefits, understanding its implementation, risks and challenges. *Renewable and sustainable energy reviews*, 75, 1046-1053.
doi:<https://doi.org/10.1016/j.rser.2016.11.083>
- Gharpedia. (2017) 3 Major Components of Daylight Factor. Retrieved October 27, 2017, Retrieved from <https://gharpedia.com/components-daylight-factor/>
- Gibson, T., & Krarti, M. (2015). Comparative analysis of prediction accuracy from daylighting simulation tools. *LEUKOS*, 11(2), 49-60.
- Glassner, A. S. (1989). *An introduction to ray tracing*: Elsevier.
- Glaudell, R., Garcia, R. T., & Garcia, J. B. (1965). Nelder-mead simplex method. *Computer Journal*, 7(4), 308-313.
- Glover, F. (1989). Tabu search—part I. *ORSA Journal on computing*, 1(3), 190-206.
- Glover, F. (1990). Tabu search—part II. *ORSA Journal on computing*, 2(1), 4-32.
- Goia, F. (2016). Search for the optimal window-to-wall ratio in office buildings in different European climates and the implications on total energy saving potential.

Solar energy, 132(Supplement C), 467-492.

doi:<https://doi.org/10.1016/j.solener.2016.03.031>

Goia, F., Haase, M., & Perino, M. (2013). Optimizing the configuration of a façade module for office buildings by means of integrated thermal and lighting simulations in a total energy perspective. *Applied Energy*, 108, 515-527.

doi:<http://dx.doi.org/10.1016/j.apenergy.2013.02.063>

Goldberg, D. E. (1989). *Genetic algorithms in search optimization and machine learning* (Vol. 412): Addison-wesley Reading Menlo Park.

González, J., & Fiorito, F. (2015). Daylight design of office buildings: optimisation of external solar shadings by using combined simulation methods. *Buildings*, 5(2), 560-580.

Hamad, M. (2018). *AutoCAD 2019 3D Modeling*: Mercury Learning & Information.

HDR. (n.d.). High dynamic range *High dynamic range*.

Hirsch, J. J. (2006). eQuest, The QUick Energy Simulation Tool. *DOE2. com*.

Hirsch, J. J. (2017) eQUEST, the QUick Energy Simulation Tool. Retrieved October 20, 2017, Retrieved from <http://www.doe2.com/equest/>

Hitchcock, R., & Osterhaus, W. (1993). SUPERLITE 2.0 User's Manual. *Lawrence Berkeley Laboratory, Berkeley*.

Hitchcock, R. J., & Carroll, W. L. (2003). DELight: A daylighting and electric lighting simulation engine. *International Building Performance Simulation Association, IBPSA BS*.

- Holland, J. H. (1992). *Adaptation in natural and artificial systems*. 1975. *Ann Arbor, MI: University of Michigan Press and*.
- Hooke, R., & Jeeves, T. A. (1961). "Direct Search" Solution of Numerical and Statistical Problems. *Journal of the ACM (JACM)*, 8(2), 212-229.
- Hopkinson, Longmore, J., & Petherbridge, P. (1954). An empirical formula for the computation of the indirect component of daylight factor. *Lighting Research and Technology*, 19(7 IEStrans), 201-219.
- Hopkinson, R. G. (1972). Glare from daylighting in buildings. *Applied Ergonomics*, 3(4), 206-215. doi:[http://dx.doi.org/10.1016/0003-6870\(72\)90102-0](http://dx.doi.org/10.1016/0003-6870(72)90102-0)
- Hopkinson, R. G., Petherbridge, P., & Longmore, J. (1966). *Daylighting*: Heinemann.
- Hou, D., Liu, G., Zhang, Q., Wang, L., & Dang, R. (2017). Integrated Building Envelope Design Process Combining Parametric Modelling and Multi-Objective Optimization. *Transactions of Tianjin University*, 23(2), 138-146.
- Huang, Y. J., Kruis, N., O'Keefe, M., Lyons, P., & Wong, J. (2019). Representative Layer-by-Layer Descriptions for Fenestration Systems with Specified Bulk Properties such as U-Factor and Solar Heat Gain Coefficient. *ASHRAE Transactions*, 125.
- IES, V. (2011). Version 12. Integrated environmental solutions virtual environment.
- IES, V. (2017) IES-Sustainable 3D Building Design, Architecture Software-Integrated Environmental Solutions. Retrieved October 20, 2017, Retrieved from <http://www.iesve.com/software/ve-for-architects>
- IESNA. (1993). *IESNA Lighting Handbook*, 8th edition: IESNA New York.

- IESNA, I. (2012). LM-83-12 IES Spatial Daylight Autonomy (sDA) and Annual Sunlight Exposure (ASE). *New York, NY, USA: IESNA Lighting Measurement Standard*
- ISO. (1994). International Standard ISO 7730 - Moderate thermal environments — determination of the PMV and PPD indices and specification of the conditions for thermal comfort. Switzerland
- ISO. (2005). *Ergonomics of the Thermal Environment: Analytical Determination and Interpretation of Thermal Comfort Using Calculation of the PMV and PPD Indices and Local Thermal Comfort Criteria*: International Organization for Standardization.
- Jakubiec, J. A., & Reinhart, C. F. (2012). The ‘adaptive zone’—A concept for assessing discomfort glare throughout daylight spaces. *Lighting Research & Technology*, 44(2), 149-170.
- Janak, M. (1997). Coupling building energy and lighting simulation. *IN: Proceedings of Proc. Building Simulation*. Vol. 2, p. 313-319.
- Kämpf, J. H., Wetter, M., & Robinson, D. (2010). A comparison of global optimization algorithms with standard benchmark functions and real-world applications using EnergyPlus. *Journal of Building Performance Simulation*, 3(2), 103-120.
doi:10.1080/19401490903494597
- Khoroshiltseva, M., Slanzi, D., & Poli, I. (2016). A Pareto-based multi-objective optimization algorithm to design energy-efficient shading devices. *Applied Energy*, 184, 1400-1410. doi:<http://dx.doi.org/10.1016/j.apenergy.2016.05.015>

- Kim, H. (2011) Design and Programming of Game Consoles. *Ray Tracing Problem*.
Retrieved October 27, 2017, Retrieved from
https://www.cc.gatech.edu/~hyesoon/spr11/lec_raytrace.pdf
- Kittler, R. (1967). Standardisation of outdoor conditions for the calculation of daylight factor with clear skies. *IN: Proceedings of CIE Intercessional Conference on Sunlight and Buildings*. p. 273-286.
- Kittler, R., Perez, R., & Darula, S. (1997). A new generation of sky standards. *IN: Proceedings of the 8th Lux Europa*. p. 359-373.
- Klein, S., Beckman, W., Mitchell, J., Duffie, J., Duffie, N., Freeman, T., . . . Kummer, J. (2004). TRNSYS 16–A TRaNsient system simulation program, user manual. *Solar Energy Laboratory. Madison: University of Wisconsin-Madison*.
- Klems, J. H. (1993). A new method for predicting the solar heat gain of complex fenestration systems I. Overview and Derivation of the Matrix Layer Calculation.
- Klems, J. H. (1994). New method for predicting the solar heat gain of complex fenestration systems - 2. Detailed description of the matrix layer calculation. *IN: Proceedings of ASHRAE Transactions*. Vol. 100, p. 1073-1086.
- Koti, R., & Addison, M. (2007). An Assessment of Aiding DOE-2's Simplified Daylighting Method With DaySim's Daylight Illuminances. *IN: Proceedings of PROCEEDINGS OF THE SOLAR CONFERENCE*. Vol. 2, p. 726. AMERICAN SOLAR ENERGY SOCIETY; AMERICAN INSTITUTE OF ARCHITECTS.
- KUMAR, V. (2011). *Multi-objective fuzzy optimization*. (Master), INDIAN INSTITUTE OF TECHNOLOGY, KHARAGPUR.

- Langtangen, H. P. (2006). *Python scripting for computational science* (Vol. 3): Springer.
- Law, L. s. C. (n.d.). Lambert's Cosine Law.
- LBL. (2019) Setting Rendering Options. Retrieved Sep. 26, 2019, Retrieved from https://floyd.lbl.gov/radiance/refer/Notes/rpict_options.html
- LBNL. (2017) LBNL Windows & Daylighting Software -- WINDOW. Retrieved October 02, 2017, Retrieved from <https://windows.lbl.gov/software/window/window.html>
- Lee, E. S., Dibartolomeo, D. L., & Selkowitz, S. E. (1998). Thermal and daylighting performance of an automated venetian blind and lighting system in a full-scale private office. *Energy and Buildings*, 29(1), 47-63.
- Li, Q., & Haberl, J. (2020). Research on Guidelines for Window Design Strategies in High Performance Office Buildings. *IN: Proceedings of 2020 Building Performance Analysis Conference & SimBuild*.
- Lin, Y.-H., Tsai, K.-T., Lin, M.-D., & Yang, M.-D. (2016). Design optimization of office building envelope configurations for energy conservation. *Applied Energy*, 171, 336-346. doi:<http://dx.doi.org/10.1016/j.apenergy.2016.03.018>
- Littlefair, P. J. (1990). Review Paper: Innovative daylighting: Review of systems and evaluation methods. *Lighting Research and Technology*, 22(1), 1-17.
- Lobaccaro, G., Fiorito, F., Masera, G., & Prasad, D. (2012). Urban solar district: a case study of geometric optimization of solar façades for a residential building in Milan. *IN: Proceedings of Proceedings of the AuSES Solar 2012 Conference, Melbourne, Australia*. Vol. 67.

- Lua. (n.d.). Lua (programming language) *Lua (programming language)*.
- Maamari, F., Fontoynt, M., & Mitanchey, R. (2002). Analytical References to Test Lighting Software Programs-Application to Lightscape 3.2. *submitted to Lighting Research and Technology*.
- Machairas, V., Tsangrassoulis, A., & Axarli, K. (2014). Algorithms for optimization of building design: A review. *Renewable and sustainable energy reviews*, *31*, 101-112. doi:<http://dx.doi.org/10.1016/j.rser.2013.11.036>
- Mangkuto, R. A., Rohmah, M., & Asri, A. D. (2016). Design optimisation for window size, orientation, and wall reflectance with regard to various daylight metrics and lighting energy demand: A case study of buildings in the tropics. *Applied Energy*, *164*(Supplement C), 211-219. doi:<https://doi.org/10.1016/j.apenergy.2015.11.046>
- Manzan, M. (2014). Genetic optimization of external fixed shading devices. *Energy and Buildings*, *72*, 431-440. doi:<http://dx.doi.org/10.1016/j.enbuild.2014.01.007>
- Mardaljevic, J. (1999). *Daylight simulation: validation, sky models and daylight coefficients*: De Montfort University.
- Mardaljevic, J. (2000). Simulation of annual daylighting profiles for internal illuminance. *International Journal of Lighting Research and Technology*, *32*(3), 111-118.
- Marsh, A. (2003). ECOTECT Tutorials. *Square One research Pty Ltd. Traducción propia*.
- Marsh, A. J. (1997). *Performance analysis and conceptual design*. (Ph.D. Dissertation), University of Western Australia, Perth, Australia.

- MATLAB. (2019) MATLAB - MathWorks - MATLAB & Simulink. Retrieved March 21, 2019, Retrieved from <https://www.mathworks.com/products/matlab.html>
- McCartney, K. J., & Fergus Nicol, J. (2002). Developing an adaptive control algorithm for Europe. *Energy and Buildings*, 34(6), 623-635.
doi:[http://dx.doi.org/10.1016/S0378-7788\(02\)00013-0](http://dx.doi.org/10.1016/S0378-7788(02)00013-0)
- McNeil, A., Jonsson, C. J., Appelfeld, D., Ward, G., & Lee, E. S. (2013). A validation of a ray-tracing tool used to generate bi-directional scattering distribution functions for complex fenestration systems. *Solar energy*, 98, 404-414.
doi:<http://dx.doi.org/10.1016/j.solener.2013.09.032>
- McNeil, A., & Lee, E. (2013). A validation of the Radiance three-phase simulation method for modelling annual daylight performance of optically complex fenestration systems. *Journal of Building Performance Simulation*, 6(1), 24-37.
- McNeil, R. (1998). Rhinoceros. *Seattle, WA: Rhino3d. com.*
- Michele, G. d., Oberegger, U., & Baglivo, L. (2015). Coupling dynamic energy and daylighting simulations for complex fenestration systems. *Pre-prints of BSA 2015-Building Simulation Application.*
- Mistrick, R. G., & An-Seop, C. (1999). A Comparison of the Visual Comfort Probability and Unified Glare Rating Systems, 94.
- Mitchell, R., Kohler, C., Klems, J., Rubin, M., Arasteh, D., Huizenga, C., . . . Curcija, D. (2008). Window 6.2/Therm 6.2 Research Version User Manual. Lawrence Berkeley National Laboratory, LBNL-941, Berkeley, CA 94720.

- Molina, G., Bustamante, W., Rao, J., Fazio, P., & Vera, S. (2015). Evaluation of radiance's genBSDF capability to assess solar bidirectional properties of complex fenestration systems. *Journal of Building Performance Simulation*, 8(4), 216-225. doi:10.1080/19401493.2014.912355
- Moon, P., & Spencer, D. E. (1942). Illumination from a non-uniform sky. *Illuminating Engineering*, 37(10), 707-726.
- Moossavi, S. M. (2014). Adaptive Thermal Comfort Model. *GREENARCS – Green Architecture and Arts Online Magazine (English)*. Retrieved from <http://greenarcs.com/?p=1291>
- Motamedi, S., & Liedl, P. (2017). Integrative algorithm to optimize skylights considering fully impacts of daylight on energy. *Energy and Buildings*, 138, 655-665. doi:<http://dx.doi.org/10.1016/j.enbuild.2016.12.045>
- Muhaisen, A. S., & Gadi, M. B. (2006). Effect of courtyard proportions on solar heat gain and energy requirement in the temperate climate of Rome. *Building and environment*, 41(3), 245-253. doi:<https://doi.org/10.1016/j.buildenv.2005.01.031>
- Murta, A. (2017) A general polygon clipping library. Retrieved October 20, 2017, Retrieved from <http://www.cs.man.ac.uk/~toby/gpc/#Features>
- Nabil, A., & Mardaljevic, J. (2005). Useful daylight illuminance: a new paradigm for assessing daylight in buildings. *Lighting Research and Technology*, 37(1), 41-57.
- Nash, S. G., & Sofer, A. (1996). Linear and nonlinear programming.

- Nazzal, A. A. (2001). A new daylight glare evaluation method: Introduction of the monitoring protocol and calculation method. *Energy and Buildings*, 33(3), 257-265.
- Nguyen, A.-T., Reiter, S., & Rigo, P. (2014). A review on simulation-based optimization methods applied to building performance analysis. *Applied Energy*, 113, 1043-1058. doi:<http://dx.doi.org/10.1016/j.apenergy.2013.08.061>
- OpenStudio. (2017) Open Studio Homepage. Retrieved October 16, 2017, Retrieved from <https://www.openstudio.net/>
- Optimization, S. (n.d.). Stochastic Optimization *Stochastic Optimization*.
- Oseland, N. (1998). Adaptive thermal comfort models. *Building Services Journal*, 20(12), 41-42.
- Ouarghi, R., & Krarti, M. (2006). Building Shape Optimization Using Neural Network and Genetic Algorithm Approach. *ASHRAE Transactions*, 112(1).
- Pellegrino, A., Cammarano, S., Lo Verso, V. R. M., & Corrado, V. (2017). Impact of daylighting on total energy use in offices of varying architectural features in Italy: Results from a parametric study. *Building and environment*, 113(Supplement C), 151-162. doi:<https://doi.org/10.1016/j.buildenv.2016.09.012>
- Perez, R., Seals, R., & Michalsky, J. (1993). All-weather model for sky luminance distribution—preliminary configuration and validation. *Solar energy*, 50(3), 235-245.
- Poles, S., Vassileva, M., & Sasaki, D. (2008). Multiobjective optimization software. *Multiobjective optimization*, 329-348.

- Rapone, G., & Saro, O. (2012). Optimisation of curtain wall façades for office buildings by means of PSO algorithm. *Energy and Buildings*, 45, 189-196.
doi:<http://dx.doi.org/10.1016/j.enbuild.2011.11.003>
- Reflectance, L. (n.d.). Lambertian Reflectance *Lambertian reflectance*.
- Reilly, M., Winkelmann, F., Arasteh, D., & Carroll, W. (1995). Modeling windows in DOE-2.1 E. *Energy and Buildings*, 22(1), 59-66.
- Reinhart, C. (2005). Tutorial on the use of Daysim/Radiance simulations for sustainable design. *NRC report, Ottawa, Canada*.
- Reinhart, C. (2010). DAYSIM 3.1 e. *Institute for Research in Construction, Ottawa, Canada*.
- Reinhart, C., Lagios, K., Niemasz, J., & Jakubiec, A. (2011) DIVA for Rhino Version 2.0. Retrieved June 10, 2015, Retrieved from
<http://diva4rhino.com/forum/categories/diva-rhino-version-2-0/listForCategory>
- Reinhart, C., & Stein, R. (2014). *Daylighting Handbook: Fundamentals, Designing with the Sun*.
- Reinhart, C. F. (2017) Daysim. *Institute for Research in Construction, National Research in Construction*. Retrieved June 20, 2017, Retrieved from
<http://www.daysim.com>
- Reinhart, C. F., & Herkel, S. (2000). The simulation of annual daylight illuminance distributions—a state-of-the-art comparison of six RADIANCE-based methods. *Energy and Buildings*, 32(2), 167-187.

- Reinhart, C. F., Mardaljevic, J., & Rogers, Z. (2006). Dynamic Daylight Performance Metrics for Sustainable Building Design. *LEUKOS*, 3(1), 7-31.
doi:10.1582/LEUKOS.2006.03.01.001
- Reinhart, C. F., & Walkenhorst, O. (2001). Validation of dynamic RADIANCE-based daylight simulations for a test office with external blinds. *Energy and Buildings*, 33(7), 683-697. doi:[http://dx.doi.org/10.1016/S0378-7788\(01\)00058-5](http://dx.doi.org/10.1016/S0378-7788(01)00058-5)
- Rossum, G. (1995). Python reference manual.
- Roudsari, M. (2016). Ladybug+ Honeybee. *Grasshopper Algorithmic*.
- Rutten, D. (2007). Grasshopper & Galapagos. *Seattle: Robert McNeel & Associates*.
- Rutten, D. (2010). Grasshopper: Generative Modeling for Rhino. Version 0.7. 0045. *Computer Software. Robert McNeel and Associates. Retrieved from www.grasshopper3d.com.*
- Rutten, D. (2013). Galapagos: On the logic and limitations of generic solvers. *Architectural Design*, 83(2), 132-135.
- Rutten, D. (2014). *Grasshopper-Algorithmic modelling for Rhino software version 0.9077*. Retrieved 5/12/2014, from <http://www.grasshopper3d.com>.
- Rutten, D. (2017) Galapagos - Grasshopper. Retrieved September 22, 2017, Retrieved from <http://www.grasshopper3d.com/group/galapagos>
- SAS. (2019). *JMP Statistical Discovery from SAS Institute Inc*. Retrieved 11/26/2019, from https://www.jmp.com/en_us/home.html.

- Saxena, M., Ward, G., Perry, T., Heschong, L., & Higa, R. (2010). Dynamic Radiance—Predicting annual daylighting with variable fenestration optics using BSDFs. *Proceedings of Simbuild*, 11-13.
- Selkowitz, S., Kim, J. J., Navvab, M., & Winkelmann, F. (1982). The DOE-2 and Superlite daylighting programs. *IN: Proceedings of Proceedings of the 7th National Passive Solar Conference*.
- Shan, R. (2014). Optimization for Heating, Cooling and Lighting Load in Building Façade Design. *Energy Procedia*, 57, 1716-1725.
doi:<http://dx.doi.org/10.1016/j.egypro.2014.10.142>
- Shen, H., & Tzempelikos, A. (2017). Daylight-linked synchronized shading operation using simplified model-based control. *Energy and Buildings*, 145(Supplement C), 200-212. doi:<https://doi.org/10.1016/j.enbuild.2017.04.021>
- Shi, Y. (2001). Particle swarm optimization: developments, applications and resources. *IN: Proceedings of evolutionary computation, 2001. Proceedings of the 2001 Congress on*. Vol. 1, p. 81-86.
- Skarning, G. C. J., Hviid, C. A., & Svendsen, S. (2017). The effect of dynamic solar shading on energy, daylighting and thermal comfort in a nearly zero-energy loft room in Rome and Copenhagen. *Energy and Buildings*, 135(Supplement C), 302-311. doi:<https://doi.org/10.1016/j.enbuild.2016.11.053>
- Solemma, L. (2017) DIVA For Rhino User Guide: Advanced Shading (Climate-Based Metrics). Retrieved October 03, 2017, Retrieved from <http://diva4rhino.com/user-guide/rhino/advanced-shading>

- Solemma, L. (n.d.-a) DIVA for Rhino 4.0. Retrieved September 06, 2017, Retrieved from <http://diva4rhino.com/>
- Solemma, L. (n.d.-b) DIVA Grasshopper Video Tutorials. Retrieved December 03, 2016, Retrieved from http://solemma.net/grasshopper_tutorials.html
- Sullivan, R., Arasteh, D., & Papamichael, K. (1987). An indices approach for evaluating the performance of fenestration systems in nonresidential buildings.
- Sullivan, R., Lee, E., & Selkowitz, S. (1992). A method of optimizing solar control and daylighting performance in commercial office buildings.
- System, E. M. (2016). Energy Management System *Energy Management System*.
- Szerman, M. (1993). Superlink, a computer tool to evaluate the impact of daylight-controlled lighting system onto the overall energetic behaviour of buildings. *IN: Proceedings of Proceedings of Right Light*. Vol. 2, p. 673-685.
- Temkin, A. (2009). Open studio. *Gabriel Orozco*, 11-21.
- Tindale, A. (2005). Designbuilder software. *Stroud, Gloucestershire, Design-Builder Software Ltd*.
- Tregenza, P., & Waters, I. (1983). Daylight coefficients. *Lighting Research and Technology*, 15(2), 65-71.
- TRNSYS. (2000). Transient System Simulation Program. *Solar Energy Laboratory. Madison: University of Wisconsin-Madison*.
- TRNSYS. (2017) TRNSYS 18: A Transient System Simulation Program Version 18. Retrieved October 12, 2017, Retrieved from <http://sel.me.wisc.edu/trnsys/>

- Trotter, A. P. (1911). *Illumination: its distribution and measurement*: Macmillan and Company, limited.
- Trubiano, F., Roudsari, M., & Ozkan, A. (2013). Building simulation and evolutionary optimization in the conceptual design of a high-performance office building. *IN: Proceedings of Proceedings of the 13th Conference of the International Building Performance Simulation Association, Chambéry, France*. Vol. 2528, p. 13061314.
- Tsangrassoulis, A., & Bourdakis, V. (2003). Comparison of radiosity and ray-tracing techniques with a practical design procedure for the prediction of daylight levels in atria. *Renewable Energy*, 28(13), 2157-2162.
- Tsangrassoulis, A., & Santamouris, M. (1997). Daylight modelling with Passport-Light. *IN: Proceedings of Fifth International IBPSA Conference*. p. 73-78.
- Tuhus-Dubrow, D., & Krarti, M. (2009). Comparative Analysis of Optimization Approaches to Design Building Envelope for Residential Buildings. *ASHRAE Transactions*, 115(2).
- Tuhus-Dubrow, D., & Krarti, M. (2010). Genetic-algorithm based approach to optimize building envelope design for residential buildings. *Building and environment*, 45(7), 1574-1581. doi:<http://dx.doi.org/10.1016/j.buildenv.2010.01.005>
- UNEP. (2016) Why Buildings. Retrieved Retrieved from <http://www.unep.org/sbci/AboutSBCI/Background.asp>
- USGBC, L. (2014). Reference Guide for Building Design and Construction (v4), US Green Building Council, 2014.

- VELUX. (2019) Daylight Visualizer. Retrieved April 24, 2019, Retrieved from <https://www.velux.com/article/2016/daylight-visualizer>
- Vera, S., Bustamante, W., Molina, G., & Uribe, D. (2016). A flexible and time-efficient schedule-based communication tool for integrated lighting and thermal simulations of spaces with controlled artificial lighting and complex fenestration systems. *Journal of Building Performance Simulation*, 9(4), 382-396.
doi:10.1080/19401493.2015.1062556
- Vera, S., Uribe, D., Bustamante, W., & Molina, G. (2017). Optimization of a fixed exterior complex fenestration system considering visual comfort and energy performance criteria. *Building and environment*, 113, 163-174.
doi:<http://dx.doi.org/10.1016/j.buildenv.2016.07.027>
- Versage, R., Melo, A. P., & Lamberts, R. (2010). Impact of different daylighting simulation results on the prediction of total energy consumption. *IBPSA-USA Journal*, 4(1), 1-7.
- Vierlinger, R. (n.d.) Octopus| Grasshopper. Retrieved December 06, 2019, Retrieved from <https://www.grasshopper3d.com/group/octopus>
- Ward, G. (1996). The RADIANCE 3.0 Synthetic Imaging System. *Lighting Systems Research Group, Lawrence Berkeley Laboratory*.
- Ward, G. (2019) rtrace - trace rays in RADIANCE scene. Retrieved Sep. 26, 2019, Retrieved from <https://floyd.lbl.gov/radiance/rtrace.1.html>

- Ward, G., Mistrick, R., Lee, E. S., McNeil, A., & Jonsson, J. (2011). Simulating the daylight performance of complex fenestration systems using bidirectional scattering distribution functions within radiance. *LEUKOS*, 7(4), 241-261.
- Ward, G. J., & Rubinstein, F. M. (1988). A new technique for computer simulation of illuminated spaces. *Journal of the Illuminating Engineering Society*, 17(1), 80-91.
- Wetter, M. (2009). GenOpt: Generic optimization program, user manual version 3.0. 0 Lawrence Berkeley National Laboratory.
- Wetter, M., & Wright, J. (2004). A comparison of deterministic and probabilistic optimization algorithms for nonsmooth simulation-based optimization. *Building and environment*, 39(8), 989-999.
doi:<http://dx.doi.org/10.1016/j.buildenv.2004.01.022>
- Wienold, J. (2004). Evalglare—A new RADIANCE-based tool to evaluate daylight glare in office spaces. *IN: Proceedings of 3rd International RADIANCE workshop 2004*.
- Wienold, J., & Christoffersen, J. (2006). Evaluation methods and development of a new glare prediction model for daylight environments with the use of CCD cameras. *Energy and Buildings*, 38(7), 743-757.
- Wilcox, S., & Marion, W. (2008). *Users manual for TMY3 data sets*: National Renewable Energy Laboratory Golden, CO.
- Winkelmann, F. (1998). Underground surfaces: How to get a better underground surface heat transfer calculation in DOE-2.1 e. *DOE-2 user news*, 19(1), 6-13.

- Winkelmann, F., Birdsall, B., Buhl, W., Ellington, K., Erdem, A., Hirsch, J., & Gates, S. (1993a). *DOE-2 supplement: version 2.1 E*. (No. LBL-34947). Lawrence Berkeley Lab., CA (United States); Hirsch (James J.) and Associates, Camarillo, CA (United States).
- Winkelmann, F., Birdsall, B., Buhl, W., Ellington, K., Erdem, A., Hirsch, J., & Gates, S. (1993b). *DOE-2, BDL summary. Version 2.1 E*. (No. LBL-34946). Lawrence Berkeley Lab., CA (United States).
- Winkelmann, F. C. (1983). *Daylighting calculation in DOE-2*. (No. LBL-11353)). Ernest Orlando Lawrence Berkeley National Laboratory, Berkeley, CA (US).
- Winkelmann, F. C., & Selkowitz, S. (1985). Daylighting simulation in the DOE-2 building energy analysis program. *Energy and Buildings*, 8(4), 271-286.
- Yang, L., Yan, H., & Lam, J. C. (2014). Thermal comfort and building energy consumption implications – A review. *Applied Energy*, 115, 164-173.
doi:<http://dx.doi.org/10.1016/j.apenergy.2013.10.062>
- Yoon, Y., Moeck, M., Mistrick, R., & Bahnfleth, W. (2008). How much energy do different toplighting strategies save? *Journal of Architectural Engineering*, 14(4), 101-110.
- York, D. A., & Cappiello, C. C. (1981). *DOE-2 engineers manual (Version 2. 1A)*. Lawrence Berkeley Lab., CA (USA); Los Alamos National Lab., NM (USA).
- Yun, G., Yoon, K. C., & Kim, K. S. (2014). The influence of shading control strategies on the visual comfort and energy demand of office buildings. *Energy and Buildings*, 84, 70-85. doi:<http://dx.doi.org/10.1016/j.enbuild.2014.07.040>

APPENDIX A

DAYLIGHTING AND THERMAL SIMULATION RESULTS

Table A-1: The Simulation Results of Different Model Conditions

Run	Room Size	Shades	O r i e n.	Window Position	WFR	FVR	sDA High	sDA Custom	ASE	Light Energy High	Light Energy Custom
1	small	NO	S	Top	20%	0.2	100	100	60	86.6	94.3
2	small	NO	S	Top	20%	0.9	100	100	60	78.8	89.5
3	small	NO	S	Centered	3%	0.2	5.3	5.3	12	545.1	584.2
4	small	NO	S	Centered	5%	0.2	16	14	22.7	433.7	456.3
5	small	NO	S	Centered	5%	0.5	24.7	19.3	22.7	358.4	439.8
6	small	NO	S	Centered	5%	0.9	34.7	24.7	22.7	297.9	385.8
7	small	NO	S	Centered	10%	0.2	42.7	38.7	32	281.5	337.1
8	small	NO	S	Centered	10%	0.5	53.3	44.7	32	228.4	276.6
9	small	NO	S	Centered	10%	0.9	66.7	53.3	32	165.9	233.2
10	small	NO	S	Centered	16%	0.2	63.3	54.7	40	178.5	224.6
11	small	NO	S	Centered	23%	0.2	100	84.7	46	107.5	135.5
12	small	NO	S	Centered	31%	0.2	100	100	46.7	90.5	94
13	small	NO	S	Centered	20%	0.2	100	66.7	40	131.7	167.4
14	small	NO	S	Top	20%	0.2	100	100	58	83.4	108.4
15	small	NO	S	Down	20%	0.2	54.7	48	26.7	217.5	256
16	small	NO	S	Down	20%	0.5	100	62.5	26.7	148.4	188.9
17	small	NO	S	Mix	20%	0.2	76.7	60	42	139.7	187.6
18	small	NO	S	Mix	20%	0.2	100	79.3	56.7	101.4	126.1
19	small	NO	S	Mix	20%	0.2	100	71.3	53.3	104.2	149.1
20	small	NO	N	Top	25%	0.9	100	81.3	0	96	128.5
21	small	NO	N	Centered	3%	0.2	2.5	2.5	0	603.5	631
22	small	NO	N	Centered	5%	0.2	10	5	0	518.9	551.3
23	small	NO	N	Centered	10%	0.2	15	15	0	431	456.6
24	small	NO	N	Centered	16%	0.2	37.5	35	0	356	413.4
25	small	NO	N	Centered	23%	0.2	50	35	0	230.9	392.7
26	small	NO	N	Centered	31%	0.2	87.5	62.5	0	134.3	187.5
27	small	NO	N	Centered	27%	0.2	62.5	57.5	0	175.5	221.4
28	small	NO	N	Centered	37%	0.2	100	100	0	99.4	123.3
29	small	NO	N	Centered	20%	0.2	46.7	46.7	0	199.9	327.5
30	small	NO	N	Centered	20%	0.5	50	50	0	219.8	303.6
31	small	NO	N	Centered	20%	0.9	67.5	50	0	161.1	255.5
32	small	NO	N	Top	20%	0.2	59.3	49.3	0	168.5	196.6
33	small	NO	N	Down	20%	0.2	33.3	30.7	0	398.1	414.8

Table A-1: The Simulation Results of Different Model Conditions (Continued)

Run	Room Size	Shades	O r i e n.	Window Position	WFR	FVR	sDA High	sDA Custom	ASE	Light Energy High	Light Energy Custom
34	small	NO	N	Mix	20%	0.2	38.7	32.7	0	325.7	373.4
35	small	NO	N	Mix	20%	0.5	46.7	36.7	0	263.4	342.3
36	small	NO	N	Mix	20%	0.9	60	40	0	193.6	317.5
37	small	NO	N	Mix	20%	0.2	43.3	34.7	0	215.8	292.3
38	small	NO	N	Mix	20%	0.2	43.3	36	0	263.4	335.6
39	small	NO	E	Centered	20%	0.2	54	50.7	35.3	192.1	214.7
40	small	NO	E	Centered	20%	0.5	66	53.3	35.3	142.3	190.8
41	small	NO	E	Top	20%	0.2	85	67.5	37.3	120.3	129.7
42	small	NO	E	Top	20%	0.5	99.3	71.3	37.3	101.8	106.2
43	small	NO	E	Down	20%	0.2	37.5	37.5	27.5	258.6	289.2
44	small	NO	E	Down	20%	0.5	48	40	27.5	216.4	241.8
45	small	NO	E	Down	20%	0.9	62.5	45	27.5	146.7	220.1
46	small	NO	E	Mix	20%	0.2	50	37.5	34	214	245.2
47	small	NO	E	Mix	20%	0.5	54.7	44	34	175.9	233.5
48	small	NO	E	Mix	20%	0.9	89.3	60	34	137.5	205.6
49	small	NO	E	Mix	20%	0.2	56.7	48.7	39.3	150	186.6
50	small	NO	E	Mix	20%	0.5	72	53.3	39.3	120	168.6
51	small	NO	E	Mix	20%	0.2	56	47.3	36.7	166.6	200.4
52	small	NO	E	Mix	20%	0.5	65.3	50	36.7	135.4	196.1
53	small	NO	E	Centered	3%	0.2	2.5	2.5	7.5	450.4	492.2
54	small	NO	E	Centered	10%	0.2	27.5	22.5	27.5	303.2	331.6
55	small	NO	E	Centered	23%	0.2	62.5	50	37.5	163.1	180.1
56	small	NO	W	Centered	20%	0.2	63.3	57.3	44	177	213
57	small	NO	W	Centered	20%	0.5	100	62.5	44	131.5	178.5
58	small	NO	W	Centered	20%	0.9	100	75	44	95.3	147.4
59	small	NO	W	Top	20%	0.2	99.3	82	52.7	108.9	127.6
60	small	NO	W	Down	20%	0.2	40	37.5	37.5	265.6	306.1
61	small	NO	W	Mix	20%	0.2	55	50	47.5	208.9	254.1
62	small	NO	W	Mix	20%	0.5	72.5	50	47.5	159.1	224.8
63	small	NO	W	Mix	20%	0.9	100	62.5	47.5	122.4	201.7
64	small	NO	W	Mix	20%	0.2	77.5	60	45	143	165.6
65	small	NO	W	Mix	20%	0.2	72.5	60	55	147.6	190.4
66	small	NO	W	Centered	5%	0.2	15	15	20	452.5	506.9
67	small	NO	W	Centered	16%	0.2	50	50	37.5	218.7	257.9
68	small	NO	W	Centered	23%	0.2	80	62.5	47.5	144.6	179.6

Table A-1: The Simulation Results of Different Model Conditions (Continued)

Run	Room Size	Shades	O r i e n.	Window Position	WFR	FVR	sDA High	sDA Custom	ASE	Light Energy High	Light Energy Custom
69	small	White Shades	S	Top	24.8	0.2	100	85.3	1.3	88.7	128.3
70	small	White Shades	S	Top	21	0.2	100	60	6.7	106.1	164.2
71	small	White Shades	S	Top	21	0.5	100	60	6.7	103.6	150.9
72	small	White Shades	S	Top	21	0.9	100	73.3	6.7	102.4	143.8
73	small	White Shades	S	Centered	3%	0.2	1.3	1.3	4.7	587.8	613.6
74	small	White Shades	S	Centered	5%	0.2	5.3	4.7	5.3	498	532
75	small	White Shades	S	Centered	10%	0.2	34	23.3	8	327.8	407.5
76	small	White Shades	S	Centered	10%	0.5	36.7	24.7	8	285.3	378.2
77	small	White Shades	S	Centered	10%	0.9	44	25.3	8	241.9	359
78	small	White Shades	S	Centered	16%	0.2	58.7	44.7	8	203.8	275.6
79	small	White Shades	S	Centered	23%	0.2	98.7	61.3	8.7	121.2	187
80	small	Dark Shades	S	Centered	23%	0.2	54	42.7	8.7	199.2	261.3
81	small	White Shades	S	Centered	31%	0.2	100	100	9.3	89.3	121.8
82	small	White Shades	S	Centered	20%	0.2	72.7	58	9.3	143.6	209.4
83	small	White Shades	S	Top	20%	0.2	96.7	58.7	9.3	122.9	152.7
84	small	White Shades	S	Down	20%	0.2	60	46.7	9.3	196.7	286.3
85	small	White Shades	S	Mix	20%	0.2	72.7	53.3	6.7	140.8	218.9
86	small	Dark Shades	S	Mix	20%	0.2	43.3	27.3	6.7	240.6	333.4
87	small	White Shades	S	Mix	20%	0.2	82.7	56.7	4.7	132.2	180
88	small	White Shades	S	Mix	20%	0.2	74	50.7	7.3	139.4	210.4
89	small	White Shades	E	Centered	20%	0.9	52.7	29.3	6.7	165.4	237
90	small	White Shades	E	Centered	35%	0.9	100	78.7	4.7	100.7	153
91	small	White Shades	E	Centered	20%	0.5	42.7	26.7	6.7	200.4	252.7
92	small	White Shades	E	Centered	20%	0.2	37.3	23.3	6.7	211.3	255.8
93	small	Dark Shades	E	Centered	20%	0.2	14	6	6.7	275.5	329.5
94	small	White Shades	E	Centered	16%	0.2	31.3	19.3	5.3	254.8	287.5

Table A-1: The Simulation Results of Different Model Conditions (Continued)

Run	Room Size	Shades	O r i e n.	Window Position	WFR	FVR	sDA High	sDA Custom	ASE	Light Energy High	Light Energy Custom
95	small	White Shades	E	Centered	16%	0.5	35.3	18	5.3	224.2	284
96	small	White Shades	E	Centered	16%	0.9	42	23.3	5.3	198.5	270.2
97	small	White Shades	E	Top	16%	0.2	22	10	13.3	205.5	239.8
98	small	White Shades	E	Down	16%	0.2	14.7	10.7	8	283.7	344
99	small	Dark Shades	E	Down	16%	0.2	3.3	2.7	8	363.1	392.7
100	small	White Shades	E	Centered	10%	0.2	13.3	9.3	5.3	320.8	352.3
101	small	White Shades	W	Centered	20%	0.2	47.3	32	7.3	225.3	286.8
102	small	White Shades	W	Centered	30%	0.9	100	70.7	8.7	79.7	151.1
103	small	White Shades	W	Centered	20%	0.5	54.7	34.7	7.3	195.9	257
104	small	White Shades	W	Centered	20%	0.9	64.7	36	7.3	171.9	255.5
105	small	White Shades	W	Centered	16%	0.2	40	26.7	6.7	256.6	313.8
106	small	White Shades	W	Centered	16%	0.5	40	26.7	6.7	243.3	310.1
107	small	White Shades	W	Centered	16%	0.9	60	33.3	6.7	209.8	291.4
108	small	White Shades	W	Centered	10%	0.2	15.3	11.3	3.3	350.6	409.1
109	small	White Shades	W	Top	10%	0.2	3.3	0.7	10	285.2	353.5
110	small	White Shades	W	Top	16%	0.2	20	6.7	0	226.9	277.9
112	small	White Shades	W	Down	16%	0.2	20	6.7	13.3	343.7	432.7
113	small	Dark Shades	W	Down	16%	0.2	6.7	6.7	13.3	413.2	472.2
114	Medium	NO	S	Centered	10%	0.2	42	35.3	24.4	925.8	1035.4
115	Medium	NO	S	Centered	10%	0.5	61.3	52.1	24.4	715.4	752.6
116	Medium	NO	S	Centered	10%	0.9	95.8	66.4	24.4	516.3	684
117	Medium	NO	S	Down	10%	0.2	25.2	23.5	16.8	1387.1	1556
118	Medium	NO	S	Top	10%	0.2	52.9	48.7	37.8	721.6	734
119	Medium	NO	S	Centered	15%	0.2	73.1	66.4	34.5	596	590.9
120	Medium	NO	S	Centered	20%	0.2	100	98.3	46.2	500.5	521.9
121	Medium	NO	S	Down	15%	0.2	52.9	41.2	21.8	846	965.8
122	Medium	NO	S	Top	15%	0.2	89.1	75.6	48.7	472.9	518.6
123	Medium	NO	S	Down	15%	0.5	96.6	67.2	21.8	570.3	729.1

Table A-1: The Simulation Results of Different Model Conditions (Continued)

Run	Room Size	Shades	O r i e n.	Window Position	WFR	FVR	sDA High	sDA Custom	ASE	Light Energy High	Light Energy Custom
124	Medium	NO	S	Down	15%	0.9	100	99.2	21.8	486.4	582.2
125	Medium	NO	N	Centered	10%	0.9	44.5	24.4	0	803.7	1124.2
126	Medium	NO	N	Centered	10%	0.5	23.5	21	0	1282.7	1461.2
127	Medium	NO	N	Centered	10%	0.2	20.2	16.8	0	1673	1859.3
128	Medium	NO	N	Centered	15%	0.9	80.7	59.7	0	551.2	666.2
129	Medium	NO	N	Centered	15%	0.5	59.7	51.3	0	645.2	816.5
130	Medium	NO	N	Centered	15%	0.2	42.9	36.1	0	799.6	965.2
131	Medium	NO	N	Centered	20%	0.9	100	98.3	0	441.7	526
132	Medium	NO	N	Top	15%	0.2	59.7	54.6	0	637.3	675.1
133	Medium	NO	N	Top	15%	0.5	68.9	59.7	0	533.8	568.9
134	Medium	NO	N	Top	15%	0.9	89.9	68.1	0	538.6	558
135	Medium	NO	N	Down	15%	0.9	67.2	42	0	684.1	971.3
136	Medium	NO	E	Centered	10%	0.2	23.5	23.5	23.5	1187.2	1221.5
137	Medium	NO	E	Centered	10%	0.5	37.8	27.7	23.5	894	927.5
138	Medium	NO	E	Centered	10%	0.9	52.9	37	23.5	578.8	814.4
139	Medium	NO	E	Centered	15%	0.2	55.5	49.6	35.3	713.3	714.3
140	Medium	NO	E	Centered	20%	0.2	95.8	82.4	45.4	531.6	571.7
141	Medium	NO	E	Down	15%	0.2	26.1	26.1	26.1	1138.5	1429.3
142	Medium	NO	E	Top	15%	0.2	67.2	62.2	42.9	566.8	523.9
143	Medium	NO	E	Centered	15%	0.5	68.9	58	35.3	535.2	586
144	Medium	NO	E	Centered	15%	0.9	93.3	68.9	35.3	511.7	568
145	Medium	NO	W	Centered	10%	0.2	31.9	28.6	30.3	1048.6	1296.4
146	Medium	NO	W	Centered	10%	0.5	46.2	36.1	30.3	787.1	937.8
147	Medium	NO	W	Centered	10%	0.9	60.5	47.1	30.3	578.7	760.7
148	Medium	NO	W	Centered	15%	0.2	62.2	55.5	42.9	616.5	597.4
149	Medium	NO	W	Centered	15%	0.5	79	67.2	42.9	456.6	546
150	Medium	NO	W	Centered	15%	0.9	96.6	78.2	42.9	432.4	466.7
151	Medium	NO	W	Centered	20%	0.2	98.3	92.4	56.3	447.4	537.2
152	Medium	NO	W	Down	15%	0.2	36.1	31.1	32.8	1023.3	1132.5
153	Medium	NO	W	Top	15%	0.2	71.4	67.2	55.5	476.7	433.5
154	Medium	White Shades	S	Centered	15%	0.2	61	47.1	5.9	661.8	831.5
155	Medium	White Shades	S	Centered	15%	0.5	71.4	51.3	5.9	618.8	841.2
156	Medium	White Shades	S	Centered	15%	0.9	89.9	55.5	5.9	619.2	738.4

Table A-1: The Simulation Results of Different Model Conditions (Continued)

Run	Room Size	Shades	O r i e n.	Window Position	WFR	FVR	sDA High	sDA Custom	ASE	Light Energy High	Light Energy Custom
157	Medium	White Shades	S	Centered	20%	0.2	98.3	78.2	8.4	618.6	695.4
158	Medium	Dark Shades	S	Centered	20%	0.2	68.1	35.3	8.4	930	1108.4
159	Medium	White Shades	S	Centered	10%	0.2	31.1	21	3.4	1039.5	1295
160	Medium	White Shades	S	Centered	10%	0.5	41.2	21.8	3.4	874	1209
161	Medium	White Shades	S	Centered	10%	0.9	50.4	25.2	3.4	754.2	1191.8
162	Medium	White Shades	S	Top	10%	0.2	41.2	23.5	0	887.4	1283
163	Medium	White Shades	S	Down	10%	0.2	20.2	15.1	0	1417.9	1794.8
164	Medium	White Shades	E	Centered	15%	0.2	40.2	24.4	8.4	868.6	1018
165	Medium	White Shades	E	Centered	15%	0.5	53.8	31.9	8.4	731.4	976
166	Medium	White Shades	E	Centered	15%	0.9	63	36.1	8.4	659.2	878.2
167	Medium	White Shades	E	Top	15%	0.2	39.5	13.4	0	864.3	1129.4
168	Medium	White Shades	E	Down	15%	0.2	22.7	17.6	16.8	1226.8	1488.4
169	Medium	White Shades	E	Centered	20%	0.2	68.1	42	0	778	1080.2
170	Medium	Dark Shades	E	Centered	20%	0.2	18.5	3.4	0	1077.5	1104
171	Medium	White Shades	E	Centered	20%	0.5	81.5	51.3	0	692.7	860.8
172	Medium	White Shades	E	Centered	20%	0.9	96.6	62.2	0	588.9	772.3
173	Medium	White Shades	W	Centered	10%	0.2	17.6	11.8	5	1503.9	1793.7
174	Medium	White Shades	W	Centered	10%	0.5	21.8	13.4	5	1326.5	1784.3
175	Medium	White Shades	W	Centered	10%	0.9	32.8	15.1	5	1125.2	1661.1
176	Medium	White Shades	W	Centered	15%	0.2	46.2	30.3	6.7	918.4	1257.7
177	Medium	White Shades	W	Centered	15%	0.5	54.6	31.5	6.7	751.1	1198.4
178	Medium	White Shades	W	Centered	15%	0.9	65.5	39.5	6.7	640.1	1219.1
179	Medium	White Shades	W	Top	15%	0.2	42	16	4.2	931.6	1258.7
180	Medium	White Shades	W	Down	15%	0.2	25.2	17.6	14.3	1345.4	1781
181	Medium	White Shades	W	Down	15%	0.2	20.2	8.4	6.7	1467.9	1787.6

Table A-1: The Simulation Results of Different Model Conditions (Continued)

Run	Room Size	Shades	Orien. n.	Window Position	WFR	FVR	sDA High	sDA Custom	ASE	Light Energy High	Light Energy Custom
182	Medium	White Shades	W	Centered	20%	0.2	76.5	54.6	10	682.9	1010.2
183	Medium	White Shades	W	Centered	20%	0.5	93.3	61.3	10	601.9	969.9
184	Medium	Dark Shades	W	Centered	20%	0.5	64.7	10.1	10	944.8	1296.3
185	Medium	Dark Shades	W	Centered	20%	0.2	32.8	4.2	10	1153.2	1319.3

Table A-2: Statistical Analysis and Predicted Results

Building Size	Shades	Orientations	Window Position	WFR	FVR	Simulated sDA_high	Simulated sDA_custom	Predicted sDA_high	Differences (Predicted vs simulated)
small	No shades	E	Centered	0.2	0.2	54	50.7	60.61	12.23%
small	No shades	E	Centered	0.2	0.5	66	53.3	70.51	6.83%
small	No shades	E	Centered	0.1	0.2	27.5	22.5	20.59	25.12%
small	No shades	E	Centered	0.23	0.2	62.5	50	62.60	0.16%
small	No shades	E	Down	0.2	0.2	37.5	37.5	42.91	14.43%
small	No shades	E	Down	0.2	0.5	48	40	52.71	9.80%
small	No shades	E	Down	0.2	0.9	62.5	45	67.58	8.13%
small	No shades	E	Top	0.2	0.2	85	67.5	83.71	1.52%
small	No shades	E	Top	0.2	0.5	99.3	71.3	94.93	4.41%
small	No shades	E	Mix	0.2	0.2	56.7	48.7	58.42	3.04%
small	No shades	E	Mix	0.2	0.5	72	53.3	70.51	2.07%
small	No shades	E	Mix	0.2	0.2	56	47.3	56.90	1.60%
small	No shades	E	Mix	0.2	0.5	65.3	50	66.91	2.47%
small	No shades	E	Mix	0.2	0.2	50	37.5	46.20	7.59%
small	No shades	E	Mix	0.2	0.5	54.7	44	60.36	10.35%
small	No shades	E	Mix	0.2	0.9	89.3	60	87.24	2.30%
small	No shades	N	Centered	0.16	0.2	37.5	35	36.87	1.69%
small	No shades	N	Centered	0.23	0.2	50	35	43.31	13.37%
small	No shades	N	Centered	0.31	0.2	87.5	62.5	80.63	7.85%
small	No shades	N	Centered	0.27	0.2	62.5	57.5	71.53	14.44%
small	No shades	N	Centered	0.2	0.2	46.7	46.7	53.32	14.18%
small	No shades	N	Centered	0.2	0.5	50	50	63.99	27.98%
small	No shades	N	Centered	0.2	0.9	67.5	50	73.41	8.76%

Table A-2: Statistical Analysis and Predicted Results (Continued)

Building Size	Shades	Orient ations	Window Position	WFR	FVR	Simulated sDA_high	Simulated sDA_custom	Predict ed sDA_high	Differences (Predict ed vs simulat ed)
small	No shades	N	Down	0.2	0.2	33.3	30.7	32.57	2.19%
small	No shades	N	Top	0.2	0.2	59.3	49.3	60.93	2.76%
small	No shades	N	Mix	0.2	0.2	43.3	34.7	40.23	7.09%
small	No shades	N	Mix	0.2	0.2	43.3	36	41.65	3.82%
small	No shades	N	Mix	0.2	0.2	38.7	32.7	38.05	1.69%
small	No shades	N	Mix	0.2	0.5	46.7	36.7	49.48	5.95%
small	No shades	N	Mix	0.2	0.9	60	40	62.50	4.17%
small	No shades	S	Centered	0.05	0.2	16	14	11.38	28.88%
small	No shades	S	Centered	0.05	0.5	24.7	19.3	24.23	1.90%
small	No shades	S	Centered	0.05	0.9	34.7	24.7	39.54	13.96%
small	No shades	S	Centered	0.1	0.2	42.7	38.7	42.99	0.67%
small	No shades	S	Centered	0.1	0.5	53.3	44.7	56.60	6.19%
small	No shades	S	Centered	0.1	0.9	66.7	53.3	75.40	13.05%
small	No shades	S	Centered	0.16	0.2	63.3	54.7	66.00	4.27%
small	No shades	S	Centered	0.2	0.2	100	66.7	82.78	17.22%
small	No shades	S	Down	0.2	0.2	54.7	48	59.09	8.02%
small	No shades	S	Mix	0.2	0.2	76.7	60	75.47	1.60%
small	No shades	W	Centered	0.2	0.2	63.3	57.3	69.57	9.91%
small	No shades	W	Centered	0.2	0.5	100	62.5	82.31	17.69%
small	No shades	W	Centered	0.16	0.2	50	50	57.92	15.84%
small	No shades	W	Centered	0.23	0.2	80	62.5	78.00	2.49%
small	No shades	W	Down	0.2	0.2	40	37.5	44.68	11.70%
small	No shades	W	Mix	0.2	0.2	77.5	60	72.52	6.43%
small	No shades	W	Mix	0.2	0.2	72.5	60	72.52	0.03%
small	No shades	W	Mix	0.2	0.2	55	50	61.61	12.02%
small	No shades	W	Mix	0.2	0.5	72.5	50	68.68	5.27%
small	No shades	W	Mix	0.2	0.9	100	62.5	91.74	8.26%
small	White shades	E	Centered	0.2	0.9	52.7	29.3	56.72	7.63%
small	White shades	E	Centered	0.2	0.5	42.7	26.7	47.90	12.19%
small	White shades	E	Centered	0.2	0.2	37.3	23.3	39.71	6.45%
small	White shades	E	Centered	0.16	0.2	31.3	19.3	31.65	1.13%
small	White shades	E	Centered	0.16	0.5	35.3	18	34.72	1.64%
small	White shades	E	Centered	0.16	0.9	42	23.3	46.49	10.68%
small	White shades	E	Centered	0.1	0.2	13.3	9.3	15.18	14.16%

Table A-2: Statistical Analysis and Predicted Results (Continued)

Building Size	Shades	Orient ations	Window Position	WFR	FVR	Simulated sDA_high	Simulated sDA_custom	Predict ed sDA_high	Differences (Predict ed vs simulat ed)
small	White shades	E	Down	0.16	0.2	14.7	10.7	18.98	29.10%
small	White shades	S	Centered	0.1	0.2	34	23.3	35.18	3.46%
small	White shades	S	Centered	0.1	0.5	36.7	24.7	41.19	12.24%
small	White shades	S	Centered	0.1	0.9	44	25.3	47.83	8.70%
small	White shades	S	Centered	0.16	0.2	58.7	44.7	64.09	9.17%
small	White shades	S	Centered	0.23	0.2	98.7	61.3	88.64	10.19%
small	White shades	S	Centered	0.2	0.2	72.7	58	82.28	13.18%
small	White shades	S	Down	0.2	0.2	60	46.7	66.66	11.10%
small	White shades	S	Top	21	0.2	100	60	97.76	2.24%
small	White shades	S	Top	21	0.5	100	60	102.24	2.24%
small	White shades	S	Top	0.2	0.2	96.7	58.7	87.83	9.18%
small	White shades	S	Mix	0.2	0.2	82.7	56.7	80.87	2.22%
small	White shades	S	Mix	0.2	0.2	74	50.7	74.32	0.43%
small	White shades	S	Mix	0.2	0.2	72.7	53.3	77.16	6.13%
small	White shades	W	Centered	0.2	0.2	47.3	32	50.97	7.75%
small	White shades	W	Centered	0.2	0.5	54.7	34.7	58.40	6.76%
small	White shades	W	Centered	0.2	0.9	64.7	36	65.80	1.70%
small	White shades	W	Centered	0.16	0.2	40	26.7	41.49	3.74%
small	White shades	W	Centered	0.16	0.5	40	26.7	45.98	14.95%
small	White shades	W	Centered	0.16	0.9	60	33.3	59.17	1.39%
small	White shades	W	Centered	0.1	0.2	15.3	11.3	19.13	25.06%
small	White shades	W	Down	0.16	0.2	20	6.7	16.38	18.10%
Medium	No shades	E	Centered	0.1	0.2	23.5	23.5	21.68	7.74%
Medium	No shades	E	Centered	0.1	0.5	37.8	27.7	33.33	11.82%
Medium	No shades	E	Centered	0.1	0.9	52.9	37	52.90	0.00%
Medium	No shades	E	Centered	0.15	0.2	55.5	49.6	54.79	1.28%
Medium	No shades	E	Centered	0.15	0.5	68.9	58	71.02	3.08%
Medium	No shades	E	Centered	0.15	0.9	93.3	68.9	92.34	1.03%
Medium	No shades	E	Down	0.15	0.2	26.1	26.1	25.86	0.92%
Medium	No shades	E	Top	0.15	0.2	67.2	62.2	73.32	9.10%
Medium	No shades	N	Centered	0.1	0.9	44.5	24.4	36.23	18.58%
Medium	No shades	N	Centered	0.1	0.5	23.5	21	23.10	1.70%
Medium	No shades	N	Centered	0.1	0.2	20.2	16.8	11.45	43.31%
Medium	No shades	N	Centered	0.15	0.9	80.7	59.7	79.38	1.63%

Table A-2: Statistical Analysis and Predicted Results (Continued)

Building Size	Shades	Orient ations	Window Position	WFR	FVR	Simulated sDA_high	Simulated sDA_custom	Predict ed sDA_high	Differences (Predict ed vs simulat ed)
Medium	No shades	N	Centered	0.15	0.5	59.7	51.3	60.79	1.83%
Medium	No shades	N	Centered	0.15	0.2	42.9	36.1	37.14	13.42%
Medium	No shades	N	Down	0.15	0.9	67.2	42	56.78	15.51%
Medium	No shades	N	Top	0.15	0.2	59.7	54.6	62.10	4.03%
Medium	No shades	N	Top	0.15	0.5	68.9	59.7	74.73	8.47%
Medium	No shades	N	Top	0.15	0.9	89.9	68.1	93.32	3.81%
Medium	No shades	S	Centered	0.1	0.2	42	35.3	39.28	6.49%
Medium	No shades	S	Centered	0.1	0.5	61.3	52.1	64.67	5.50%
Medium	No shades	S	Centered	0.1	0.9	95.8	66.4	89.70	6.37%
Medium	No shades	S	Centered	0.15	0.2	73.1	66.4	77.84	6.49%
Medium	No shades	S	Down	0.1	0.2	25.2	23.5	23.11	8.30%
Medium	No shades	S	Down	0.15	0.2	52.9	41.2	47.05	11.05%
Medium	No shades	S	Down	0.15	0.5	96.6	67.2	82.49	14.61%
Medium	No shades	S	Top	0.1	0.2	52.9	48.7	58.67	10.91%
Medium	No shades	W	Centered	0.1	0.2	31.9	28.6	29.01	9.05%
Medium	No shades	W	Centered	0.1	0.5	46.2	36.1	44.26	4.19%
Medium	No shades	W	Centered	0.1	0.9	60.5	47.1	65.69	8.58%
Medium	No shades	W	Centered	0.15	0.2	62.2	55.5	63.00	1.28%
Medium	No shades	W	Centered	0.15	0.5	79	67.2	82.83	4.85%
Medium	No shades	W	Down	0.15	0.2	36.1	31.1	33.08	8.36%
Medium	No shades	W	Top	0.15	0.2	71.4	67.2	80.54	12.80%
Medium	White shades	E	Centered	0.15	0.2	40.2	24.4	36.29	9.72%
Medium	White shades	E	Centered	0.15	0.5	53.8	31.9	48.96	8.99%
Medium	White shades	E	Centered	0.15	0.9	63	36.1	59.53	5.51%
Medium	White shades	E	Centered	0.2	0.2	68.1	42	60.11	11.74%
Medium	White shades	E	Centered	0.2	0.5	81.5	51.3	74.74	8.29%
Medium	White shades	E	Centered	0.2	0.9	96.6	62.2	92.62	4.12%
Medium	White shades	E	Down	0.15	0.2	22.7	17.6	25.58	12.69%
Medium	White shades	E	Top	0.15	0.2	39.5	13.4	29.07	26.41%
Medium	White shades	S	Centered	0.15	0.2	61	47.1	65.78	7.83%
Medium	White shades	S	Centered	0.15	0.5	71.4	51.3	74.85	4.83%
Medium	White shades	S	Centered	0.15	0.9	89.9	55.5	85.41	4.99%
Medium	White shades	S	Centered	0.1	0.2	31.1	21	32.67	5.04%
Medium	White shades	S	Centered	0.1	0.5	41.2	21.8	38.03	7.70%

Table A-2: Statistical Analysis and Predicted Results (Continued)

Building Size	Shades	Orient ations	Window Position	WFR	FVR	Simulated sDA_high	Simulated sDA_custom	Predict ed sDA_high	Differences (Predict ed vs simulat ed)
Medium	White shades	S	Centered	0.1	0.9	50.4	25.2	47.72	5.32%
Medium	White shades	S	Down	0.1	0.2	20.2	15.1	22.94	13.55%
Medium	White shades	S	Top	0.1	0.2	41.2	23.5	40.17	2.49%
Medium	White shades	W	Centered	0.1	0.2	17.6	11.8	19.68	11.81%
Medium	White shades	W	Centered	0.1	0.5	21.8	13.4	25.91	18.86%
Medium	White shades	W	Centered	0.1	0.9	32.8	15.1	33.75	2.89%
Medium	White shades	W	Centered	0.15	0.2	46.2	30.3	44.50	3.68%
Medium	White shades	W	Centered	0.15	0.5	54.6	31.5	50.29	7.89%
Medium	White shades	W	Centered	0.15	0.9	65.5	39.5	65.00	0.76%
Medium	White shades	W	Centered	0.2	0.2	76.5	54.6	75.62	1.15%
Medium	White shades	W	Centered	0.2	0.5	93.3	61.3	87.42	6.30%
Medium	White shades	W	Down	0.15	0.2	25.2	17.6	27.35	8.52%
Medium	White shades	W	Down	0.15	0.2	20.2	8.4	17.31	14.30%
Medium	White shades	W	Top	0.15	0.2	42	16	33.67	19.82%